THE SEDIMENTOLOGY OF THE LOWER FARS FORMATION (MIOCENE) OF NORTHERN IRAQ

by

MUDHAR G. SHAWKAT

Thesis presented for the degree of
Doctor of Philosophy
in the
University of Newcastle upon Tyne

September 1979

CONTENTS

ABSTRACT

This thesis incorporates a study of the petrology and sedimentology of rocks of the Gachsaran Formation (formerly Lower Fars) (Miocene) in northern Iraq.

Field study led to the recognition of three basic lithofacies: mudrock, limestone and gypsum-anhydrite, which are arranged into cycles. The lithofacies are interpreted as the deposits of subtidal, intertidal and supratidal environments by comparison with Recent sediments, particularly those developing along the Trucial Coast, Arabian Gulf.

Petrological studies show that the gypsum is secondary after anhydrite. Several types of sulphate textures are distinguished, each of which is described and its origin interpreted. The dominant nodular nature of the sulphates and their occurrence in repeated mudrock, limestone, sulphate cycles are consistent with a supratidal (sabkha) origin. Geochemical data were also used to aid in the interpretation of the depositional environment and diagenesis of the sulphates.

Detailed petrographic examination of the limestones has led to the distinction of twelve carbonate lithofacies. The most common types are peloidal and bioclastic limestones as well as oolitic and oncolitic varieties. Stromatolites and cryptalgal laminites are also present and their significance is discussed. In general the limestones are interpreted as deposited in shallow subtidal to intertidal situations. Diagenetic events in the limestones include early and late cementation, dissolution and some dolomitization. Early diagenetic cementation appears to have been widespread. Two types of dolomite are recognised: an early non-rhombohedral variety resembling micrite, and a much coarser, later diagenetic dolomite. Geochemical data indicate diagenesis in both open and closed systems. The limestones possess average Fe and Mn contents, but Mg is

relatively low compared with published limestone analyses. The very high content of Sr in some of the carbonate rocks is taken to indicate that aragonite has been an important early mineral in these rocks. The Na content, a reflection of salinity, indicates hypersalinity, especially for the dolostones.

With regard to the mudrocks, illite is the dominant clay mineral with montmorillonite, mixed-layer clays and kaolinite less common. On the basis of colour, mineralogy and type of Foraminifera present, two types of mudrock are recognised: a green variety with benthic Foraminifera, other fossils and higher kaolinite, interpreted as deposited in hypersaline lagoons, and a red variety with planktonic Foraminifera and a lower kaolinite content, interpreted as of relatively deep water origin.

Cycles of mudrock - limestone - gypsum, limestone - gypsum and mudrock - gypsum are interpreted as sabkha cycles produced through the progradation of sabkhas over intertidal and subtidal sediments. A consideration of the tectonic context of the Mesopotamian Basin suggests that vertical tectonic movements may well have been an important factor in Gachsaran deposition and the development of the cyclicity, as well as eustatic sea-level changes through variations in the extent of polar glaciation and plate tectonic movements.

ACKNOWLEDGEMENTS

I sincerely acknowledge the guidance and help of Dr. M.E. Tucker, who supervised this work. His assistance, patience, guidance and the stimulation of my interest in sulphate and carbonate rocks were invaluable.

My thanks are due to Professor T.S. Westoll and Professor J.R. Cann for the use of the facilities of the Department of Geology at the University of Newcastle upon Tyne. I would also like to thank the academic staff, particularly Dr. M.H. Battey and Dr. C.T. Scrutton, postgraduate colleagues and technical staff of the department, for the fruitful discussions and help throughout the time of research.

I owe special thanks to my family, particularly my grandfather, Mr Ali Kamal, for their support both spiritually and financially. My sincerest thanks are also extended to my wife for her patience and guidance without which this work would have been very difficult to perform.

Finally, I am most indebted to Miss P. Webb for typing the manuscript and for her patience and perseverance throughout.

CHAPTER 1

INTRODUCTION

1.1 Previous work and background geology

1.2 Aim of research

CHAPTER 1

INTRODUCTION

The Gachsaran Formation (formerly Lower Fars) occurs in Syria, Iraq and Iran. The thickness of the formation is variable, with a maximum thickness of some 600m. in the central part of the basin in Iraq. The formation is an evaporitic sequence and consists mainly of repeated cycles of mudrock limestone and gypsum, locally with halite. In Iraq, the formation is of Middle Miocene age.

The Gachsaran Formation in the Middle East is important for a number of reasons. It is the cap rock to the major oil fields of Iraq, Iran and Syria; it contains reserves of sulphur in Iraq, and an inexhaustable supply of limestone and gypsum which is used for construction purposes.

This thesis arises from the field work in the Shaqlawa, Bashiqa, Mosul, Tall-afar, Sheikh Ibrahim and Makhul regions of northern Iraq (Fig.2-1) and laboratory studies of material collected there and from three boreholes at Mishraq.

1.1 Previous work and background geology

The vast resources of oil in the Middle East have attracted many geologists to investigate its origin and relation to the sedimentary rock sequence and tectonic history of the area. Many of these studies touched upon the Gachsaran Formation in one way or another.

Henson (1951) divided the Middle East into seven stratigraphic-tectonic zones. These were the Arabo-Nubian and Arabo-Somali shields, the stable shelf, the unstable shelf, the zone of marginal upper Cretaceous troughs, the zone of marginal Neogene troughs, the zone of Neogene autochthonous folds and the orogeosynclinal zone of thrusting. A simpler structural division was employed by Baker and Henson (1952) and Stocklin (1968): the Anatolian-Iranian ranges in the northeast, the Arabian shield in the southwest and a broad transitional shelf zone in the centre. Iraq,

on the other hand, was subdivided structurally into three main zones by Dunnington (1955): the nappe zone, the folded zone, and the unfolded zone (Fig.1-1). These zones were differentiated during the late Tertiary Alpine orogeny. The boundary between the folded and unfolded zone is abrupt. The folds increase in both amplitude and tightness as the nappe zone is approached (Dunnington, 1958). Exceptions to this generalisation do occur as in the anticlinal folds of Hemrin, Makhul, Sheikh-Ibrahim and Jabal Sinjar. These folds have a greater amplitude and length compared to those surrounding them. Such discrepancies, together with seismic data, led Henson (1951) and Henson and Baker (1952) to suggest that the folding was affected by pre-existing basement block faults. This caused the sedimentary sequence to react in an irregular and complex fashion to the tangential forces exerted. In general the folds are steeper on their southwestern limbs than their northeastern ones, indicating that the main forces exerted were from the northeast (Lees, 1938). On the basis of tectonic behaviour of the stratigraphic column in Iran, O'Brien (1950) divided it into four groups; upper incompetent group, mobile group, competent group, and lower mobile group. Dunnington (1968) employed the same division for the stratigraphic column in Iraq.

Earlier ideas concerning the deposition of the Gachsaran succession considered sedimentation to have taken place in an immense gulf which stretched from the present Turkish frontier to the Arabian Gulf (Lees, 1938). Sugden (1951) did not object to this idea but added that this basin was restricted and he further suggested that a strait to the open ocean existed near the present strait of Hormuz. Dunnington (1958) postulated that the Gachsaran was deposited in an intermittently barred, basinal lagoonal environment, and Bellen et al. (1959) considered the basin to be semibarred. The configuration of this basin was discussed by Stocklin (1968), who considered the western shore of the basin to be somewhat east of the present

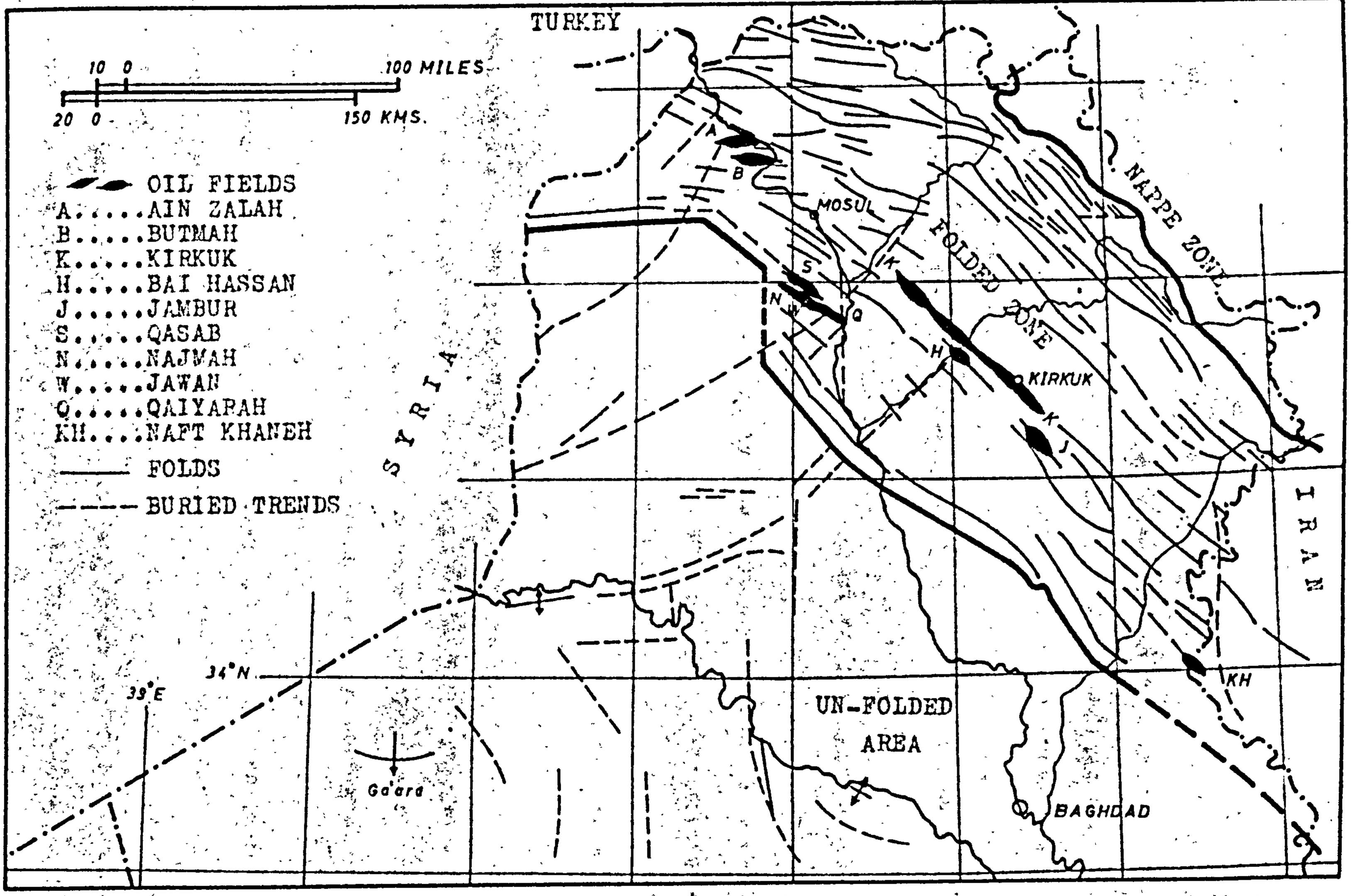

Fig. 1-1. Tectonic framework of Northern Iraq (After Dunnington, 1958).

western coastline of the Arabian Gulf, and to extend west of the River Euphrates through Iraq into Syria. He further suggested that a branch of this basin extended southward between Qatar and the Oman range. Like Sugden (1951), he put the emphasis on the point that the basin must have had a connection with the Indian Ocean over a shallow, submarine swell, and suggested its position to be off the Oman Peninsula. He further proposed that on the eastern side, the basin might have extended further into central and northwest Iran, and into Anatolia (Turkey) through some gaps north of Bandar Abbas and near Hamadan. Dunnington (1958), on the other hand, suggested separate basins of Miocene age in Turkey and Iran.

The stratigraphic column of Iraq was studied by Bellen et al. (1959). James and Wynd (1965) revised the nomenclature and other aspects of the stratigraphic column in Iran. Gill and Ala (1972) and Shawkat and Tucker (1978) discounted the previously suggested evaporating dish model for the Gachsaran deposition. They compared the Gachsaran succession with recent examples of carbonate-sulphate deposits along the Arabian Gulf and other intertidal-supratidal environments. Al-Saadooni (1978) discussed certain aspects of the formation using cuttings from wells in Kirkuk. Other work which has touched upon the Gachsaran Formation in Iraq includes that of Al-Ansari (1973) and Al Mubarak (1975).

1.2 Aim of Research

The aim of this study is to determine the sedimentological characteristics of the Gachsaran Formation and establish the depositional environments. In order to accomplish this, sections over a wide area of northern and central Iraq were studied and sampled. The petrography of the carbonates and sulphates and their sedimentological context have been investigated. The fine-grained clastics (mudrocks) have been qualitatively and quantitatively examined, and Foraminiferal content investigated. The Gachsaran sediments have been described and interpreted with reference to

Recent sediments and ancient sequences. The tectonic context of the formation has also been considered.

CHAPTER 2

STRATIGRAPHY

2.1 Introduction

2.2 Terminology and age

2.3 Iraq

2.4 Iran

2.5 Syria

2.6 Regional distribution and variation

2.7 Thickness variation

2.8 Other Miocene evaporites in the Middle East

CHAPTER 2

STRATIGRAPHY

2.1 Introduction

In Iraq the formation under study has been widely referred to as the Lower Fars Formation. The name Gachsaran is now proposed for this formation (see below). This formation is characterised by repeated cycles of marl and/or clay, limestone and gypsum. Halite is locally developed. Good exposures along wadis cutting across the flanks of anticlines in the Bashiqa-Mosul-Tallafar-Sheikh Ibrahim-Makhul regions of northern Iraq (fig.2-1), allowed detailed study of this formation. The Gachsaran Formation was studied along 11 sections in 8 localities in northern Iraq.

In this chapter a brief account is given of the formation in Iraq, Iran and Syria. The formation is compared with other Miocene evaporite formations in the Middle East.

2.2 Terminology and age

The name Fars Series was first introduced by Pilgrim (1908) to designate a thick sequence of Miocene deposits cropping out in the Fars Province of south-west Iran. The Fars Series was later subdivided into lithostratigraphic units, Lower, Middle and Upper Fars Formations by geologists working for the British Petroleum Company in the area. The three formations were later described from Iran by Busk and Mayo (1918). The names applied to the three formations in Iran were used to describe similar lithostratigraphical units in Kuwait, Iraq and Syria.

The term series is applied to a unit in the conventional chrono-stratigraphic hierarchy, ranking above a stage and below a system, and hence it is wrong to use it as a lithostratigraphic term more or less equivalent to a group (American Commission on Stratigraphic Nomenclature; 1961: Hedberg, 1976). Chronostratigraphic units are defined as encompassing all rocks formed within a certain time span of Earth history regardless of their lithology. By definition these units everywhere

Fig. 2-1 Map of northern Iraq showing localities referred to in text. Isopachytes for the Gachsaran Formation (formerly Lower Fars) are based on Dunnington (1958). The shaded area on inset map represents the location of the Miocene depositional basin in the Middle East.

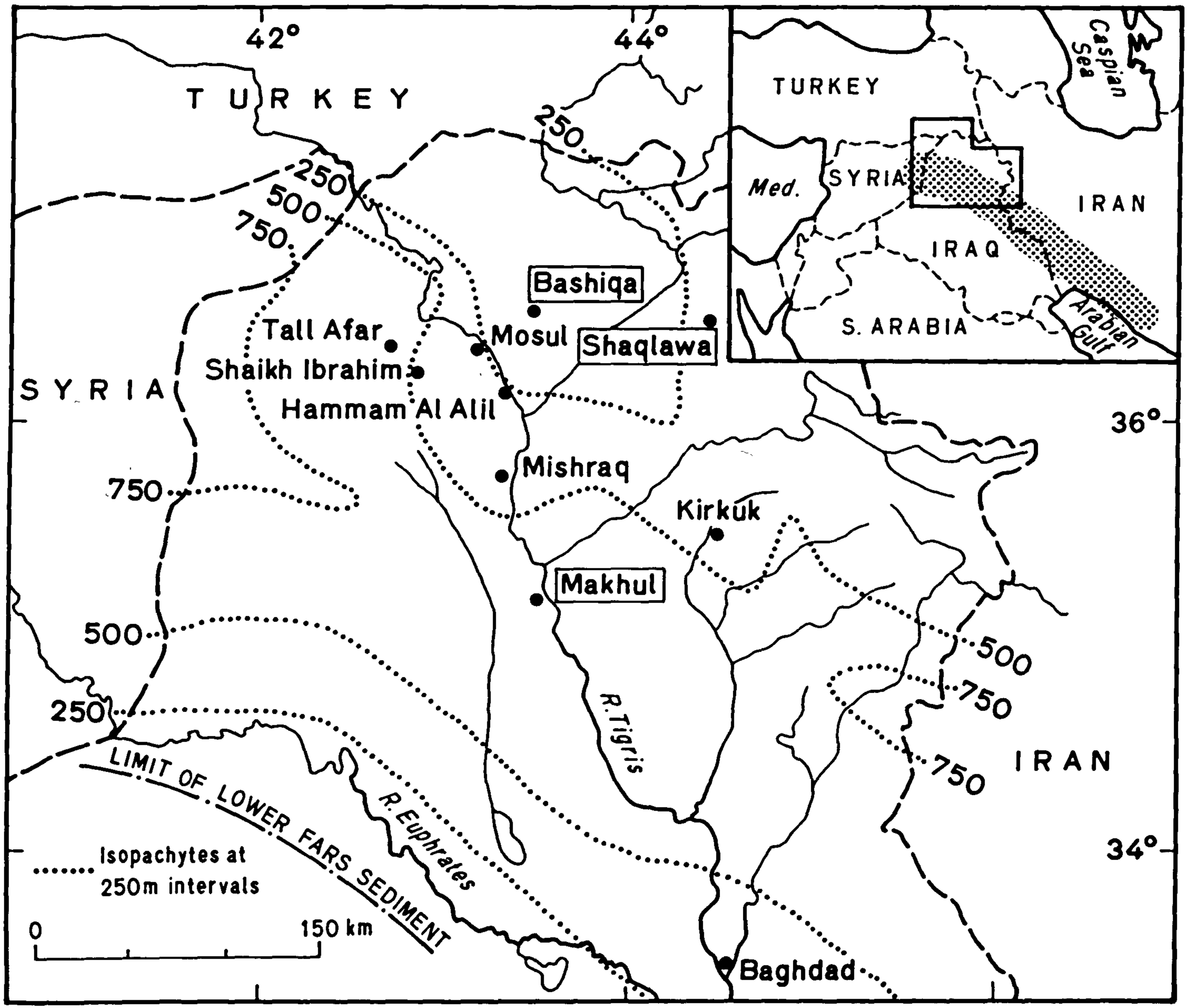
42°
44°
36°
34°
TURKEY
SYRIA
IRAQ
IRAN
S. ARABIA
Med.
Caspian Sea
Arabian Gulf
250
500
750
Bashiqa
Tall Afar
Mosul
Shaqlawa
Shaikh Ibrahim
Hammam Al Alil
Mishraq
Kirkuk
Makhul
R. Tigris
R. Euphrates
LIMIT OF LOWER FARS SEDIMENT
Isopachytes at 250m intervals
0
150 km
Baghdad

include rocks of only a certain age and their boundaries are everywhere isochronous (Hedberg, 1976). It is therefore erroneous, from the chronological point of view, to call formations in Iraq, Syria and indeed even in Iran (see James and Wynd, 1965) by the same chronological term when they are diachronous (see below). Furthermore, the terms Lower, Middle and Upper, together with the System name, are frequently used for Series divisions (International Subcommission on Stratigraphic Classification, 1972) and should not be used as formal names to designate different lithostratigraphic units (Hedberg, 1976; Holland, 1978). Following the recommendations and definitions proposed by the International Sub-Commission on Stratigraphic Terminology (1961) and the American Commission on Stratigraphic Nomenclature (1961), James and Wynd (1965) re-named the Lower Fars Formation the Gachsaran Formation, the Middle Farsthe Mishan Formation and the Upper Fars the Agha Jari Formation. They also designated type sections and type localities for each formation. These names are now widely accepted by geologists in Iran. There is no doubt, however, that the Lower Fars Formation, the Middle Fars Formation (although limited to the central part of the Mesopotamian basin in Iraq) and the Upper Fars Formation in Syria, Iraq and Kuwait are continuations of the re-named formations (Gachsaran, Mishan and Agha Jari) of Iran, as they belong to the same basin of deposition. Their lithologies, if not the same, are similar. The former names, however, are still being used for the formations in Kuwait, Iraq and Syria. Geologists should seek the easiest and simplest ways to communicate, interpret and understand their subject, and complications such as giving different names to the same formation should be avoided. Furthermore, stratigraphic units should not be limited by international borders (Hedberg, 1976). For the above mentioned reasons and discussions, and following the re-naming of the formations under discussion in Iran, the author recommends that, at

least in Iraq, the Lower Fars Formation be re-named the Gachsaran Formation, the Middle Fars the Mishan and the Upper Fars the Agha Jari Formation.

In Iraq the precise age of the Gachsaran Formation has been a matter of some controversy. A Middle Miocene age was assigned by Bellen et al. (1959), Lower Middle Miocene by Owen and Nasr (1958) and Lower Miocene by Sayyab and Kureshy (1967). More recently, Al-Omari and Sadik (1972) considered the formation to be Lower Middle Miocene in age. In the western desert, the Gachsaran Formation conformably overlies the Euphrates Limestone Formation. The latter formation was dated Burdigalian by Ctyroky et al. (1975). This dating seems to confirm that the Gachsaran Formation is of Middle Miocene age, possibly Langhian to Serravallian (Fig.2-2), at least in this particular locality. James and Wynd (1965), however, considered the Gachsaran Formation to be Early Miocene in interior Fars and late Early Miocene throughout Khuzestan and Lurestan (Fig.2-10,11),while Metwalli et al. (1974) assigned the formation to an Upper Miocene age in Syria. It is likely that the base of the Gachsaran Formation is diachronous (older in the southeast, younger in the north-west). The exact age of the formation in different parts of the depositional basin, however, must remain in doubt.

2.3 Iraq

The Gachsaran Formation in northern Iraq is characterised by repeated cycles of marl, limestone, gypsum with individual cycles varying from 3 to 25 metres in thickness, and sulphate horizons 1.5 to 15 metres in thickness (see Figs. 2-3 - 9). . Halite occurs in several cycles in the middle part of the Gachsaran, in the central part of the basin (e.g. Naft-Khaneh and Kirkuk) in Iraq (Jones and Hudson, 1949; Dunnington, 1958). Salt horizons occur in the lower part of the sequence and attain a total thickness of about 45 metres in Naft Khaneh (Jones and Hudson,

Fig. 2-2 Tertiary formations in Iraq plotted against the Miocene stages of the Mediterranean.

Miocene stages are after Rogl and Muller (1978).

Million Years	Epochs		Mediterranean European Stages	Formations in Iraq
5	PLIOCENE		Zanclian	Bakhtiari Formation
	MIOCENE	late	Messinian	Agha Jari Formation
10			Tortonian	
				Mishan Formation
15		middle	Serravallian	Gachsaran Formation (formerly Lower Fars)
			Langhian	
			Burdigalian	Jeribe Formation
20		early	Aquitanian	Dhiban/ Euphrates/ Sirikagni Formation
25	OLIGOCENE			Anah/Azkland/Ibrahim Fms.

Fig.2-3
SECTION IN LOWER FARS FORMATION NEAR SHEIKH IBRAHIM, N.W. IRAQ.

TELAFAR
Section 3

Upper
Fars Fm.

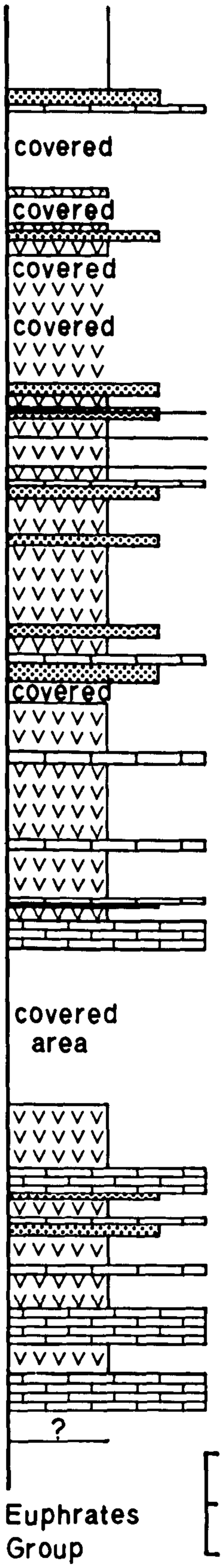

Euphrates
Group

Fig. 2-4

JABAL ALAN
Section 5

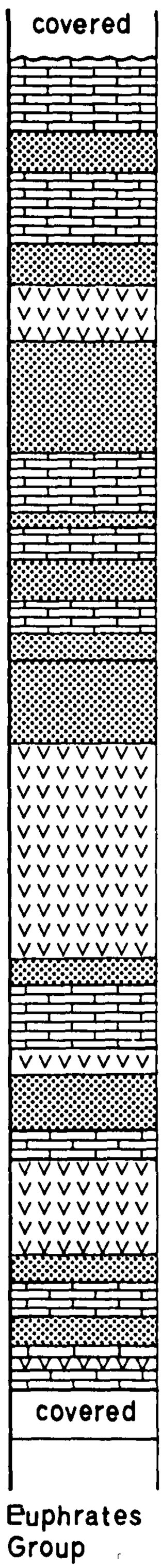

Euphrates
Group

Fig. 2-5

HAMAM ALIL
Section 2

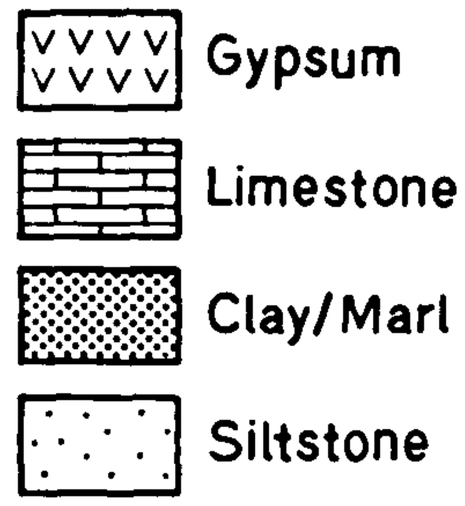

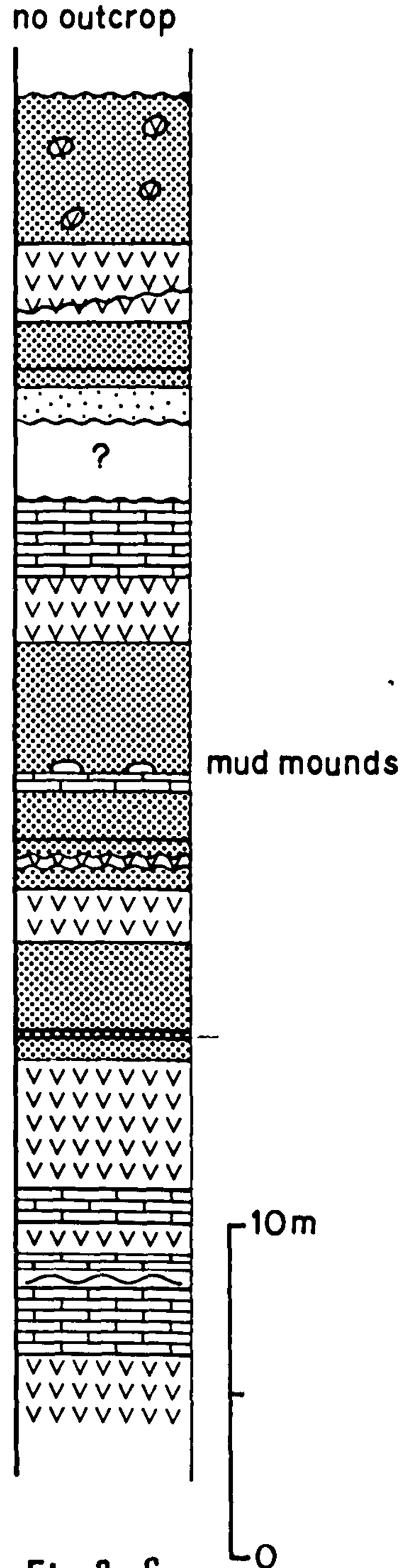

Fig. 2-6

MAKHUL
Section 10

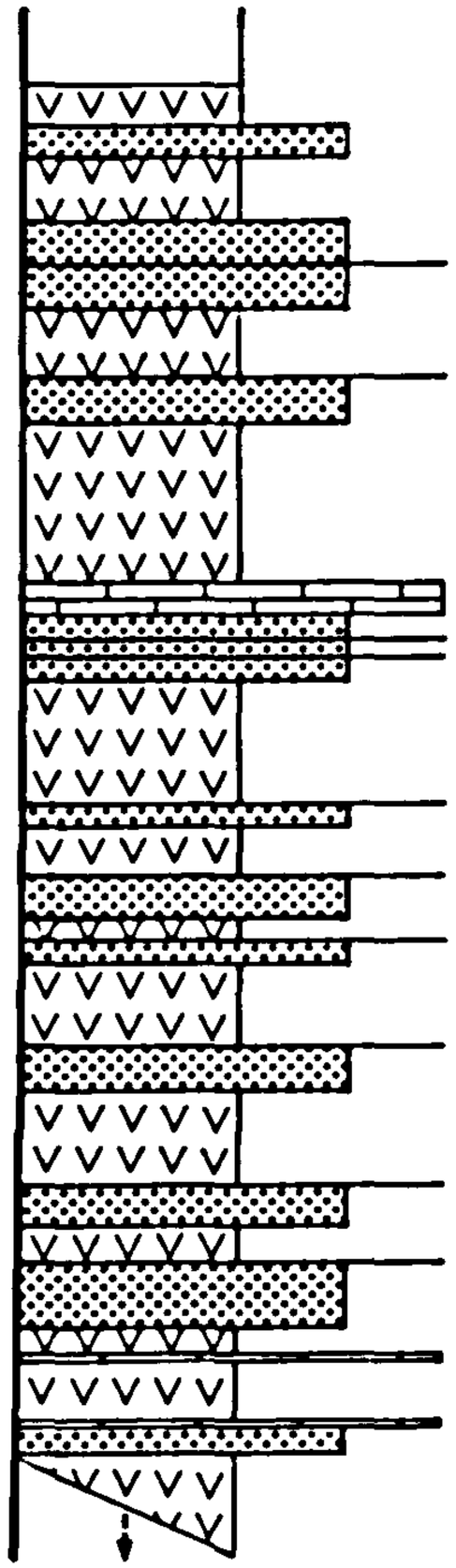

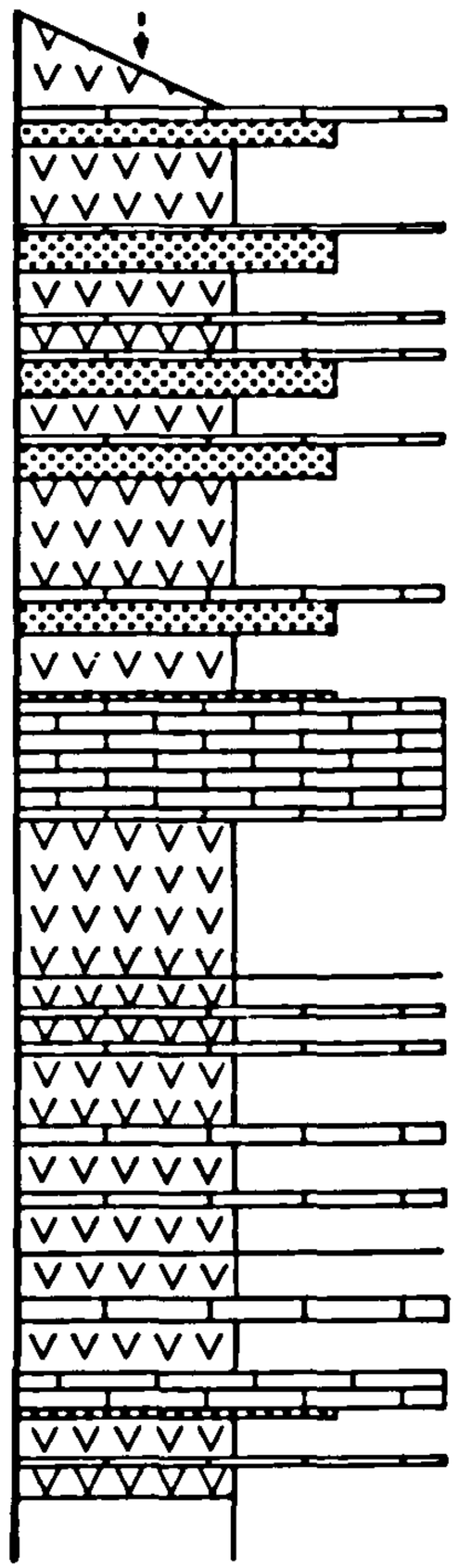

Fig. 2-7

SHAQLAWA
Section 6

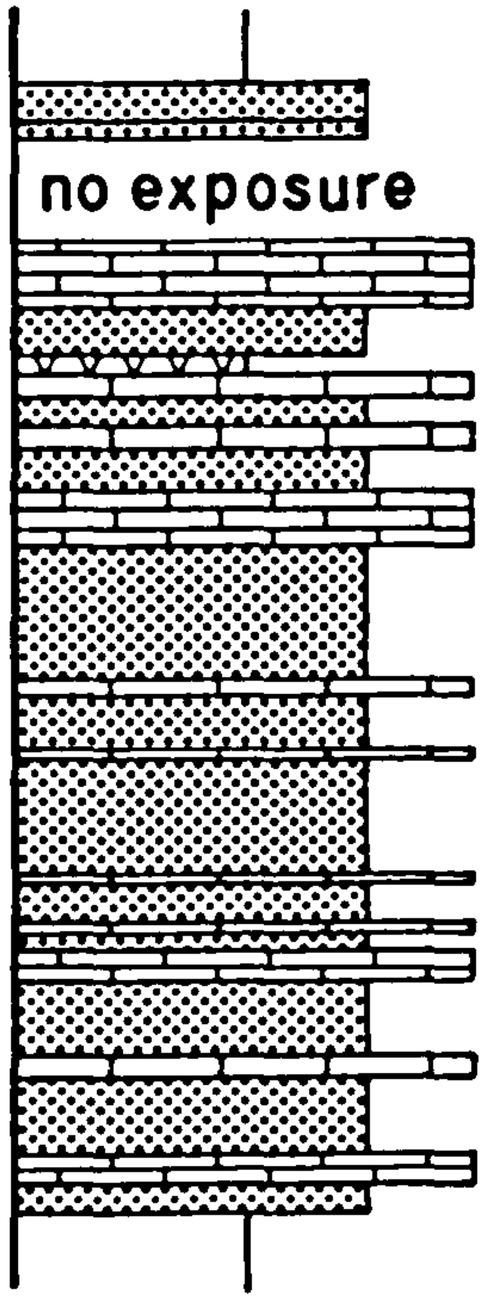

Fig. 2-8

BASHIQA
Section 1

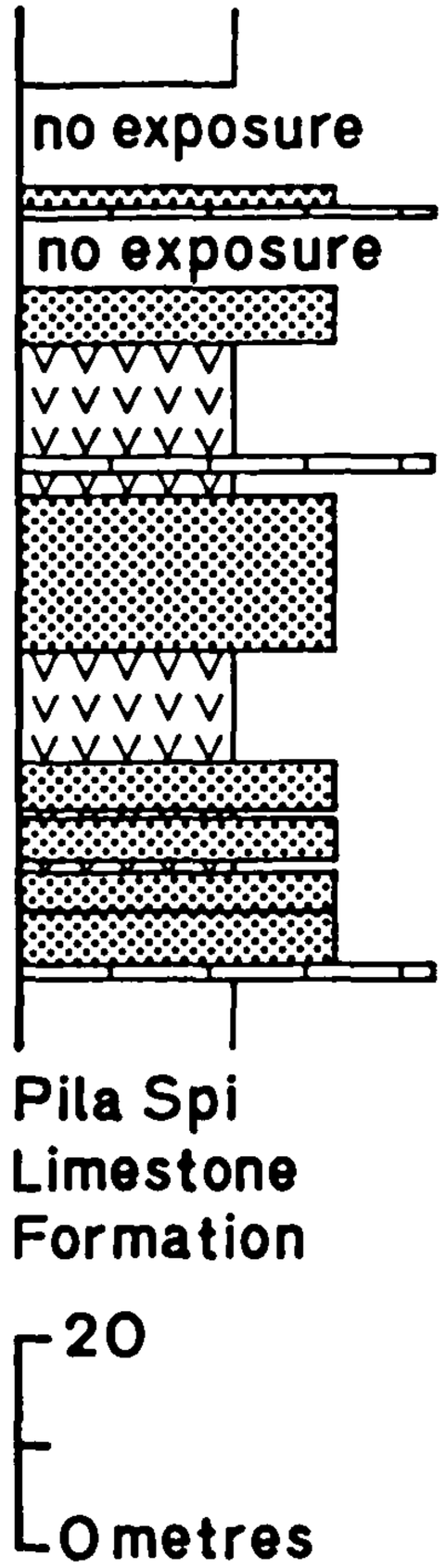

Fig. 2-9


Gypsum

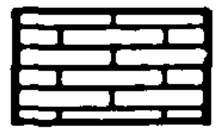
Limestone

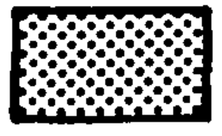
Clay/Marl

FORMATION CORRELATION CHART

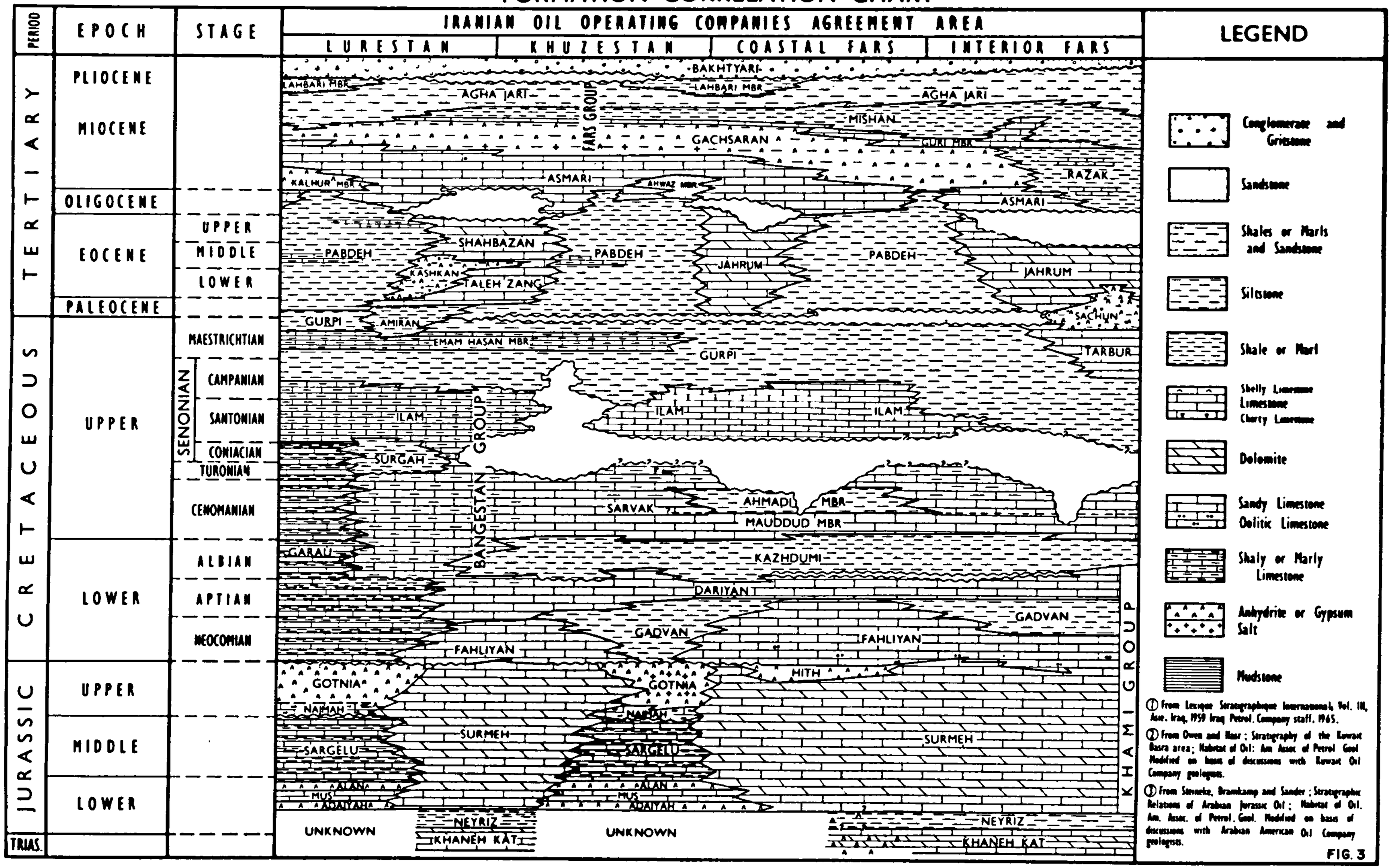

FIG. 3

Fig. 2-10 - After James and Wynd (1965).

FORMATION CORRELATION CHART OF IRAQ, IRANIAN AGREEMENT AREA, KUWAIT AND SAUDI ARABIA

PERIOD	EPOCH	STAGE	IRAQ ① SEE FIG 3	IRANIAN AGREEMENT AREA: LURESTAN	IRANIAN AGREEMENT AREA: KHUZESTAN	KUWAIT AND SE IRAQ ② SEE FIG 3	SAUDI ARABIA ③ SEE FIG 3
TERTIARY	PLIOCENE		UPPER FARS	BAKHTYARI		DIBDIBBA	HOFUF
	MIOCENE		LOWER FARS	LAHBARI MBR	LAHBARI MBR	LOWER FARS	DAM
			JERIBE	AGHA JARI		GHAR	HADRUKH
			DHIBAN	MISHAN			
			EUPHRATES	GACHSARAN			
				ASMARI			
	OLIGOCENE		KIRKUK GROUP	KALHUR MBR	AHWAZ MBR		
	EOCENE	UPPER	JADDALA	PILA SPI AND AVANAH	SHAHBAZAN	DAMMAM	DAMMAM
		MIDDLE	AALIJI	GERCUS	PABDEH	PABDEH	RUS
		LOWER		KHURMALA AND SINJAR	KASHKAN	RUS	
				KOLOSH	TALEH ZANG	RADHUMA	RADHUMA
	PALEOCENE				AMIRAN	TAYARAT	
JURASSIC CRETACEOUS	UPPER	MAESTRICHTIAN	AQRA BEKHME	TANJERO	EMAM HASAN MBR	QURNA	
		SENONIAN CAMPANIAN	SHIRANISH		GURPI	HARTHA	ARUMA
		SANTONIAN		ILAM	ILAM	SADI	
		CONIACIAN	KOMETAN	SURGAH		MUTRIBA	
		TURONIAN	GULNAR			TANUMA	
		CENOMANIAN	DOKAN	SARVAK		KHASIB	
						MISHRIF	MISHRIF MBR
						RUMAILA	RUMAILA MBR
						AHMADI	AHMADI MBR
						WARA	WARA MBR
						MAUDDUD	MAUDDUD MBR
	LOWER	ALBIAN	QAMCHUQA	GARAU	KAZHDUMI	BURGAN	
		APTIAN		BALAMBO	DARIYAN	SHU'AIBA	BIYADH
			GARAGU			ZUBAIR	
		NEOCOMIAN	SARMORD		GADVAN	RATAWI	BUWAIB
				FAHLIYAN		MINAGISH	YAMAMA - SULAIY
			RAKHIA			MAKHUL	HITH
	UPPER		GOTNIA	GOTNIA	GOTNIA	GOTNIA	ARAB
			BARSARIN				JUBAILA
			NAJMAH	NAJMAH	NAJMAH	NAJMAH	HANIFA
			NAOKELEKAN				TUWAIQ MT
	MIDDLE		SARGELU	SARGELU	SURMEH SARGELU	SARGELU	DHRUMA
	LOWER		ALAN	ALAN	ALAN		
			MUS	MUS	MUS		
			ADAIYAH	ADAIYAH	ADAIYAH		
			SEHKANIYAN				MARRAT
			BUTMAH				
			SARKI	UNKNOWN	NEYRIZ KHANEH KAT UNKNOWN		MINJUR
TRIAS			BALUTI				

FIG. 4

Fig. 2.11. After James and Wynd (1965).

1949). Halite is developed to a much greater extent in southwest Iran (O'Brien, 1957; Gill and Ala, 1972). Towards the margin of the basin, the thickness of the cycles is reduced and red marls and siltstones dominate. In Shaqlawa, the sulphate horizons are reduced to only one gypsum bed (2 m.) within the sequence.

W. Kitchin (Unpub.reports in Bellen et al., 1959) was the first to subdivide the Gachsaran from studies of boreholes from the Kirkuk structure, northern Iraq, into a number of informal units. He recognised 29 limestone marker horizons within the formation. From bottom to top, Kitchin designated four units, a) the transition beds, b) the saliferous beds, c) the seepage beds, and d) the upper red beds. Elsewhere in Iraq the formation is divided into two units on the basis of the presence of marl or clay beds, where thicker developments of these horizons occur in the upper part (Al-Ansari, 1973; Agha et al., 1978; this work, see sections 2.3 - 9).

2.4 Iran

The type sequence of the Gachsaran Formation is in Gachsaran, southwest Iran. There the formation, about 2000 m. thick, has been divided into seven informal members (Fig.8-2; James and Wynd, 1965). The formation in Iran consists dominantly of alternating beds of marl or mudstone, limestone and gypsum or anhydrite with occasional thick salt beds in the lower and middle part of the sequence.

2.5 Syria

The Gachsaran Formation covers extensive areas in Gebel Abd-El-Aziz, Jebissa, north-eastern Syria. The formation here overlies the transition zone (Middle Miocene) which in turn overlies the Jeribe Limestone Formation. Metwalli et al. (1974) subdivided the Tortonian deposits into a lower Transitional Zone and an upper part (Gachsaran Formation). The Transitional Zone (71-98 m.) is mainly composed of

gypsum (70-85%), intercalated with limestone, marl and, in some places, rock salt. The Gachsaran Formation was subdivided by Metwalli et al. (1974) into an upper and a lower part. The lower part is composed mainly of thick bedded salt (147-382 m.) with a fairly large proportion of greyish-blue siltstone. The upper part of the Gachsaran Formation is composed mainly of anhydrite, siltstone and thin interbeds of shaly gypsiferous limestone. The observed thickness of this zone is 257 m.; total thickness is not known but was estimated by Junphert (1969, in Metwalli et al., 1974) to be 600-700 metres.

2.6 Regional distribution and variation

In Iran, the Gachsaran Formation overlies the Asmari Formation (Oligocene to Early Miocene). The contact between the two formations is conformable. The Asmari Formation consists of about 312 metres of limestone with shelly intercalations through most of south-western Iran (James and Wynd, 1965). An evaporite wedge, the Kalhur member, replaces the limestone of the middle part of the Asmari Formation in south-western Lurestan (Fig.2-10). In south-western Khuzestan, sandstone of the Ahwaz Member, interfingers with limestone of the middle and lower parts of the Asmari Formation, and near Bandar Abbas in south-eastern Fars Province, the Asmari passes into marl of the Paddeh Formation towards the south-east (Fig.2-10)(James and Wynd, 1965). The Asmari Formation is a synonym of the Kalhur Limestone (Naft Khaneh) which is also a synonym of the Euphrates and Jeribe Limestone Formations in the interior of Iraq (Bellen et al., 1959). The Kalhur Member of the Asmari Formation is equivalent to the Dhiban Anhydrite which lies between the Euphrates and Jeribe Limestone Formations in Iraq (Fig.2-11). In the central part of the Mesopotamian basin in Iraq, the Gachsaran Evaporite Formation rests disconformably of the Basal Fars Conglomerates which belong to the Jeribe Limestone (Lower Miocene). Where this Basal Fars Conglomerate is missing,

the contact between the two formations is assumed to be conformable (Fig 2-11). The Jeribe Limestone Formation is composed of massive, recrystallised and dolomitised limestone, having a maximum thickness of 73 metres in its type locality seen near Jaddala Village (Bellen et al., 1959). The Jeribe Limestone Formation thins and disappears towards the south, south-western and north-eastern parts of Iraq, and the Gachsaran Formation rests conformably on the Euphrates Limestone Formation. Al-Khersan and Al-Saddiki (1970 and 1972) suggested that the Ghar Formation is a clastic equivalent of the Jeribe Limestone Formation to the south of Iraq and in Kuwait. The Gachsaran Evaporite Formation rests on successively older strata towards the basin margin so that in Bashiga and Shaqlawa, north and north-east of Iraq, it rests on the Pila Spi Limestone Formation (Upper Eocene) and further to the north-east, on Upper Cretaceous marls (Dunnington, 1958).

In Syria, the Gachsaran Formation conformably rests on the Transitional Zone which in turn overlies the Jeribe Limestone Formation (Metwalli et al., 1974). From published descriptions, it appears that the Transitional Zone could well be considered as part of the Gachsaran Formation and so here it is treated in this manner. This may facilitate regional stratigraphic correlation.

In Iran, the Gachsaran Formation is succeeded by the Mishan Formation (Early to Middle Miocene). The Mishan Formation is a transitional marine sequence separating the Gachsaran Formation (conformable contact) from the sub-continental Agha Jari Formation. The Mishan Formation in Iran consists of 706 metres of grey marl and shelly limestone with abundant microfauna (James and Wynd, 1965). From the oil fields area towards Lurestan, south-eastern Iraq, Kuwait and Saudi Arabia, the Mishan Formation passes vertically into the clastics of the Agha Jari Formation (Fig 2-11). The Mishan Formation in Iraq is poorly developed and has only

been reported from Kirkuk (86 metres) and Naft Khaneh (122 metres). Generally, the Mishan Formation in Iraq consists of marine limestones, shales, siltstones, sandstones and some anhydrite. In other localities of Iraq, the Gachsaran Formation almost always passes upward into a more transitional marly to silty sequence (e.g. Hamam al-alil, Mishraq, Tal-Afar etc.). This transitional sequence, however, has always been considered to be part of the upper part of the Gachsaran Formation. It remains to be seen if such a separation serves any purpose in Iraq. However, much more detailed stratigraphic and lithological work is needed on this subject before one can draw any conclusions.

In Iran, the Mishan Formation is succeeded transitionally by the Agha Jari Formation (Late Miocene to Pliocene), which in turn is unconformably overlain by the Bakhtiari Conglomerate, a coarse Pliocene fluviatile deposit ('molasse') derived from erosion of the rising Zagros Mountains. The Agha Jari Formation in Iran ranges from 606 to 3030 metres in thickness and consists mainly of siltstones, silty marl and subordinate sandstones and gypsum beds (James and Wynd, 1965). Also in Iran the Agha Jari Formation is diachronous, becomming younger from north-west to south-east and north-east to south-west (James and Wynd, 1965). Towards Kuwait and Saudi Arabia, the Agha Jari Formation thins and merges with the Dibdibba and Hofuf Formations. In Iraq, the Mishan Formation or the Gachsaran Formation is succeeded by the Agha Jari Formation, which has similar lithologies to that in Iran. It is widespread in northern Iraq but southward it loses its identity and merges with the Dibdibba Formation.

The Gachsaran Formation attains a maximum but variable thickness in south-western Iran, The thickest part of the formation in Iran seems to fall on an axis extending in a north-west - south-east direction, passing through Gesham, Gachsaran Masjid-I-Sulaiman and Lali

(Fig.2-12). In Iraq, the axis continues north-westwards through Naft Khaneh, Kirkuk and then swings westward and continues through Sinjar to Jebbisa (north-east Syria)(Fig.2-12). The maximum thickness of the formation as detected from wells in the Gachsaran oil field is about 2000 metres (James and Wynd, 1965). In Naft Khaneh, the formation is about 600 metres (Jones et al.,1949) in Kirkuk about 600 metres (Bellen et al., 1959) and in and around Mosul, about 270 metres. In south Iraq, the Gachsaran Formation ranges from 100 metres at Rumaila to 304 metres at Nahr Umr (Owen and Nasr, 1958). In the Western Desert the formation, according to Al-Naqib (1967), crops out in the area of Qasr, Shaqrah, Dafina, Qars Naba, Qasr Abu Ghar, Al Busayyah, Al Buwaib and Khashmat ibn Hallaf. Extensive outcrops occur also west of An Najaf in the area around Zigla and Gur al Hibari. Westward from the Euphrates River, the Gachsaran Formation becomes generally and gradually less evaporitic and passes into clastic sedimentary rocks laterally and vertically (Al-Naqib, 1967). In south-western Iran, the Gachsaran Formation passes into the Razak Formation in a north-easterly direction towards the interior of Iran (Fig.2-10). The Razak Formation attains a maximum thickness of about 758 metres and consists chiefly of silty marl with subordinate silty limestone (James and Wynd, 1965). On the south-westerly flank of the axis, however, the Gachsaran Formation in south-west Iran decreases in thickness dramatically towards the Arabian Gulf, Saudi Arabia, Kuwait and Rumaila in Iraq (Figs,2-13, 14, 15). In Kuwait, the formation, according to Owen and Nasr (1958), is readily recognisable in Raudhatain between drilled depths of 100 and 200 metres. Further south in Kuwait, the formation has its equivalent in the Zor Formation and in Saudi Arabia the formation has its equivalent in the Dam Formation which is strongly dominated by terrigeneous clastics (Al-Naqib, 1967). As one progresses along the axis northwards to Iraq, the Gachsaran Formation is characterised by repeated

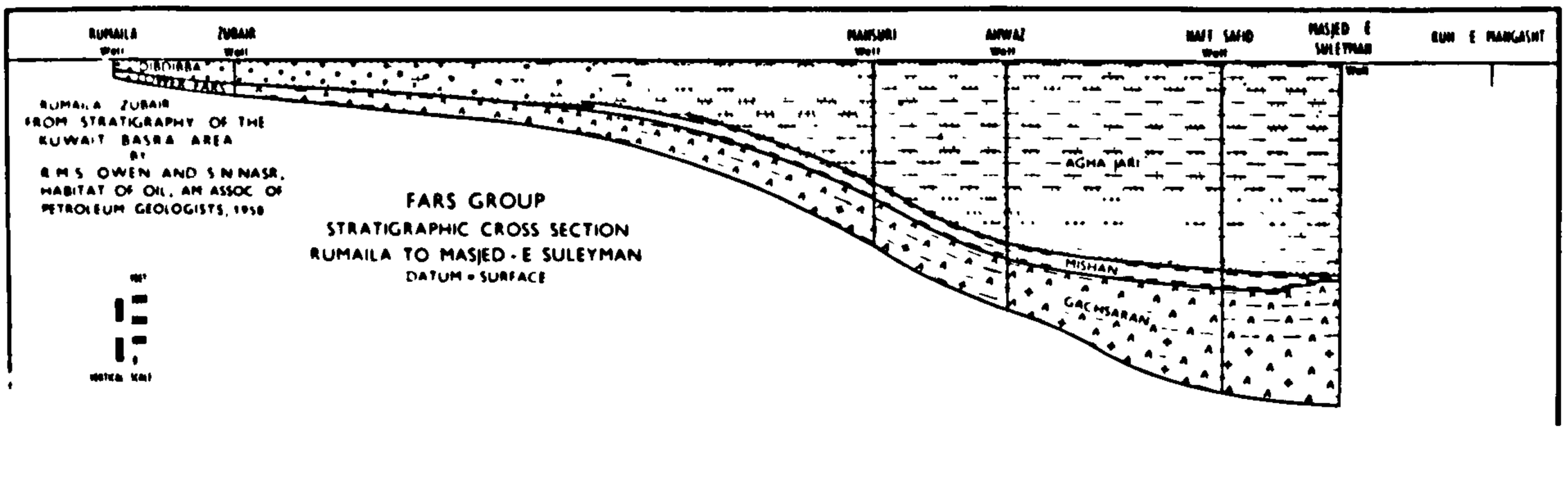

Fig. 2-13

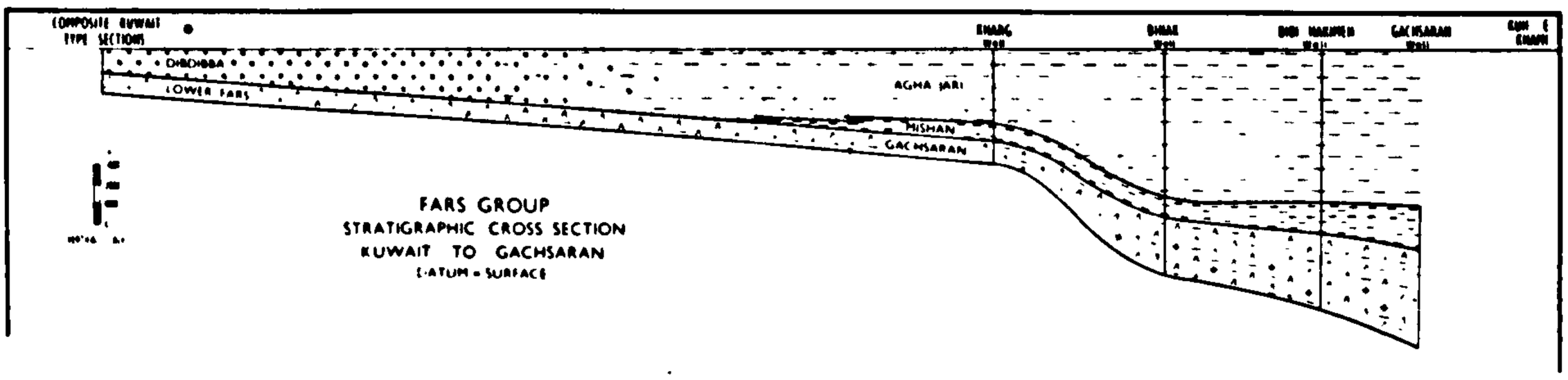

Fig. 2-14

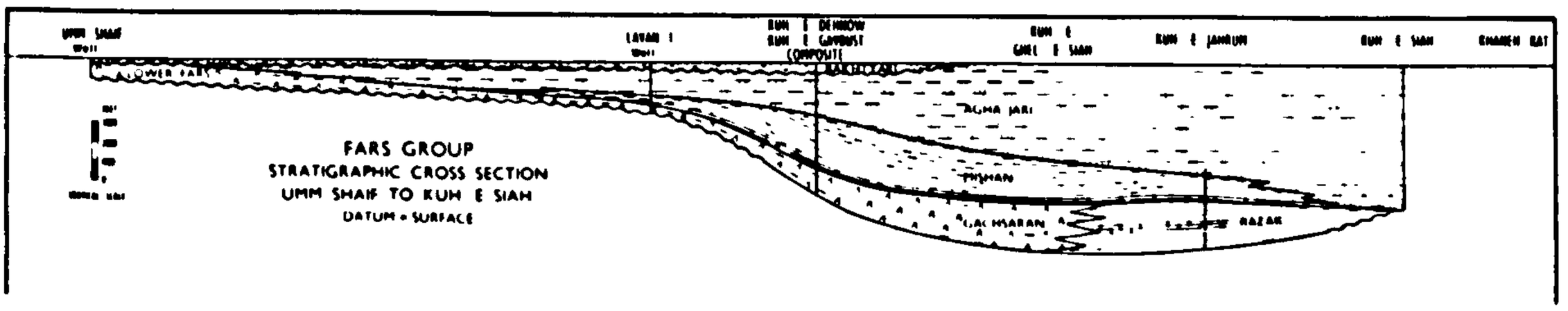

Fig. 2-15

Fig.2-12 Map of the Middle East showing localities referred to in text. The shaded area on the right of the diagram represents the Gachsaran deposit.
The shaded area to the left represents another evaporite deposit (also referred to in text) in the Middle East.


TURKEY
CASPIAN SEA
MEDITERRANEAN SEA
SYRIA
Mosul
Hamadan
Kermanshah
IRAN
Baghdad
Isfahan
JORDAN
IRAQ
Lali
Masjed Suleyman
Ahwaz
Abadan
Basra
Agha Jari
Gachsaran
Shiraz
KUWAIT
ARABIAN GULF
Bandar Abbas
Qeshm Ist.
EGYPT
RED SEA
SAUDI ARABIA
QATAR
TRUCIAL OMAN
0
500km

cycles of marl, limestone and gypsum with individual cycles varying from 3 to 25 metres in thickness. Halite occurs in several cycles in the middle part of the formation, in the central part of the basin in Iraq (Dunnington, 1958). Halite, however, is developed to a much greater extent in south-west Iran (O'Brien, 1957). The upper part of the formation in Iraq is dominated much more by marl than the lower part. Towards the margin of the basin, in a north-northeasterly direction away from the basin axis in Iraq, the thickness and the cyclic pattern of the formation is reduced and mudstones dominate (Fig.2-9). In Shaqlawa, north-east of Iraq (Fig.2-8), the sequence is dominated by marls and limestones, it is possible therefore that this sequence is correlated more with the Razak Formation of Iran than with the Gachsaran Formation. In south-east Turkey, similar Middle Miocene rocks to the Gachsaran Formation occur (Temple and Perry, 1962; Ilhan, 1967).

From the above description, the Gachsaran Formation seems to vary greatly in thickness, even over short distances and along the axis of the basin, and this in part is controlled by the structure. The thickness of the formation at the flanks of the folds differs from its thickness on the crests. In Kirkuk, and over the Kirkuk structure, the thickness of the formation varies from about 305 metres in the north-west to about 610 metres in the south-east (Bellen, et al., 1959). Over part of the Masjid-I-Sulaiman field, stage 1 of the formation is absent, while at Zeloi, 20km. to the northwest, Stage 1 of the formation is well developed reaching its base at 3237 metres (Lees, 1938).

2.7 Thickness variation

The thickness variations of the Gachsaran Formation is thought to be controlled by tectonic factors. Two factors are considered here to be the most important.

1. Variations in thickness of the Gachsaran Formation reflect a

more positive or more negative behaviour of the basin floor, producing areas with a lower or higher rate of subsidence. The underlying control is thought to be block fault movements in the basement. Such a movement is thought to be about the most important contribution to the cyclicity of the formation. This subject is dealt with and discussed in Chapter 8.

2. Salt tectonics:

In order to assess this factor, one has to consider the disharmonic structures and salt tectonics in Iran (O'Brien, 1950) and in Iraq (Dunnington, 1968).

O'Brien (1950; 1957) divided the geological succession in Iran into three groups; this division based purely on tectonic behaviour of rocks was later employed by Dunnington (1968) in Iraq. O'Brien recognised three groups (Fig.2-16):

a) competent group which is made up mainly of massive limestones with intervening calcareous shale and marl formations. This group as a whole reacted competently to tangential compression during the Miocene-Pliocene phases of the Zagros- Taurus Orogeny, and resulted in a very thorough transmission of stress throughout the region (Dunnington, 1968).

b) mobile group comprises the saliferous beds in Kirkuk (salt, anhydrite and marls) or the stage 1 (salt, anhydrite and marls) in Iran. To quote Dunnington "....the original cycles are extremely difficult to recognise within the saliferous beds of Kirkuk because of the high degree of flowage and internal shear that has been imposed upon the salt-bearing beds during stress episodes.". He also added that there has been a wholesale squeezing and translation of the salt and its associated sediments from the north-eastern flank region and crest to high flank positions on the south-western flank of the anticlines. The whole of the Saliferous Beds has been involved in this viscous-fluid translation in some instances,

but in other instances only the upper parts have undergone extensive movement. The underlying Transition Beds have not been involved in incompetent translation movements, nor have the overlying Seepage and Upper Red Beds of the Gachsaran Formation.

c) passive group in both Iraq and Iran has similar components and comprises marls, limestones and anhydrites of the Gachsaran Formation, the marls and limestones of the Mishan Formation, the marls and sandstones of the Agha Jari Formation and the conglomerate of the Bakhtiari Formation (Fig.2-16). The detailed tectonic behaviour of the passive group is discussed in Dunnington (1968).

The development of disharmonic structures in Iran are illustrated in Fig. 2-17, and by Dunnington (1968), which clearly show the effect of tectonics on sequence thickness. The problem of determining the original thickness of the Saliferous Beds in Kirkuk, Iraq, or stage 1 of Iran prior to flowage, is complex and a quantitative assessment of the degree of flowage is difficult (Dunnington, 1968).

2.8 Other Miocene Evaporites in the Middle East

Evaporites occur elsewhere in the Middle East. Equivalents of the Gachsaran Formation are found in central Iran, Azerbaijan and Turkey, and their deposition could be considered contemporaneous with the Gachsaran Formation (Stocklin, 1968). In the Qum area, salt (about 200 m.) immediately overlies the marine marls and limestones of the Qum Formation (Oligocene to Miocene) and is separated from the Qum Formation by a thin basal anhydrite. Further east, in the Great Kawir, the Miocene sequence consists of a cyclic repetition of salt beds alternating with gypsum and silty marl, and individual cycles from base to top consist of salt, gypsum, green-grey gypsiferous silty marl, and red saliferous marl. A marine origin for these deposits has been postulated (Stocklin, 1968). Stocklin also suggested that the Gachsaran basin might have been connected with

Fig. 2-16 Generalised stratigraphic columns for areas of Miocene salt disharmonies in Iran and Iraq (after Dunnington, 1968, fig.3).

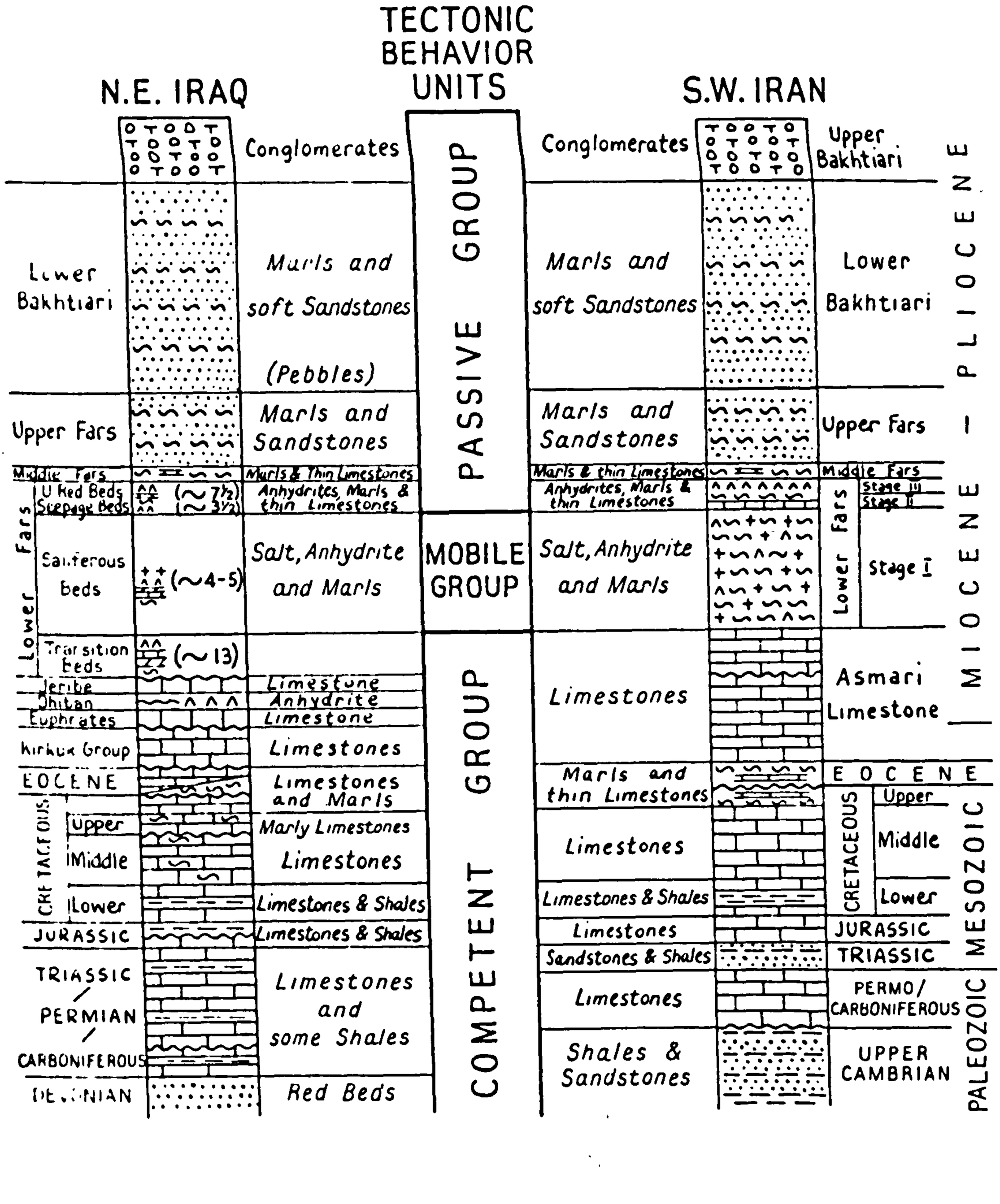
TECTONIC BEHAVIOR UNITS
N.E. IRAQ
S.W. IRAN
Conglomerates
Conglomerates
Upper Bakhtiari
Lower Bakhtiari
Marls and soft Sandstones
(Pebbles)
Marls and soft Sandstones
Upper Fars
Marls and Sandstones
Marls and Sandstones
Middle Fars
Marls & Thin Limestones
Marls & thin Limestones
U Red Beds
Seepage Beds
(~7½)
(~3½)
Anhydrites, Marls & thin Limestones
Anhydrites, Marls & thin Limestones
Stage III
Stage II
Lower Fars
Salt, Anhydrite and Marls
(~4-5)
Salt, Anhydrite and Marls
Stage I
Transition Beds
(~13)
Jeribe
Dhiban
Euphrates
Limestone
Anhydrite
Limestone
Limestones
Asmari Limestone
Kirkuk Group
Limestones
EOCENE
Limestones and Marls
Marls and thin Limestones
EOCENE
Upper
Middle
Lower
CRETACEOUS
Marly Limestones
Limestones
Limestones
Limestones & Shales
Limestones & Shales
Limestones & Shales
JURASSIC
Limestones
JURASSIC
TRIASSIC / PERMIAN / CARBONIFEROUS
Limestones and some Shales
Sandstones & Shales
TRIASSIC
Limestones
PERMO/ CARBONIFEROUS
DEVONIAN
Red Beds
Shales & Sandstones
UPPER CAMBRIAN
COMPETENT GROUP
PASSIVE GROUP
MOBILE GROUP
MIOCENE
PLIOC
PALEOZOIC
MESOZOIC

Fig. 2-17 Development of disharmonic structure in Iran by the folding of the evaporitic Competent Group beneath the Passive Group (after Dunnington, 1968, fig.10).

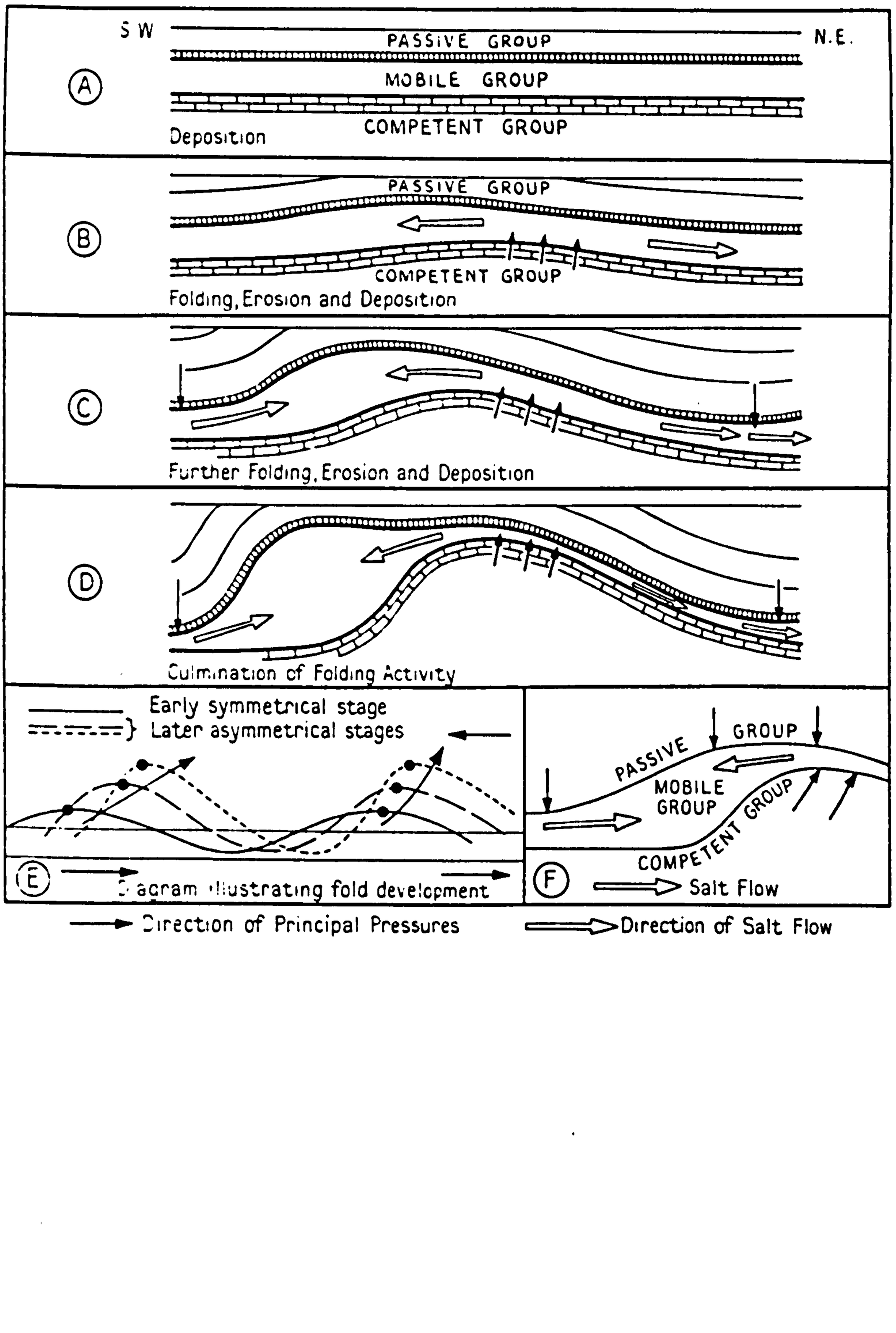
S W
N.E.
PASSIVE GROUP
MOBILE GROUP
COMPETENT GROUP
A
Deposition
PASSIVE GROUP
B
COMPETENT GROUP
Folding, Erosion and Deposition
C
Further Folding, Erosion and Deposition
D
Culmination of Folding Activity
Early symmetrical stage
Later asymmetrical stages
E
Diagram illustrating fold development
PASSIVE GROUP
MOBILE GROUP
COMPETENT GROUP
F
Salt Flow
Direction of Principal Pressures
Direction of Salt Flow

these basins through gaps, north of Bandar Abbas and near Hamadan, or they had a link with the open sea through some channels in Azerbeigan and Turkey. More recently, a connection of the Mesopotamian Basin and the Paratethys through eastern Turkey and Azerbejan has been suggested (Rogl et al., 1978).

Another great basin of evaporite deposition is the Miocene Clysmic Gulf which extended about 200 km. from the Gulf of Suez area, to approximately the southern end of the Red Sea in a north-west - south-east direction (Fig.2-12). This basin was filled by two main groups; the Gharandal Group , which is mainly composed of clastics, conglomerates, sandstones, marls and clays, and an overlying group consisting mainly of gypsum, anhydrite and salt with numerous intercalations of shale and sandstone. In the Gulf of Suez, the Evaporite Group is subdivided into the Kareen, Belavim, South Gharib and Zeit Formations (EGPC, 1964 from Hassan et al., 1970), and the group attains a maximum thickness of 3600 metres. It ranges in age from Aquitanian to Helvetian (Said and Heiny, 1967). Rapid lateral facies changes are a feature of this Evaporite Group, lateral grading of gypsum into gypsiferous clays and marls, and there is a very substantial decrease in thickness when the group is followed laterally. Hassan et al. (1970) concluded that these lateral and sometimes abrupt changes may have been the result of fault movements which resulted in the creation of microbasins with variable salinity gradients. The rock salt is confined to the deeper, more rapidly subsiding parts of the graben, whilst locally on highs and in the marginal near-shore areas, algal reef limestones were found; the gypsum, anhydrite, dolomites and marls occurred between these extremes (Heybroek, 1965). Heybroek also concluded that the whole of the Clysmic Gulf and Red Sea formed an inland evaporite basin, almost closed off by a bar in the north from the Mediterranean, and completely closed off by a land barrier in

the south from the Indian Ocean during the deposition of this group. In the Red Sea area, these Miocene evaporite outcrops are restricted to the coastal belts of Sudan, Eritrea, Yemen and Saudi Arabia (Heybroek, 1965). In Sudan, the Maghersen Formation (Middle Miocene), 1435 metres thick, is composed of 465 metres of salt overlain by a succession of gypsum-anhydrite interbedded with sandstones (Heybroek, 1965).

Desiccation periods persisted throughout the Mediterranean during the Messinian stage (Late Miocene) which led to thick deposits of evaporites (Hsü *et al.*, 1978).

CHAPTER 3

SULPHATES

Petrology, sedimentology and geochemistry

3.1 Introduction

3.2 Gachsaran evaporites

3.3 Gypsum-anhydrite structures

3.4 Petrography of the Gachsaran sulphates

3.5 Secondary gypsum

3.6 Gypsum veins

3.7 Celestite

3.8 X-ray analysis

3.9 Summary

CHAPTER 3

SUPHATES

3.1 Introduction

At outcrop, the sulphate horizons of the Gachsaran Formation are seen as gypsum but at depth anhydrite is present. The origin of anhydrite, whether it is primary or secondary after gypsum has been a matter of some controversy and speculation. At the present time, gypsum crystals are a common precipitate in the intertidal-supratidal sediments of semi-arid coastlines. For anhydrite, however, there are few known marine occurrences, save for the now well-documented supratidal nodular and enterolithic anhydrite of the Trucial Coast sabkhas, Arabian Gulf. There, the anhydrite forms first from the dissolution of gypsum and then with continued evaporation and an increase in sediment-porewater salinities anhydrite is precipitated directly within the sediment (Butler, 1970). The high annual mean temperature (above 22°C) of the Trucial Coast, together with the very high seasonal temperatures (above 35°C) are thought to be the prime factor in this anhydrite precipitation. Pseudomorphs of anhydrite after gypsum have been identified in deeply buried evaporites (Schaller and Henderson, 1932; Kerr and Thompson, 1963; and others). It is also a matter of observation that gypsum converts into anhydrite when buried at depths in excess of 850 to 1220 m., and that the opposite takes place with the formation of secondary gypsum when exhumation brings anhydrite near to the surface again (Deer et al., 1962; Murray, 1964; Hardie, 1967). For the most part secondary gypsum rocks are restricted to within 100 m. of the surface, but locally they are found at depths in excess of 1000 m. (Murray, 1964). Hydration of anhydrite to gypsum starts near aquifers and along fault planes (Deer et al., 1962). On a microscopic scale, hydration may proceed from cleavage planes, fissures and cracks (Goldman, 1952; Ogniben, 1957; Ham, 1962; Holliday, 1967). Hydration may also take place around the edges of anhydrite nodules, occurring within sediment (this work). Gypsum is stable below 42°C, where it is less soluble and

can therefore be precipitated or replace other minerals (Posnjak, 1938; MacDonald, 1953). Several authors have argued that the concentration of sodium chloride in the host solution lowers the transition temperature of gypsum to anhydrite (MacDonald, 1953; Dickson*, 1973). Zen (1965), after re-calculating results of previous workers, put the transition temperature at $46^{\circ} \mp 21^{\circ}C$. This was well supported by the experiments carried out by Hardie (1967) on the gypsum-anhydrite equilibrium.

The hydration of anhydrite to gypsum should theoretically bring about a substantial increase in volume. This was calculated by comparing the unit-cell volumes of anhydrite and gypsum and found to be 63% (Allen, 1971). In practice, however, there is often no indication of such a volume increase (Gaurtner, 1932; Goldman, 1952; Mcwhae, 1953; Holliday, 1967, 1970; Mossop and Shearman, 1973). It has been suggested, therefore, that the excess volume of calcium sulphate was removed during hydration (Goldman, 1952; Gaurtner, 1932; Bundy, 1956; West, 1965; Holliday, 1967; Mossop and Shearman, 1973). The water supply for the hydration of anhydrite has three possible sources; connate water buried with evaporitic sediments, water introduced from underlying water-bearing formations and surface water moving into the anhydrite rocks as they are uplifted (Mossop and Shearman, 1973; Burgess and Holliday, 1974). The processes by which anhydrite converts into gypsum are reviewed by Holliday (1970) and Mossop and Shearman (1973).

3.2 Gachsaran Evaporites

In this section, the petrology and structures of the sulphate rocks (gypsum/anhydrite) are described. By comparison with ancient and recent analogues, a model for their formation is proposed. For the sake of completeness, a small section on halite is given.

A. Halite

Halite is absent at outcrops, but is present at subsurface and is

* Dickson (1973) is in Mossop and Shearman, 1973.

reported from boreholes from the centre of the basin (Jones et al., 1949; Bellen et al., 1959; Dunnington, 1968; Stöcklin, 1968; Gill and Ala, 1972). The halite is mostly concentrated in the lower to middle part of the Gachsaran Formation in northern Iraq and attains a maximum thickness of 45 metres in Naft Khaneh (Jones and Hudson, 1949). Lack of information on the halite textures hinders the identification of the depositional environment. Polyhalite was reported to occur in association with the halite in south-western Iran by Stöcklin (1968). Halite can be precipitated subaerially in sabkha situations (e.g. Shearman, 1970) and subaqueously in shallow or deep water environments (e.g. King, 1947). It is most probable that the halite of the Gachsaran was deposited at a time when the Mesopotamian basin was partially or completely cut off from the world's ocean. The reported polyhalite occurrence from south-western Iran may suggest that at least in some places, the basin was desiccated leading to the precipitation of potash salts, since the latter typically form subaerially in sabkha or playa situations towards the end of an evaporation cycle.

B. Gypsum and anhydrite

These rocks constitute about 70% of the Gachsaran Formation in the central parts of the Mesopotamian basin. Towards the margins, they are, however, less well devloped and the formation is dominated by the marl/claystone lithofacies. It is worth noting that the gypsum beds are sulphur-bearing in some parts of Iraq, especially in Makhul near Fatha Gorge and Mishraq. Where sulphur is developed, gypsum beds have been converted into a very cavernous limestone.

3.3 Gypsum-anhydrite structures

The evaporite rocks of the Gachsaran Formation exposed in northern Iraq consist of nodular, structureless and bedded gypsum. At depth, as seen in cores from Mishraq, south of Mosul (Fig.2-1), and recorded by

Dunnington (1958) and Bellen et al. (1959) from other borehole locations, the sulphate is anhydrite, with the same macro-structures as gypsum at outcrop. There are basically two types of nodular sulphates, a primary and a secondary variety. These two types are differentiated according to their different types of matrix and origin.

3.3.1 Primary nodular structure

Sulphate nodules are composed either of gypsum or anhydrite with stringers of calcite and clay between nodules (Fig.3-1). They are spherical to flattened in the plane of the bedding. The nodules typically range in diameter from 1 to 3 cm., but do reach 15 cm. In any one nodular horizon, nodules attain different shapes and sizes (Fig.3-1). Some of the larger nodules (3 cm. in diameter), as defined by the matrix surrounding them, show internal structures of a mosaic to wispy nature. Secondary gypsum comprises these structures at outcrop and commonly anhydrite in cores. The spacing of nodules and the degree of packing are the main features used in their terminology (Maiklem et al., 1968; Holliday, 1971). In some cases, thin beds of nodular anhydrite (5 to 20 cm. thick) or scattered, isolated nodules of anhydrite occur within or towards the tops of limestone beds. Laths of anhydrite commonly protrude from the nodules into the surrounding limestone (Fig.3-2). Occasionally some of these nodular anhydrites have been completely replaced by calcite spar and sulphur (Fig.3-3).

3.3.2 Secondary nodular structures

These nodules are composed of anhydrite and they attain different shapes and sizes (Fig.3-4b,c). The shapes of the smaller nodules are spherical, ovate and rectangular but become more irregular as they decrease in size. These nodules range in diameter from 1 mm. to 6 cm. with the larger varieties being mostly rectangular in section. The matrix between the nodules ranges in thickness from .02 to .5 cm. and is composed of

Fig. 3-1 A close-up of the common nodular nature of the outcropping gypsum in the Gachsaran Formation. At depth the nodules are of anhydrite. Note the composite structure of some of the larger nodules. Bashiqa, Iraq.

Fig. 3-2 Laths of anhydrite protruding from the nodules into the surrounding limestone. These laths are primary. Peel Mishraq, Iraq.

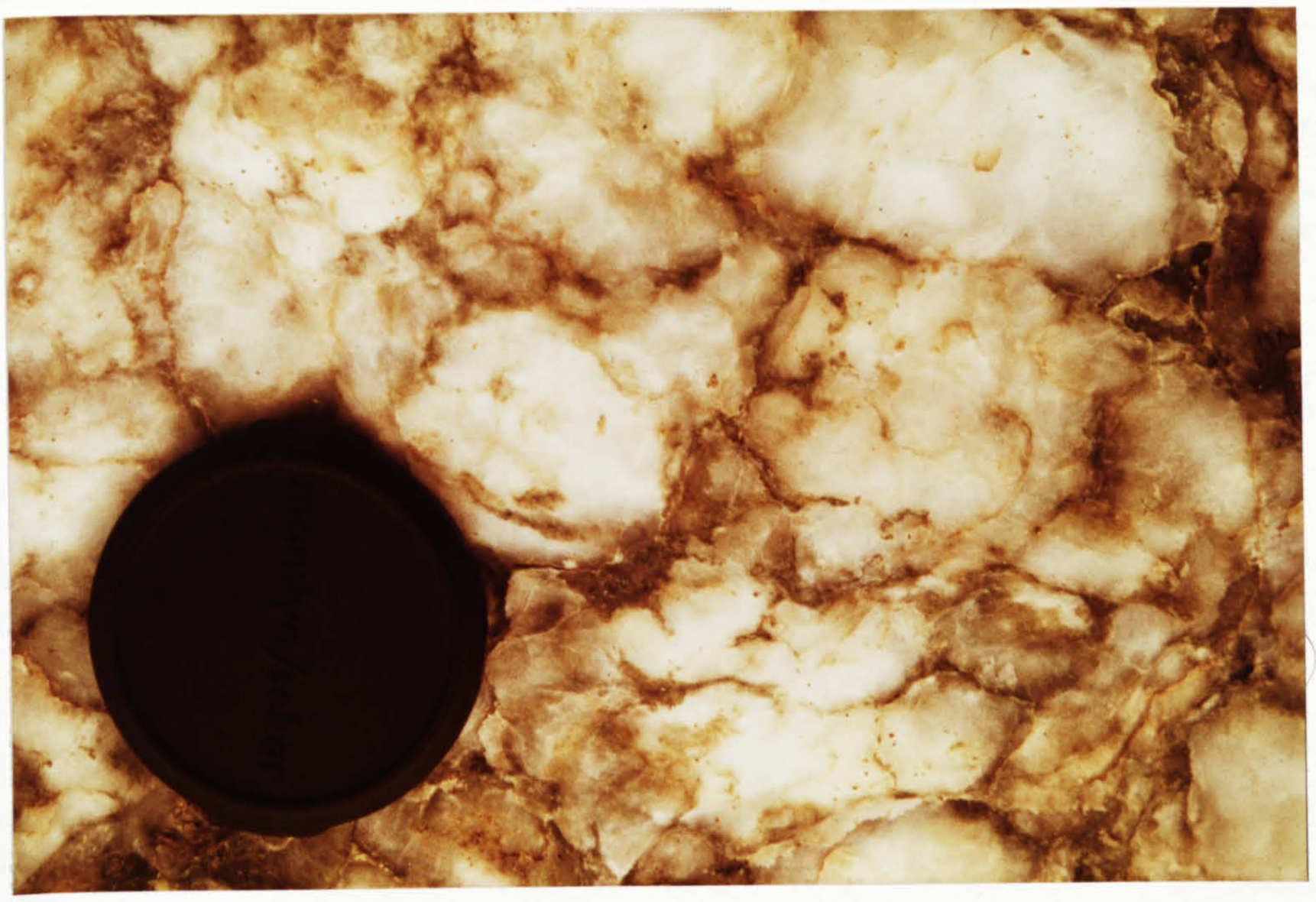


0.17mm.

Fig. 3-3 Nodular anhydrite replaced completely by sparry calcite and sulphur. The sulphur is in the middle of the photograph (dissolved). Slice crossed nicoles, Mishraq, Iraq.

Fig. 3-4 A, structureless anhydrite with wisps of sediment. B, nodular anhydrite. The matrix between the nodules is of alabastrine gypsum. C, smaller nodular structure. D, structureless alabastrine gypsum with wisps of sediment. Mishraq, Iraq.

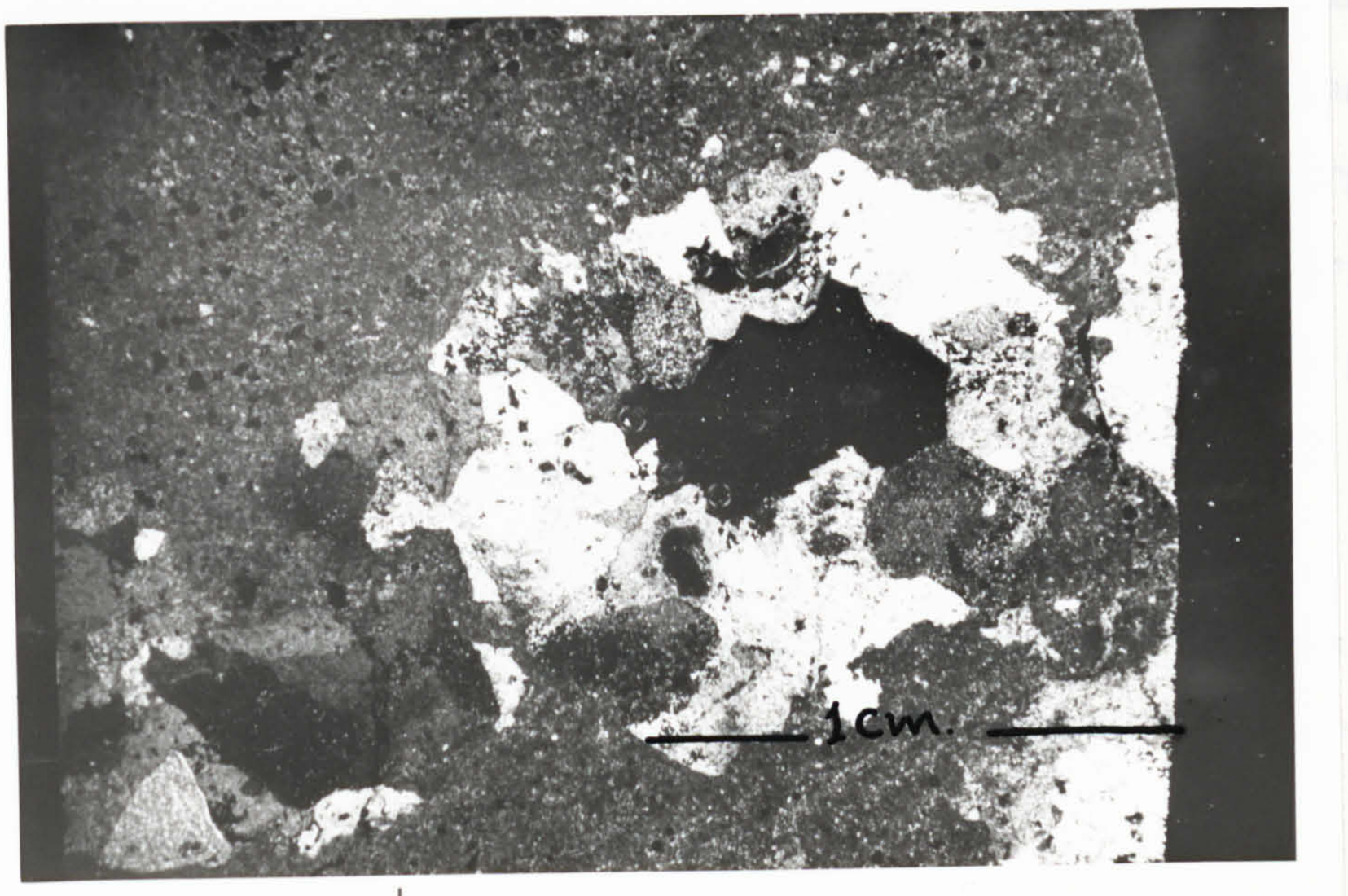
1cm.

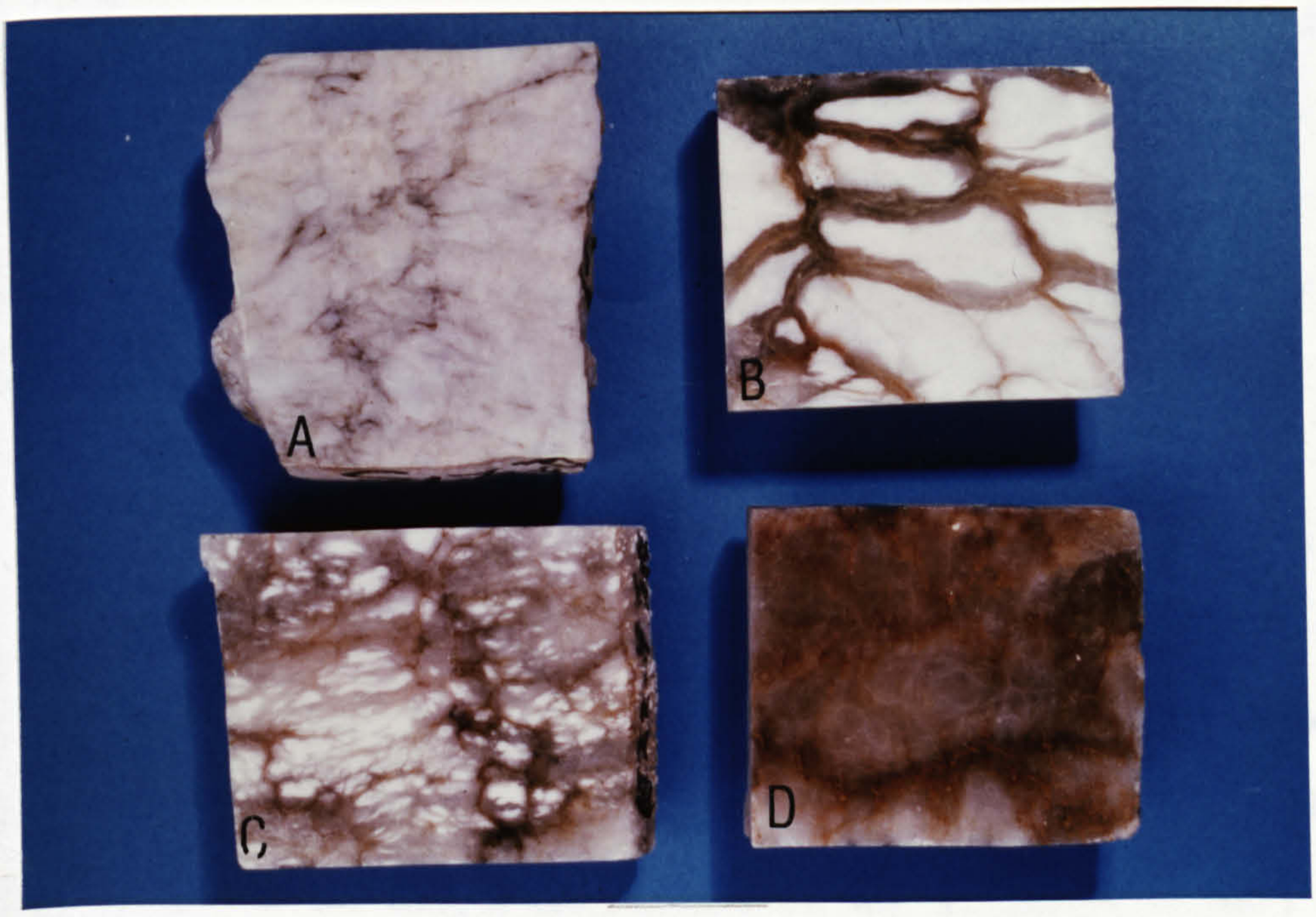
A
B
C
D
8cm.

alabastrine secondary gypsum together with streaks of sediment; quartz, silt and clay, carbonate grains and micrite, and organic matter (Fig.3-6). Very thin streaks of sediment are also present within the individual anhydrite nodules. In some samples, alabastrine secondary gypsum is found associated with these thin streaks of sediment, thus differentiating individual anhydrite nodules into segments (smaller nodules)(Fig.3-6). Such features were found within thick anhydrite beds in cores from the Mishraq area about 190 m. below the surface.

3.3.3 Wispy to structureless sulphates

Some sulphate beds are massive with no nodular structure. However, they do contain wisps and streaks of sediment. These beds may be composed of anhydrite or gypsum (Fig. 3-4a,c, 5a,f).

3.3.4 Bedded sulphates

In thicker developments of sulphate beds, the nodular gypsum is overlain by a bedded variety (Fig.3-7). These beds consist of an alternation of pure, white alabastrine gypsum and less pure, clayey or marly, grey to green alabastrine gypsum with traces of organic matter. The bedding is on the scale of 2 to 5 cm. and is laterally continuous over many metres of outcrop. The bedding is rarely planar, it is generally slightly irregular, with low undulations, occasional contortions and buckles. These bedded sulphate rocks are well represented in the Bashiqa area (Fig.2-1).and the area south of Mosul.

3.3.5 Interpretations

Although nodular and bedded gypsum-anhydrite can form in deep water environments (Dean et al., 1975), the features and context of the Gachsaran sulphates in northern Iraq are consistent with sabkha deposition. In particular, the nodular character of the gypsum-anhydrite is very reminiscent of the anhydrite nodules of the Abu Dhabi sabkha, Trucial Coast. A sabkha origin is also indicated by the lithofacies of the

Fig. 3-5 Stages leading to the development of secondary nodular anhydrite structure. (a). Water percolates through the weak zones in the anhydrite (sediment wisps) hydrating the anhydrite along these planes into secondary alabastrine gypsum. This will lead to the formation of anhydrite mosaic (b). As these planes widen, nodular anhydrite structure would result (c). Further hydration would differentiate the nodular structure into nodular mosaic (d). This will lead to smaller structure (e) and then further hydration will result in the complete transformation of anhydrite to gypsum. The end result is a wispy secondary alabastrine gypsum. (f).

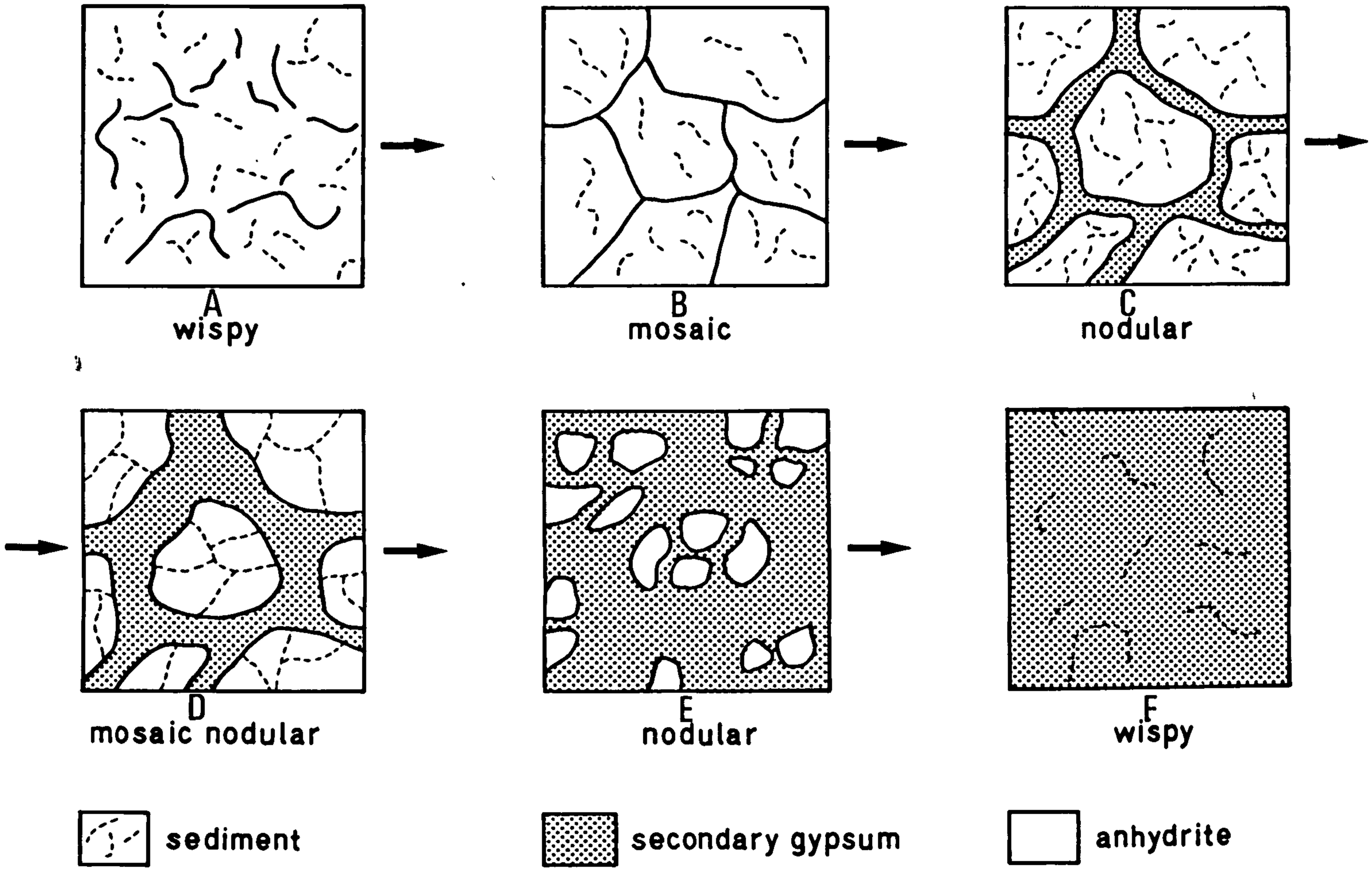

EVOLUTION OF SECONDARY ANHYDRITE NODULES

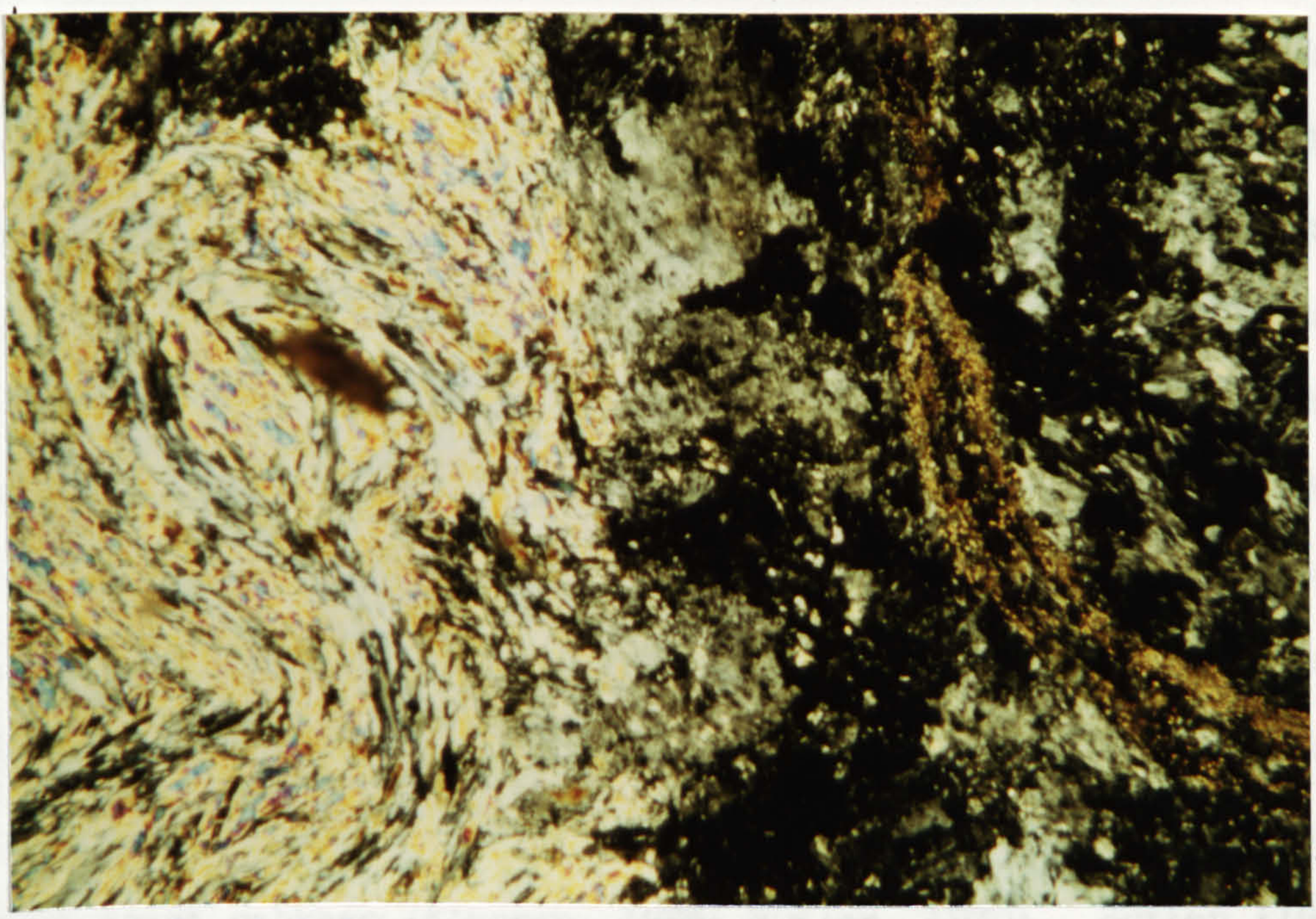

Fig. 3-6 Photomicrograph of secondary nodular anhydrite. Note the thin streak of sediment in between two anhydrite nodules and surrounded by alabastrine secondary gypsum. Slice. crossed nicoles, Mishraq, Iraq.

sediments immediately underlying the sulphates, especially the stomatolitic and cryptalgal limestones of intertidal origin (Shawkat and Tucker, 1978) and the limestone with calcite pseudomorphs after gypsum of the high intertidal. (see Chapters 5 and 6).

Several processes have been suggested for the origin of primary nodular anhydrite; replacement of gypsum crystals and rosettes (Kerr and Thompson, 1963; Murray, 1964; Butler, 1970), nodular anhydrite growth in the sediment by displacement (Butler, 1965; Kinsman, 1969) and the interstitial precipitation of anhydrite within supratidal sediments (Kinsman, 1966; Rooney and French, 1968). It is possible that more than one process may be involved in the formation of one anhydrite nodule. It is also possible that different processes and diagenetic events may generate similar nodules. The anhydrite nodules of the Gachsaran resemble those forming in recent environments, especially those forming in the Trucial Coast sabkhas (Kinsman, 1966; Butler, 1970). Butler (1970) has suggested that the size of the anhydrite nodules is directly proportional to the size of the parent gypsum crystals. The close correspondence between the smaller anhydrite nodules of the Gachsaran (1-3 cm. in diameter) and the larger discoidal gypsum crystals (2 cm. in diameter) of the Abu Dhabi sabkha (Butler, 1970) is striking, and these smaller nodules may thus have had a gypsum precursor.

It is possible that some larger nodules are compound, having formed by the coalescence of a number of smaller nodules. The packing of the anhydrite nodules could be attributed, at least in part, to the packing of the crystals in the original gypsum mush (Holliday, 1971). In recent sabkhas, the pseudomorphs of anhydrite after gypsum lose their shape with time, as a result of the 'toothpaste' consistency of the sediment and the precipitation of further primary diagenetic anhydrite with no gypsum precursor. The latter precipitates between the anhydrite pseudomorphs

after gypsum crystals to form larger ovoid and variously shaped anhydrite nodules (Kinsman, 1969). Through the processes of packing of the initial gypsum mush (Holliday, 1971) which is replaced by anhydrite and later precipitation of diagenetic anhydrite between the anhydrite pseudomorphs after gypsum, a number of anhydrite nodules may coalesce. The replacing and displacing behaviour of the anhydrite laths between adjacent nodules (Fig.3-2) is in accordance with this fact.

The secondary nodular structures have no recent analogue. This is believed to be mainly due to the fact that these secondary structures were the result of later diagenetic processes. The formation of these nodular structures is envisaged as follows:

1. Water percolates through thin sediment streaks or wisps, as these constitute porous planes within the anhydrite (Fig. 3-5a,b).The water percolation leads to the hydration of the anhydrite along the sediment streaks and wisps into secondary alabastrine gypsum. Eventually, this results in the differentiation of the anhydrite into a mosaic structure (Fig. 3-5b)

2. Along these planes, now occupied by sediment and alabastrine secondary gypsum, water continues to percolate, and alabastrine gypsum continues to replace anhydrite. The widening of these partition planes by more replacement of anhydrite eventually leads to a secondary nodular anhydrite structure (Fig.3-5c). At a later stage, very thin streaks of sediment still present within some secondary nodules, now act as pathways for water movement and bring about further gypsification of anhydrite. This further divides individual nodules into yet smaller nodules separated by alabastrine secondary gypsum (Fig. 3-5d,e).

3. This cycle will eventually come to an end when all the anhydrite is replaced by secondary gypsum. The product of this hydration of anhydrite is thus massive secondary gypsum with sediment wisps (Fig. 3-5f).

The bedded alabastrine gypsum of the Gachsaran Formation is regarded as a replacement of bedded anhydrite. This bedded sulphate may be similar to enterolithic anhydrite of the Abu Dhabi sabkhas, forming in a high supratidal setting (Butler, 1970). Bedded anhydrite can also form as basinal varves (Dean et al., 1975) or as coalescing nodules (Shearman and Fuller, 1969). In ancient sequences, distinction between beds of laminated anhydrite and beds of packed nodules may prove essential in differentiating the mode of origin of bedded anhydrite (Kerr and Thompson, 1963). With the Gachsaran case the planar to irregular nature of the layering and the nodular nature of the bedding suggest otherwise. An alternative is that it is analogous to algal mat-gypsum mush deposit. In the Abu Dhabi sabkha (Butler, 1970) and in the Laguna Madre (Masson, 1955; Kerr and Thompson, 1963) algal mats with scattered gypsum crystals alternate with gypsum-crystal mush. Continued precipitation of gypsum and interstitial anhydrite can be expected to replace the algal-mat layers, producing a clayey, organic-rich gypsum bed.

Whatever the exact mode of origin of the bedded sulphate, its occurrence above nodular sulphate indicates formation in a more landward situation. It is suggested that it formed either in or around lagoons or lakes in a back-sabkha setting. The high Na_2O and K_2O contents of the bedded sulphates in comparison with the nodular and structureless varieties (Table 3-1)is consistent with formation in a more highly evaporite, back-sabkha lagoon. These lagoons would have formed in areas of more rapid subsidence within the sabkha plain, but sufficiently distant from the open sea, so that higher salinities could be maintained. Similar layered anhydrite has been described from the Arab-Hith anhydrite of Jurassic age in Saudi Arabia (Ieeder and Zeidan, 1977).

3.4 Petrography of the Gachsaran Sulphates - anhydrite textures.

Four main textural types are distinguished within the Gachsaran

TABLE 3-1

Sample No.	Rock	Na_2O ppm	K_2O ppm	Zn ppm	Fe_2O_3 ppm	MnO ppm	MgO ppm
22-4-18	nodular anhydrite	225	50	-	260	<9	557
P9-17	nodular anhydrite	293	109	18	230	<9	975
22-4-4	nodular gypsum	59	64	13	83	9	218
P9-1	nodular gypsum	102	206	12	289	17	543
P9-4	nodular gypsum	33	187	32	326	17	490
P9-5	nodular gypsum	29	57	45	113	<9	310
226	nodular gypsum	79	81	13	54	<9	92
73	bedded gypsum	133	499	264	1537	36	3097
43	nodular gypsum	81	83	38	55	17	4720
17	bedded gypsum	216	882	16	2136	38	4786
xa	nodular gypsum	67	116	< 3	133	<6	905

Fig. 3-7 Nodular gypsum overlain by a bedded variety. Note the low undulations, contortions and buckles of the bedded gypsum. Bashiqa, Iraq.

Fig. 3-8 Secondary gypsum crystals replacing subfelted lath texture anhydrite. Note how the crystal boundaries and cleavage planes of the gypsum crystals are accentuated by the concentration of organic matter and sediment along them. The gypsum crystals are full of subfelted anhydrite relics. Slice. crossed nicoles, Mishraq, Iraq.

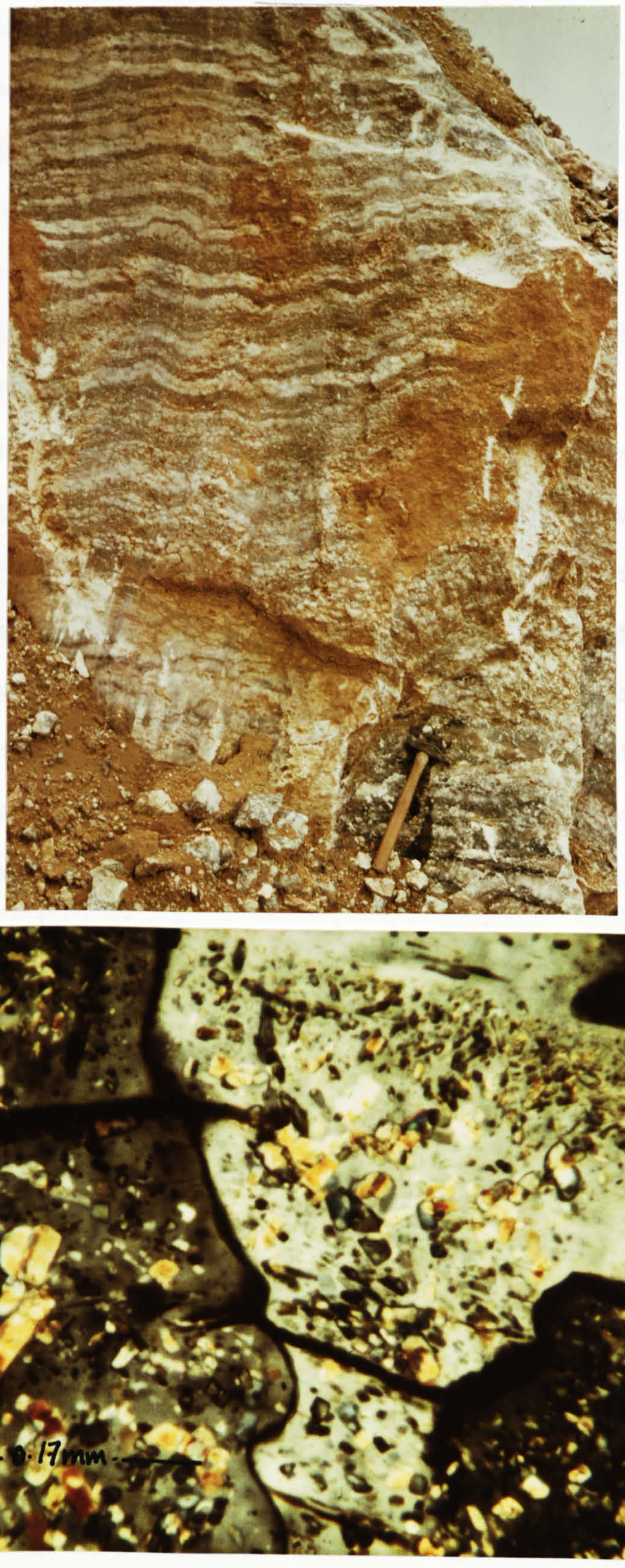
0·17mm

anhydrite rocks from borehole samples; 1) subfelted texture, 2) felted-lath texture, 3) fibroradiate and pile-of-bricks lath textures, and 4) blocky-granular texture.

1 - The subfelted texture has been referred to as aphanitic by Holliday (1966, 1973), Arthurton and Hemingway (1972) and others. This texture consists of mosaics of microcrystalline, rounded, irregular, rectangular, subhedral to anhedral anhydrite crystals. These crystals have an average diameter of about 4 μ. The subfelted texture is often interrupted by areas which consist of larger irregular and granular to lath-shaped crystals of anhydrite. These elongate crystals often have a preferred orientation. Also, isolated large rectangular to lath-shaped anhydrite crystals occur scattered within the subfelted mosaic. These crystals, however, have no preferred orientation and often occur cross-cutting the subfelted laths and each other. Organic matter and sediment are found dispersed between the anhydrite crystals giving the anhydrite a brownish appearance. In some samples the subfelted anhydrite crystals occur in isolated nodules of anhydrite set in a secondary alabastrine gypsum matrix, which has large prominent crystals. The secondary gypsum crystal boundaries and cleavage planes are accentuated by the concentration of organic matter and sediment along them (Fig.3-8).

2 - Felted-lath texture consists of lath-shaped crystals of anhydrite. They range in length from 30 to 400 μ. and width from 4 to 12 μ. The laths may sometimes reach a length of 800 μ, and a width of 200 μ. These laths are sometimes parallel to each other but they may form wavy or folded patterns (Fig.3-9). The laths also occur with no obvious orientation, and in many instances they cross-cut each other (Fig.3-10). The laths are sometimes found packed together with indistinguishable boundaries, which may form large areas of massive anhydrite. In the latter case the laths can only be distinguished through rotation

Fig. 3-9 Felted-lath texture. Lath-shaped crystals of anhydrite forming a wavy or folded pattern. Slice. crossed nicoles, Mishraq, Iraq.

Fig. 3-10. Felted-lath texture with no obvious orientation. Note the largest lath in the middle of the photomicrograph being bent. Slice. crossed nicoles, Mishraq, Iraq.

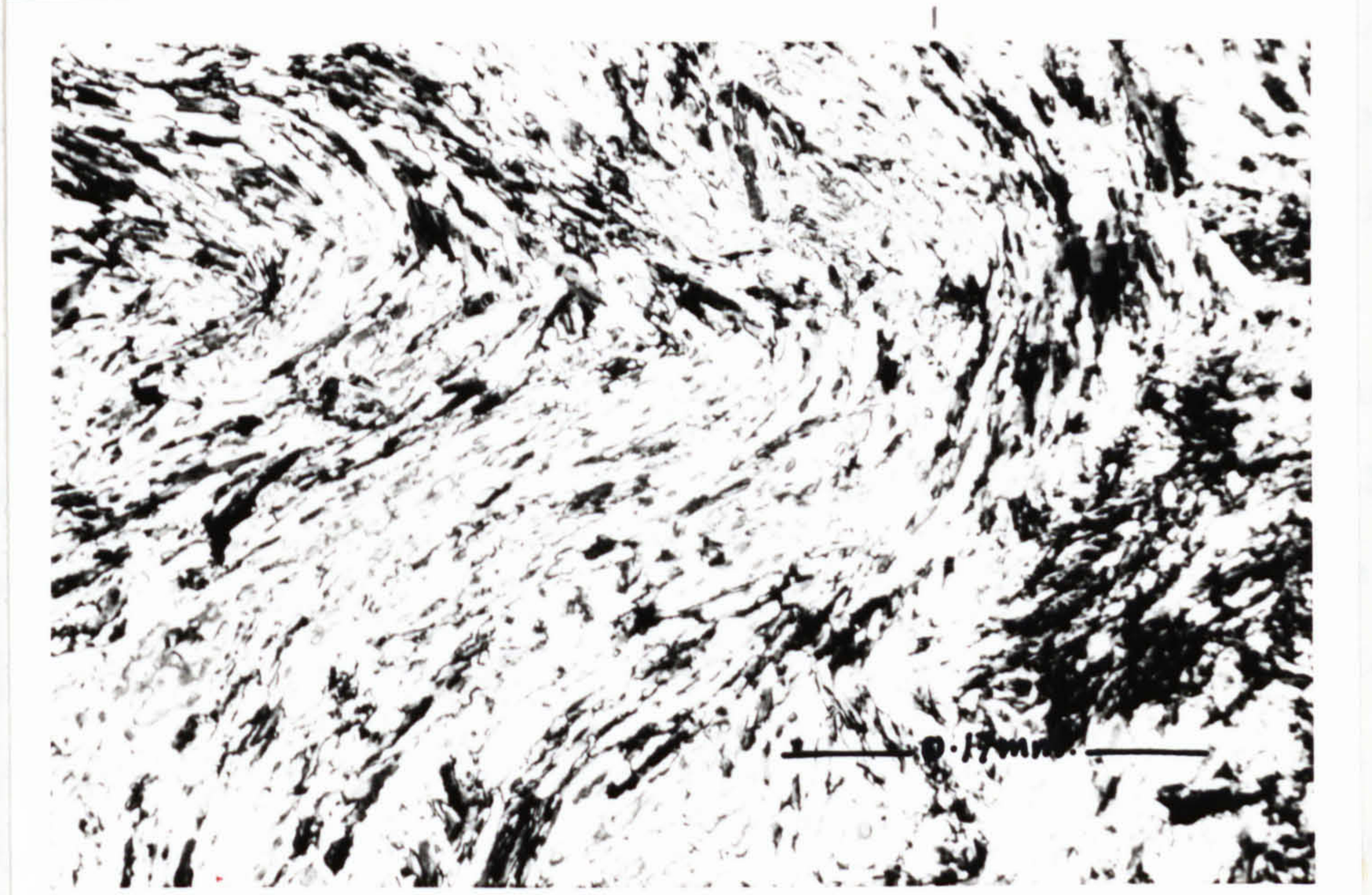
0·1mm

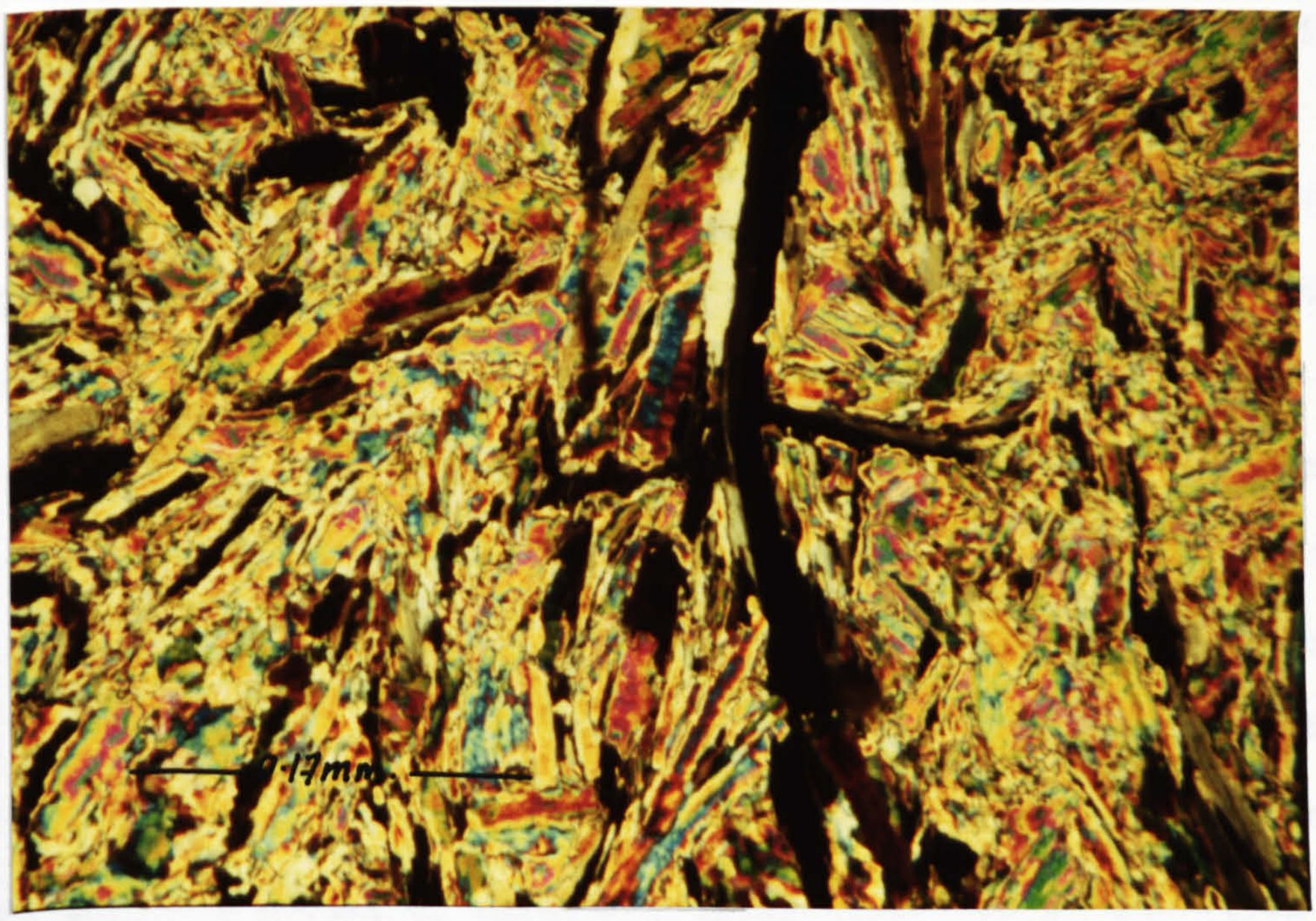
0·1mm

of the microscope stage, noting that the laths extinguish in different positions. Some of the larger laths are bent (Fig. 3-10). Some of the laths are primary. These laths project from the nodules replacing and displacing the surrounding carbonate sediment. Similar laths were described from the Carboniferous of Spitsbergen by Holliday (1968).

3 - The fibroradiate and pile of bricks lath textures. These textures are composed of large laths of anhydrite. These laths have a maximum length of 2.5 mm. and a maximum width of 0.2 mm. (Fig.3-11). When these laths are found packed together, they form what is known as the pile of bricks texture (Brown, 1931). These laths sometimes form radiating groups referred to as fibroradiate texture (Stewart, 1949) (Fig.3-11). Whatever texture these laths form, they almost always have a very high concentration of organic matter along their cleavage planes and surrounding boundaries.

4 - The blocky anhydrite texture is mostly found associated with the pile of bricks texture. This texture is composed of large blocky, rectangular to lath-shaped crystals of anhydrite, which are packed together very closely to form large discrete areas of anhydrite (Fig. 3-12).

3.4.1 Interpretation of anhydrite fabrics

Dehydration of gypsum results in the formation of subfelted or aphanitic anhydrite (Holliday, 1973). The origin of lath texture anhydrite is however more of a problematic matter. There is, however, little doubt as to the primary origin of laths projecting from the nodules into the surrounding matrix (Fig.3-2). The presence of laths in such a context indicates that the anhydrite nodules formed within the host sediment before consolidation (Holliday, 1968). No positive textural distinction was found between primary laths and secondary lath crystals forming as a result of direct re-crystallisation of subfelted anhydrite. The presence of lath to rectangular anhydrite suggests a re-crystallisation

Fig. 3-11 Larger laths of anhydrite. In this photomicrograph they form radiating groups referred to as fibroradiate texture. Slice. crossed nicoles, Mishraq, Iraq.

Fig. 3-12 Blocky textured anhydrite forming a discrete area of anhydrite. The blocky to lath-shaped crystals of anhydrite are still recognisable. Slice. crossed nicoles, Mishraq, Iraq.

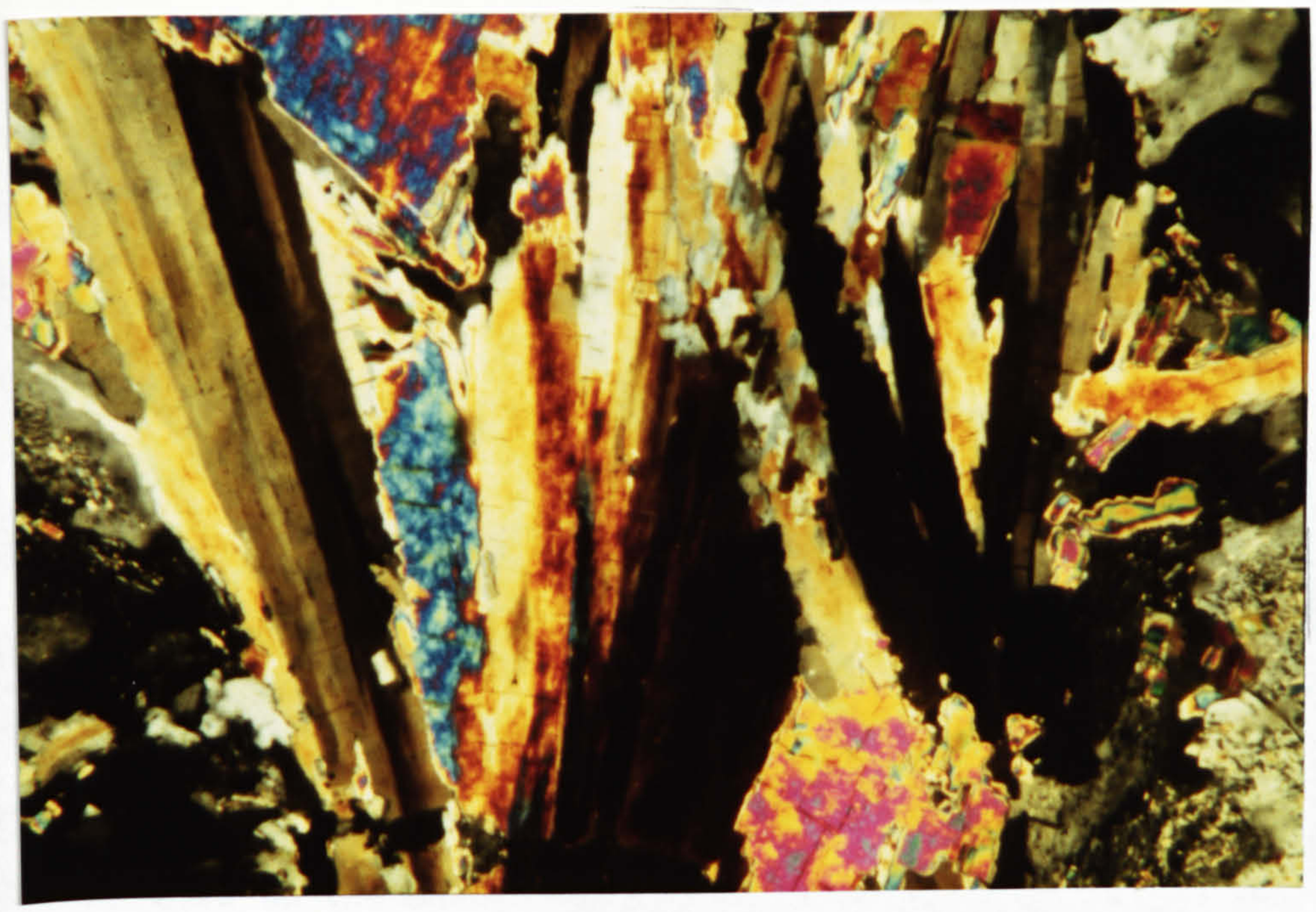

0·6mm.

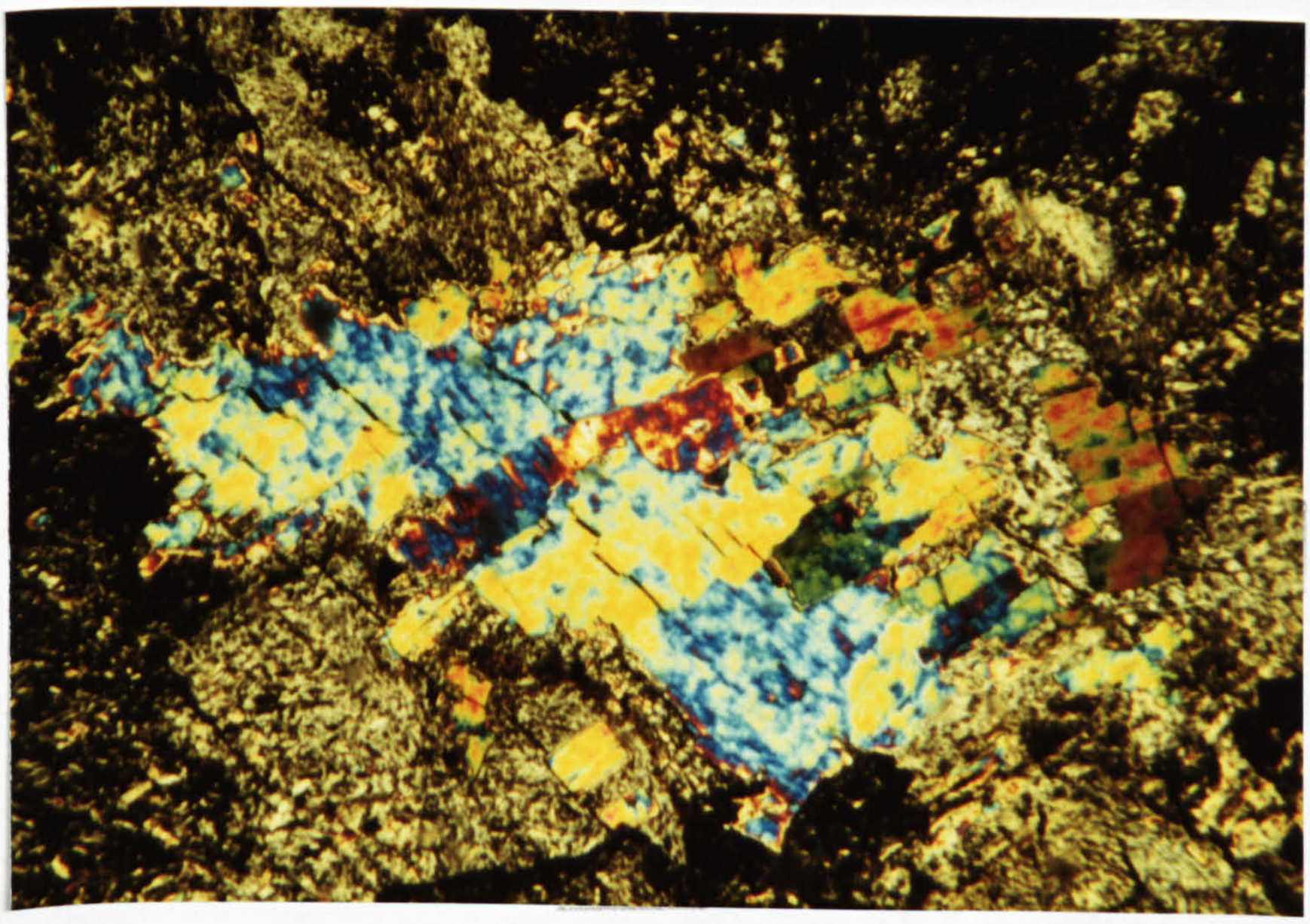

0·6mm.

form (secondary) for some of the laths. Further re-crystallisation of these laths may yet form larger laths and rectangular crystals of anhydrite, which may lead to the formation of the pile of bricks or the fibroradiate textures. Laths are bent or even broken and this may be caused by overburden pressure.

3.5 Secondary gypsum

Terminology and classification

Ogniben (1957) was the first to classify secondary gypsum rocks, from the Miocene Sulphur Series of Sicily, into two main types: porphyroblastic secondary gypsum and alabastrine secondary gypsum. Holliday (1967, 1970) further subdivided the alabastrine secondary gypsum into three varieties. The Gachsaran secondary gypsum rocks show many petrographic similarities to the secondary gypsum rocks described previously by Bundy (1952), Ogniben (1957), Forbes (1958), Ham (1962), West (1964, 1965), Holliday (1967, 1970), Mossop and Shearman (1973) and others. The similarities and dissimilarities of the Gachsaran secondary gypsum rocks with ancient analogues has resulted in the need for a slight adjustment to the petrographical classification proposed by Holliday (1970). Four types of alabastrine secondary gypsum are recognised here.

3.5.1 Alabastrine secondary gypsum

Type A - At first sight, this texture is seen under cross-polars to be composed entirely of discrete gypsum crystals 4 μ in diameter. On closer inspection, however, the rock is seen to consist of much larger ill-defined areas (Fig.3-13). In each of these areas the small gypsum crystals are orientated in a direction different from the orientation of crystals in an adjacent area (Fig.3-13). On rotating the stage under cross-polars, the areas extinguish uniformly. This feature could indicate that the gypsum crystals are actually subcrystals of large crystals with lattice linkages as suggested by Mossop and Shearman (1973) for similar

large gypsum crystals. When the stage is further rotated, the gypsum subcrystals break down and no discrete crystals as such are recognised. This textural type of gypsum was found replacing different textural types of anhydrite; the abundant relics of anhydrite within this secondary gypsum may reflect the textural type of the parent anhydrite. Mostly, however, this gypsum was seen replacing large lath and blocky types of anhydrite. The gypsum subcrystals replacing the anhydrite laths line themselves parallel to the cleavage planes of the anhydrite laths they are replacing (Fig.3-14,15). These boundaries are very distinctive due to the concentration of organic matter along them. This texture is often seen in thin section adjacent to and replacing anhydrite. This fact, together with the presence of relic anhydrite, may suggest that this texture is an early hydrational form of anhydrite. Of importance in this respect is the re-crystallisation of this type A gypsum to type B alabastrine secondary gypsum (Fig.3-16).

Type B - Type B gypsum consists of crystals which neither have definite boundaries nor uniform extinction properties as the stage is rotated (Fig.3-17). Gypsum crystals of this type attain different ranges of sizes and shapes.

A defined area of gypsum may become undefined with parts of it apparently belonging to other defined areas, when the stage is rotated. These areas were termed superindividuals by Ogniben (1957). This type of texture was described by Ver Plank (1952), Goldman (1952), Williams et al. (1954), and most recently by Holliday (1967, 1970), Mossop and Shearman (1973) and others. This texture was found adjacent to anhydrite and contained abundant relics of anhydrite. This suggests that this type of alabastrine gypsum is a hydration texture of anhydrite. Similar observations and conclusions were noted by Ver Plank (1952), Ogniben (1957), and Holliday (1967, 1970).

Fig. 3-13 Secondary alabastrine gypsum consisting of large ill-defined areas. Each area consists of small ill-defined sub-crystals which are oriented differently in adjacent areas. This texture is type A alabastrine gypsum. Slice. crossed nicoles, Mishraq, Iraq.

Fig. 3-14 A photomicrograph showing gypsum subcrystals replacing anhydrite laths parallel to its cleavage planes. Slice. crossed nicoles, Mishraq, Iraq.

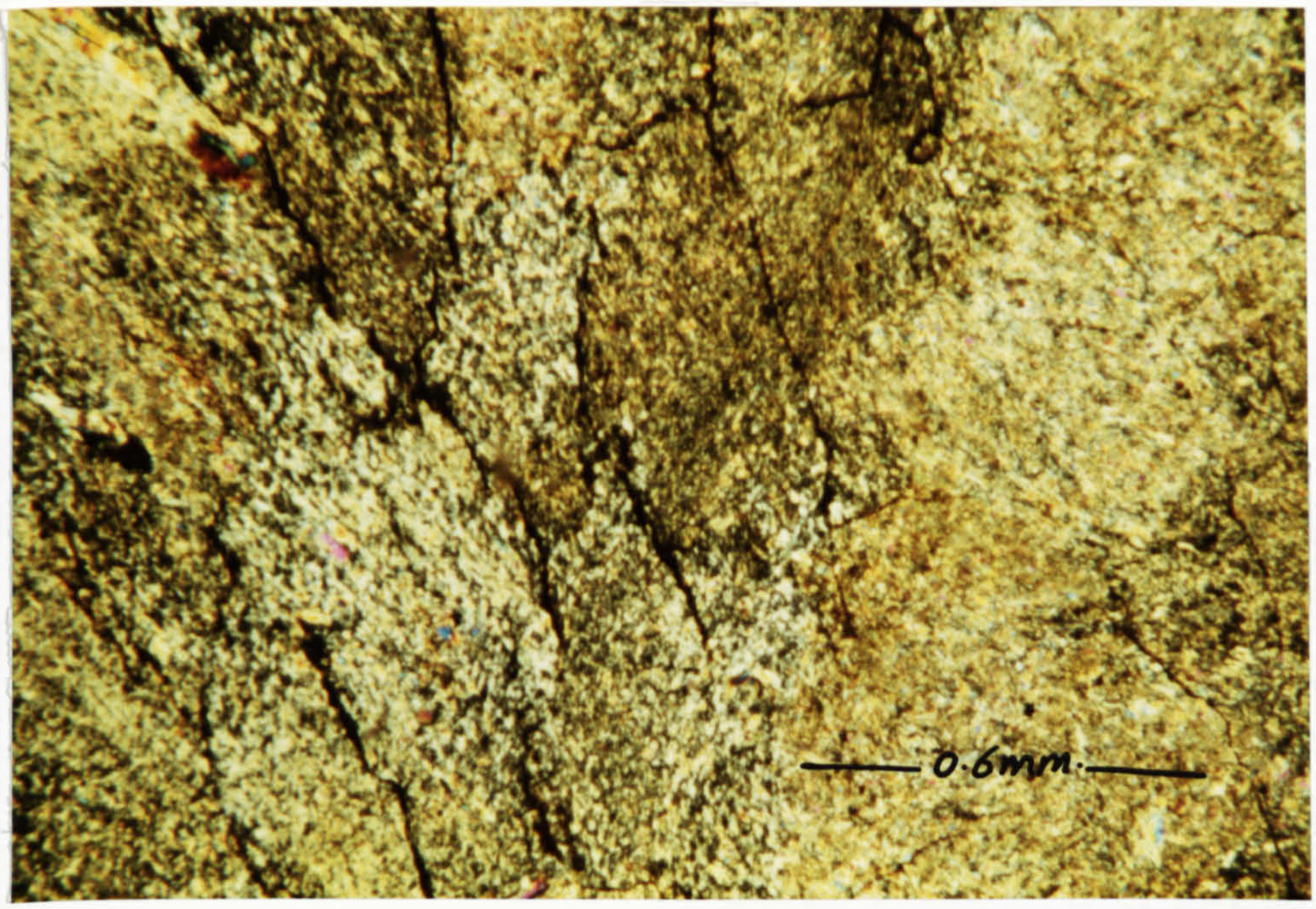
0·6mm

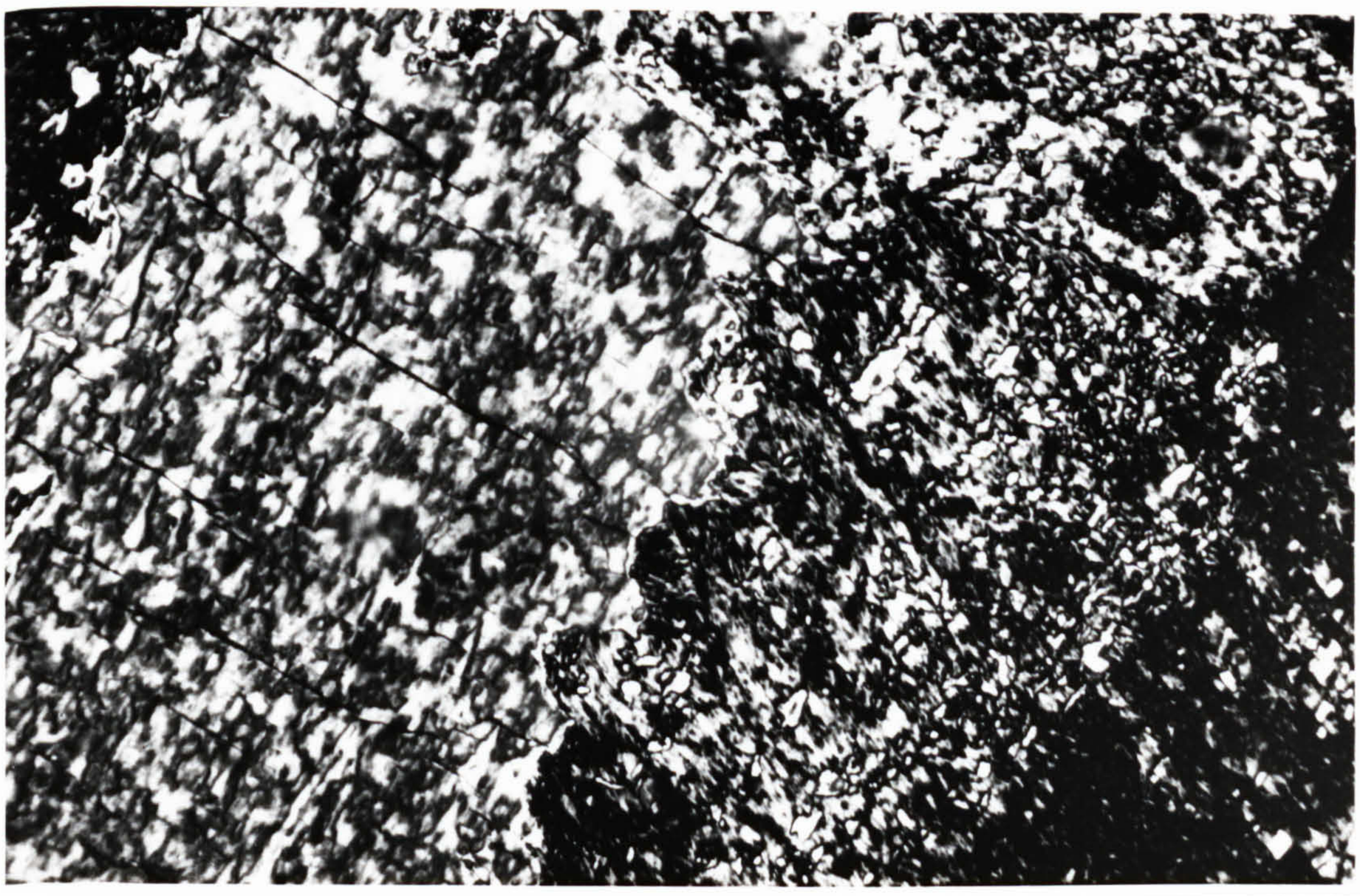

Fig. 3-15 A diagramatic section showing the replacing habit of type A texture alabastrine gypsum (a). The gypsum subcrystals lining themselves parallel to the two perpendicular cleavage -planes of one anhydrite lath (b). The larger the laths, the larger the areas containing a set of oriented gypsum subcrystals; the smaller the laths, the more diffusive the nature of type A becomes.

Fig. 3-16 Gypsum subcrystals (type A) replaced by ill-defined areas of alabastrine gypsum (type B). Slice. crossed nicoles, Bashiqa, Iraq.

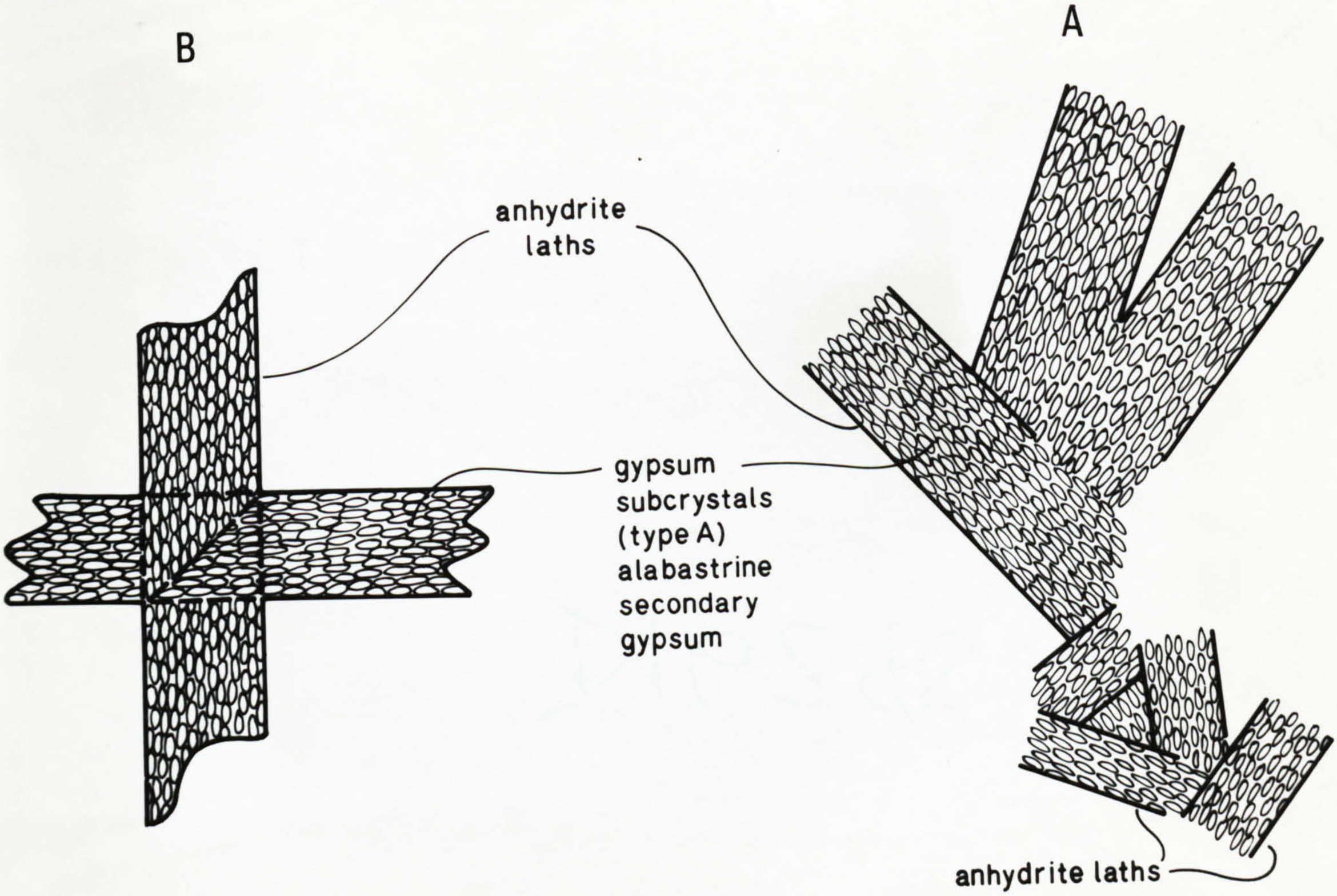
B
A
anhydrite
laths
gypsum
subcrystals
(type A)
alabastrine
secondary
gypsum
anhydrite laths

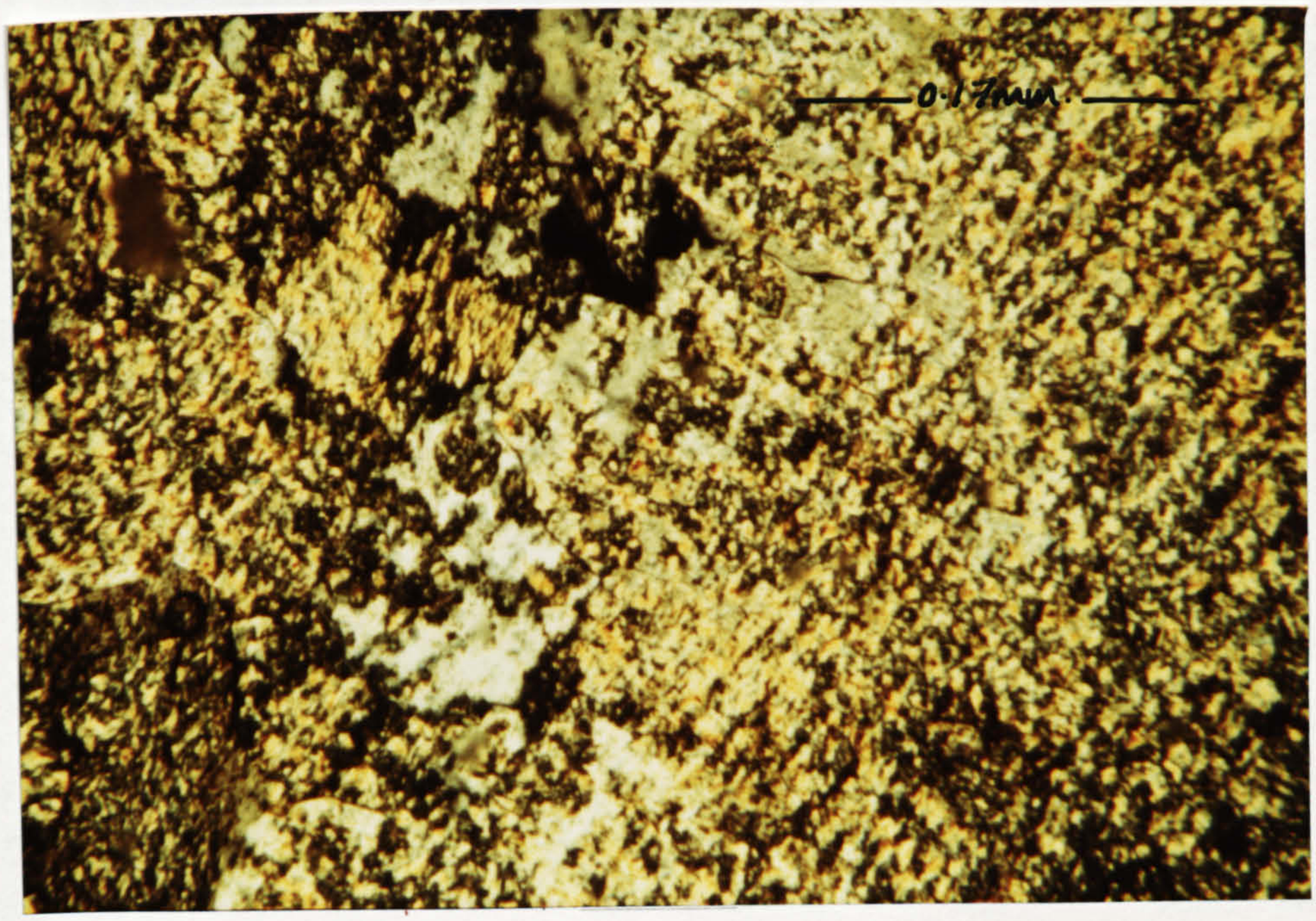
0·17mm.

Fig. 3-17 Ill-defined areas of secondary alabastrine gypsum. These areas neither have definite boundaries nor uniform extinction properties. This texture of alabastrine gypsum is referred to as type B. Slice. crossed nicoles, Bashiqa, Iraq.

Fig. 3-18 Small gypsum anhedra (type C) occurring adjacent to sub-felted texture anhydrite. The gypsum crystals nearest the anhydrite contain abundant relics. The amount of relics decreases away from the contact zone with the anhydrite. Slice. crossed nicoles, Mishraq, Iraq.

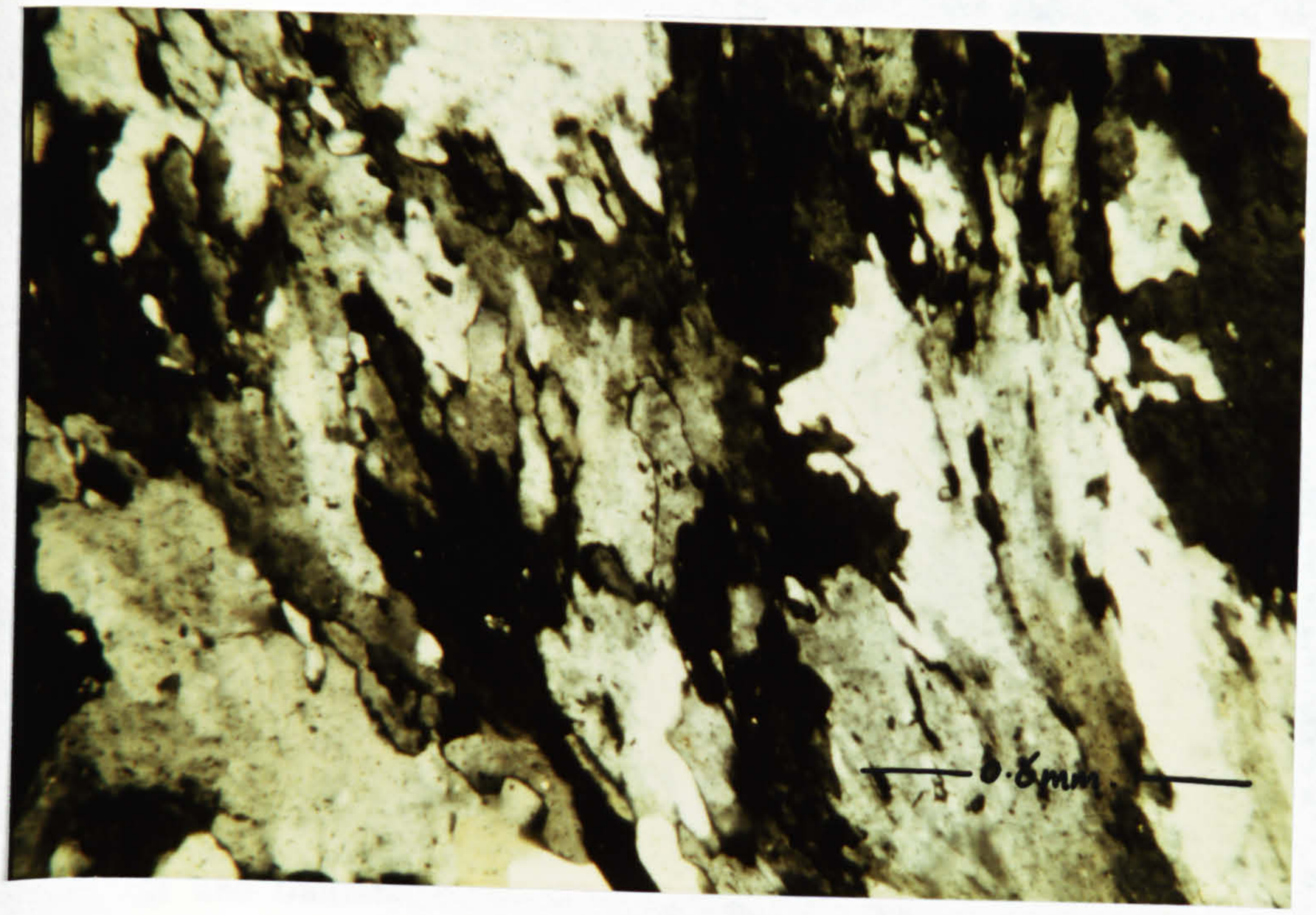
0·5mm.

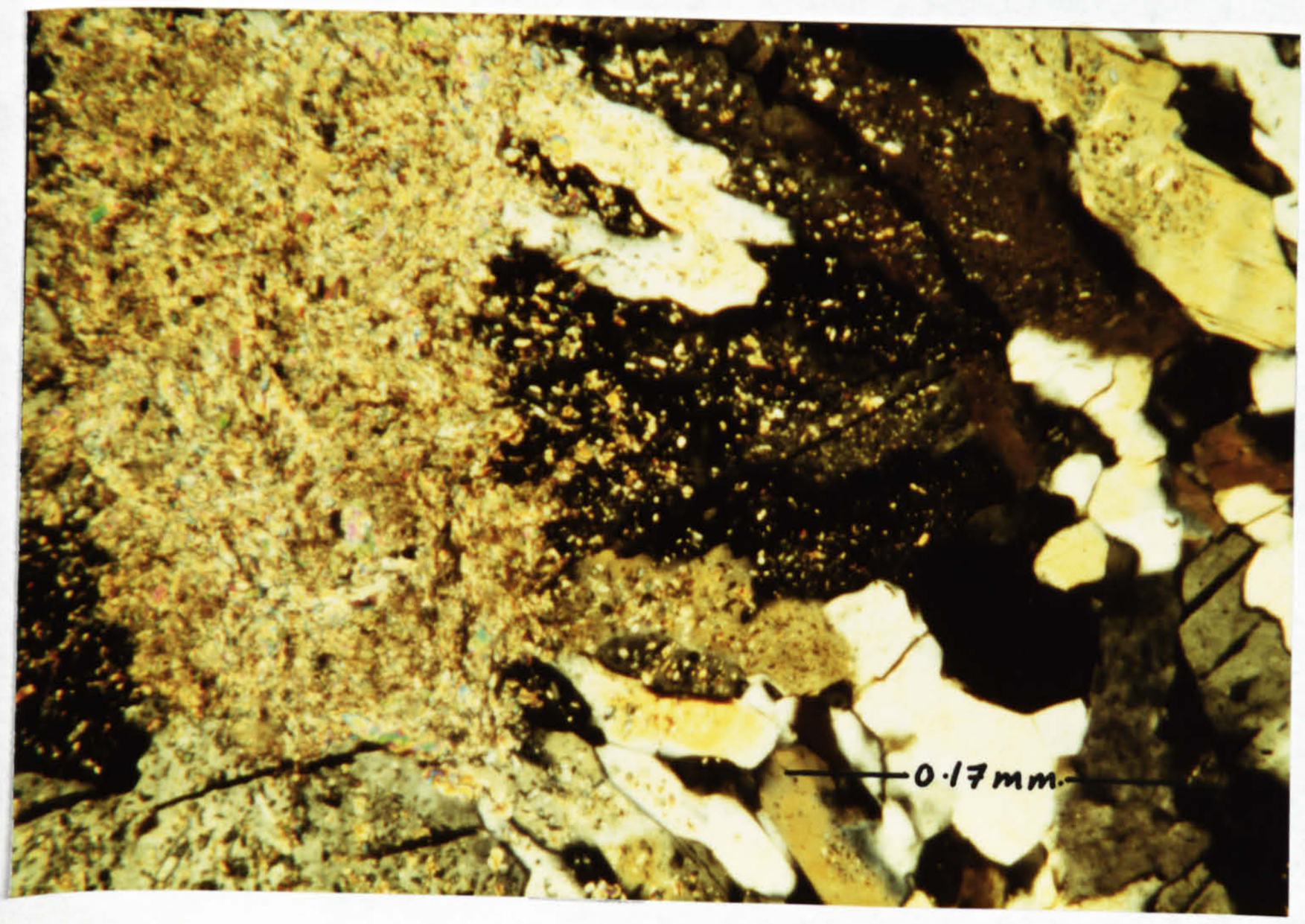
0·17mm.

Type C - This type consists of small gypsum anhedra, with an average diameter of 30 μ. These crystals are equidimensional and interlocking, and have curved boundaries. This type was described by Ham (1962), West (1964, 1965) and Holliday (1967, 1970). Holliday (1967) used the term 'granoblastic' to describe this type of gypsum mosaic and referred to it as type 2 alabastrine gypsum. This type of secondary gypsum occurs adjacent to and grades into type D gypsum (see below). Ogniben (1957) and Holliday (1967, 1970) considered this type to be the re-crystallised form of type B alabastrine secondary gypsum. They also concluded that this type never occurs adjacent to anhydrite or contains relics of anhydrite. This led them to believe that this type could not be a direct hydrational form of anhydrite.

In the Gachsaran evaporites this type of alabastrine secondary gypsum does occur adjacent to anhydrite and contains abundant relics of anhydrite (Fig.3-18). The relics, however, are present in abundant quantities in the crystals near the contact and decrease in quantity away from the contact zone till they are completely absent. These observations may question the conclusions of Ogniben and Holliday, and therefore may suggest that this type could be a direct hydrational texture of anhydrite.

Type D - This type was not found within the secondary gypsum textures of the Gachsaran Formation. According to Holliday (1967), gypsum crystals of this type are coarse, subhedral and euhedral, highly re-crystallised alabastrine secondary gypsum (Plate XI, Holliday, 1967). This type was classified as G_{13} gypsum by Ham (1962) and stage 3 alabastrine secondary gypsum by Holliday (1967). Ham (1962) and Holliday (1967) distinguish between these crystals and secondary gypsum porphyroblasts by their cross-cutting relationship with the surrounding gypsum and also by the lack of anhydrite relics within the stage 3 type.

3.6 Gypsum veins

Gypsum veins cut various types of rocks within the Gachsaran Formation, limestones, marls, shales and gypsum rocks. On the basis of their nature and structure, two types are distinguished. The first type of vein occurs either in a solitary manner or as a group, cutting each other at low angles and forming a network of veins (Fig.3-19). These veins which only occur in gypsum rocks, are aligned either parallel or at an angle to the bedding. The veins are short, with lengths of only a few millimetres. They range in thickness from 0.1 mm. to 1 mm. but have an average thickness of 0.4 mm. (Fig. 3-20). These veins are occupied by type C alabastrine secondary gypsum (crystals around 0.07 mm. in diameter) which may pass laterally into satin spar gypsum. A common feature of these veins is that all of them are bounded on both sides by porphyroblastic secondary gypsum. These porphyroblasts are elongated, full of anhydrite relics and their longest axes are arranged perpendicular to the vein walls. These longitudinal porphyroblasts were termed transverse gypsum by Goldman (1952). Shearman et al. (1972) noticed similar structures within Permian anhydrite rocks from northern England. They suggested that these porphyroblasts were the result of hydration of anhydrite caused by the percolation of water through the veins. They further suggested that these veins were caused by hydraulic fracture, through the upward movement of water caused by the erosion of the overburden which accounted for the former pressure on the water (Shearman, et al., 1972).

The second type of vein is found in marls, shales, siltstones, limestones and gypsum and is most abundant within marls and shales. They have a wide range of thicknesses, between 0.15 mm. and 3.5 cms. The gypsum occupying these veins is referred to as satin spar or fibre cross type in the literature. The satin spar gypsum consists of fibres

Fig. 3-19 A secondary gypsum rock composed completely of secondary alabastrine gypsum-filled veins. The veins either occur in a solitary manner or in a group cutting each other at low angles. Mishraq, Iraq.

Fig. 3-20 A photomicrograph of the above rock. Note that the veins contain type C alabastrine secondary gypsum which, in many places, passes into satin spar gypsum. Note also the large porphyroblasts of gypsum bounding the veins from each side. Slice. crossed nicoles, Mishraq, Iraq.

5 cm.

1 cm.

which are arranged in a vertical manner, which in many instances line themselves normal to the vein walls. On first sight the fibres look like individual discrete crystals, but microscopically, this is not the case. Cleavage planes pass from fibre to fibre without any deviation and there are no boundaries which define individual crystals (Shearman et al., 1972). Shearman et al. (1972) therefore concluded that these fibres are all parts of one and the same crystal, and suggested that the fibrous form of the satin spar gypsum is the result of the strain produced by the overburden on the formerly water-filled fractures (now filled with gypsum) as the water was squeezed out.

The source of the gypsum precipitated in the veins could be the excess sulphate produced as a result of the hydration of anhydrite (Shearman et al., 1972), and/or connate brines concentrated with $CaSO_4$ within the evaporite- bearing strata (Burgess and Holliday, 1974).

3.7 Celestite

Celestite was found in small amounts within the gypsum rocks of the Gachsaran Formation and within the hydrated parts of the anhydrite rocks, but was never seen within anhydrite rocks. In thin section, it occurs as irregular to anhedral plates of an average diameter of 80 μ. (Fig.3-21). These plates are sometimes composed of clusters of grains up to 400 μ. across, forming a cellular structure (Fig.3-22).

The strontium contents of two anhydrite and nine gypsum rocks from the Gachsaran Formation were determined by atomic absorption techniques (Table 3-2). The average strontium contents are compared with other ancient and modern examples in Table 3-3).

The results for the sulphate rocks of the Gachsaran Formation (Table 3-2)plus the results of several authors from other areas (Table 3-3) suggest that the anhydrite usually has 1/3 to 2/3 more strontium than the secondary alabastrine gypsum. It is reasonable to believe therefore

Fig. 3-21 Irregular to anhedral plates of celestite. Slice. p.p.l. Bashiqa, Iraq.

Fig. 3-22 The above plates are in cases composed of a cluster of grains forming a cellular structure. Slice.p.p.l. Mishraq, Iraq.

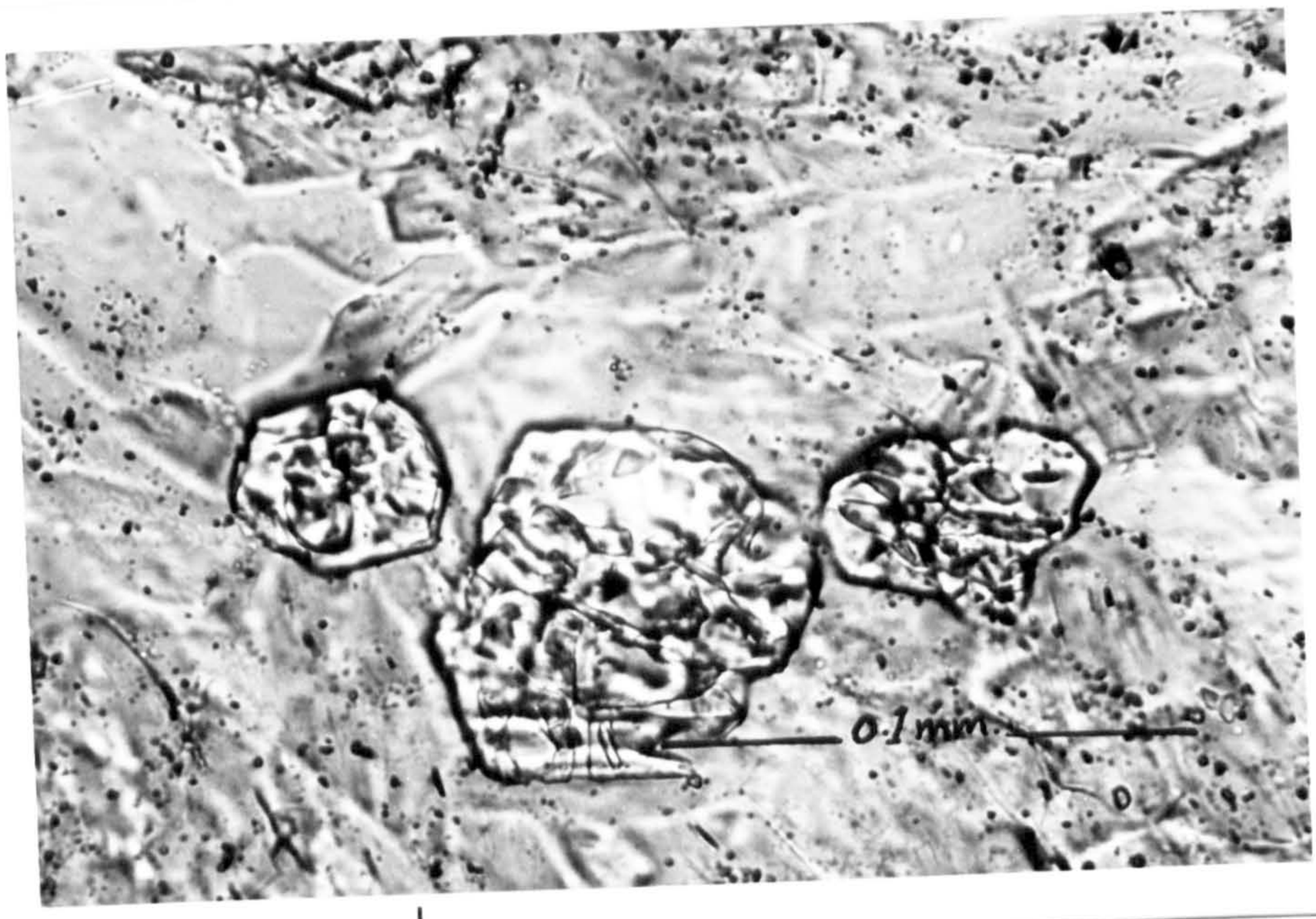
0.1 mm

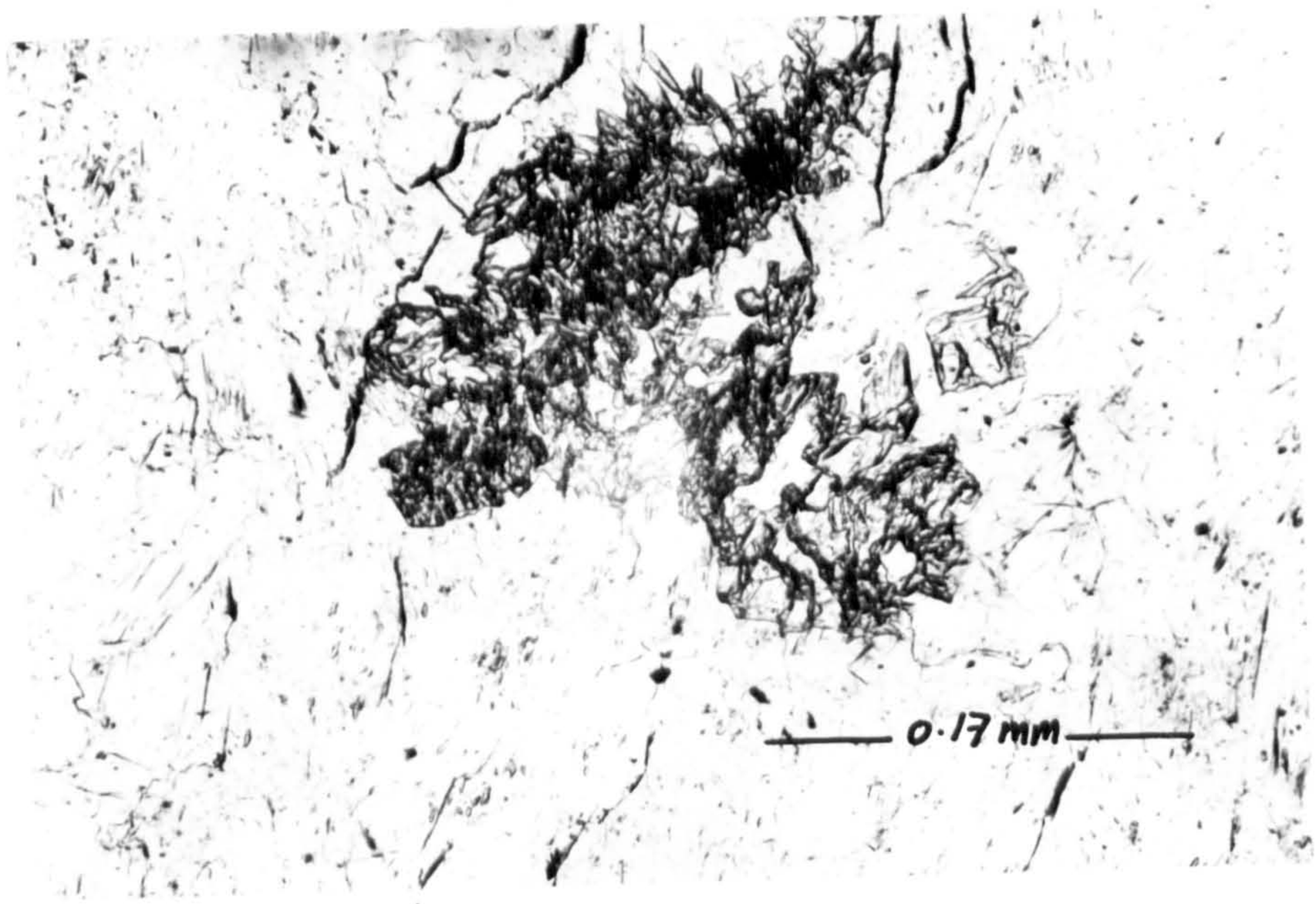
0.17 mm

TABIE 3-2

Sample No.	Rock	Sr-ppm	Sample No.	Rock	Sr-ppm
22-4-18	Anhydrite	1234	P9-5	Gypsum	713
P9-17	Anhydrite	1142	226	Gypsum	208
22-4-4	Gypsum	883	73	Gypsum	1063
P9-1	Gypsum	150	43	Gypsum	1608
P9-4	Gypsum	597	17	Gypsum	1104
			xa	Gypsum	623

TABIE 3-3

Source	Location	Age/Formation	Gyp/Anhy.	Av. Sr-ppm
This work	Northern Iraq	Middle Miocene Gachsaran Fm.	Gypsum	772
			Anhydrite	1188
Holliday (1965)	Spitsbergen	M.Carboniferous Ebbadalen & Nordenskioldbrean	Gypsum	680
			Anhydrite	1420
Johnson & Ham (1970) unpub.data from Butler 1973.	W.Oklahoma	Permian - cloud chief	Gypsum	860
			Anhydrite	1000
	S.W.Oklahoma	Permian - Dog Creek & Baline	Gypsum	380
			Anhydrite	1290
Butler (1973)	Baja Calif.	Recent	Gypsum	750
			Anhydrite	1154
Butler (1973)	Abu-Dhabi	Recent Trucial Coast	Gypsum	802
			Anhydrite	2175
Ham (1962)	Oklahoma	Blaine Form	Gypsum	970
			Anhydrite	1475

that the celestite formed within the secondary gypsum rocks was the result of the release of strontium ions from the hydrated anhydrite. The reduction in strontium content in secondary gypsum rocks is considered to indicate hydration of anhydrite in an open rather than a closed system (Holliday, 1965). Celestite was found in greater quantities in type C secondary alabastrine gypsum than in types A and B. Holliday (1965) recorded similar observations and suggested that the strontium released by the anhydrite could well have been retained by secondary gypsum type B and released as type B re-crystallised into types C and D secondary gypsum.

3.8 X-ray analysis

X-ray diffraction analyses were undertaken of the Gachsaran sulphates to check the crystal ordering. The peaks obtained were sharp and well-ordered. Using X-ray diffraction methods, Cuff (1969) compared anhydrite Jurassic rocks from the borehole at Warlingham, south London, with late diagenetic anhydrite from Abu-Dhabi and found that the peak profiles exhibited by the Warlingham samples were sharp and well-ordered, whereas those from the recent anhydrite were broad and disordered. The analysis of these Miocene sulphates suggests that the ordering of anhydrite takes place at least within a few million years.

3.9 Summary

This chapter has been concerned with the petrology and origin of the gypsum-anhydrite evaporites of the Miocene Gachsaran Formation in northern Iraq. The dominant nodular nature of the sulphate, its occurrence in repeated marl, limestone, sulphate cycles and the presence of stromatolites and cryptalgal laminates (see 5.9) are all consistent with a supratidal sabkha origin for the sulphates. Bedded sulphate developed above nodular sulphate is thought to have developed in back-sabkha lagoons. Petrological studies show that the gypsum is secondary after anhydrite.

The anhydrite, preserved at depth is present as subfelted lath, felted lath, blocky and fibroradiate types. There is evidence for a gypsum precursor to subfelted anhydrite. The other types of anhydrite are interpreted as re-crystallisation products of subfelted anhydrite. Four types of secondary gypsum were recognised, with three varieties interpreted as forming by direct hydration of anhydrite. Strontium contents of secondary gypsum are much lower than those of anhydrites. This is interpreted as reflecting an open pore-water system during the hydration process.

CHAPTER 4

MUDROCKS OF THE GACHSARAN FORMATION

CHAPTER 4

MUDROCKS OF THE GACHSARAN FORMATION

4.1 Introduction

The term claystone is here used to refer to a non-fissile sedimentary rock consisting chiefly of clay-grade material. Shale is the fissile equivalent of claystone. Marls are claystones with a considerable amount of calcareous material. An inclusive general term (mudrock) is used here to refer to all the above rock types.

Mudrocks of the Gachsaran are cyclically arranged with the limestones and sulphates. The mudrocks range from .3 to 20 metres in thickness, and are generally found underlying limestone beds which in turn are overlain by sulphate beds. They are often featureless and apparently structureless. Very thin limestone beds are occasionally present within these rocks. Mudrocks, however, do not occur uniformly throughout the Gachsaran sequence. They are more prevalent in the upper part of the sequence in the central parts of the basin and towards the margins of the basin, and they predominate over limestone and gypsum (see Figs.2-3 to 9).

The clay mineralogy of mudrocks can be used in palaeoenvironmental studies, although it must be remembered that most clays are detrital and, to a large extent, reflect the source area climate and geology. X-ray diffraction analysis of the Gachsaran mudrocks was thus undertaken and the abundances of the various clay minerals were estimated semi-quantitatively. Further information on the depositional environments of mudrocks can be obtained from their contained microfossils and so study of the Foraminifera within these sediments was also undertaken.

4.2 The colour of the mudrocks

Pigmentation of mudrocks is caused mainly by the oxidation state of iron oxides and the amount of organic matter and pyrite present. A red colour generally prevails when iron is present in the ferric state, while

many green mudrocks contain iron in the ferrous state. A dark grey to black colour is caused by the presence of organic material.

The origin of the red pigmentation has been a matter of some controversy and discussion. Walker (1967) concluded that the red pigmentation of arkosic sandstones of Baja California (Mexico) was caused by the diagenetic oxidation of iron-bearing minerals of igneous and metamorphic origin. An alternative view is that the red pigmentation of sandstones is derived from the breakdown of a detrital hematite precursor, formed in soils of the source area. For mudrocks from Baja California, Walker (1967) suggested that the red colour was caused by the oxidation and transfer of iron from within clay minerals to their exterior. Hubert and Reed (1978) envisaged the pigmentation of red mudrocks in the East Berlin Formation (Jurassic of the Connecticut Valley, USA) to be mainly the result of the conversion of limonite stains adsorbed on clay particles to hematite, by an aging process. Braunagel and Stanley (1977), in an attempt to investigate the origin of the variegated red beds of the Cathedral Bluffs Tongue of the Wasatch Formation (Eocene), attributed the formation of red and green couplets to the effect of wet and dry seasons. Reducing solutions removed the iron during the wet season while desiccation removed the water during the dry season, increasing the oxygen potential and leading to the oxidation of the ferrous iron.

On the basis of colour, two types of mudrocks in the Gachsaran are distinguished; (1) purple to red mudrocks, and (2) green mudrock.

Purple to red mudrocks generally have green laminae or lenses averaging one to several centimentres in thickness. Small greens spots in the red mudrocks also occur. The boundaries between the red and green laminae are sharp. Although these mudrocks rarely contain macrofossils, they do contain a considerable amount of planktonic Foraminifera (see sections 4.6, 7), suggesting that these are of relatively deep marine origin.

Bivalves also occur in the red mudrocks, but they are not common. They are invariably small forms (5 mm or less across) with thin shells. Several types are present, including forms with radial and concentric ornamentation patterns. Unfortunately the preservation is not sufficiently good for accurate identification. Bivalves are adapted to a wide range of modes of life. Many are benthonic, both infaunal and epifaunal whereas others are nektonic or epiplanktonic. The small size and thin-shelled nature of the bivalves in the red mudrocks suggest that they may be epiplanktonic. Such an interpretation would be in keeping with the dominantly planktonic nature of the Foraminifera in the red mudrocks. Further work on the bivalve fauna of the red and green mudrocks is required, and this could give valuable information on the depositional environment of these fine-grained sediments.

The explanation offered by Braunagel and Stanley (1977), mentioned above, of the effects of wet and dry seasons, cannot be applicable to these mudrocks. The iron most probably was adsorbed on to the clay particles when transported and deposited. This iron was later oxidixed to hematite. The mechanism by which the green laminae were formed must remain in question. Generally iron oxides may be reduced and leached either by the action of pore water or by migration of petroleum (Thompson, 1970; McBride, 1974). The impermeable nature of these clayey mudrocks, however, makes it difficult to envisage such migration fluids without any external pressure. Compaction in mudrocks expels water and reduces the mudrock thickness by a factor of up to ten (Ricke and Chilingarian, 1974). Compaction could have contributed to the movement of reducing solutions.

Green mudrocks are characterised by a high fossil content. The fossils are dominated by benthic Foraminifera, but echinoderms, bivalves, ostracods and gastropods are also common. Green mudrocks are characterised by a relatively high $CaCO_3$ content and they usually contain much organic material. The non red character of these rocks can be explained by the organic content which led to the reduction of any colloidal or adsorbed ferric iron oxides. Compared with the red mudrocks, depths of deposition were much less (see section 4.7).

4.3 Mineralogy of the mudrocks

X-ray diffraction techniques were used to identify the mineral suite of the Gachsaran mudrocks.

The mudrocks studied consisted predominantly of clay minerals. Accessary minerals such as quartz, feldspar, muscovite, carbonate and pyrite were also found. Such minerals act as dilutents of clays (Van der Marel, 1966) and so affect the reflection intensity of the clay minerals. Because the interest lies in the clay minerals, certain techniques were applied for their isolation, and attention was focussed on the clay minerals. Clay

minerals identified belonged to the three main groups; kaolinite, illite and smectite.

4.3.1 Kaolinite (or kandite) group

This group, in addition to kaolinite, includes dickite, nactite, halloysite and meta-halloysite. Although all these minerals have more or less similar X-ray reflections, there exist certain reflections or relative intensities which are specific to a particular mineral of the group (Douillet and Nicolas, 1969, in Thorez, 1976). These minerals are all pure hydrous aluminium silicates with an $Al_4Si_4O_{10}(OH)_8$ chemical composition (Deer, Howie and Zussman, 1962). These do not expand when treated with glycol except for halloysite; heating, however, causes the complete destruction of their diffraction patterns.

Of this group, the mineral kaolinite was the only mineral found. It existed in all the samples analysed but in a low concentration (Table 4-1). The mineral kaolinite was identified on the evidence shown on the diffractogram by the reflections of 7.15Å (001), 3.57Å (002) and 2.38Å (003).

Thorez (1976) stated that "a well-ordered (well-crystallised) kaolinite can be assumed by the presence of a narrow symmetric and relatively intense 7.1 and 3.5Å reflections." The intensity of the (001) and (002) reflections decreases with an increasing asymmetry of the clay mineral. He further suggested that the disordered kaolinites display, beside the low intensity and asymmetric nature, a more or less pronounced diffraction effect at about 4.4Å. The Gachsaran kaolinites display sharp and narrow reflections with a very slight asymmetry (Fig.4-1). Accordingly, therefore, these kaolinites can be assumed to be fairly well crystallised.

The (001) reflection of kaolinite is interfered with when chlorite is present. To overcome this problem, the normal procedure was followed involving heating of the smear at 560°C for one hour. As a result, the (001) reflection diminished leaving only a very small (002) chlorite

Table 4-1

Sample No	Location	Colour	Illite % + Mixed layers%	Montmorillonite	Kaolinite
21	Hammam Al-Alil	Green	62%	21%	16%
25	" "	Green	60%	25%	15%
211	" "	Green	56%	30%	14%
23	" "	Green	55%	27%	16%
13	Bashiqa	Green	58%	30%	12%
111	"	Red-Green banded	47%	47%	6%
18	"	"	50%	40%	10%
93	Khaniqeen	"	52%	35%	13%
86	Mishraq	"	50%	40%	10%
8X	"	Red with green spots	52%	42%	6%

reflection (Fig.4-1). The percentage of this chlorite in different samples can be considered negligible. This process is used to differentiate between the similar reflections of the two minerals.

4.3.2 Illite group

Illite, the hydromicas and glauconite are the principal members of this group. The general chemical formula for this group is $K_{1.0-1.5}Al_4(Si_1Al)_8O_{20}(OH)_4$ (Deer, Howie and Zussman, 1962).

In the Gachsaran mudstones, illite was discovered to be the dominant clay mineral (Table 4-1).

Illites are recognised by their strong reflections at 10Å and 3.3Å. The latter reflection also coincides with the strongest quartz reflection.

The Gachsaran illites are recognised as dioctahedral because of the presence of a medium strong (002) reflection which occurs at a d-spacing of 5Å. In a trioctahedral variety, this reflection is very weak or absent (Thorez, 1976). Dioctahedral illites have also an intensity ratio of I(001) / I(002) of less than four (see Thorez, 1976). The difference between illite and muscovite is in the greater range of compositional variation (degraded with respect to potassium ions) of illite, which in turn causes a lower degree of crystallinity (Thorez, 1976; Ziam, 1977). The (001) reflections of these illites are asymmetric. Although the apex of the (001) reflection of illite is at 10Å, its base shifts towards the higher angle. This is caused mainly by the stripping of K ions. The asymmetric nature of illite (001) reflections is a feature attributed by some to be indicative of a transition to mixed-layer systems (Reynolds and Hower, 1970; Kodama et al., 1969).

4.3.3 Smectite group

Montmorillonite, nontronite, hectorite and saponite are the principal members of this group. Montmorillonite has a similar structure to illites but has interlayer water instead of K ions between layers. Depending upon

Fig.4-1 X-ray diffraction pattern of the three major clay minerals; kaolinite, illite, and montmorillonite, in a representative Gachsaran mudrock.

Upper - non treated

Middle - glycolated

Lower - heated at 560°C

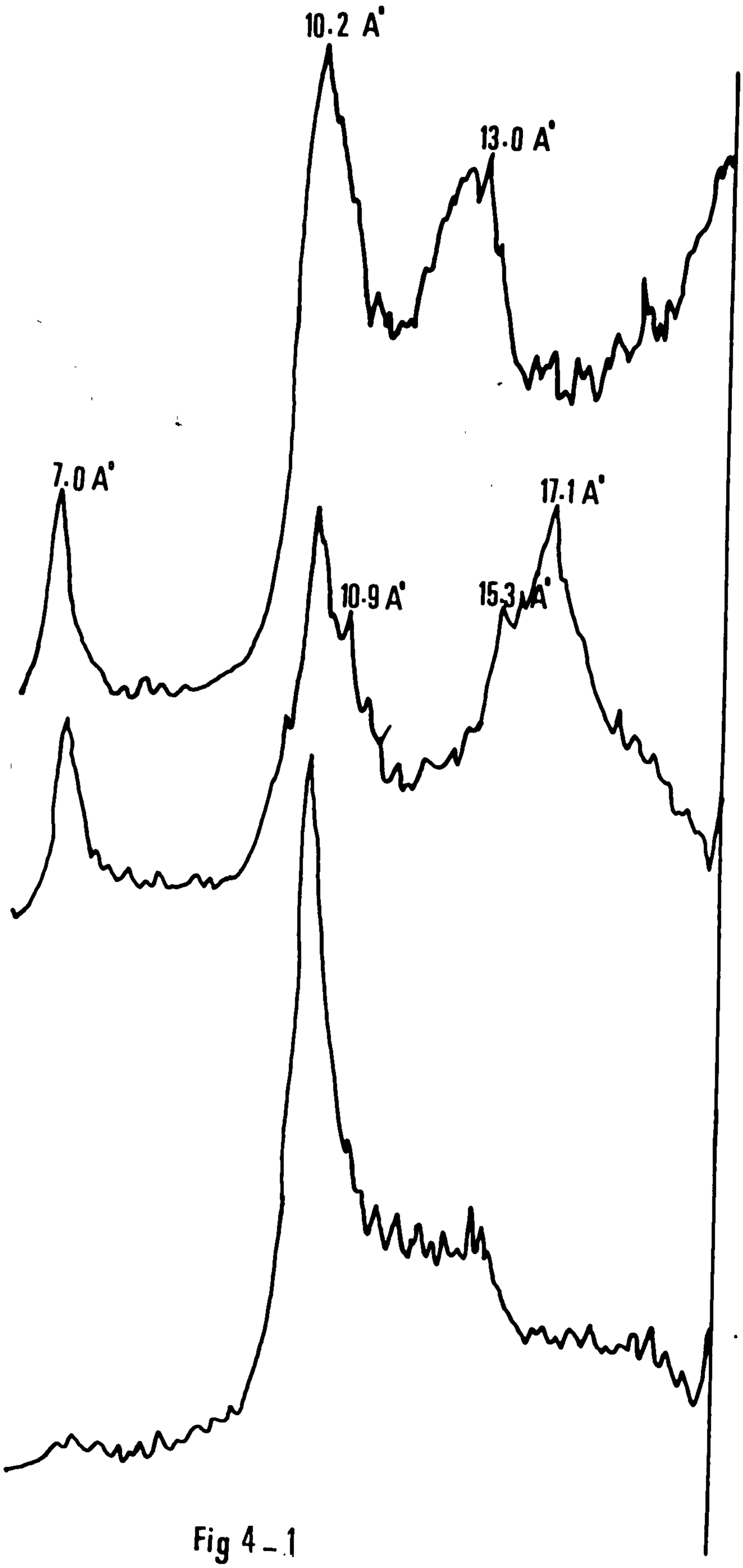

Fig 4 – 1

the number of water layers the mineral montmorillonite shows an intense (001) peak ranging from 12-15Å. This peak expands to 17Å when the sample is glycolated and collapses to about 10Å upon heating at 550°C for one hour.

Montmorillonite was found to be the second dominant clay mineral in the Gachsaran samples (Table 4-1). Generally speaking, the sample analysed by X-ray diffraction showed broad patterned (001) peaks (Fig.4-1). The reflections ranged from 12-13Å at (001) with their base shifting towards the lower Å. Upon glycolation the reflections became more symmetrical but expanded to about 17Å. This reflection collapsed to 10Å after heating. The base shifting to lower angles was interpreted by Thorez to be an indication of mixed layering.

Thorez emphasised the fact that not all clay minerals that expanded to 17Å upon glycolation are smectites. Mixed-layer clays containing montmorillonite as a major constituent may behave in the same manner. The identification of the various mixed-layer clays is based upon their behaviour under different treatments (Lucas et al., 1959 in Millot, 1970, p.17 fig.2). According to this figure, three types of mixed layering occur within the Gachsaran mudrocks: montmorillonite-vermiculite, montmorillonite-chlorite and illite-montmorillonite.

4.4 Processes in the formation and distribution of clay minerals

Clay minerals form as a result of several different processes. These include hydrothermal processes, weathering and pedogenesis from which most of the detrital clays in sedimentary rocks are derived, and the clays formed during diagenesis (Millot, 1970). The most important of these clays are those of detrital origin, which are thus directly related to the processes of weathering. Processes involved in generating these clays include variations of temperature, hydration, oxidation and reduction, hydrolysis and biochemical activity (Millot, 1970). The nature of the parent rock, as well as the physico-chemical conditions that prevail in the source

area, determine the type of clay minerals produced. Field occurrences and observations indicate that the rocks which weather to kaolinite are usually of an acidic nature, particularly of granites and acid gneisses, while montmorillonite is generally produced as a result of the weathering of calcium or sodium-rich rocks and volcanic deposits. The ordinary of most rocks with common conditions of pH would lead to the formation of illite. With regard to the chemical conditions of formation, kaolinite chiefly forms in acid environments under the influence of humic acids, in association with the oxidation of sulphides and through strong leaching (Ross, 1945). He also noticed that the formation of montmorillonite is favoured by alkaline conditions, while minimal leaching would normally produce illite. As an example of the effect of climate on clay mineral formation, Beaven (1966) made a detailed study of the clays of the islands of Trinidad, Jamaica and Grenada, and found that the volcanic rocks of these islands were weathered to kaolinite during the wet season, and montmorillonite during the dry season. The close control of clay facies patterns in modern marine muds by climatic conditions on the adjacent land mass is evident from maps constructed by Biscaye (1965) and Rateev et al. (1969).

In addition to the obvious importance of the geology and climate of the source area on clay mineralogy, other factors affecting clay distribution include grain size and clay mineral transformation. Clay minerals differ in their grain size, with kaolinite being coarser in its size of flakes compared to illite and montmorillonite. Montmorillonite is composed of the finest grain size. In studies of shallow marine clays, it has been shown that kaolinite is generally most abundant near shore, while illite and montmorillonite dominate further offshore (Porrenga, 1967; Baker, 1973).

It was thought at one stage that transformation of clays as they are suspended in sea water or lying on the sea floor played a part in clay

distribution and formation. Caroll and Starkey (1959) believed that clay minerals lose appreciable amounts of SiO_2, Al_2O_3 and FeO when transported from fresh waters into sea waters. They concluded that the amount of loss of these oxides to sea water can be directly used as a measure of the mineral stability in a marine environment. General agreement among workers about diagenetic changes of clay minerals in suspension has now been achieved with the conclusion that the effect of such operations is minimal and of little significance. Clay alteration during diagenesis after burial, however, is significant. Compaction reduces the deposited clay sediment to about 1/10 its original thickness, and removes its high water content (Ricke and Chilingarian, 1974). When clays are deeply buried much alteration is expected. Weaver (1959) reported that montmorillonite alters to montmorillonite - illite mixed layer below a depth of 3000 metres. Other studies indicate that substantial diagenetic changes in clay mineral accompany burial below 3000 metres and/or increase in temperature to about 100°C. This is also supported by the predominance of clay minerals such as illite and chlorite in the lower Palaeozoic and Precambrian mudrocks. Foster (1972) summarised the changes that can take place in clay minerals during diagenesis and the relationship of the various groups.

4.5 The Gachsaran mudrocks: interpretations

In the Gachsaran Formation the mudrocks are more dominant in the northeast marginal sections than in the sections from near the centre of the basin. This obviously led to the conclusion that the source area for this detrital material was towards the northeast where the Zagros mountain chain was being uplifted during Miocene times. Igneous and metamorphic rocks are common in the Zagros Mountain range (Pamić et al., 1979) and weathering of these could explain the predominance of illite and montmorillonite in the Gachsaran rocks. These clays would also have been supplied by weathering of Mesozoic sedimentary rocks in the Zagros area. The clay mineralogy also

suggests that an arid to semi-arid climate prevailed in the source area, with minimal leaching. The predominance of mudrocks in the upper part of the succession in the central part of the basin is, however, attributed to a change in the pattern of deposition.

Table 4-1 shows small but noticeable differences in the clay mineral content of the dominantly green and the red mudrocks. Illite is clearly predominant in the green mudrocks but its amount decreases in the red mudrocks with an increase in the montmorillonite and mixed-layer clays. The amount of kaolinite also decreases in the latter. This is attributed to the size of the clay mineral's flakes involved, i.e. the larger kaolinite and illite flakes were deposited in the relatively shallow near-shore areas, whereas the montmorillonite was deposited predominantly in relatively deeper water offshore areas because of its finer size. This can be supported by the fact that the dominantly green mudrocks contain an appreciable amount of $CaCO_3$ which is negligible in the red mudrocks. Palaeontological evidence is further advanced to support the above conclusion (see later sections).

Some mudrocks from the Gachsaran Formation (Iran) were reported to be of Aeolian origin (Gill and Ala, 1972). The possibility that some mudrocks in the Gachsaran Formation of Iraq are also Aeolian cannot of course be excluded, but all those examined in this study are of subaqueous origin.

No diagenetic alterations are expected for these mudrocks because of their relatively shallow burial.

4.6 Foraminifera of the Gachsaran mudrocks

The mudrocks of the Gachsaran are generally fossiliferous. Fossils include Foraminifera, gastropods, bivalves, echinoderms, ostracods and bryozoa. The Foraminifera of these mudrocks have been extracted and studied both qualitatively and quantitatively. In all, eleven samples were analysed.

On the basis of Foraminiferal content and other fossils, the Gachsaran mudrocks are divided into two types:

1. Very fossiliferous mudrocks. Fossils include mostly benthic Foraminifera, but gastropods, bivalves, echinoderms, ostracods and bryozoa are also common. The benthic Foraminifera are dominated by Ammonia. Others include Elphidium, Quinqueloculina, Triloculina, Rotalia, Discorbis, Nonion, Borelis and Textularia (Plates 4-1, 2). The average percentages of these genera in the various samples are given in Table 4-2.

It is also of importance to point out that the colour of these mudrocks is dominantly green. The $CaCO_3$ content is also high as compared to the other type.

2. Less fossiliferous mudrocks dominated by planktonic Foraminifera. The Foraminifera are few in number individually and species. The dominating genera are Globogerina, Globorotalia and Globotruncana (Plate 4-3). The number of benthic Foraminifera do not comprise more than 20% of the Foraminiferal content. No other associated fossils were detected. The colour of these mudrocks is dominantly red with green bands and/or spots. The amount of $CaCO_3$ content is very low.

4.7 Depositional environment

Foraminifera of the Miliolidae group are characteristic of shallow water sequences in both Recent and ancient sediments. They are abundant in the inner part of continental shelf environment (Bandy and Arnal, 1957). Two particular genera, Quinqueloculina and Triloculina, are usually reliable indicators of shallow water environments (Bandy and Arnal, 1960). Table 4-3 shows that most of the genera associated with the first type of mudrocks are found to live between 0-50 metres depth in Recent marine environments.

Murray (1973) summarised the ecological characteristics of living Foraminiferal genera in terms of salinity, temperature and depth. These data are given for each identified benthic genus within the Gachsaran mudrocks in Table 4-2. The terms hyposaline (salinity 33%), normal marine (33-37 per mille), hypersaline (37 per mille) are after Murray (1973).

Table 4-2

Genus	Salinity	Temp. °C	Depth (m)	Environment	% Average
Ammonia	Hyposaline, marine, hypersaline	15-30	0-50	Hyposaline and hypersaline lagoons, inner shelf	53
Elphidium (Unkeeled)	0 - 70 per mille	1-30	0-50	Hyposaline to hypersaline tidal marshes and lagoons	10
Triloculina	> 32 per mille	Tropical	0-40	Inner shelf, normal marine and hypersaline lagoons	12
Quinqueloculina	> 32 per mille	Tropical	0-40	" " "	9
Rotalia	36 - 38 per mille	14-25	0-40	Inner shelf	6
Borelis	39 - 50 per mille	18-26	0- 6	Inner shelf, and lagoons	3
Textularia	Normal marine	Arctic-tropical	50-640	Shelf and upper bathyl	3
Discorbis	Normal marine	> 12	0-50	Inner shelf	2
Nonion	Hyposaline to normal marine	Cold to tropical	0-180	Shelf	2

Plate 4-1

Fig.1-a,b,c — Ammonia : diameter 0.6-0.8mm

Fig.2-a,b — Elphidium : diameter 0.35mm

Fig.3-a,b,c — Quinqueloculina : length 0.4mm

Fig.4-a,b,c — Triloculina : length 0.8mm

Fig.5-a,b,c — Rotalia

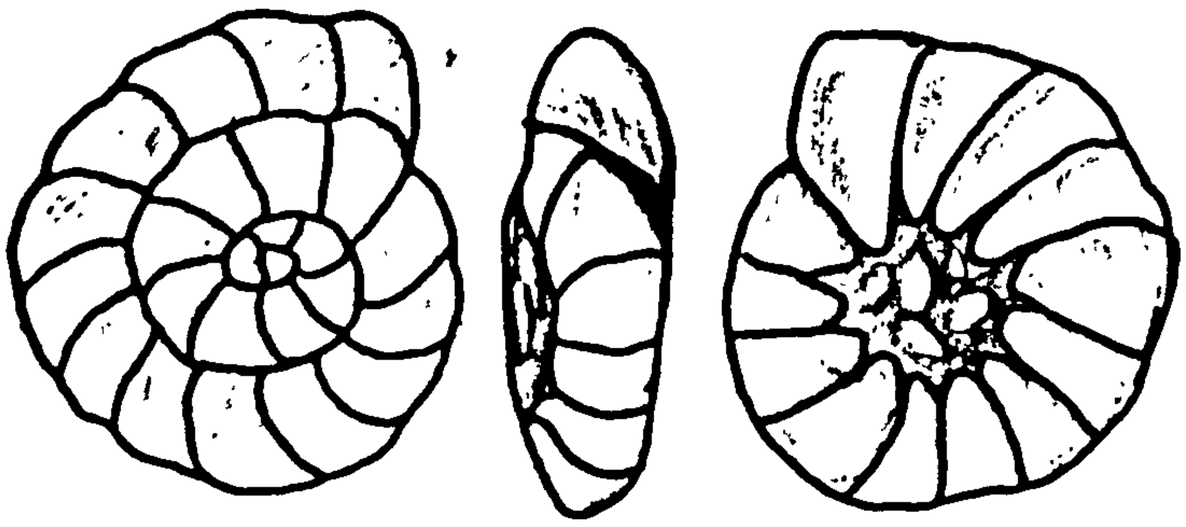

a b c

Fig - 1

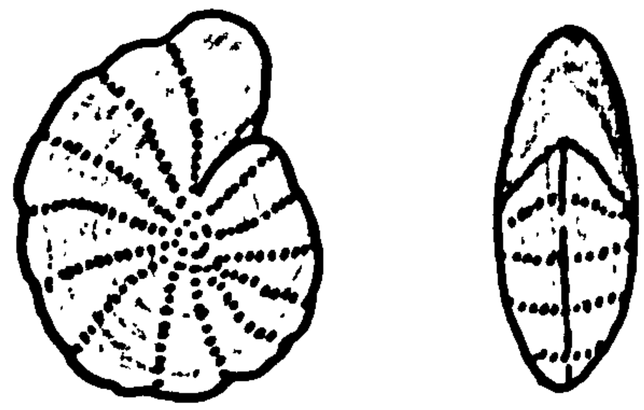

a b

Fig - 2

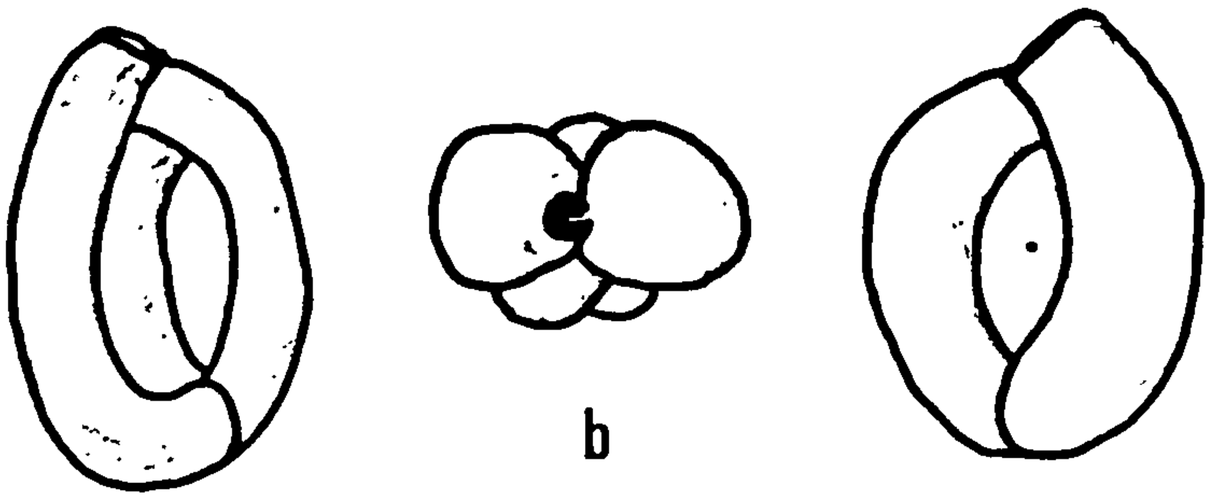

a b c

Fig - 3

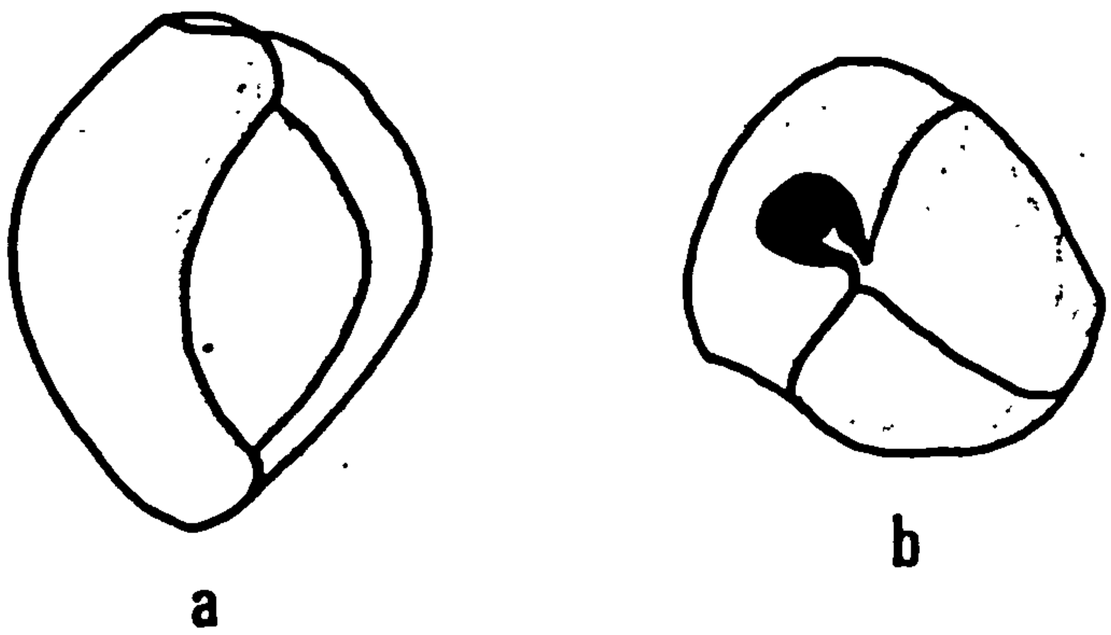

a b c

Fig - 4

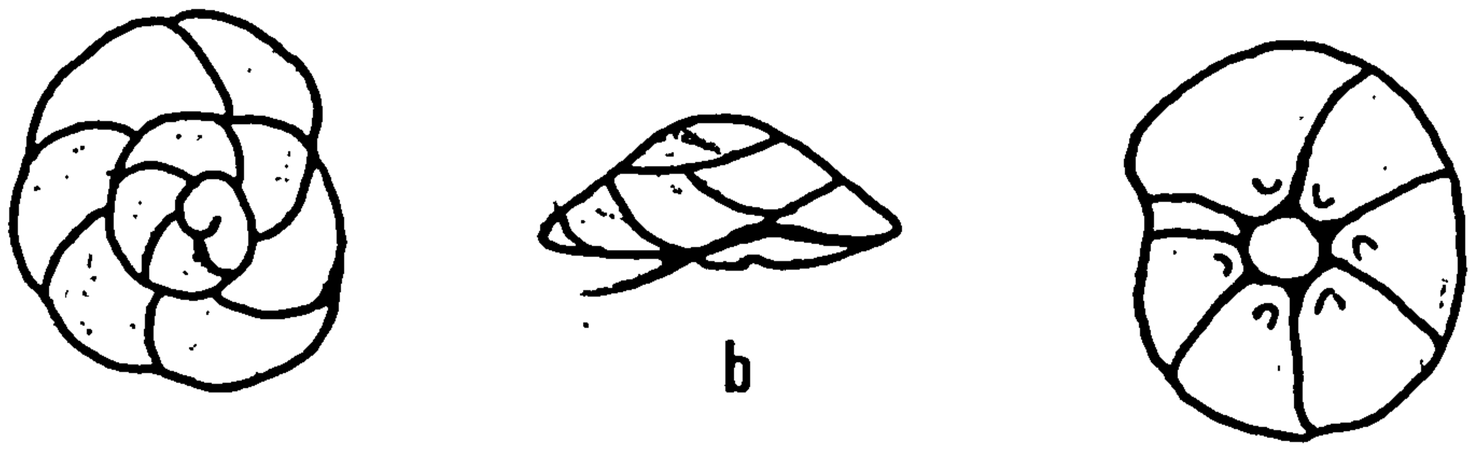

a b c

Fig - 5

Plate 4-2

Fig.1-a,b,c — Discorbis : diameter 0.6mm

Fig.2-a,b — Nonion

Fig.3-a,b — Borelis : diameter 0.35mm

Fig.4-a,b — Textularia : length 0.63mm

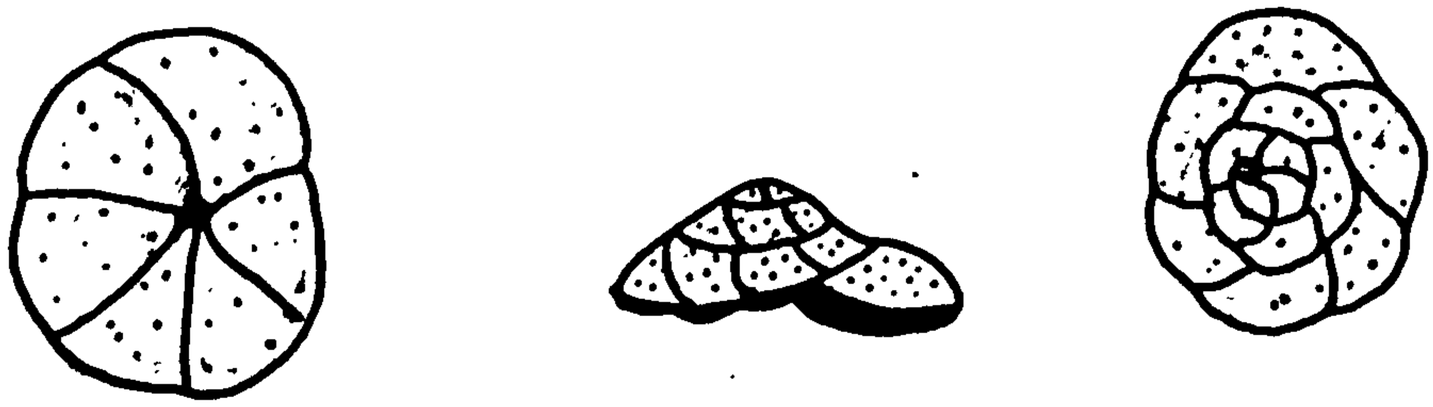

à b c

Fig - 1

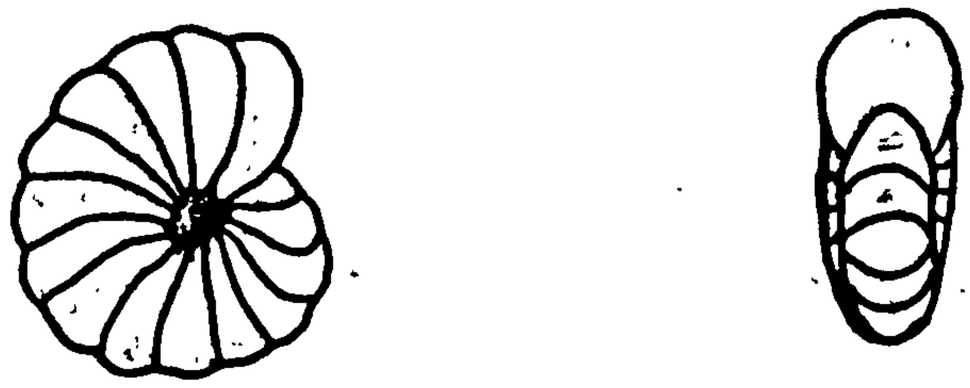

a b

Fig - 2

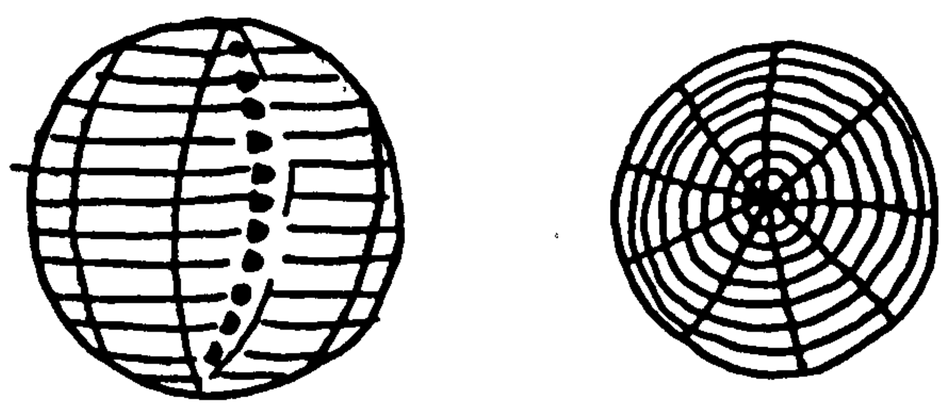

a b

Fig - 3

a b

Fig - 4

Plate 4 -3

Fig.1-a,b — Globogerina : diameter 0.2mm

Fig.2-a,b,c — Globorotalia : diameter 0.18-0.2mm

Fig.3-a,b,c — Globotruncana : diameter 0.25-0.3mm

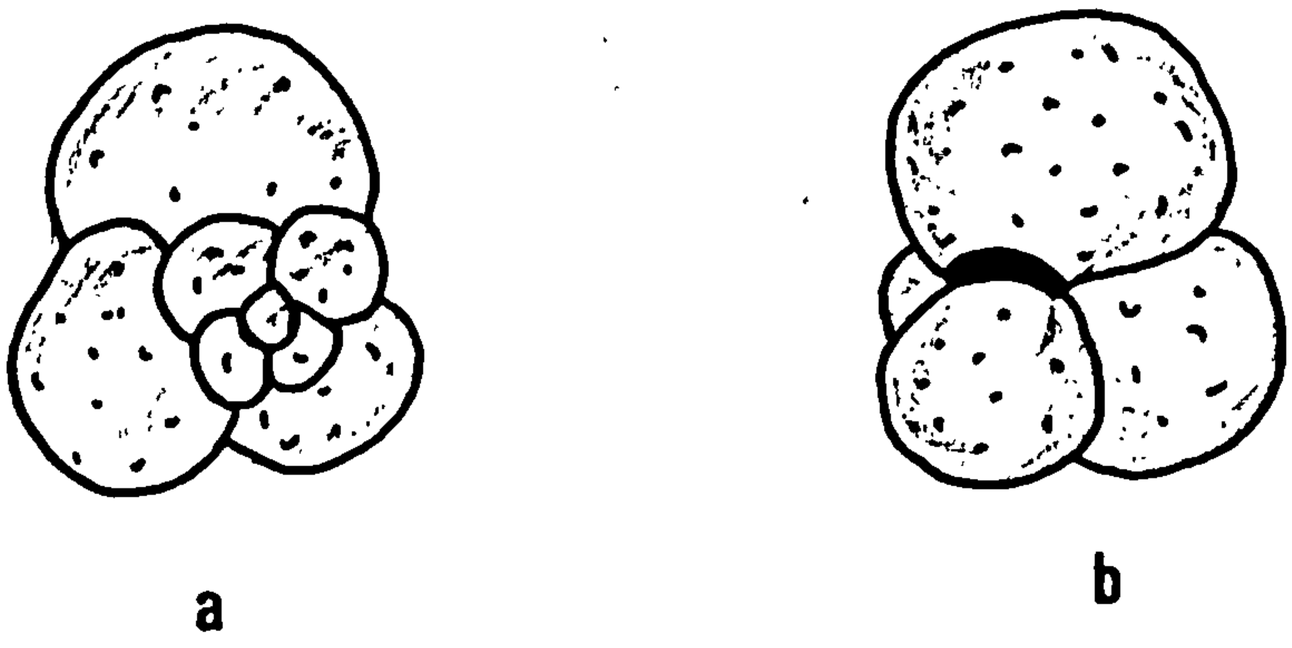

a b

Fig - 1

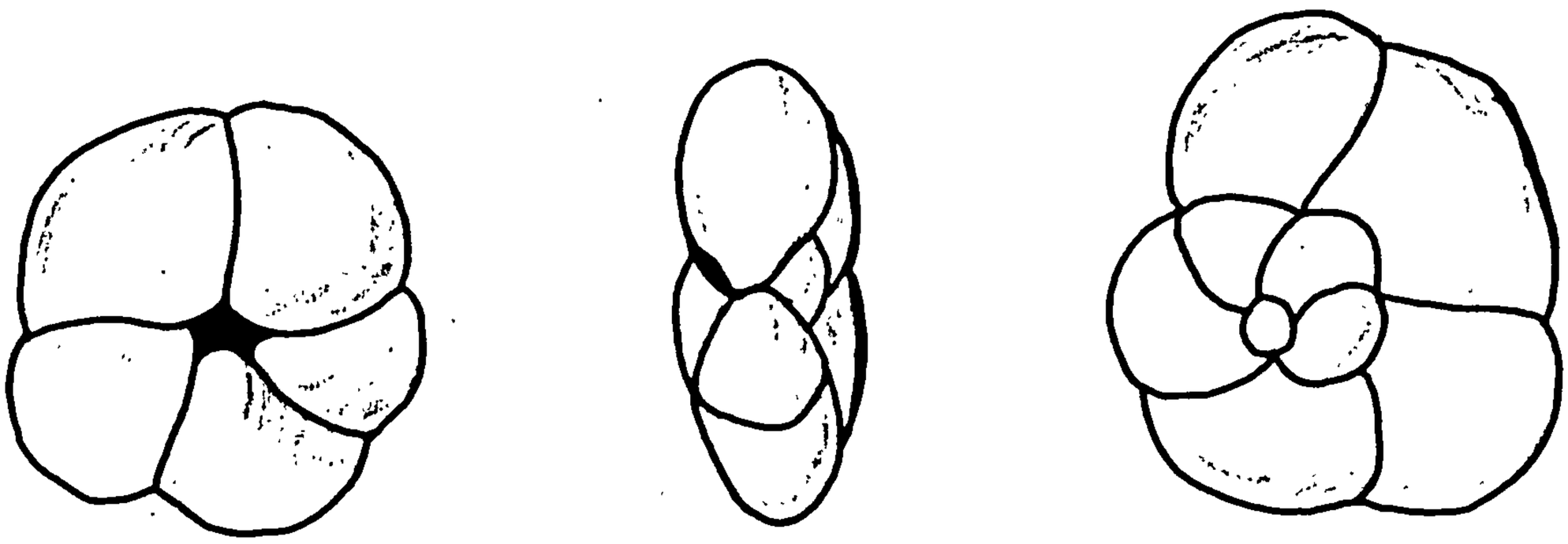

a b c

Fig - 2

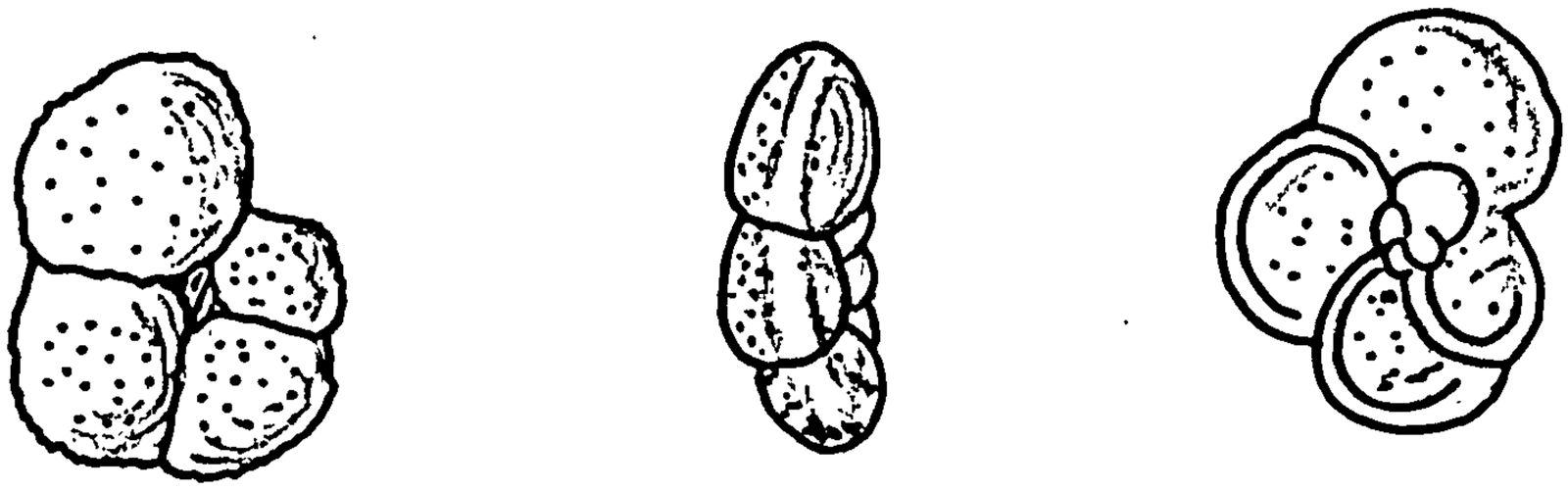

a b c

Fig - 3

The benthic Foraminifera generally fall into three major suborders: Textularia, Milliolina and Rotalina (Loeblich and Tappan, 1964). Murray (1973) undertook an investigation into the occurrence of Foraminifera in Recent environments. He combined his work with that of others and plotted the relative percentages of Foraminifera in each sample collected from a particular locality and environment on a triangular diagram with the three major suborders as end-members. The result was clusters of points representing the different environments. This enabled Murray to draw boundaries between each environment (Fig.4-1b). Six samples of the Gachsaran mudrocks have been plotted in this triangular diagram (Fig.4-1a). Each point represents the relative percentages of the three suborders in that sample (Table 4-3). When these points are overprojected over figure (4-1b) of Murray, it is seen that they fall close to the boundary of two environments: normal marine lagoons and hypersaline lagoons. The ecological data of the genera from Table 4-2 can now be used to separate these two environments. The dominant genus of Type 1 mudrock samples is Ammonia (Table 4-2). This genus is usually found in hyposaline to hypersaline lagoons in Recent environments. Thus, the environment of deposition of mudrocks containing these Foraminifera is most likely to be hypersaline lagoons.

Table 4-3

Sample No.	Rotalina	Milliolina	Textularia
211	68%	30%	2%
23	57%	42%	1%
13	36%	64%	-
25	60%	35%	5%
27	70%	30%	-
26	73%	27%	-

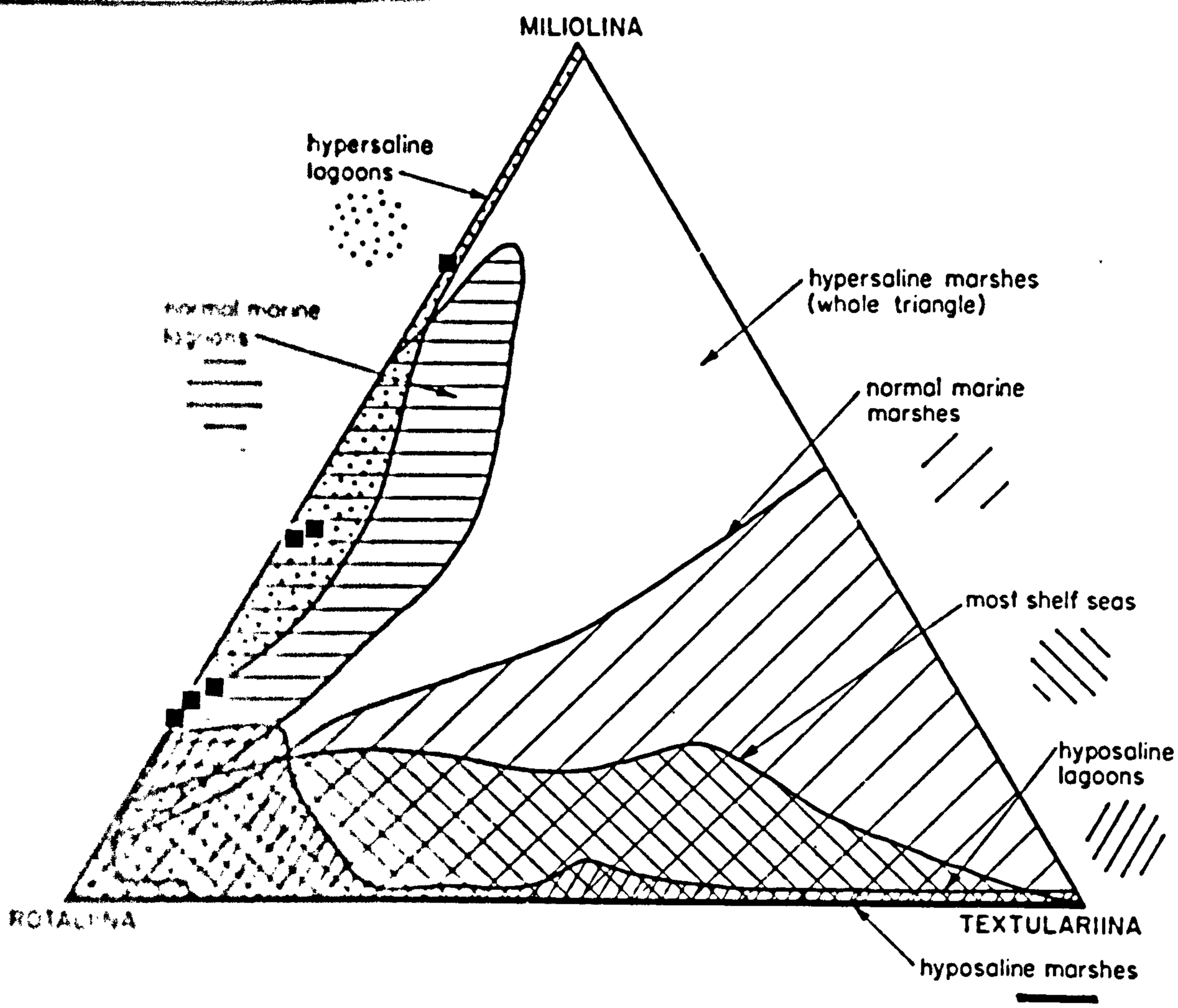

Fig.4-1a A triangular diagram with the major suborders, Textulariina Milliolina, and Rotaliina as end-members. The relative percentages of Foraminifera representing these three suborders of six samples in the Gachsaran are plotted. Overprojecting Fig.4-1a over Fig.4-1b, the plotted points of the Gachsaran samples fall close to the boundary of two environments, normal marine and hypersaline lagoons.

Fig.4-1b A triangular diagram of Murray (1973) representing different environments. These environments were the result of plotting samples representing different environments in a triangular diagram with the three major suborders, Textulariina Milliolina, and Rotaliina as end-members.

It is now well established from modern environments that both the number of species and individuals of Foraminifera increase with greater distance from shore (Parker, 1954; Bandy and Arnal, 1960). Such an increase has been attributed to decreasing dilution by sediment (Phleger, 1951; Walton, 1955). Exceptions to this rule, however, do occur in closed basins such as the Santa Cruz basin of southern California (Resig, 1958) and the Red Sea (Said, 1949). The data of Said (1949) show that the number of species is not less than 50 at shallow depths but it decreases dramatically to not more than 20 at greater depths. The low microfossil content of the Type 2 Gachsaran mudrocks thus could indicate deposition in a closed, or at least restricted, basin. The dominant planktonic nature of the Foraminifera in these mudrocks is also taken to indicate greater depth. Planktonic Foraminifera are known to increase in concentration relative to benthic Foraminifera with greater depth (eg. Bandy, 1956; Bandy and Arnal, 1960).

In conclusion, the Gachsaran mudrocks can be divided into two types based on their Foraminiferal content. These mudrocks were interpreted on the basis of consistent association with Foraminifera which have representatives today in Recent environments. By comparison with studies of Recent Foraminifera, the first type of mudrocks are interpreted as shallow water in origin, with deposition possibly taking place in hypersaline lagoons. The second type are considered to have been deposited in relatively deeper water environments but in a closed or restricted basin.

4.8 Summary

The predominance of illite and montmorillonite in the Gachsaran mudrocks is consistent with the general geology of the source area. An arid to semi-arid climate with minimal leaching is suggested. The colour, calcium content and fossil content of the mudrocks suggest two probable environments of deposition:

1. The green mudrocks with a high $CaCO_3$ content and benthic

Foraminifera suggest deposition in hypersaline shallow lagoons. The above conclusion is compatible with the predominance of illite over montmorillonite.

2. The dominantly red mudrocks are less fossiliferous than the first type but they are dominated by planktonic Foraminifera. These were deposited in a deeper water environment but in a closed or a restricted basin. The above conclusibn is also consistent with the higher amount of montmorillonite and lower quantity of kaolinite compared to the green mudrocks.

CHAPTER 5

CARBONATE ROCKS OF THE GACHSARAN

Microfacies, Lithofacies and Sedimentary Structures

CHAPTER 5

CARBONATE ROCKS OF THE GACHSARAN

5.1 Carbonate Rocks

In this account of the limestones of the Gachsaran Formation, the classification scheme of Folk (1959, 1962) is used. The scheme is based on the composition of the limestones, whether the principal components are skeletal grains (bioclasts), peloids, ooids, oncolites or intraclasts, and on whether the rock possesses (or is composed of) a micritic matrix or the grains are cemented by sparite.

An alternative and widely used classification is that of Dunham (1962), which is based on texture. The terms of Grabau (1904) inferring grain size (calcilutite, calcarenite, and calcirudite) can be useful in some instances.

Within the Gachsaran Formation twelve principal carbonate lithofacies/ rock types occur: micrites, pelmicrites, pelsparites, oomicrites, oosparites, biomicrites, biosparites, intramicrites, intrasparites, intrabiomicrites, intrabiosparites and oncolitic limestones. These different lithofacies are described and then compared with similar sedimentary facies in Recent settings and with ancient analogues. Churned bedding and sediments of cryptalgal origin are described separately.

It is hoped that this approach may help in establishing the conditions under which each type of lithofacies was deposited.

5.2 Micrites

There is every gradation between micrites and pelmicrites, and it is very difficult sometimes to separate between the two classes when there are very poorly defined peloids in the micritic rocks. Brown (1964) believed that all homogeneous micrites were derived from pelmicrites by the 'merging together' of the peloids during compaction. Although this theory may be applicable to some of the Gachsaran micrites, it can not be applicable to them all, since evidence of compaction in most cases is lacking. The Gachsaran micritic rocks are composed chiefly of micrite. The micrites have

Fig. 5-1 A micritic limestone showing calcite-filled cavities. Note the lensoid shapes of these cavities. These are interpreted as calcite pseudomorphs after gypsum. Slice.p.p.l. Mishraq, Iraq.

Fig. 5-2 A micritic limestone showing calcite-filled cavities. Note the lath-shaped crystals projecting from these cavities into the micrite matrix. The cavities are interpreted as calcite pseudomorphs after nodular anhydrite and the lath crystals as calcite pseudomorphs after anhydrite laths. Slice.p.p.l. Mishraq, Iraq.

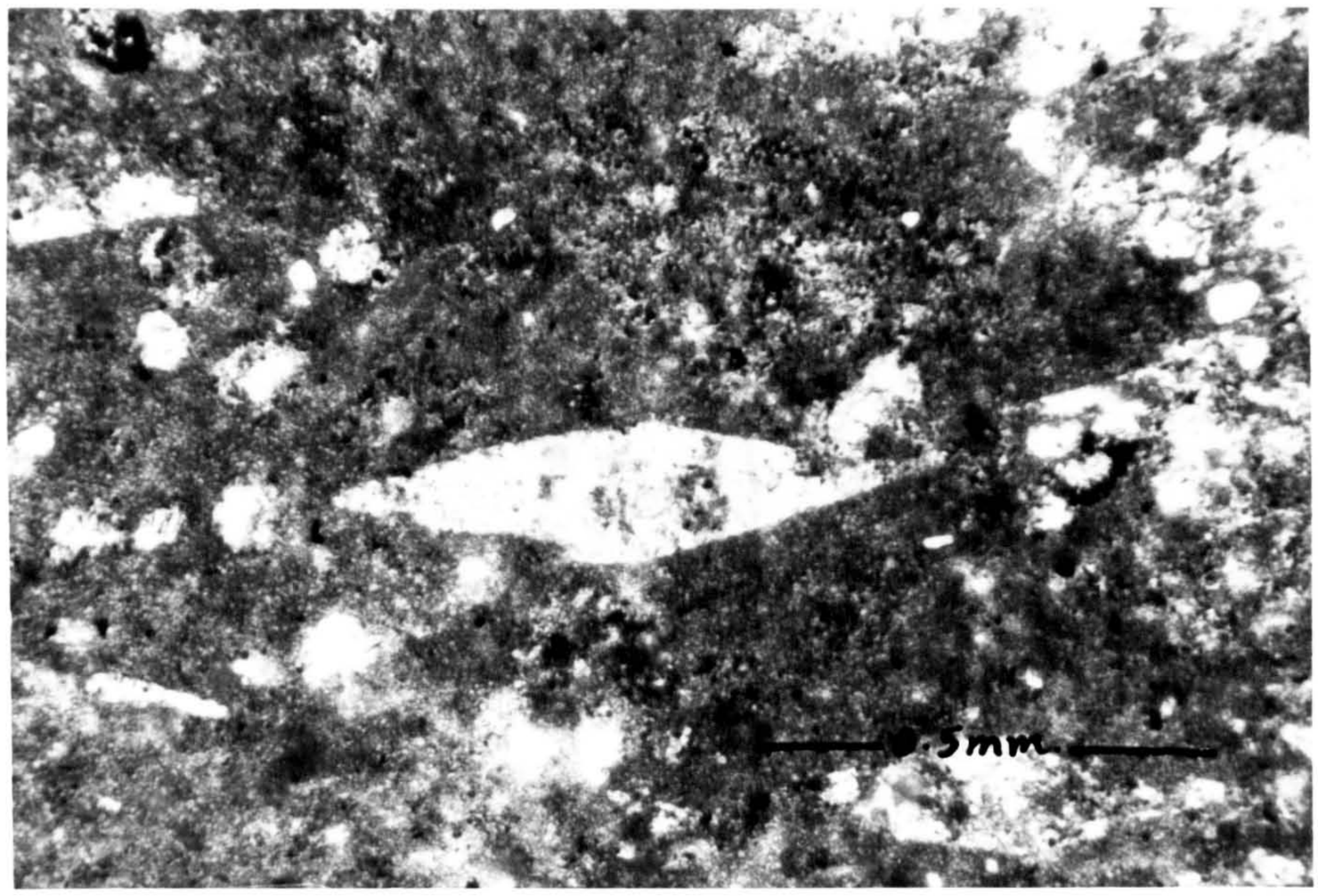
.5mm

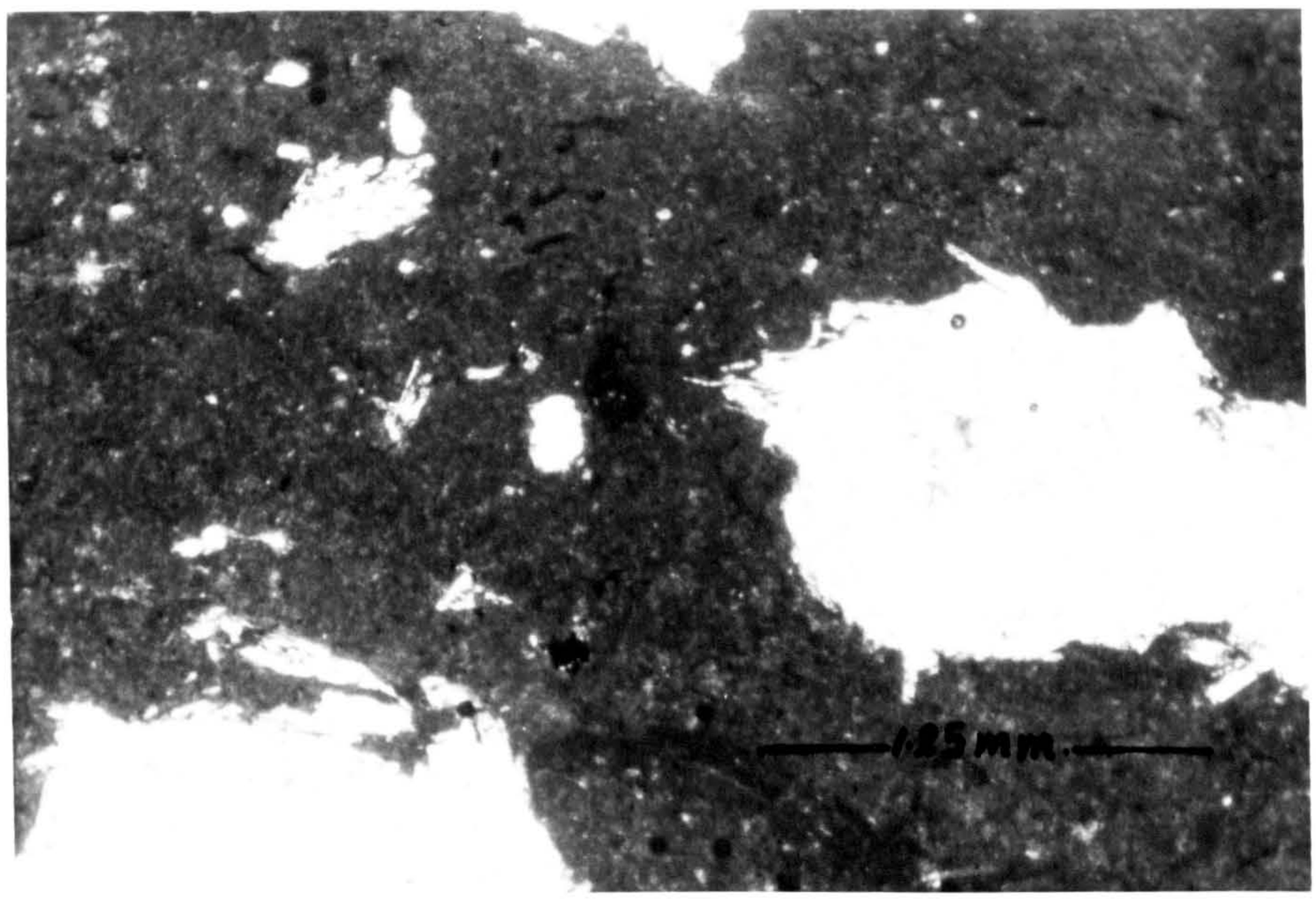
1.25 mm

an average diameter of 3-4μ, and silt-sized calcite grains are not uncommon. These micrites consist of either calcite or dolomite and it is difficult to distinguish between the two microscopically or by using staining techniques (see Chapter 6, Section 6.9.1).

The micrites range in colour from grey to brown, the brownish colour being caused mainly by organic matter. A common feature of most of these micrites is the presence of pyrite crystals (up to 7%) which are not uniformly distributed in the rock but rather occur in clusters. Fossil content is generally less than 5%. Calcite pseudomorphs after gypsum are also common (fig.5-1), and some contain calcite pseudomorphs after nodular anhydrite (fig.5-2).

Many of the Gachsaran micrites show clotted or grumelous texture, first defined by Cayeux (1935). The clots appear cloudy and brownish in colour and are of finer crystals than those surrounding them (see 6-4-A2).

The micrites typically range in thickness from 20cm. to 2 metres. They usually overlie gypsum beds or in other cases fossiliferous limestones and marls. In all cases they were found to be overlain by gypsum beds. These micritic rocks are often structureless; sometimes, however, they are interlaminated with pelmicrites or pelsparites (see Section 5.9), forming in some cases stromatolites or cryptalgal laminites.

5.2.1 Origin of Micrite

The origin of micrite is somewhat controversial. Cloud and Barnes (1948) and Cloud (1962) considered the lime mud of the Bahamian sediments as a non-skeletal precipitate, largely physiochemical. However, Lowenstam and Epstein (1957) by O^{18} analysis have shown that the sedimentary aragonite needles of these sediments may be a decay product of calcification of calcareous algae. It was suggested that soon after deposition and some compaction, the needles lost their acicular shape. Recent work has shown that lime mud is produced by:

1. Calcareous green algae, following the disintegration of their fragile skeletons. Stockman et al. (1967) and Neuman and Land (1975) concluded that there was more than sufficient lime mud produced in south Florida and the Bahamas by algal disintegration (particularly by the green algae Penicillus) to account for the lime mud there.

2. Biological and mechanical breakdown of resistant skeletons such as molluscas, algae and foraminifera.

Mathews (1966), in a study of the genesis of Recent lime mud from southern British Honduras, found that physical breakage and abrasion in an agitated environment are the dominant processes by which lime mud is produced on the carbonate shoals, whereas the main factors in the in situ production of lagoonal mud appears to be (a) the inherently fragile nature of the mollusc shells and foraminifera tests of the lagoonal environment, (b) the removal of binding organic matter from mollusc shells, (c) the weakening of larger skeletal particles by the activity of boring micro-organisms, and (d) the mastication, ingestion and perhaps even simple movement of sediment by the vagrant benthos.

Within micrites in the Gachsaran Formation, the often close association of micrites with skeletal grains may suggest an origin through biological and mechanical breakdown of less resistant skeletal grains. However, it is difficult to exclude other origins such as algal disintegration or direct physiochemical precipitation of $CaCO_3$.

5.2.2 Environment of deposition

Micrite can form as a result of the different processes noted above. Depending on the level of agitation within the area of formation, the lime mud may either accumulate in situ if calm conditions persist, or be removed by waves and tidal currents to be carried to other parts of the basin if the energy level is relatively high. Many of these micrites are associated

with calcite pseudomorphs after gypsum, some with nodular anhydrite. This, together with the above mentioned position in the sequence, suggests that these micrites were deposited in an intertidal environment (it should be noted that fenestral fabric does not occur in these sediments).

Other micrites probably accumulated in protected lagoons and some may have formed in deep water offshore areas, below wave base.

5.3 Pelmicrites and Pelsparites

5.3.1 Pellets and Peloids

The term 'peloid', first introduced by McKee and Gutshick (1969) to denote all aggregated bodies (micritic pellets) without implying any particular mode of formation, is used in this work. Illing (1954) noted the formation of abundant pellets and aggregate grains partly by a process of faecal agglutination and partly by precipitation of aragonite on and in grains and clusters. Hadding (1958), however, attributed the apparent pelleting to clotting of the sediment following the appearance of local centres of crystallisation associated with the bacterial decomposition of algae and concurrent deposition of more carbonate. Beales (1965), on the other hand, attributed pelleting to organic agglutination, inorganic precipitation and cementation, recrystallisation, or a combination of these processes. Ginsburg (pers. Comm. in Beales, 1965), considered that varieties of Foraminifera played an important part in the binding of pellets and debris into aggregate grains and lumps.

Peloids in the Gachsaran limestones are of several different shapes, ranging from ellipsoidal to spherical, and are similar to those described by Illing (1954), Folk (1962), Brown (1964), Beales (1965) and others. They are distinguished from ooids by a lack of radial or concentric structures and from intraclasts by a lack of complex internal structures, uniformity of shape and size (Folk, 1959). The Gachsaran intraclasts are distinguished

from peloids by their irregular and large size as many of the intraclasts lack any internal structure. The Gachsaran peloids are devoid of any internal structure and their crystals are equigranular, generally ranging from 3-5μ in diameter. A mottled appearance, however, may show, due to the inorganic framework set in the peloid (fig.5-3). Generally speaking, peloids have a brownish colour, probably due to the high organic content. Other peloids may show a deeper brown colour which is caused by the presence of opaque organic specks, irregular in shape, and ranging from 4 to 8μ in diameter (fig.5-4). The organic matter is concentrated between the calcite crystals of the peloids; the finer the crystals of the peloids are, the higher the concentration of organic matter, and consequently the peloid would look darker. Brown (1964), working on the petrography of Upper Jurassic beds from Dorset, England, attributed the colour difference to the crystal size of the micrite and suggested that brown pellets have crystals with diameters of 2μ or less, and pellets of a grey colour have crystals with diameters of 4 microns. The features of the Gachsaran peloids indicate that the colour is not only a factor of crystal size but of organic content too, since some peloids are richer in organic matter than others. Individual peloids range in diameter from 0.12mm. to 0.24mm. in their longest diameter.

Within the micrite of some peloids, large, often rectangular shaped calcite crystals are present. Black (1961) noticed similar crystals and attributed them to replacement of anhydrite. These coarser crystals in the peloids may be original sediment or the result of neomorphism of the original micrite or intra-pellet aragonite cement.

The margins of many peloids are often poorly defined, which is probably a neomorphic effect (fig.6-28). Recent faecal pellets consist of ultra fine-grained calcareous mud with some organic matter, chitinous flakes and siliceous remains (Illing, 1954). In time this mixture changes to a uniform micrite (Purdy, 1963a). Faecal pellets of the Gachsaran are identified by

Fig. 5-3 A pelmicrite showing a mottled appearance caused by different concentrations of organic matter. Slice.p.p.l. Mishraq, Iraq.

Fig. 5-4 A pelmicrite. Note the black colour of some of the peloids caused by the high concentration of opaque organic specks. Slice.p.p.l. Hammam Al-Alil, Iraq.

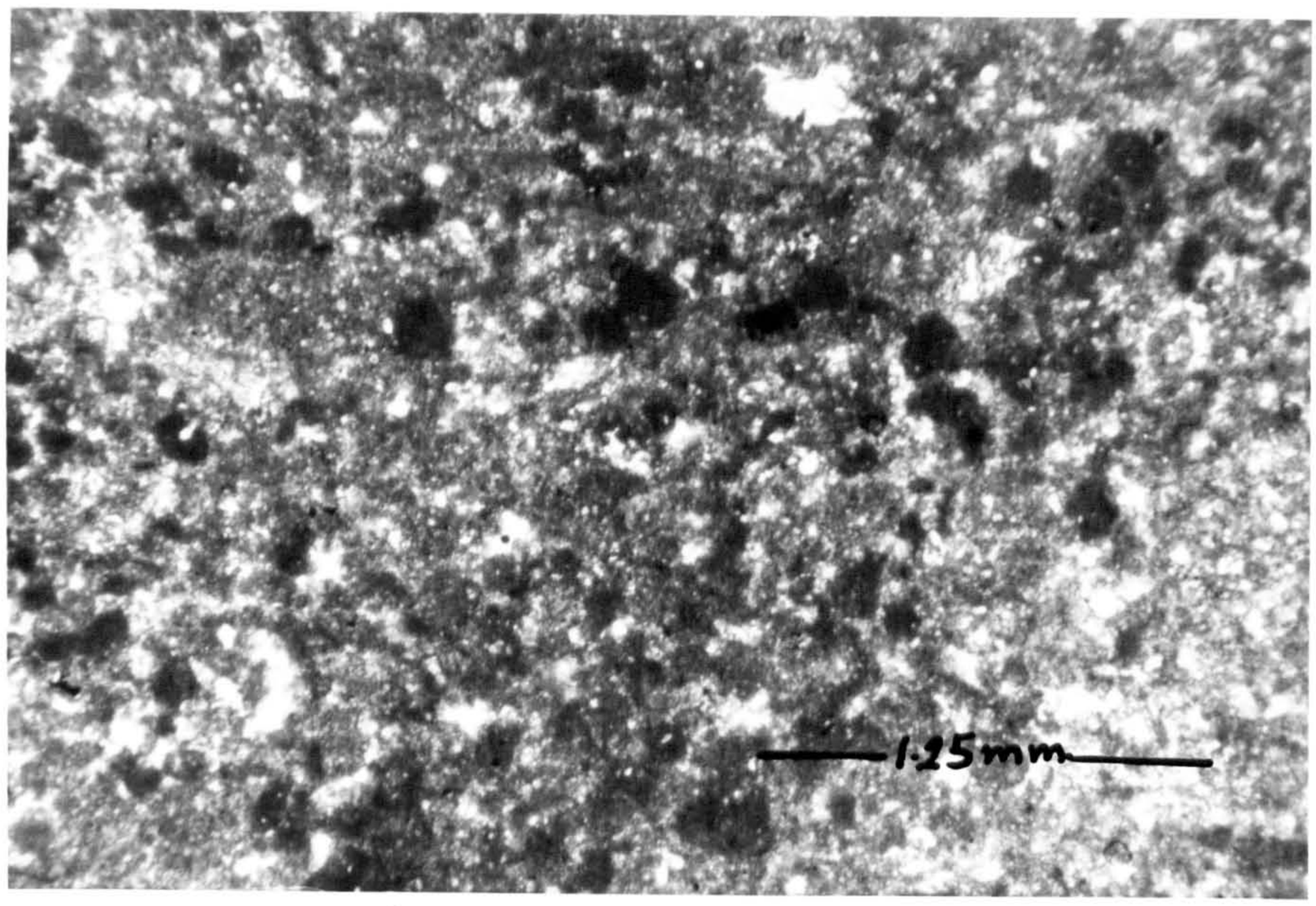
1.25mm

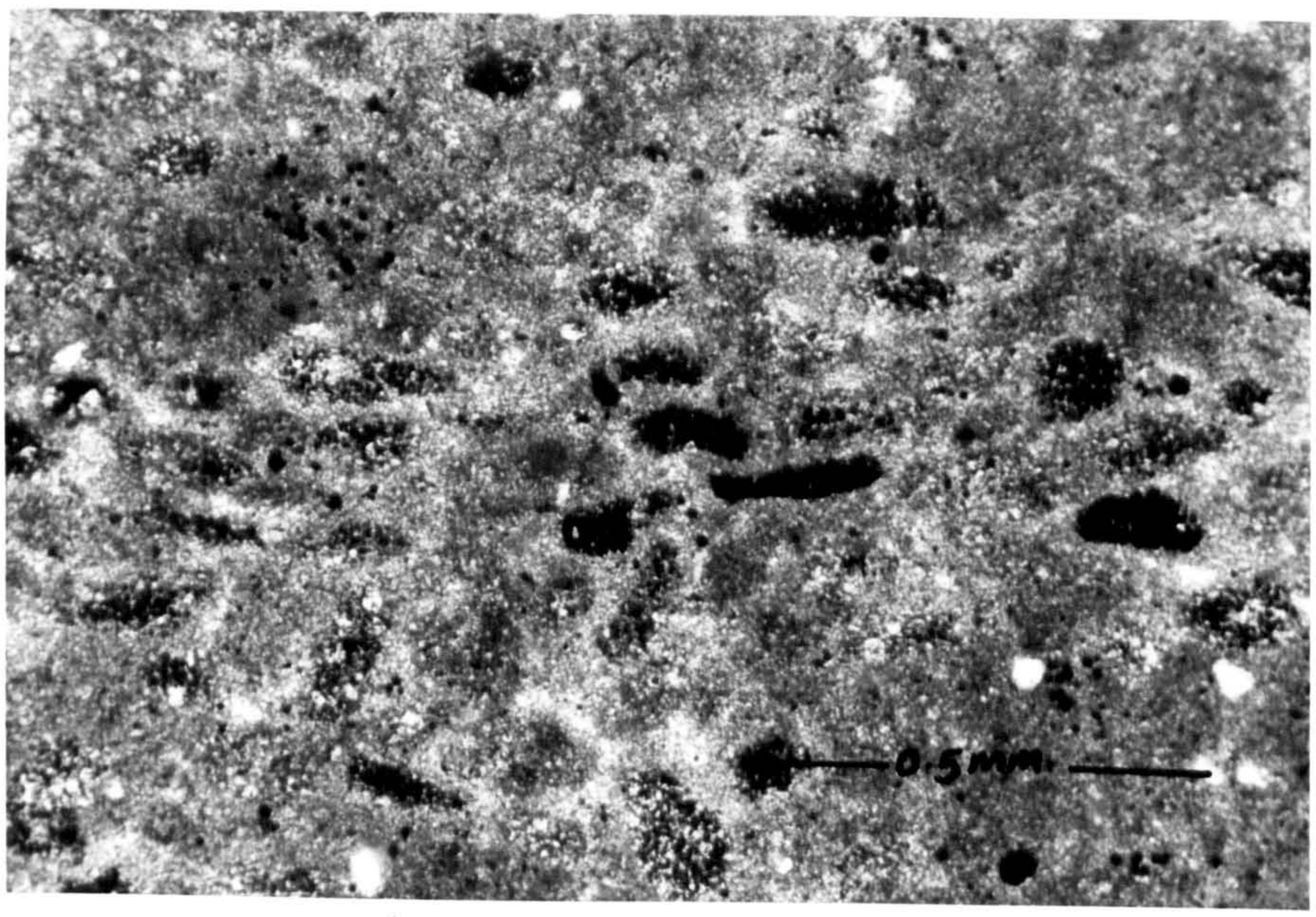
0.5mm.

their ellipsoidal shapes and uniform size (fig.5-5).

5.3.2 Pelmicrites

Pelmicrites of the Gachsaran are not very fossiliferous but fossils present include Foraminifera, bivalves, gastropods and algae. Gypsum is present as pore filling and calcite pseudomorphs after gypsum is often present. It is not uncommon to find that in some pelmicrites, the peloids are represented by moulds (fig.6-37). This type of texture can be referred to as pelmouldic porosity. This term is analogous to the oomouldic porosity described from the dolomitised Jurassic limestone in Arkansas (Bathurst, 1975).

Pelmicritic beds of the Gachsaran usually range in thickness from 20cm. to 4 metres. They frequently overlie marls, and so form the lower part of the limestone members, but they are also interbedded with biosparites and biomicrites. Laminations and other sedimentary structures associated with pelmicrites are described below.

Alternating laminae of organic-rich pelmicrites with organic-poor, very fine micrite laminae are common (fig.5-6). These laminae range from 4 to 3.5mm. in thickness, but it may exhibit much thicker developments (1.5cm.). The laminae are fairly uniform in thickness, thinner laminae die out laterally. In some cases, the organic-rich pelmicritic laminae fine upwards into organic-poor micrite (fig.5-7). In one instance, laminites pass upwards into churned bedding (through bioturbation). Calcite replaced nodular anhydrite layers (fig.5-8), solitary nodules of calcite after nodular anhydrite (fig.5-6), and calcite pseudomorphs after gypsum are common. In another sample, when these laminae are followed vertically upwards, they pass into thicker developments of calcite replaced nodular anhydrite (fig.5-9). The laminae occurring directly beneath the nodules are crinkly (fig.5-9). In other instances, these laminae were found to be wave-rippled (fig.5-10). The ripple offsets of these wave ripples are generally composed

Fig. 5-5 A pelmicrite showing faecal pellets. Note the uniform ellipsoidal shapes of these pellets. Slice.p.p.l. Mishraq, Iraq.

Fig. 5-6 Alternating laminae of organic-rich pelmicrites with organic-poor very fine micrite laminae (grey). The laminae are graded (see Fig.5-7). The lower part of the sample shows the presence of tubular extensions of a burrow system. The upper part of the sample is extensively bioturbated so that the laminae are destroyed. Note also the presence of solitary nodules of calcite after anhydrite. (arrows). Mishraq, Iraq.

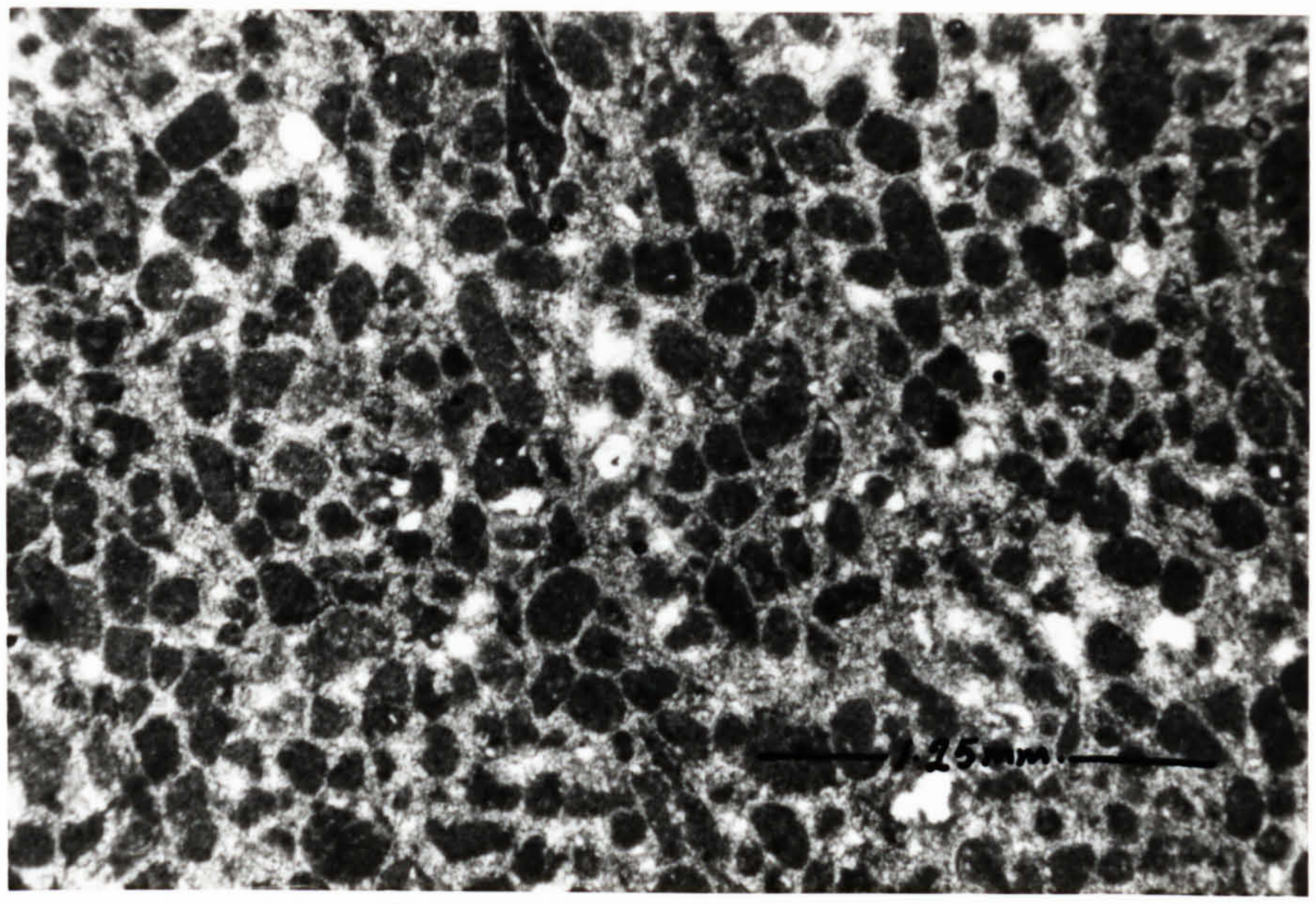
1.25mm

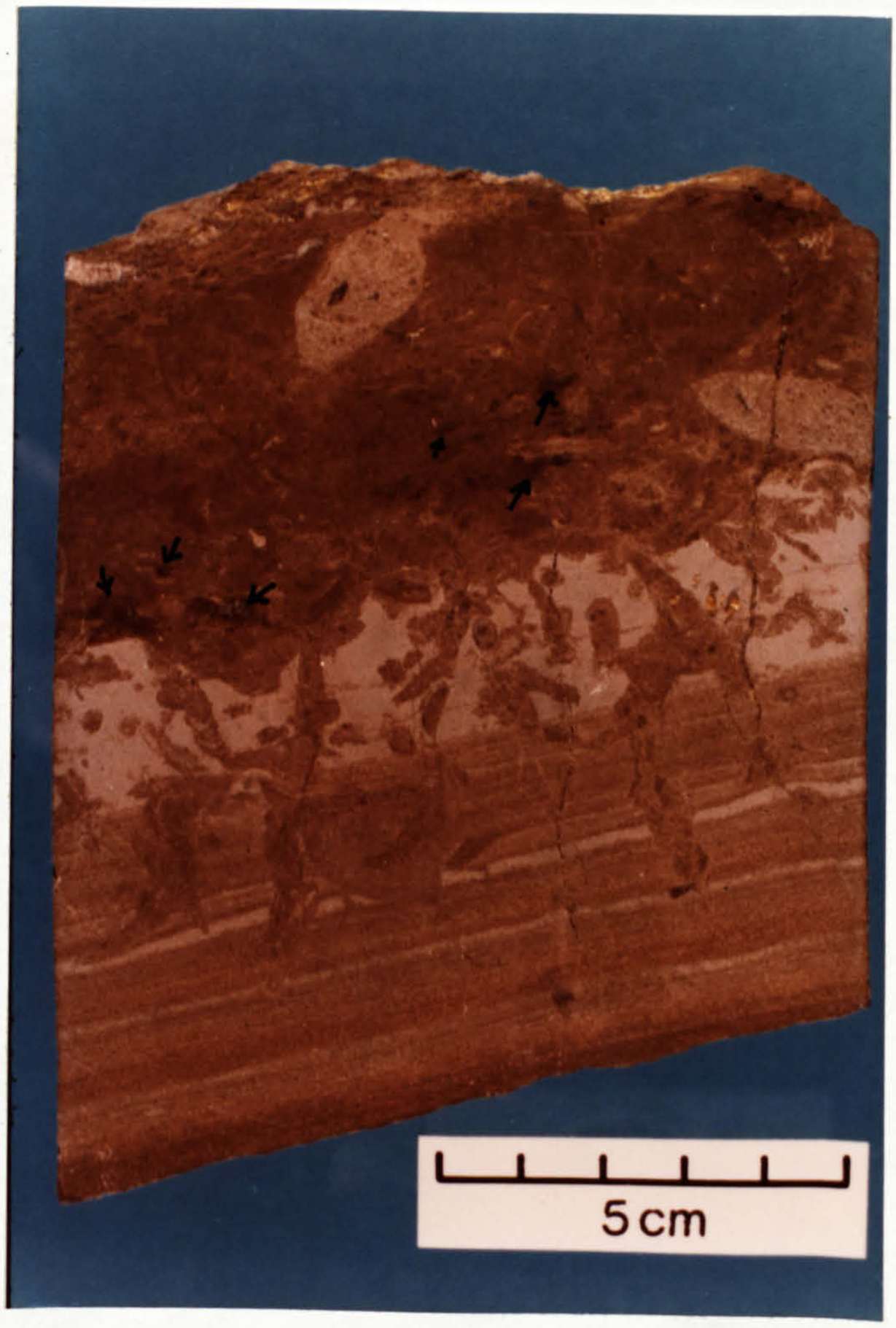
5 cm

Fig. 5-7 Graded laminae. The organic-rich pelmicrite laminae fine upwards into very fine organic-poor laminae. Mishraq, Iraq.

Fig. 5-8 Alternating laminae of calcite after anhydrite nodules. Note the presence of sulphur in the centre of some of these nodules. Mishraq, Iraq.


1cm


5 cm

Fig. 5-9 Alternating pelmicrite-micritic laminae passing upward into thick development of calcite pseudomorphs after nodular anhydrite. Notice the crinkly nature of the laminae directly beneath the nodules. Mishraq, Iraq.

Fig. 5-10 Pelmicritic-micritic wave rippled laminae. Mishraq, Iraq.


5cm


5cm

of cross laminae arranged in groups forming cross-stratal offshoots.

The pelmicrite-micrite laminae clearly formed in a protected environment and in their organic matter show many similarities to oil shales. Their depositional environment is likely to be lagoons or ponds within a supratidal environment. The replaced nodules of anhydrite are taken to indicate subaerial conditions and desiccation of the lagoon or pond. The churned bedding was formed as a result of increased bioturbation, possibly brought about by slower sedimentation.

Pelmicrites of algal origin are described elsewhere (see Section 5.9).

5.3.3 Pelsparites

These peloids are very much like those associated with pelmicrites. The peloids have sharp contacts because of the large calcite crystals of the surrounding matrix. The size of the sparry calcite crystals depends on the degree of packing of the peloids, i.e. larger sparry crystals are present when the peloids are loosely packed and smaller when the peloids are densely packed. The peloids of this type of facies are better sorted and possess more of a preferred orientation compared with those in the pelmicrites. This probably arises from deposition under more agitated conditions. Pelsparites are not as common as pelmicrites but they occur in beds ranging in thickness from tens of centimetres up to 10 metres in thickness, as in Ooti Limestone of Makhul (fig.5-11). There, occasional thin beds of oriented fossils occur within the pelsparite bed (fig.5-12).

In some examples, pelsparites in the Gachsaran are associated with ripple marks, as in Hamam Al-Alil (fig.5-13). These are symmetrical, wave-formed ripples. Their crests are rounded to flattened in shape. The ripples show crest bifurcation, and the wave length of these ripples average about 40cm., and 10cm. in height. The ripple index L/H is about 4. This type of ripple mark can form in tidal flats and shallow subtidal situations (Reinech

Fig. 5-11 Ooti limestone of Makhul.

Makhul, Iraq.

Fig. 5-12 Thin laminae of oriented fossils representing storm deposits. Makhul, Iraq.

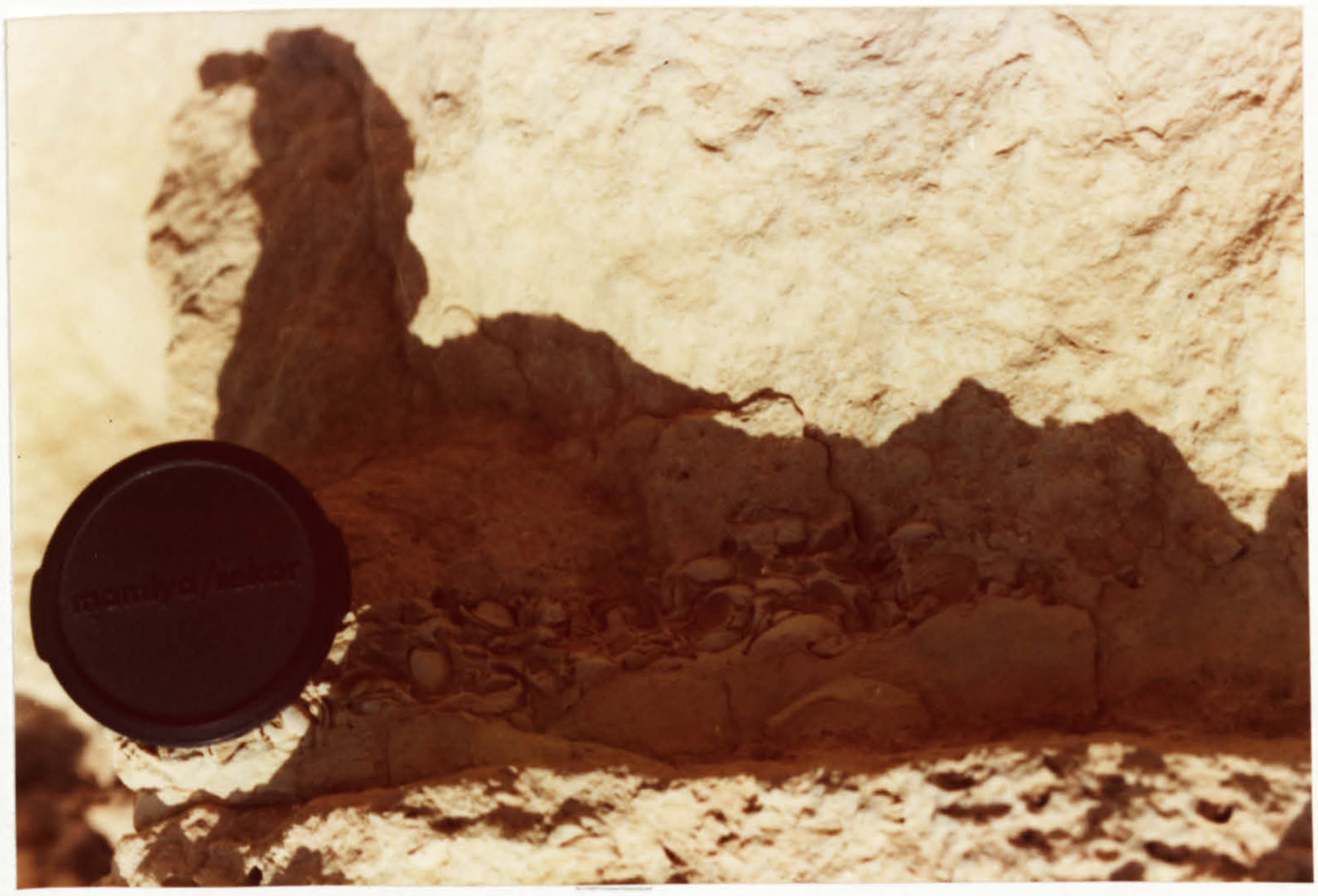

Fig. 5-13 Ripple marks. Note the symmetrical form of these ripples. The rock is a pelsparite. Hammam Al-Alil, Iraq.

Fig. 6-14 Oomicrite showing ooids with recognisable cortical layers. Slice.p.p.l. Mishraq, Iraq.

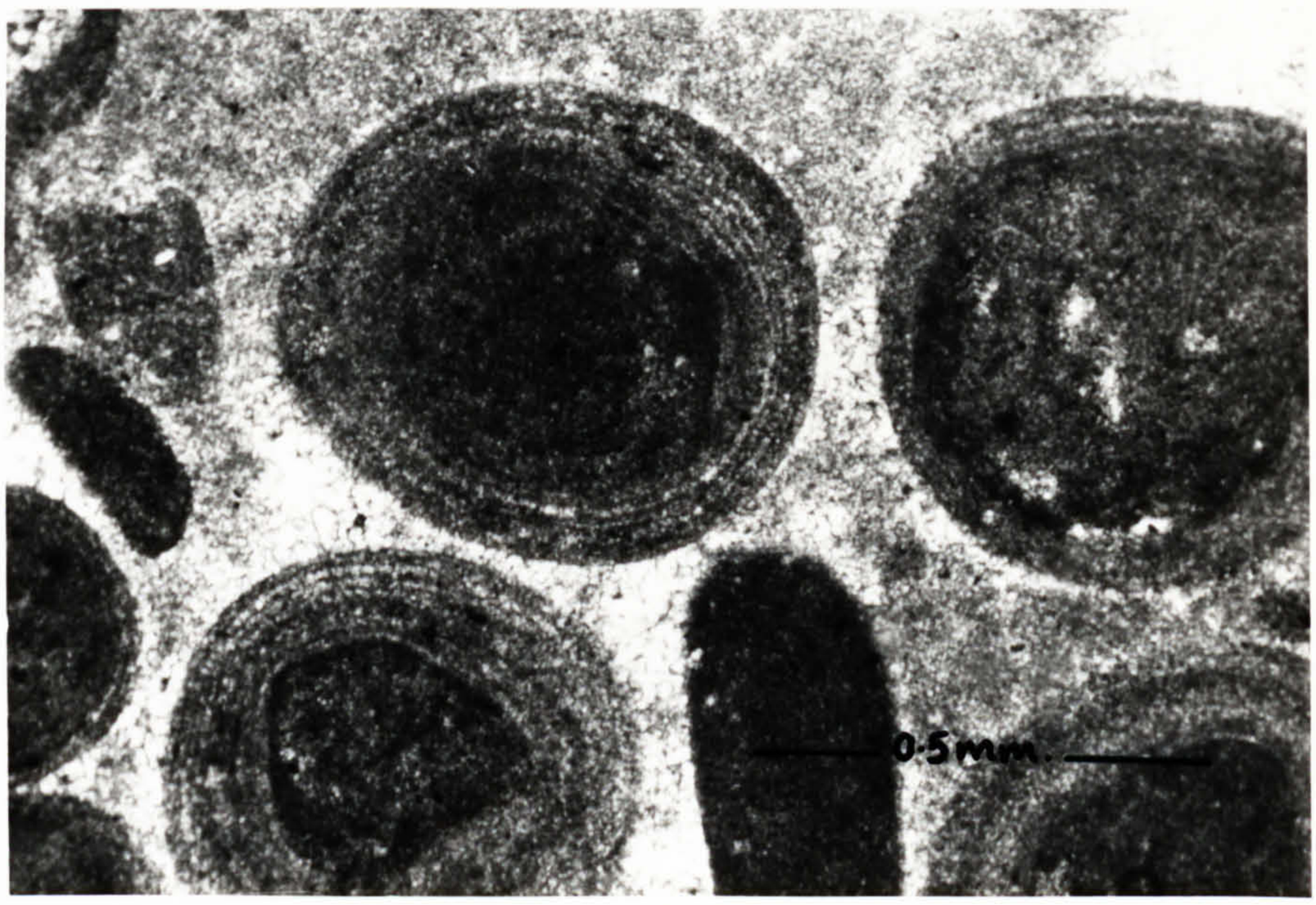
0·5mm.

and Singh, 1973). Pelsparites interlaminated with pelmicrites are not uncommon (see Section 5.9).

5.3.4 Depositional Environment

In the Arabian Gulf, peloids associated with Foraminifera occur at depths of less than 5 metres and are typical of wide tidal flats (Wagner, et al., 1973). Also, peloids with skeletal fragments are the predominant sediment type of subtidal and intertidal environments of NE Qatar (Shinn, 1973). Peloidal sediments occur also on lagoon terraces in the Arabian Gulf (Evans, et al., 1973).

It is inferred here that both types of pelleted rocks of the Gachsaran (pelsparites and pelmicrites) deposited in shallow subtidal-intertidal environments. The pelsparites were deposited in more agitated conditions than pelmicrites. This is indicated by the better sorting and preferred orientation of the peloids and the occurrence of wave ripples.

5.4 Oosparites and Oomicrites

Ooids are small spheroidal to ellipsoidal bodies, distinguished by the possession of concentrically laminated cortical layers around a nucleus. In modern examples the ooids are composed of cryptocrystalline or acicular aragonite, whilst ancient ooids are of calcite.

The ooids present within the Gachsaran limestones range from 1 to 1.2mm. in diameter. Their cortical thickness ranges from 20 to 120μ. The contrast between the diameter of the ooids and their cortical thicknesses illustrates that it is chiefly the nuclei which determine the size of the ooids. The ooids have generally suffered micritization which has caused the obliteration of their internal structure. Hence, it is very difficult to determine the thickness of the individual cortical layers (fig.6-32). Where individual cortical layers could be discerned, they had an average thickness of about

6μ (fig.5-14). The cortex chiefly consists of equidimensional interlocking calcite crystals (fig.5-15). Closer examination reveals that crystals are anhedral to subhedral with boundaries that are straight, curved, or irregular (fig.5-16). The average diameter of these calcite crystal is 5μ. No laminae can be discerned within the cortex of the ooids using S.E.M., and calcite crystals do not appear to show any preferred orientation. Organic matter, commonly associated with pyrite and clay minerals (identified by Edax)(fig.5-17), are distributed evenly throughout the ooid, possibly forming a network around individual calcite crystals.

Pellets generally serve as nucleii to the ooids, also quartz grains, skeletal fragments and small intraclasts. Most of the ooids are micritized and in many cases it is impossible to distinguish the nucleus from the cortex. More often, however, vague laminations surrounding the nucleus can be discerned. Radial structures were not observed within these ooids. If radial structures were originally present, then micritization is thought to be the main cause of its obliteration and destruction.

In some oolitic limestones, coated grains are present. These have an average diameter of 4mm. and exhibit various morphologies. Most of the grains are skeletal fragments and the external morphology of the grain depends primarily on the shape and size of the component skeletal fragments (figs. 5-18, 19). Coated grains of this type have been termed pisoliths by Shinn (1973) and compound ooids by others.

Three different microfacies can be recognised within the Gachsaran oolitic limestones:

5.4.1 <u>Oolitic Microfacies</u>

A - The ooids (.2mm. in diameter) are well sorted in this microfacies and are interlaminated with laminae of bivalve fragments. The latter are thinner than the oolitic laminae and range from 1 to 4mm. in thickness. The bivalves are aligned parallel to the plane of the bedding. The oolitic

Fig. 5-15 SEM Micrograph of a cortex of ooids in the Gachsaran. The crystals are anhedral to subhedral with straight, curved or irregular boundaries. Note that no laminae could be identified within the cortex using SEM. Hammam Al-Alil, Iraq.

Fig. 5-16 A close up of the above figure.

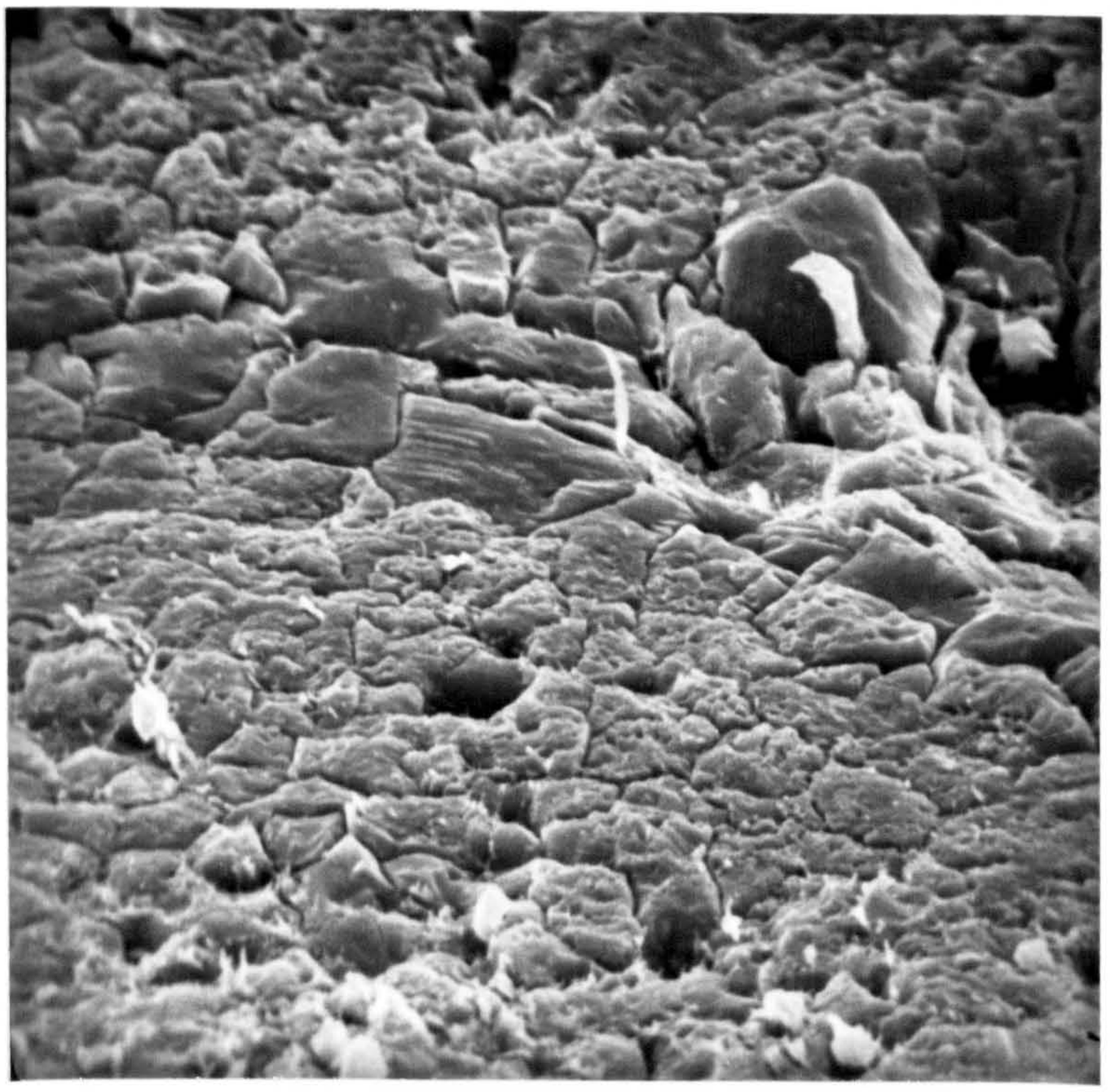

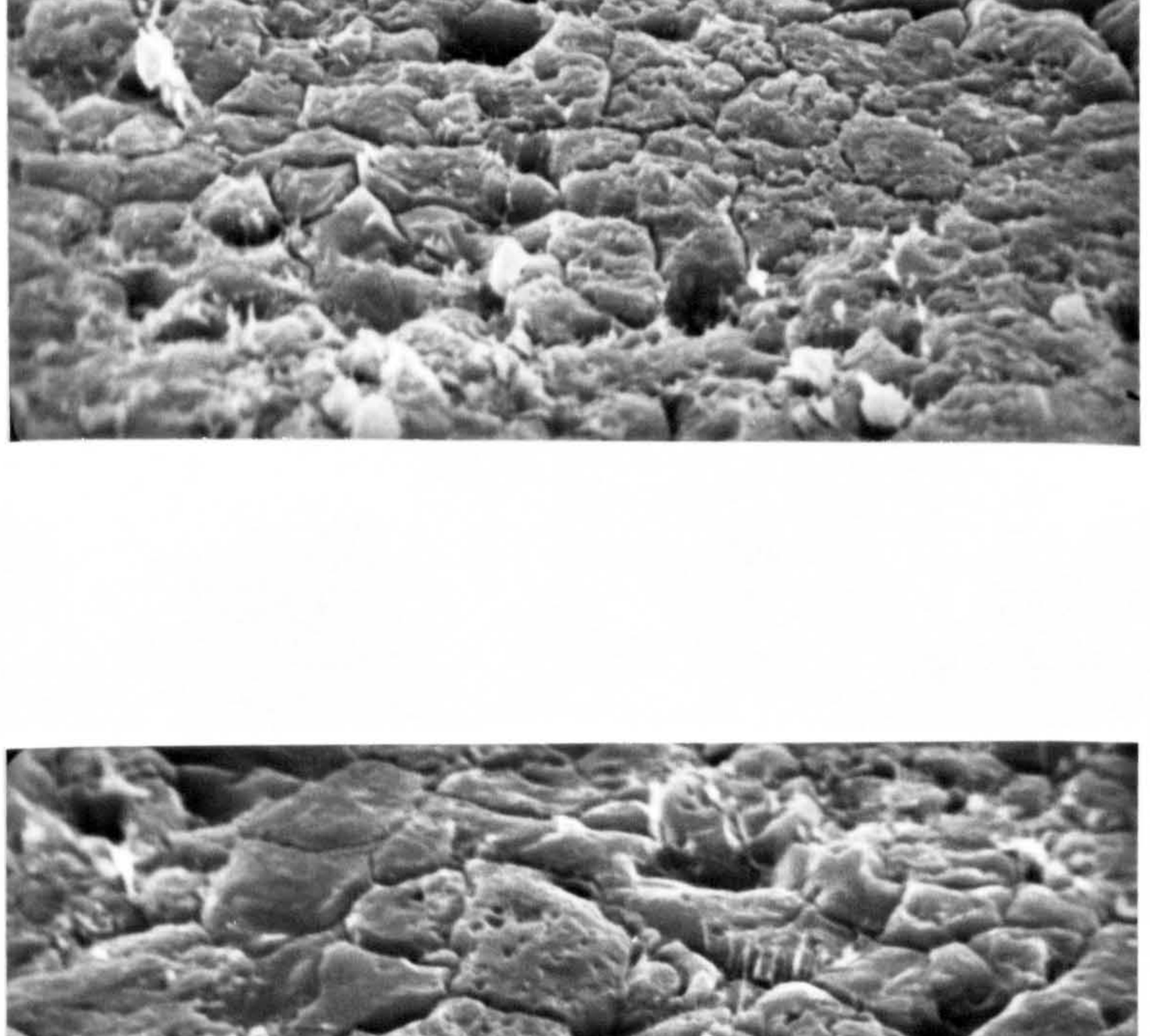

Fig. 5-17 Chemistry of ooids.

(a) Element distribution map for calcium of the region shown in Figs.5-15, 16.

(b) A 'spot' EDAX analysis showing the distribution of elements in a calcite crystal in an ooid cortex.

(c) A 'spot' EDAX analysis showing the distribution of elements in between the calcite crystals in an ooid cortex.

Fig. 5-18 A skeletal fragment with an oolitic coating. Note the thicker coating on the depressed part of the allochem. Slice.p.p.l. Hammam Al-Alil, Iraq.

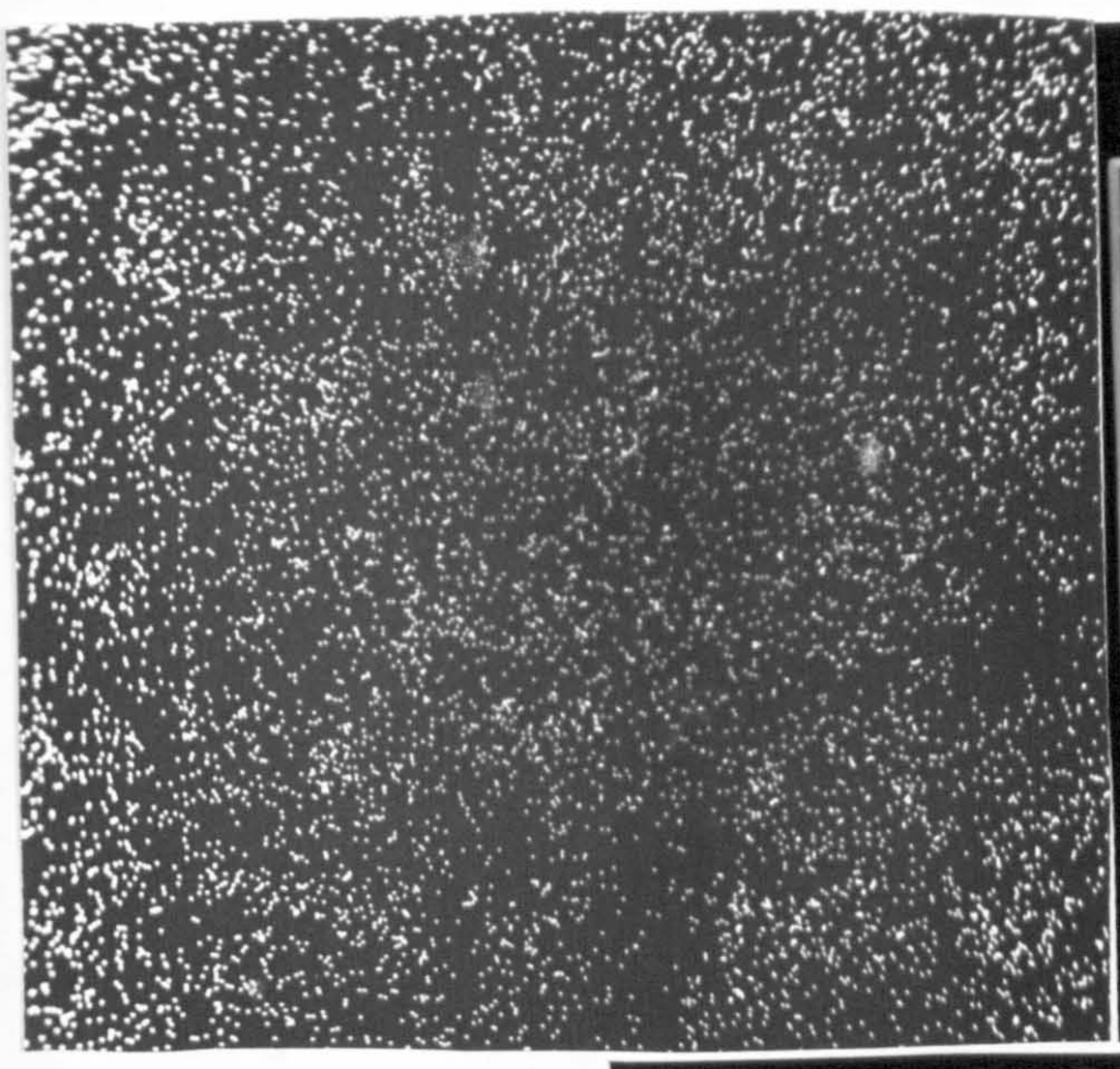

a

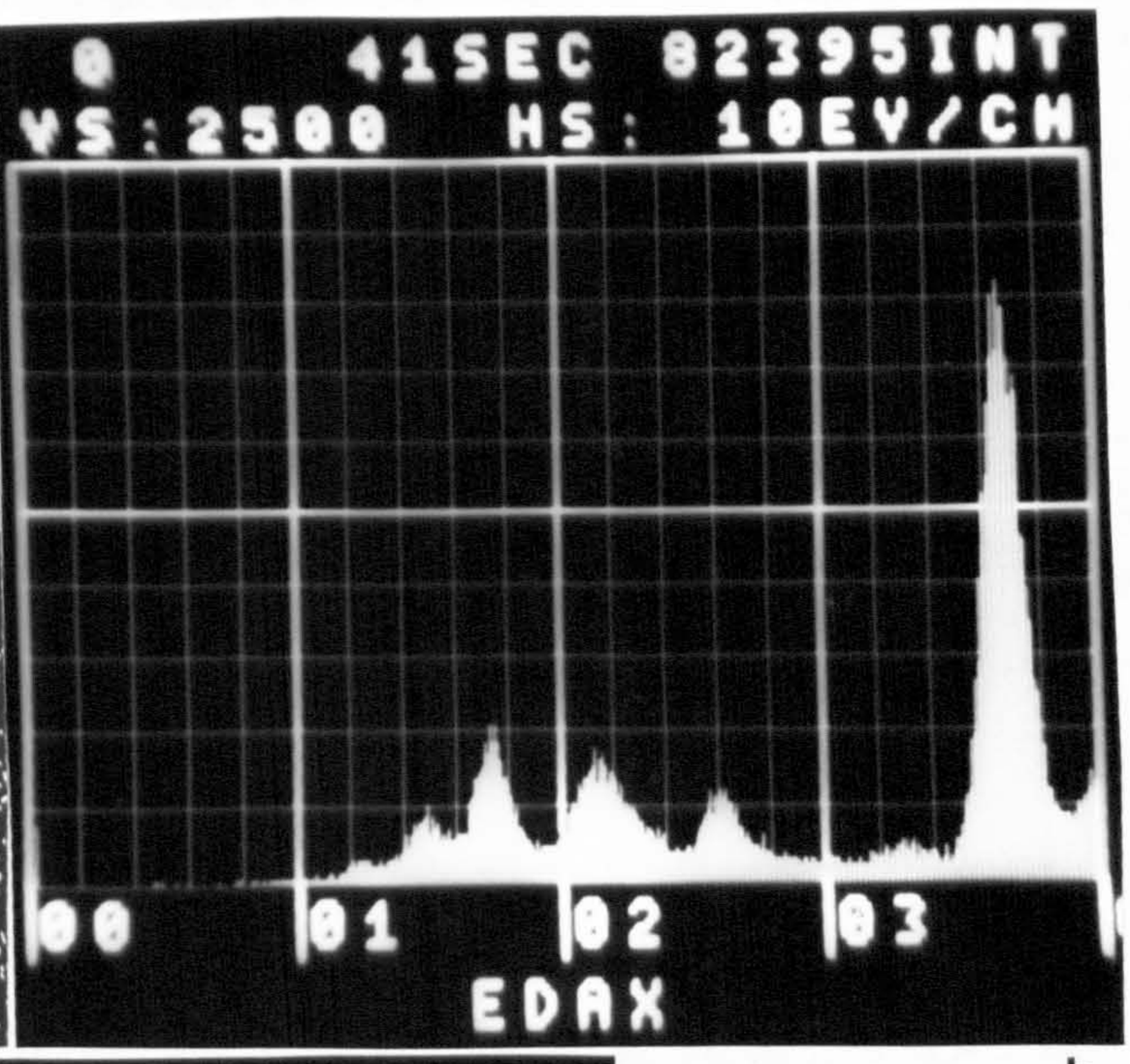
0 41SEC 82395INT
VS:2500 HS: 10EV/CH
00 01 02 03
EDAX

b

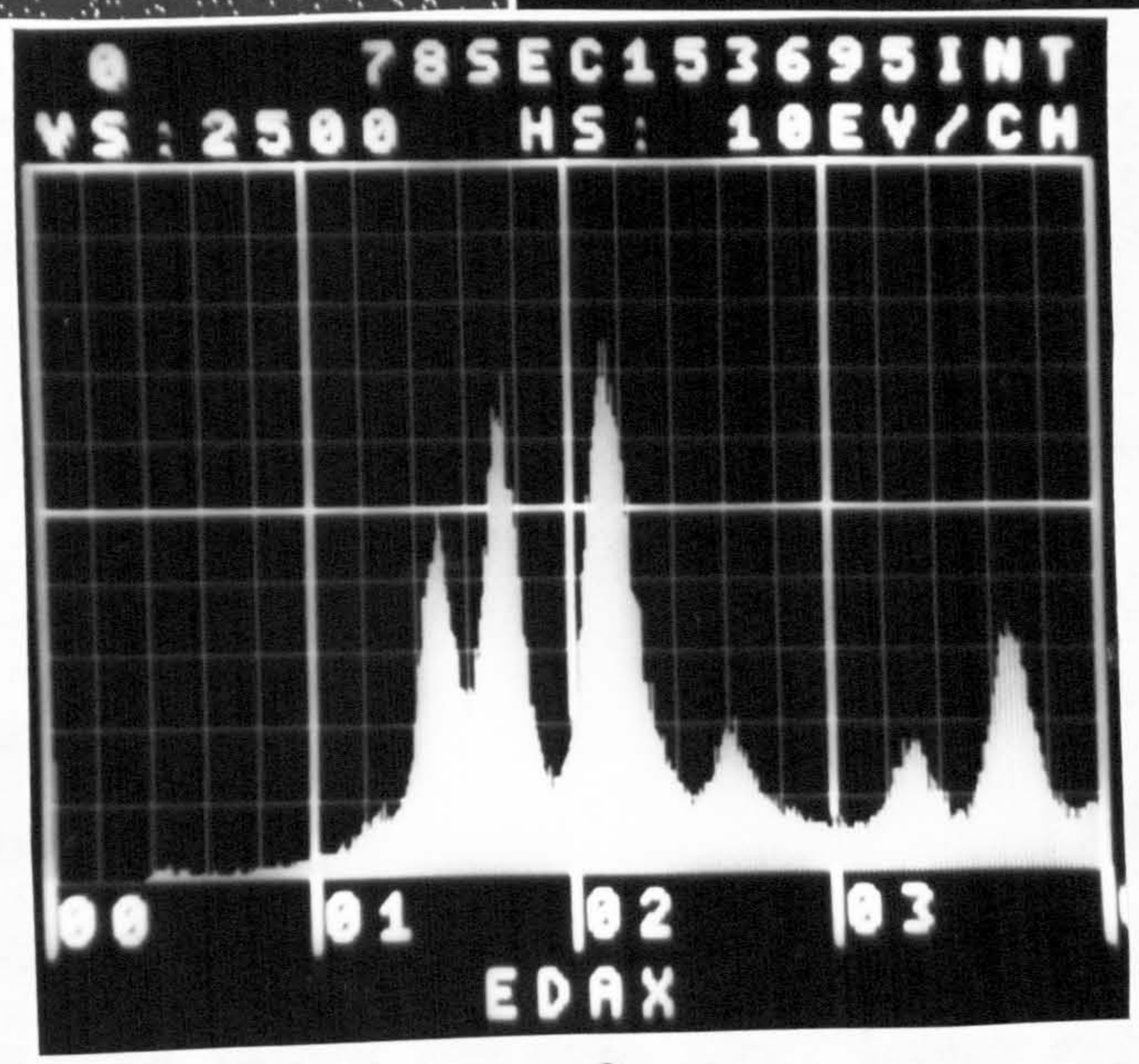
0 78SEC153695INT
VS:2500 HS: 10EV/CH
00 01 02 03
EDAX

C

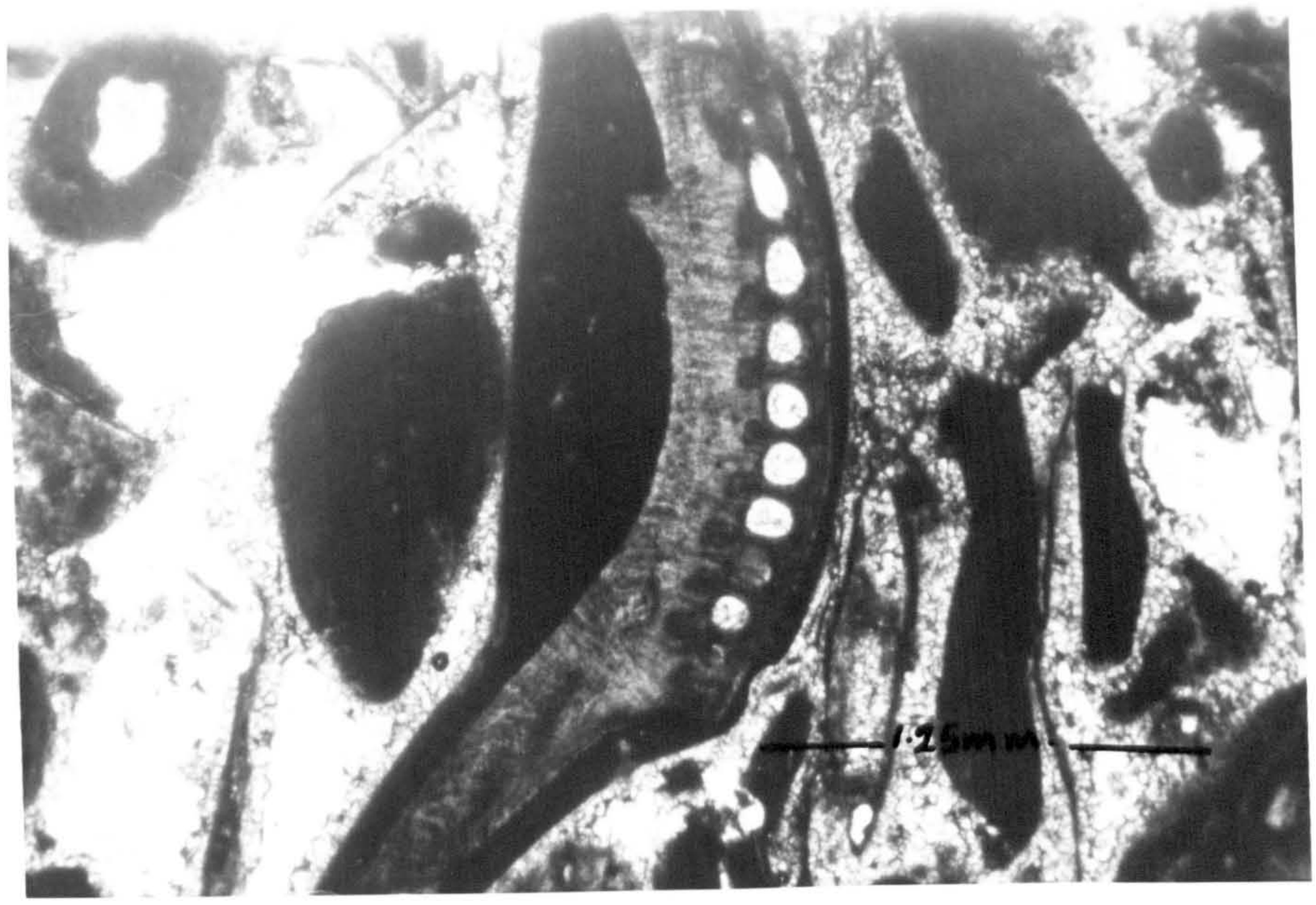
1.25mm

1

laminae are cemented by sparite (fig.6-42). Herring-bone cross-bedding is also associated with this facies type (fig.5-20). This type of cross-bedding consists of foreset laminae dipping in opposite directions. Set thicknesses are 3 to 13cm. and dip up to 25°. Herring-bone cross-bedding is indicative of tidal environments (Reineck and Singh, 1973).

B - These oolitic limestones consist almost entirely of ooids (≻ 90%), with diameters ranging from 0.1 to 0.6mm., contained within a micritic matrix. No associated sedimentary structures were detected.

C - These oolitic limestones contain a fair proportion of pellets and coated skeletal grains (fig.5-19) within a micritic matrix. The percentage of ooids in these rocks ranges from 25 to 40% and diameters of ooids from 0.6 to 1mm.

In general, oolitic limestones of the Gachsaran occur in beds ranging from 1 to 3 metres in thickness.

5.4.2 Depositional Environment

Ooids are usually considered to form in shallow, agitated environments (Eardley, 1938; Newell, et al., 1960; Purdy, 1963a, b). They are also known to form in shallow quiet waters (Freeman, 1962; Loreau and Purser, 1973). The optimum conditions for ooid growth in the Bahama Banks is around 1.8 metres below low water (Bathurst, 1975). In the Arabian Gulf, the environment most favourable for ooid formation is a tidal delta (Kinsman, 1964; Loreau and Purser, 1973), but they also form in protected areas such as tidal flats. An attempt here is made to compare as closely as possible the Gachsaran oolitic facies with those occurring today along the coasts of the Arabian Gulf. The comparison is based upon size of ooids, cortex thickness, percentage of ooids in any one sample, and sedimentary structures.

Oolitic sand (ooids 100-400u in diameter) and skeletal fragments occur along the subtidal and intertidal flats of Sabkha Matti. These beach deposits

Fig. 5-19 Limestone consisting mostly of ooids together with some peloids and skeletal grains with oolitic envelopes. Slice.p.p.l. Mishraq, Iraq.

Fig. 5-20 Herring-bone cross-bedding. Limestone is composed of ooid-bivalve laminae. Tell-Afar, Iraq.

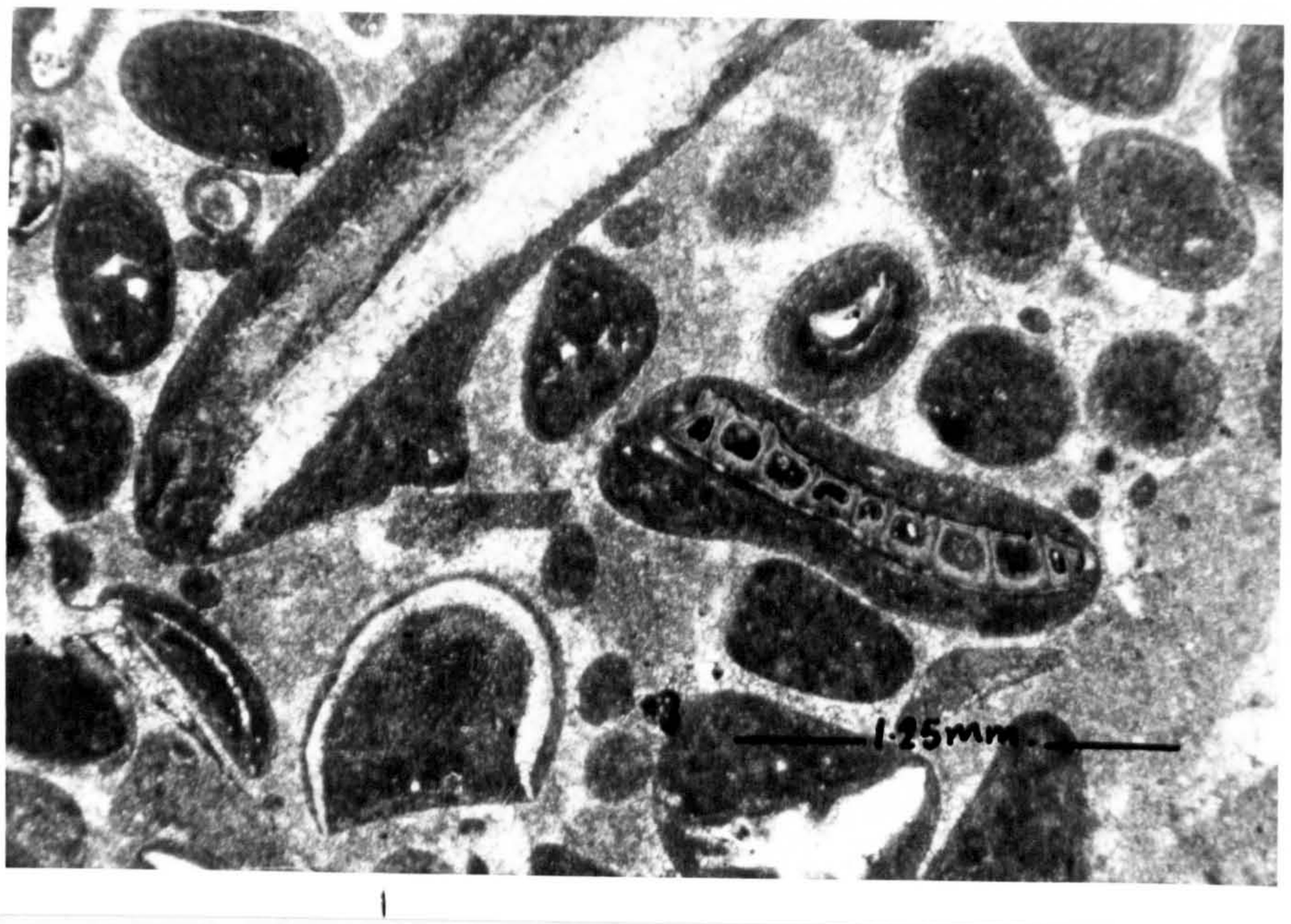
1·25mm

are associated with mega ripples (Loreau and Purser, 1973). Type A microfacies may be correlated with these deposits.

The size and dominance of ooids in microfacies B suggest comparisons with ooids occurring along the outer tidal delta between Sadiyat and Gharab Islands.

The coated grains which typify oolitic microfacies C were observed by Shinn (1973) in high intertidal/supratidal zones along the SE coast of the Qatar Peninsula. The size of ooids in microfacies C is comparable to those occurring in inner tidal deltas between Sadiyat and Gharab Islands. It is possible, therefore, that ooids of microfacies C were deposited in an alluvial channel-inner tidal delta situation, where the coated grains were derived from a tidal flat. The presence of a large percentage of a micrite matrix may suggest a more protected environment. Alternatively, therefore, the ooids may have been transported to the tidal flats by storms.

5.4.3 Growth and Origin

The problem concerning the growth and origin of ooids has been tackled by many workers including Bucher (1918), Cayeux (1935), Eardley (1938), Illing (1954), Newell, et al. (1960), Bathurst (1968, 1975), Shearman, et al., (1970), and, more recently, by Davies et al. (1978). Donahue (1965) put the requirements for ooid growth as

1. super saturation of the solution in $CaCO_3$
2. availability of detrital nucleii
3. agitation of grains
4. a splash cup

These requirements were based on Donahue's experience with cave ooliths and ooid growth in the laboratory.

There are many questions concerning ooid growth, fabric and mineralogy which until recently have been difficult to answer. The first, and probably

the most important, concerns the conditions under which there is a continuous build up of tangentially-arranged calcium carbonate crystals. Sorby (1879) envisaged the growth process as mechanical, involving the adhesion of loose detrital aragonite needles onto a nucleus. Bathurst (1975), however, argued that such adhesive capabilities do not exist and noted that it should be prevented by the constant agitation to which ooids are subjected. By way of an alternative process, Bathurst suggested that the aragonite needles grow by the addition of ions, first to suitable nucleii embedded in the ooid surface, and then through normal precipitation on crystal faces. This process would lead to the evolution of a radial fibrous fabric with a preferred orientation of C-axes perpendicular to the ooid surface. Such an orientation, he added, arises naturally as a result of competition between aragonite (or calcite) crystals which grow most rapidly in the direction of the C-crystallographic axis. The latter property of $CaCO_3$ is directly concerned with the second question concerning ooid growth, i.e. tangential versus radial-fibrous growth.

This problem was considered by Rusnack (1960) and Usdowski (1963). They concluded that during collisions, the radially-arranged needles were broken and abraded through being less resistant to abrasion. The more resistant fabric of tangentially-arranged needles remained.

Loreau and Purser (1973) observed that the radial structure of ooids along the Trucial Coast of the Arabian Gulf existed only in very protected settings. Davies, et al. (1978), through laboratory studies, postulated that quiet water ooids exhibited a radial orientation of carbonate crystals, while ooids formed in agitated conditions exhibited a tangential orientation.

The third question concerns the original mineralogy of ancient ooids; whether they were calcitic or aragonitic. Shearman, et al. (1970) stated that since all known Recent marine ooids are composed of aragonite, on the basis of uniformitarianism, ancient marine ooids were also made of aragonite

and were later replaced by calcite in the course of diagenesis. Shearman, et al. (1970) observed that in many ancient ooids, the detrital nucleus, originally consisting of aragonite, has been replaced by calcite. The ooid cortex, on the other hand, which in ancient limestones is also calcite, retains an original concentric structure. Shearman, et al., therefore, suggested that during diagenesis the original aragonite of the ooid coat was dissolved, but the organic matter present between individual calcium carbonate crystals remained and acted as a template on which tiny crystals of calcite cement grew with the typical preferred orientation that accompanies competitive growth. Owing to the concentric arrangement of the ooid surfaces, the resultant fabric was radial-fibrous. Sandberg (1975), on the other hand, compared modern and ancient ooids with ancient skeletal carbonate grains and noticed that during diagenesis, aragonite skeletal grains may alter to a coarse neomorphic calcite spar with or without relic organic inclusions, or pass through a solution precipitation stage to be preserved as a sparite pseudomorph. In Sandberg's opinion, skeletal grains possess an organic framework similar to that in ooids. The question then arises as to why the organic matter in skeletal grains cannot play the same role as that in ooids, if the views of Shearman, et al. are correct. Sandberg suggested that ancient ooids were calcitic and not aragonitic. He based his assumption on the fact that pre-Cainozoic sea-water contained a lower Mg/Ca ratio than it does now. The Gachsaran ooids are of interest in this debate since their age (Miocene) is around the time that Sandberg envisaged the change in mineralogy. Subrecent ooids composed of calcite of a high Mg type have recently been described from the Great Barrier Reef and the Amazon Shelf (Marshall and Davies, 1975; Milliman and Barreto, 1975) so that there is no reason why ancient ooids should not be calcitic.

5.5 Biosparites and Biomicrites

In these limestones, skeletal components constitute more than 10% of the rock volume. The dominant skeletal components of both the biosparites and biomicrites are bivalves and Foraminifera, other skeletal grains include gastropods, ostracods, bryozoa, echinoderms and crustacean fragments (figs. 5-21, 22). Shallow water, benthonic Foraminifera are the most common in these rocks (see Chapter 7). In some cases skeletal layers are interlaminated with pelsparites (fig.5-11) or oosparites (fig.6-42). Geopetal structures are not uncommon (fig.6-13).

The amount of organic matter present within these rocks varies considerably. Quartz grains are usually present but in small quantities. Most of the bivalves are replaced by drusy or fibrous calcite. Chambers of gastropods and Foraminifera are often filled with cryptocrystalline calcite or drusy spar. Their walls, however, are preserved as sparry calcite in the case of gastropods, and micrite or radial-fibrous calcite with the Foraminifera (see diagenesis). Most of the skeletal grains show the effects of boring algae and possess a micrite envelope.

In some of the samples, skeletal grains are broken and fractured.

Biomicrites and biosparites occur either in laminae or in beds. Beds containing them are up to 4 metres thick. These types of rocks are almost always underlain by marl (fig.5-23) or, in some cases, gypsum beds and overlain by pelmicrites or pelsparites. Sedimentary structures are poorly developed or absent. It is inferred here that these types of rocks were originally deposited in shallow subtidal environments.

5.6 Intrasparites and Intramicrites

Intrasparites and intramicrites are limestones containing more than 25% intraclasts. An intraclast is a fragment of partly to wholly consolidated carbonate sediment that has been eroded from nearby and re-

% OF FOSSILS IN INDIVIDUAL BIOMICRITE SAMPLES

	FORAMS	BIVALVES	GASTROPODS	BRYOZOA	ECHINODERMS	OSTRACODS	WORM TUBES
Sample 66	14%	45%	17%	14%	-	9%	-
Sample 27	37%	26%	9%	14%	14%	-	-
Sample 26	40%	19%	-	5%	35%	-	-
Sample 1011	39%	4%	-	3%	37%	-	-
Sample 103	40%	7%	53%	-	-	-	-
Sample 110	-	6%	-	94%	-	-	-
Sample 22	4%	94%	-	-	-	-	-
Sample 71	18%	25%	7%	-	-	-	50%

TABLE 5-1

Average fossil content in biomicrites

Foraminifera	24%
Bivalves	28%
Gastropods	11%
Bryozoa	16%
Echinoderms mostly crinoids	11%
Ostracods	1%
Bone fragments	6%

BIOSPARITES

	FORAMS	BIVALVES	GASTROPODS	BRYOZOA	ECHINOIDS	OSTRACODS	WORM TUBES
Sample 72	9%.	13%	23%	13%	4%	1%	37%
Sample 81	7%	4%	34%	11%	3%	6%	35%
Sample 12	21%	9%	18%	20%	-	-	32%
Sample 311	32%	46%	-	-	-	-	22%
Sample 14	9%	49%	3%	-	-	-	40%
Sample 312	52%	32%	6%	4%	4%	-	3%
Sample 1010	48%	34%	-	-	18%	-	-
Sample 109	-	90%	5%	-	-	-	5%

TABLE 5-2

Forams	22%
Bivalves	34%
Gastropods	11%
Bryozoa	6%
Echinoids	4%
Ostracods	1%
Worm tubes	22%

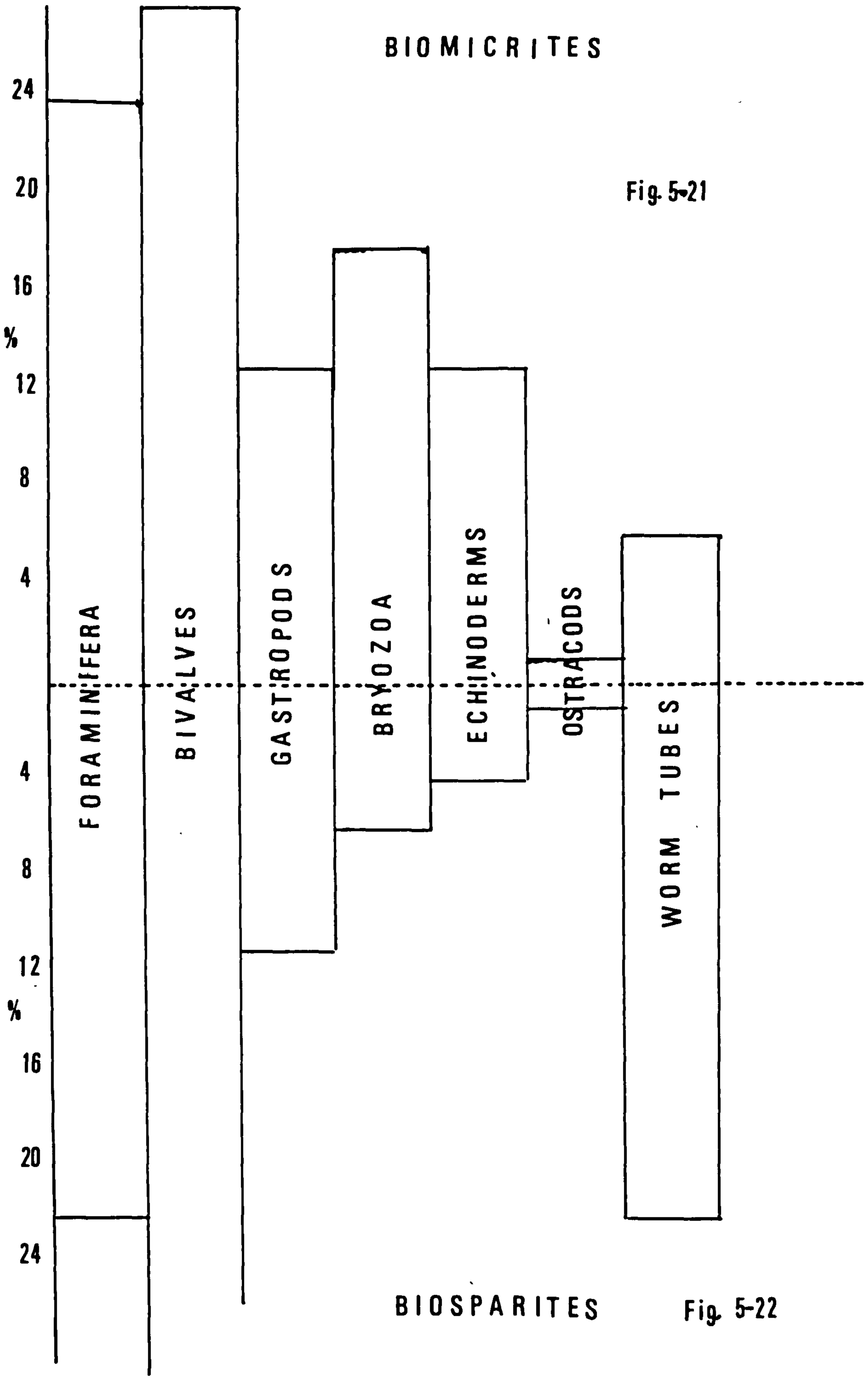
BIOMICRITES
Fig. 5-21
24
20
16
%
12
8
4
FORAMINIFERA
BIVALVES
GASTROPODS
BRYOZOA
ECHINODERMS
OSTRACODS
WORM TUBES
4
8
12
%
16
20
24
BIOSPARITES
Fig. 5-22

deposited to form the intraclast. The intraclasts in these types of rock consist of micrite and are structureless. They range from 1mm. to 3cm. in their longest diameter. Smaller intraclasts are more common and they are angular to rounded in shape. The larger intraclasts are more tabular in cross section and some show a preferred orientation (fig.5-24). These types of intraclastic rocks are usually devoid of any skeletal fragments. Calcite pseudomorphs after nodular anhydrite occur within some intramicrites (fig. 5-25) within the micritic matrix.

Subaerial exposure in the supratidal environment frequently leads to desiccation of the sediments. Intraclasts can be produced through such desiccation and then transported and deposited in adjacent environments. The presence of calcite replaced anhydrite nodules in some of the intramicrites suggests high intertidal/supratidal setting, and thus, little transportation.

5.7 Intrabiomicrites and Intrabiosparites

When intrasparites or intramicrites have a considerable amount of skeletal grains, the rock is referred to as intrabiomicrite or intrabiosparite, depending on the relative ratio of spar to micrite.

The intraclasts here are either structureless (fig.5-26), pelleted (fig.5-27) or composite. These rocks are generally poorly sorted consisting of a mixture of allochems. These are intraclasts, pellets, oncolites and skeletal debris including fragments of bivalves, gastropods, Foraminifera and crustacea. Some of the intraclasts show features of leaching and subsequent sparry calcite filling.

These sediments were probably deposited in a high energy environment with the intraclasts derived from penecontemporaneous erosion in intertidal and shallow subtidal areas.

Fig. 5-23 A red claystone overlain by marl and then by a bioclastic limestone. Shallowing sequence. Bashiqa, Iraq.

Fig. 5-24 An intraclastic limestone. Note the oriented nature of the intraclasts. Mishraq, Iraq.


5 cm

Fig. 5-25 Calcite pseudomorphs after nodular anhydrite associated with intraclasts. Mishraq, Iraq.

Fig.5-26 An intraclastic limestone showing a structureless intraclast. Slice.p.p.l. Jabal Alan, Iraq.


5cm


1.25mm

Fig. 5-27 An intra-biomicrite limestone showing a composite intraclast. Slice.p.p.l. Hammam Al-Alil, Iraq.

Fig.5-28 Oncolitic limestone. The oncoids are of type C of Logan. Slice.p.p.l. Mishraq, Iraq.

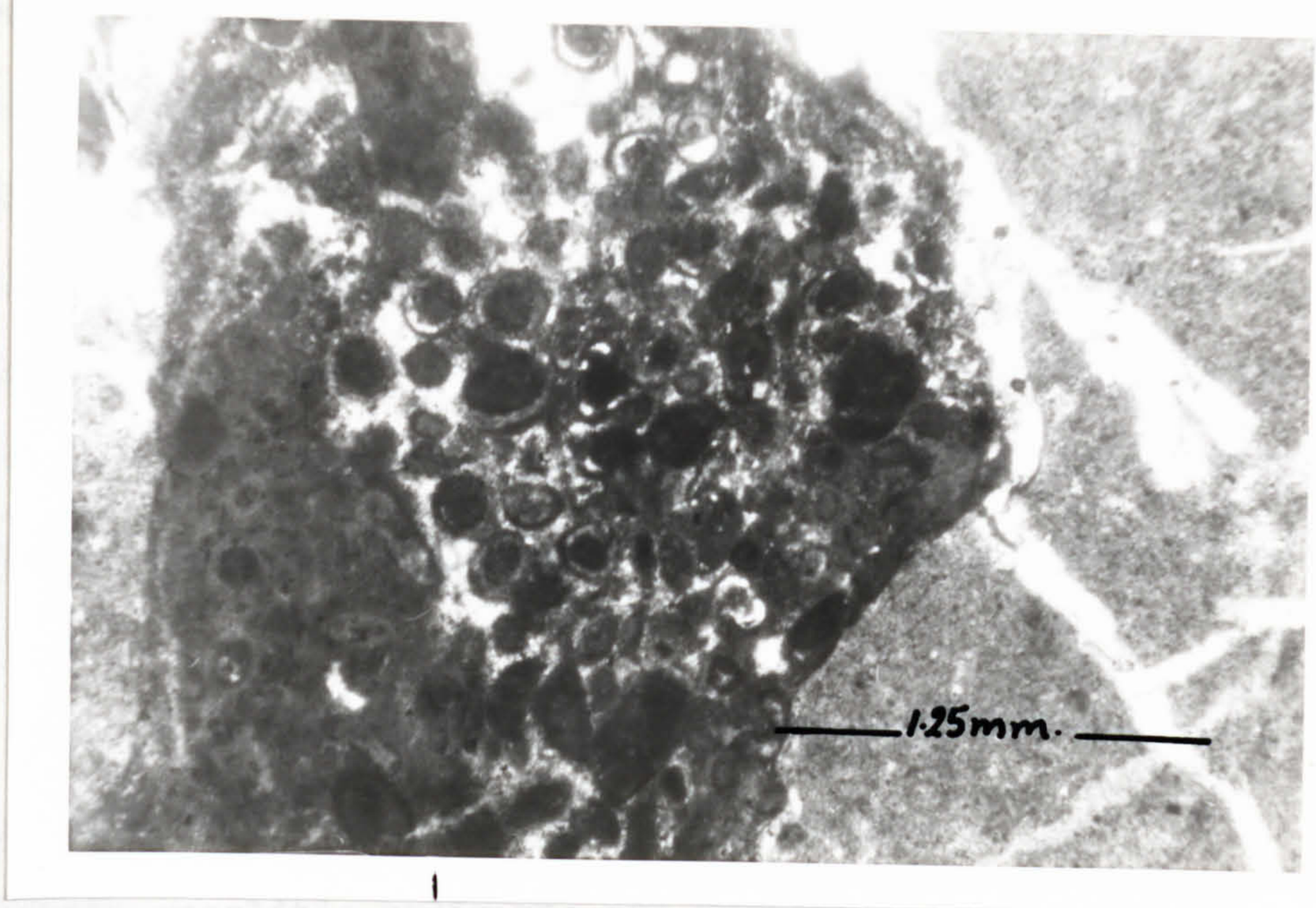

Fig. 1

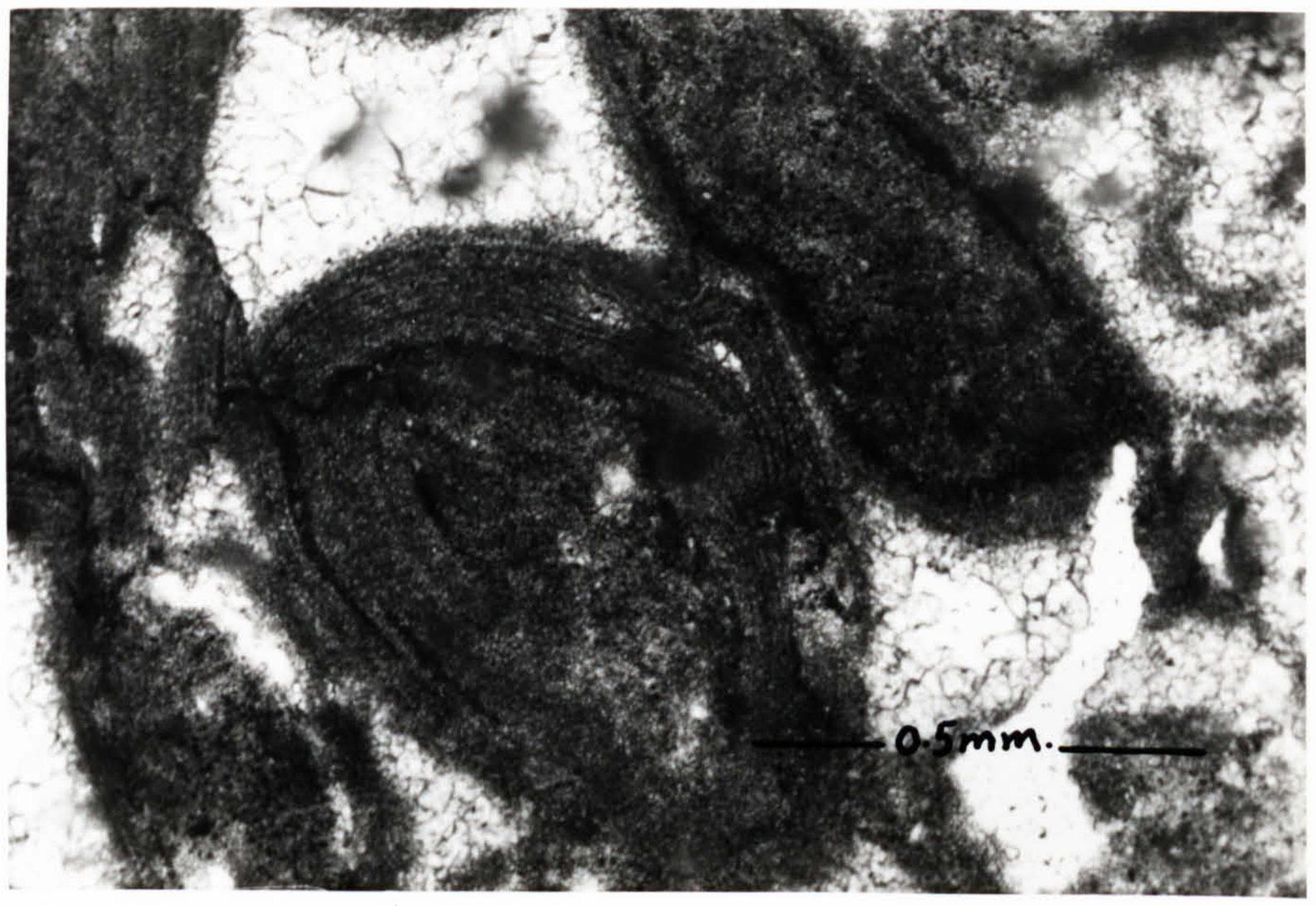

Fig. 1

5.8 Oncolitic Limestones

These rocks are composed largely of oncoids. The oncoids observed within these rocks are of mode C of Logan, et al. (1964)(fig.5-28). In general the oncoids consist of concentrically-laminated envelopes made up of very fine micrite. Larger oncoids, however, are more irregularly laminated. Many of these oncoids are squashed and broken (fig 5-29) skeletal fragments; quartz grains, intraclasts and other material generally serve as nucleii for these oncoids. The breakage and scattering of laminae in the rock hindered the identification of any composite structures pointed out by Logan, et al. (1964).

Oncoids generally differ from ooids by their irregular form, absence of crystal orientation and frequent asymmetry.

These oncolitic sediments are typical of agitated lower intertidal and shallow subtidal zones (Ginsburg, 1960; Logan, et al., 1964). Oncoids vary from soft elastic bodies (Ginsburg, 1960) to structures with a rigid filamentous fabric (Aitken, 1967). The oncoids of the Gachsaran seem to be of the first type. Compaction during early burial, before any cementation, has resulted in the fracture and compression of the oncoids.

5.9 Stromatolites and Cryptalgal Laminites (Published work)

Stromatolites and cryptalgal laminites are only locally developed in the limestone horizons. The best domed and columnar stromatolites were found in a limestone horizon towards the base of the succession near Shaikh Ibrahim (45km. west-southwest of Mosul). In this case the stromatolites are overlain by a 10 metre thick gypsum bed, and underlain by a pelleted limestone (0.5m. thick) before the gypsum at the top of the cycle below (fig.5-30). Planar cryptalgal laminites occur in this cycle, in others in the Shaikh Ibrahim area, and were also noted in limestones near Tall-Afar. Vague, often undulating laminations are present in many limestone at other

Fig. 5-29 A general view of the previous sample. Note the compacted and fractured nature of the oncoids. Slice.p.p.l.

Fig. 5-30 Cycle in the Gachsaran Formation. The prominent limestone in the centre of the photograph is composed of planar, domed and columnar stromatolites. This bed is overlain by nodular gypsum and underlain by pelleted limestone (behind hammer). Shaikh Ibrahim, Iraq.

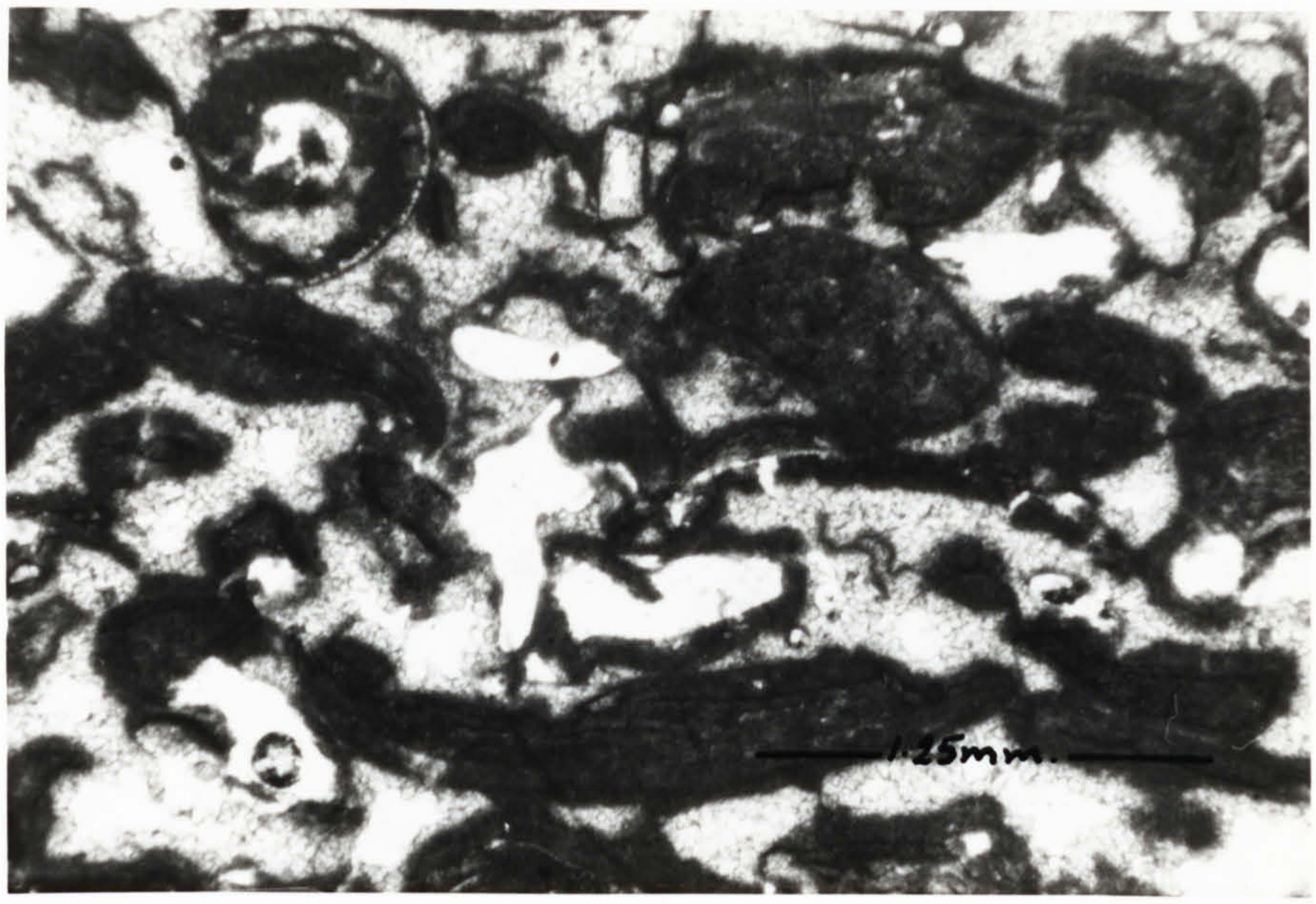

1

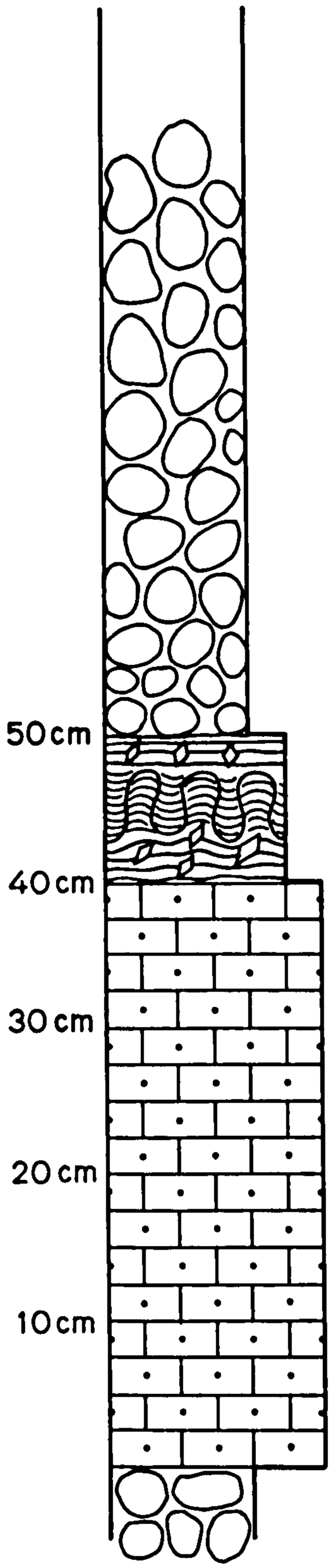

Gypsum 10m thick

Stromatolite Horizon 0·1m

Pelleted Limestone 0·4m

Fig. 5-31 Cryptalgal laminites, consisting of an alternation of micritic and pellet-packstone or pelsparite laminae. Note slight irregularities but persistence of micritic laminae. Tall-Afar, Iraq.

Fig. 5-32 Domed and columnar stromatolites from Shaikh Abrahim. Planar cryptalgal laminites are developed above the stromatolites. Shaikh, Abrahim, Iraq.

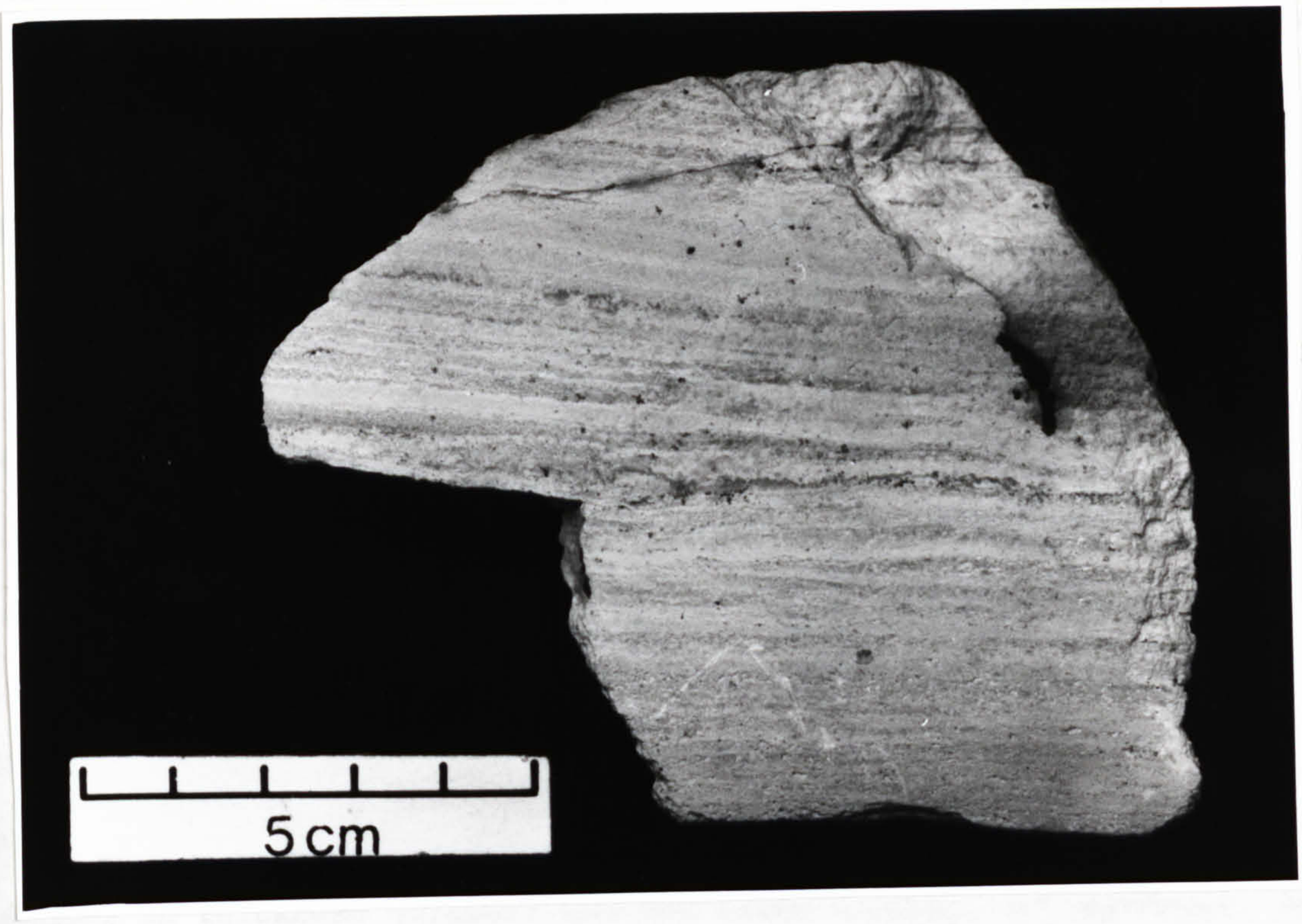
5 cm


5 cm

localities (such as at Hammam al Alil, and Makhul) and were noted in cores from the Mishraq area. These may well be of cryptalgal origin, but for reasons of weathering or diagenesis, an algal origin is not definite.

5.9.1 Cryptalgal laminites

Planar laminated sediments of cryptalgal origin are more widely developed than domed or columnar stromatolites. Laminites (fig.5-31) form units up to 2 metres thick, composed of dense micritic laminae alternating with pelsparite or pellet-packstone laminae. The pellets average 0.1mm. in diameter and form laminae from 2 to 15mm. in thickness. The micritic laminae tend to be thinner and, although commonly smooth and continuous, often exhibit small irregularities or corrugations (fig.5-31). In fact there appear to be two types of micritic lamina, one very thin and generally constant in thickness (0.1mm.) and the other thicker, but variable, reaching 5mm. Laminae of the first type are most common between and immediately above the stromatolitic columns described below. Some of these thin micritic laminae only persist for several or tens of millimetres, as wisps, while others join laterally to form single laminae. Laminae of the second type are more common and constitute most planar cryptalgal laminites. They are chiefly composed of dense micrite but pellets may be vaguely discerned. Possible algal-filament moulds (diameter 0.05mm.) occur in a vertical position in some laminae. Laminoid fenestrae and small irregular birdseye structures are present, the former immediately below micritic laminae, and are filled with drusy calcite spar, poikilotopic calcite, or gypsum. Some calcite-filled cavities have a lozenge or convex-lens shape in cross section, or are triangular. Their shape suggests that they are calcite pseudomorphs after small discoidal gypsum crystals which formed displacively within the sediment (cf. Hudson, 1970; Tucker, 1976).

5.9.2 Domed and columnar stromatolites

The stromatolites from Shaikh Ibrahim are on a small scale and consist of both columnar and domed forms (fig.5-32). The domes are up to 3cm. in diameter and 2cm. high and possess laminae of the LLH-S type of Logan, et al. (1964). Vertically, the domes commonly give rise to two or three columns, in the 'furcate' branching style of Hofmann (1969). The linked domes occur upon planar cryptalgal laminae, locally desiccated and with rare lozenge-shaped pseudomorphs after gypsum (fig.5-33). The sediment above the domed and columnar stromatolites mainly consists of pelsparite, with thin micritic laminae of cryptalgal origin (fig.5-34A). In other cases, however, large micritic interclasts (flakes) occur (figs.5-34C and D) and reworked gypsum crystals (the latter pseudomorphed by calcite). In one instance a centimetre-sized flake had been incorporated into a growing column (fig.5-34D). When traced laterally, the domed and columnar stromatoites give way to pelsparite, only locally with cryptalgal laminae.

There are several different aspects to the microstructure of the domes and columns. In the majority, there is a lamination of dense, micritic layers alternating with pellet packstone or pelsparite (fig.5-35). In the columns the laminae are of the SH-C and SH-V types of Logan, et al., (1964) although individual micritic laminae are frequently irregular in thickness. Small laminoid fenestrae are locally present below the micritic layers, and irregular fenestrae occur within the pellet laminae. In a few columns, laminations are not developed or only weakly so, and the microstructure consists of pelsparite with many irregular fenestrae.

Some of the latter show a vague alignment, concentric with the curvature of the column. The pelsparite which constitutes the columns has a characteristic 'clotted' fabric of very poorly organised pellets, and is comparable with the textures of thrombolitic stromatolites (Aitken, 1967; Gebelein, 1974). This clotted fabric forms the upper part of some

Fig. 5-33 Calcite-filled cavities within a planar laminated cryptalgal limestone, which are interpreted as pseudomorphs after gypsum. Slice.p.p.l. Shaikh Ibrahim, Iraq.

Fig. 5-34 Sketches of stromatolites from Shaikh Abrahim. A, showing columns developed upon domes, thin micrite laminae between columns and pelsparite above with cryptalgal laminae. B, detail of columnar stromatolite showing fractured outer micritic rind. C, columnar stromatolites showing branching, with one column developing a bulbous head. Coarse matrix with micrite flakes. D, columnar upon domed stromatolites, surrounded by matrix of coarse pelsparite and micrite flakes.

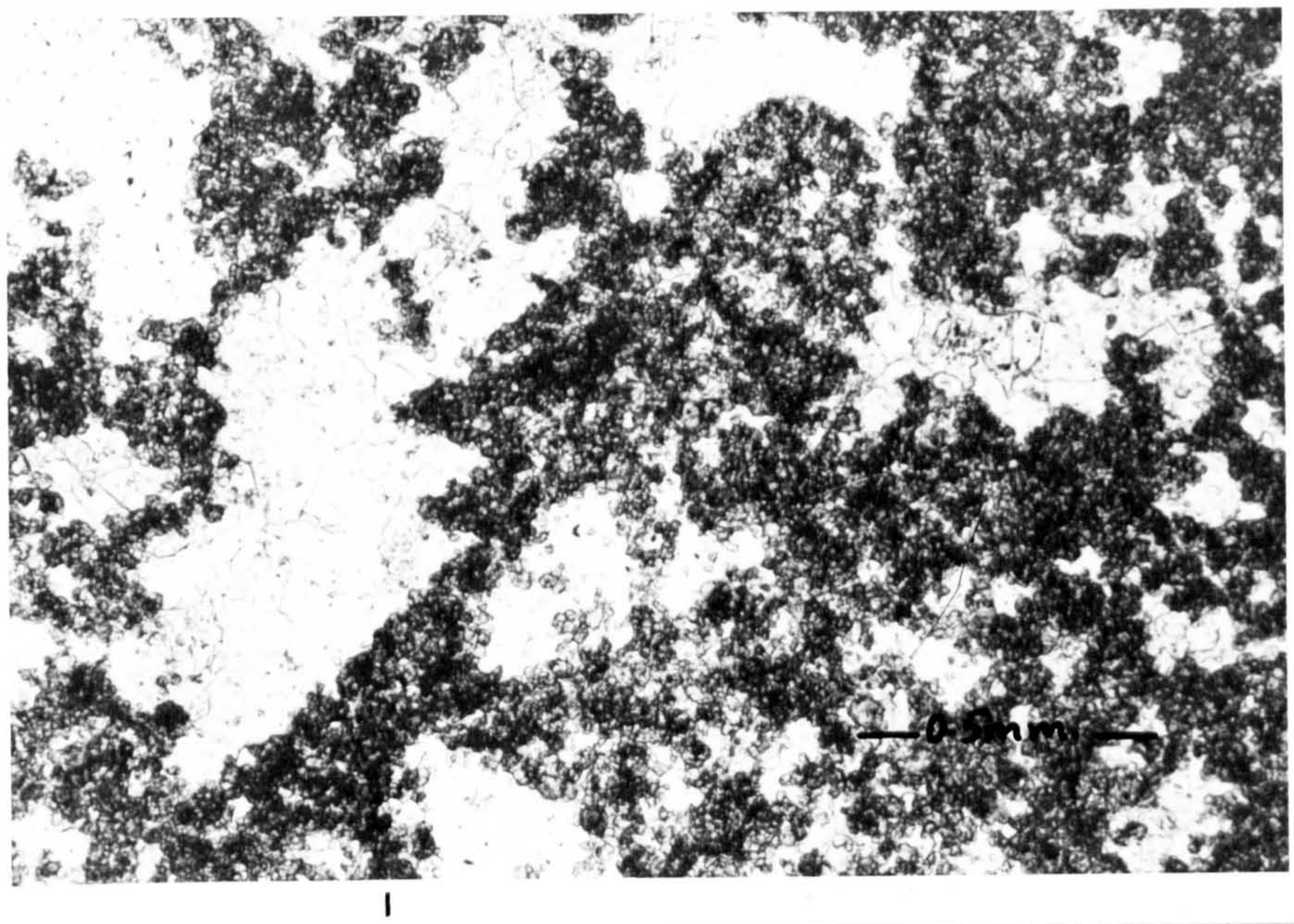

1

Aufsätze

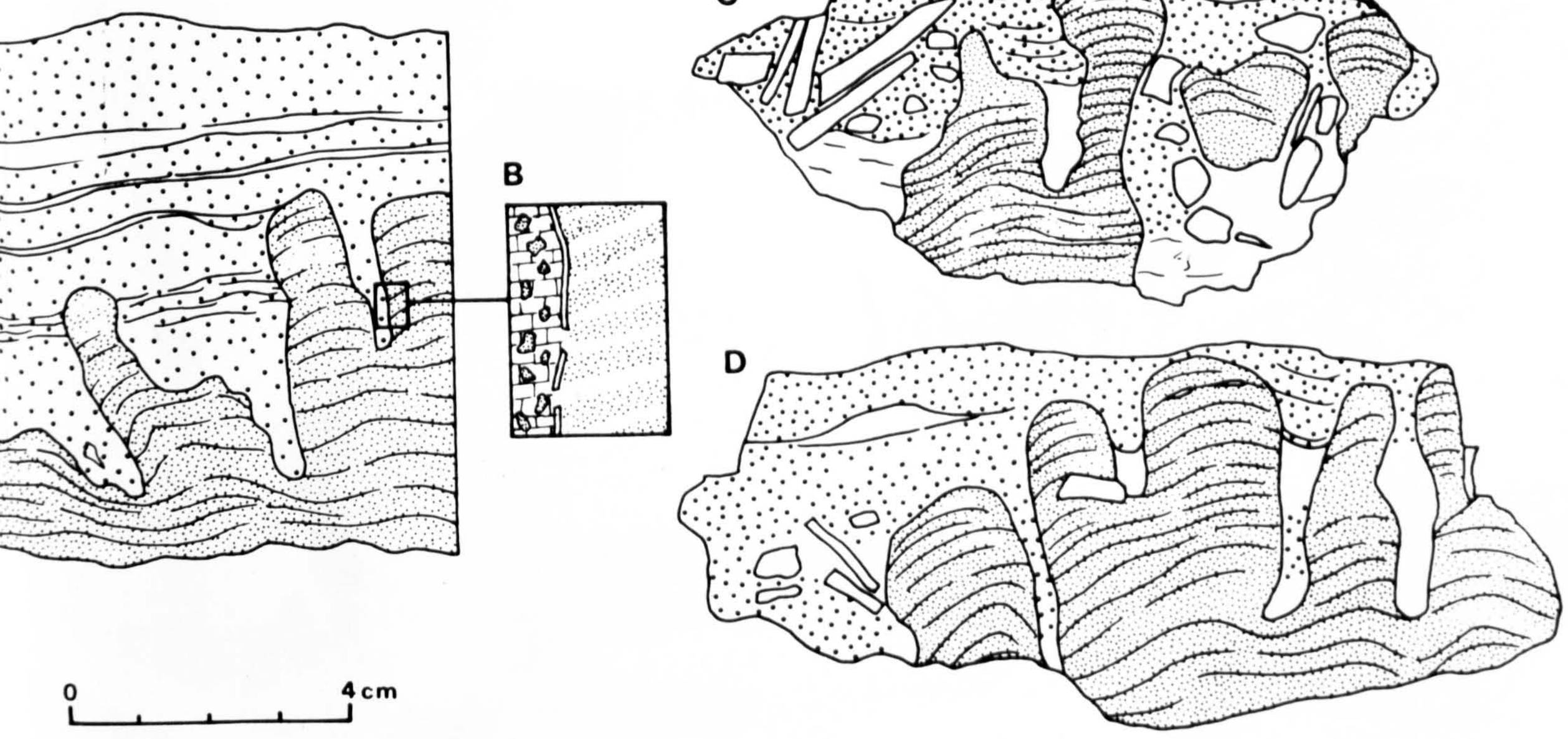

Fig. 5-35 Fabric of domed stromatolite consisting of dense micritic layer (centre) resting sharply upon, and passing up into, pelsparite. Irregular and laminated cavities are present immediately below the micritic laminae and within the pelsparite. Slice p.p.l. Sheikh Ibrahim, Iraq.

Fig. 5-36 Photomicrograph showing fractured micritic rind developed around a columnar stromatolite. Slice p.p.l. Sheikh Ibrahim, Iraq.

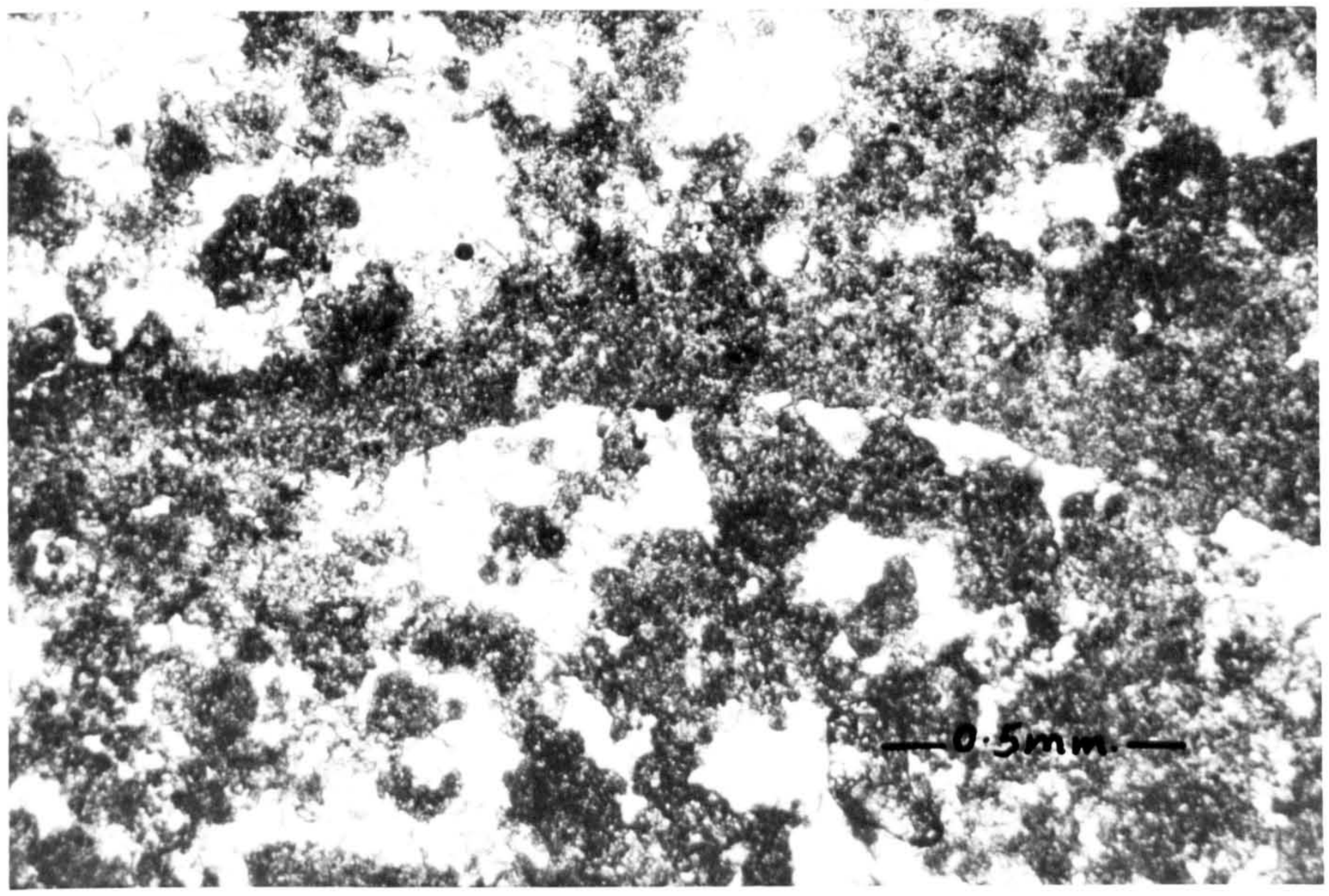
0·5mm

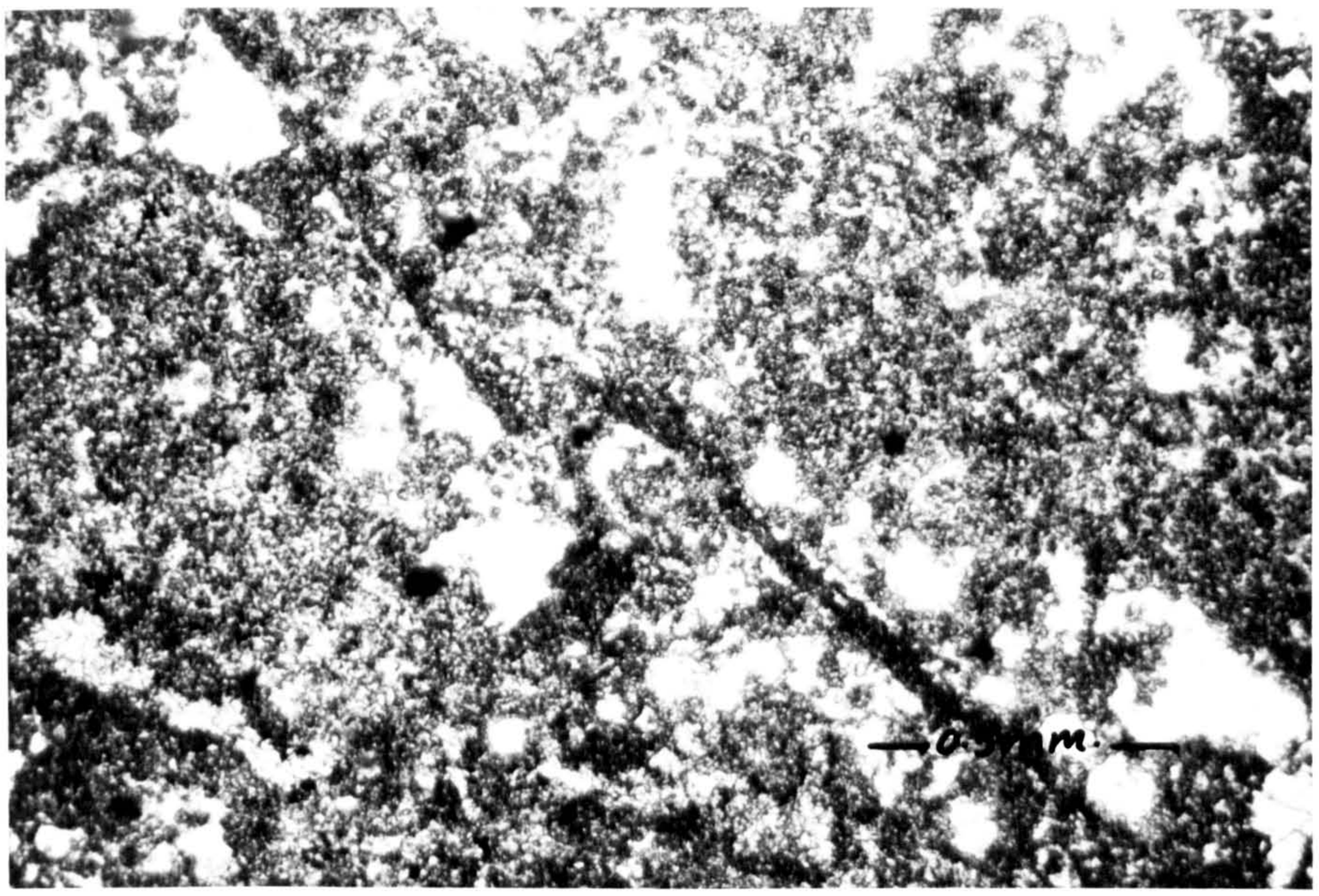
0·5mm

columns, above the laminated fabrics. Irrespective of internal microstructure (laminated or clotted) columns possess a thin outer rind or wall (0.04mm. thick)(fig.5-36) which follows the stromatolite topography, with negligible thickening in troughs between columns. This rind may be entirely micritic or consist of an inner and outer micritic lamina, separated by a zone of honey-coloured (presumably organic-rich) microsparite, or clear sparite. The rind is commonly cracked and slightly displaced (figs.5-34B, 36). In several places, it appears to have been bored.

The microsparite, which constitutes many cryptalgal laminae, consists of anhedral to subhedral, often rounded crystals. They are commonly brownish in colour, with opaque inclusions of organic matter.

5.9.3 Interpretation of Stromatolites

Recent work on modern algal mats has shown that they are of several different types, each composed of a different blue-green algal community (Gebelein, 1974; Logan et al., 1974; Hofmann, 1976). The microstructure produced by the sediment trapping and binding properties of the algal mat varies according to the mat type. The planar cryptalgal laminites in the Gachsaran limestones are directly analogous to many recorded from modern carbonate environments such as the Bahamas (Black,. 1933; Monty, 1965, 1972), the Trucial Coast (Kendall and Shipwith, 1968) and Shark Bay, Western Australia (Davies, 1970; Logan et al., 1974). The alternating micritic/pelleted fabric of many laminites (fig.5-31) suggested comparison with cryptalgal sheets composed of smooth mat, described from the Trucial Coast by Kinsman and Park (1976) and from Shark Bay by Davies (1970), Logan et al., (1974) and Hofmann (1976). Along the Trucial Coast, smooth mat is the most important form as far as producing laminated sediments is concerned. It is characteristic of a large part of the intertidal zone (where it is commonly desiccated) but it also occurs subtidally in high salinity pools and channels. The paucity of desiccation in the Miocene cryptalgal laminites may suggest a similar shallow subtidal or low intertidal setting. The presence of

calcite pseudomorphs after gypsum in some cryptalgal limestones (fig.5-33) indicates a higher intertidal situation, with the development of hypersaline sediment pore-waters. The pelleted laminae represent clastic sediment transported over and deposited upon the surficial algal mat, the latter represented by the micritic laminae. The significance of the lamination in cryptalgal structures of this type, as to whether it is diurnal, tidal or seasonal, is still in question. Monty (1976) has demonstrated the importance of compaction in reducing the thickness of the algal laminae in Recent deposits. In addition, Park (1976) has shown that algal mat growth can be very slow, and that clastic laminae generally represent sporadic storm activity. Similar tidal-flat cryptalgal structures have been described from many other ancient sequences (e.g. Aitken, 1967; Matter, 1967; Hudson, 1970; Tucker, 1977).

Modern columnar and domed stromatolitic structures are only extensively developed in the Shark Bay area (Logan, 1961; Logan, et al., 1964; Logan, et al., 1974; Hoffman, 1976; Playford and Cockbain, 1976). They tend to occur in relatively high energy intertidal and shallow subtidal areas. The association of flakes with the Miocene stromatolites also indicates agitated conditions. The majority of columnar stromatolites at Shark Bay are much larger than those in the Gachsaran and are developed in headland situations. However, small discrete columns similar in size to the Miocene examples do occur in the bights of Hamelin Pool and also show an analogous type of branching (Logan, et al., 1974; Hoffman, 1976; fig. 6d,6e). These digitate stromatolites occur in the low intertidal zone and are composed of the smooth type of algal mat. In fact, the microstructure of the Iraqi domes and columns, with alternations of pelsparite and micrite, suggest that a smooth type of algal mat may also have been involved (e.g. compare fig.5-33 with Logan, et al., 1974, fig.17D). The local clotted microstructure of some

columns suggests that coccoid algae (rather than filamentous) may have been an important constituent of the algal mat community (Gebelein, 1974; Logan, et al., 1974; Monty, 1976). Recent algal mats of Shark Bay, composed chiefly of coccoid algae (referred to as pustular mat) typically have an unlaminated, highly fenestral fabric. The features of the thin, micritic double wall around the columns indicate the development of a third type of algal structure. This was clearly a sheet which enveloped the stromatolite surface, after cessation of columnar growth. It appears to be similar to the film mat of Shark Bay which develops in the high intertidal-low supratidal zone. The cracked nature of the micritic layer suggests a similar high intertidal position. Film mat coats columnar stromatolites in Shark Bay and produces a cryptocrystalline aragonitic or pelleted rind.

The changes in algal-mat type, as indicated by the cryptalgal fabrics, and the changes in gross morphology of the stromatolites, could be reflections of algal mat growth (from one zone into another) and/or of some variations in the tidal flooding frequency (controlling the turbulence of the environment). Cryptalgal fabric sequences, as a result of growth or slight sea-level fall, have been described from Shark Bay by Logan, et al. (1974), e.g. fig.29. The occurrence of stromatolites and cryptalgal laminites in the Gachsaran Formation indicates that intertidal (and perhaps locally shallow subtidal) conditions were periodically established. The presence of calcite pseudomorphs after gypsum also indicates the intertidal environment.

It is perhaps surprising that stromatolites and cryptalgal laminites are not more widely developed in the Gachsaran limestones. There are two possible reasons for this apparent anomaly. Algal mats may have been more widely developed but were disrupted and obliterated in the displacive growth of the supratidal sulphate, as has been shown to take place with Recent algal

mats by Park (1976) and Kinsman and Park (1976). However, the presence of some algal limestones and the development of gypsum pseudomorphs in others, shows that intertidal carbonates have been preserved and were not engulfed by a downward growing 'front' of supratidal sulphate. Algal mats of higher intertidal and low supratidal areas may well have been obliterated in this manner. Algal mats may have been prevented from developing extensively by the grazing activities of metazoans - particularly the gastropods (cf. Garrett, 1970; Awramik, 1970). The lack of grazing organisms (due to high salinities) is thought to be the principal reason for the diverse assemblage of algal mats present in Hamelin Pool, Shark Bay (Playford and Cockbain, 1976). Gastropods are common in Gachsaran limestones so it may well have been their activities which prevented widespread algal mat growth. Local higher salinities may have excluded gastropods and allowed algal mat formation there.

5.10 Churned Bedding and Burrows

'Burrow' is used herein for penetration of soft substrates and 'boring' for penetration of any hard substrate. This usage follows the suggestions of Bromley (1970a), Alexandersson (1972) and Frey (1973).

During sedimentation, there is competition between the rate of sedimentation and the rate at which organisms burrow and disrupt the sediment. This could be considered the most important factor in the preservation or destruction of laminations. The term 'churned bedding' implies reworking of sediments by burrowing organisms causing mottling and giving the sediment a mixed appearance (Conybeare and Crook, 1968). Churned bedding within the Gachsaran Formation is identified by a mottled, irregular appearance and lack of laminations (fig.5-6). Two main burrow systems are distinguished:

1. Irregular burrows, but generally parallel to the bedding (fig.5-37).

They range in diameter from .5 to 1.8cm. but are mainly around 1 cm. in diameter. These burrows are cylindrical to tabular and flattened in the plane of bedding, forming ribs projecting over the bedding plane. They form irregular and randomly overlapping branching systems. Petrographically, these burrows are filled with peloidal micritic and skeletal fragments which include Foràminifera, gastropods and small bivalves. Frey (1970) termed horizontal branched burrows planolites. These burrows were probably caused by crustaceans. They appear similar to Callianassa burrows described by Farrow (1971). Callianassa burrows usually have vertical extensions forming galleries (Shinn, 1969; Farrow, 1971), but in strongly current swept areas with relatively thin sediment cover, possess dominantly horizontal systems (Farrow, 1971).

2. Vertical pipes of oval cross section were recorded at various levels in boreholes from Mishraq. The best preserved example was encountered at a depth of 163 metres in a laminated limestone bed. In this bed the tubes range up to 4cm. in length and have elliptical cross sections (fig.5-6), which generally range from 3 to 5mm. in diameter. Around each tube there is usually a zone of disturbance within which the sedimentary laminations are bent upwards or downwards, the direction of bedding possibly indicating the direction of animal movement. The burrows sometimes have lateral but short extensions forming U-shaped structures. These extensions may be in order for the animal to maintain a position relative to sediment water interface (Goldring, 1964). The burrows are filled with pelmicrite with the peloids usually concentrated towards the burrow walls. No internal laminations were observed. The burrows were probably caused by annelids in shallow subtidal conditions. The sediment overlying these burrows is intensely bioturbated and no structure is observed. Additional unidentified burrowers may also have contributed to this bioturbation. The intensive

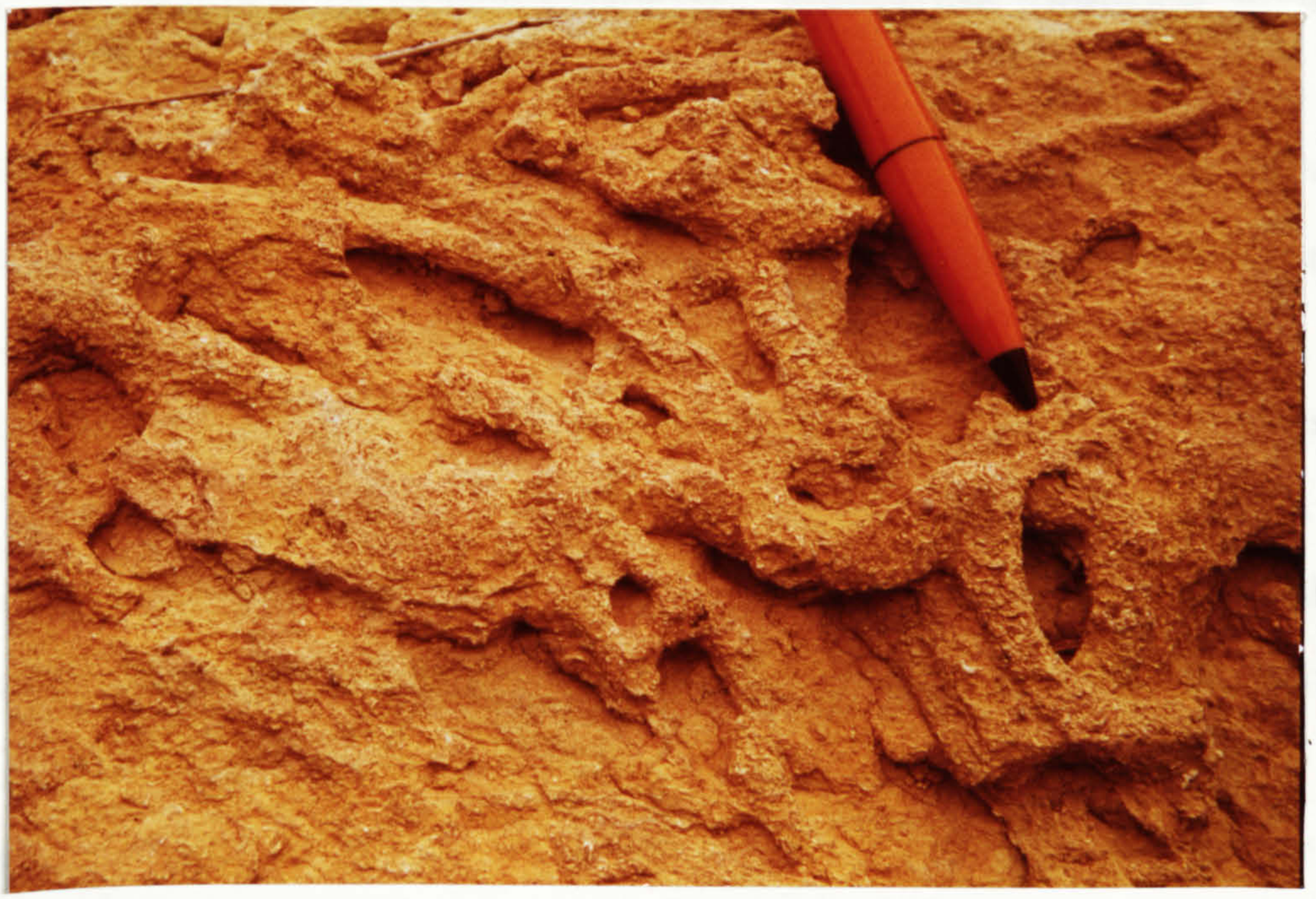

Fig. 5-37 Burrow systems in the Gachsaran. Note the horizontal to bedding nature of the burrows. Bashiqa, Iraq.

upward bioturbation may indicate slower sedimentation.

5.II Summary

Within the Gachsaran Formation twelve carbonate lithofacies are recognised, each of which has been described and discussed. In general, rocks of the Gachsaran occur in cycles. They are generally underlain by marl/clay and overlain by gypsum-anhydrite. Within the limestone members the carbonate lithofacies are rarely organised in any pattern or sequence, rather one lithofacies may be underlain or overlain by another carbonate lithofacies. In general, however, the carbonate rocks represent environments ranging from shallow subtidal to lower supratidal settings.

Cryptalgal laminites and stromatolites discovered within the carbonate members of the Gachsaran have been described as indicating intertidal conditions. Apart from the cryptalgal laminites and stromatolites, other limestone lithofacies also have parellels in the Recent carbonate sediments forming along the Trucial Coast, Arabian Gulf. Pelleted limestones, occurring, for example, below the stromatolites at Shaikh Ibrahim, or in other cases overlying bioclastic rocks, are similar to the deposits of lagoonal and low energy areas, while wave-rippled and cross-bedded biosparites are analogous to many skeletal and oolitic carbonates of more agitated, shallow subtidal regions (Wagner and Van der Togt, 1973).

CHAPTER 6

CARBONATE'S DIAGENESIS

CHAPTER 6

CARBONATE'S DIAGENESIS

6.1. Introduction

Carbonate diagenesis can take place in submarine (e.g. Milliman, 1966), intertidal to shallow subtidal (e.g. De Groot, 1969; Shinn, 1969; Taylor and Illing, 1969), subaerial environments (e.g. Friedman, et al., 1971; Land, 1971) and during deep burial.

The fabrics of any indurated carbonate rock can be the product of the various diagenetic processes that take place in these four environments. Such processes are reflected in the Gachsaran carbonates by the evidence for early and late cementation, early and late dolomitisation, replacement, neomorphism, compaction, leaching and cavity infilling. Some early diagenetic changes which took place while the sediments were still in contact with sea water may have been obscured during subsequent changes following burial or subaerial exposure. Nevertheless, there is still considerable evidence for early diagenetic events in these carbonates.

This chapter describes the diagenesis of the Gachsaran carbonates involving all changes that took place in the sediments from immediately after deposition up to their present state.

6.2 Early Cementation

Observations regarding the mineralogy of Pleistocene and Recent marine carbonate cements demonstrate that most marine cements are composed of either high Mg-calcite or aragonite. These two minerals both have a typical fabric; aragonite commonly forms acicular crystals, whereas high Mg-calcite forms cryptocrystalline crystals (e.g. Shinn, 1969). There are records, however, of cryptocrystalline aragonite cements and fibrous high Mg-calcite cements. In certain beach rocks from Qatar, Arabian Gulf, Taylor and Illing (1969) described cryptocrystalline and acicular fibrous crystals of both aragonite and high Mg-calcite. This relation was also observed on the Bermuda reefs by Ginsburg, et al. (1967).

Studies of the distribution of these cements suggest that aragonite is more prevalent in higher tidal flats, while Mg-calcite in lower and subtidal areas. Aragonite cement is more common in slightly supersaline conditions (Friedman, 1968b), whereas high Mg-calcite cement is more frequent where the level of supersaturation is lower (De Groot, 1969).

The distinction between cryptocrystalline (micritic) cement and micrite resulting from algal diminution is not easy to make, even in Recent sediments. Alexandersson (1969), for example, found that cryptocrystalline cement (high Mg-calcite) is identical in texture and colour to the micrite in a lithified algal framework.

The fabrics and textures exhibited by the Gachsaran cements are compared with those of Recent cements. Four major types of early cements were identified:

1. Closely-packed fibrous crystals of non-ferroan calcite which form a single layer or fringe around allochems (fig.6-1). These crystals range in length from 7 to 20μ and their width is usually about one third of their length. In any one fringe, fibres are remarkably uniform in length, producing an isopachous texture.

The overlying generation of cement is invariably equant drusy sparite and the contact between the two generations is sharp.

The fibrous cement does not appear to develop preferentially around any particular type of allochem. It envelops skeletal grains, ooids, pellets as well as intraclasts. This fabric is somewhat comparable to Recent beach rock and shallow subtidal cements of high Mg-calcite, although the latter have more equant crystals (for comparison see Tietz and Muller, 1971). Another possibility is that they could be the neomorphosed form of early fibrous aragonite cement.

2. Small radiating non-ferroan calcite crystals up to 20μ in diameter surrounding allochems (fig.6-2). This cement is very similar to

Fig. 6-1 A bio-pelsparite showing early cementation. Notice the closely packed fibrous crystals of calcite forming a fringe around allochems. Slice p.p.l. Mishraq, Iraq.

Fig. 6-2 A biosparite showing early cementation. Crystals of calcite surrounding allochems show well developed terminations forming more of a zig-zag line. The rest of the cavity is filled by a later generation of sparry calcite cement. Note the difference in shape, size and behaviour of the two generations of cement. Slice p.p.l. Sheikh Ibrahim, Iraq.

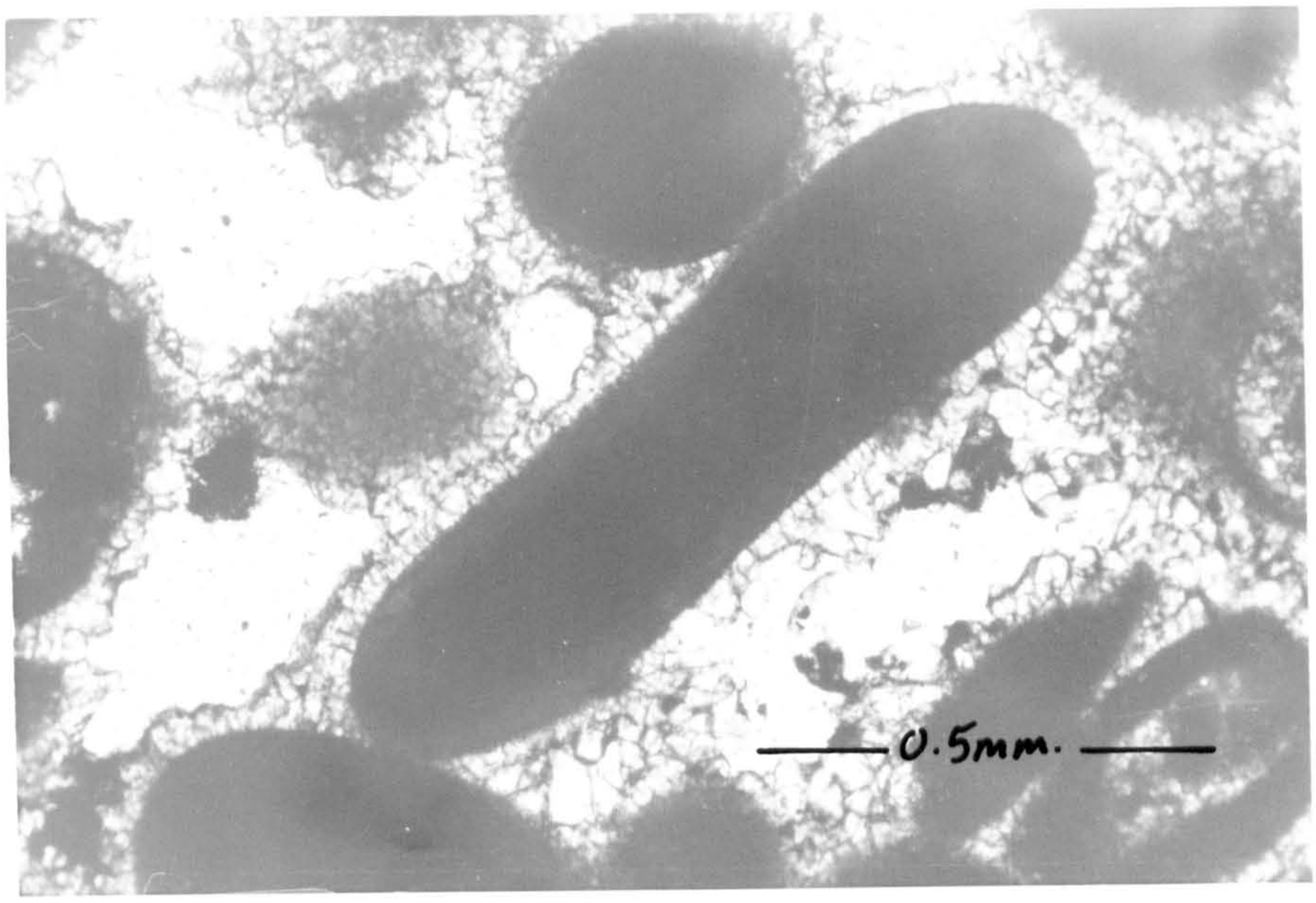

1

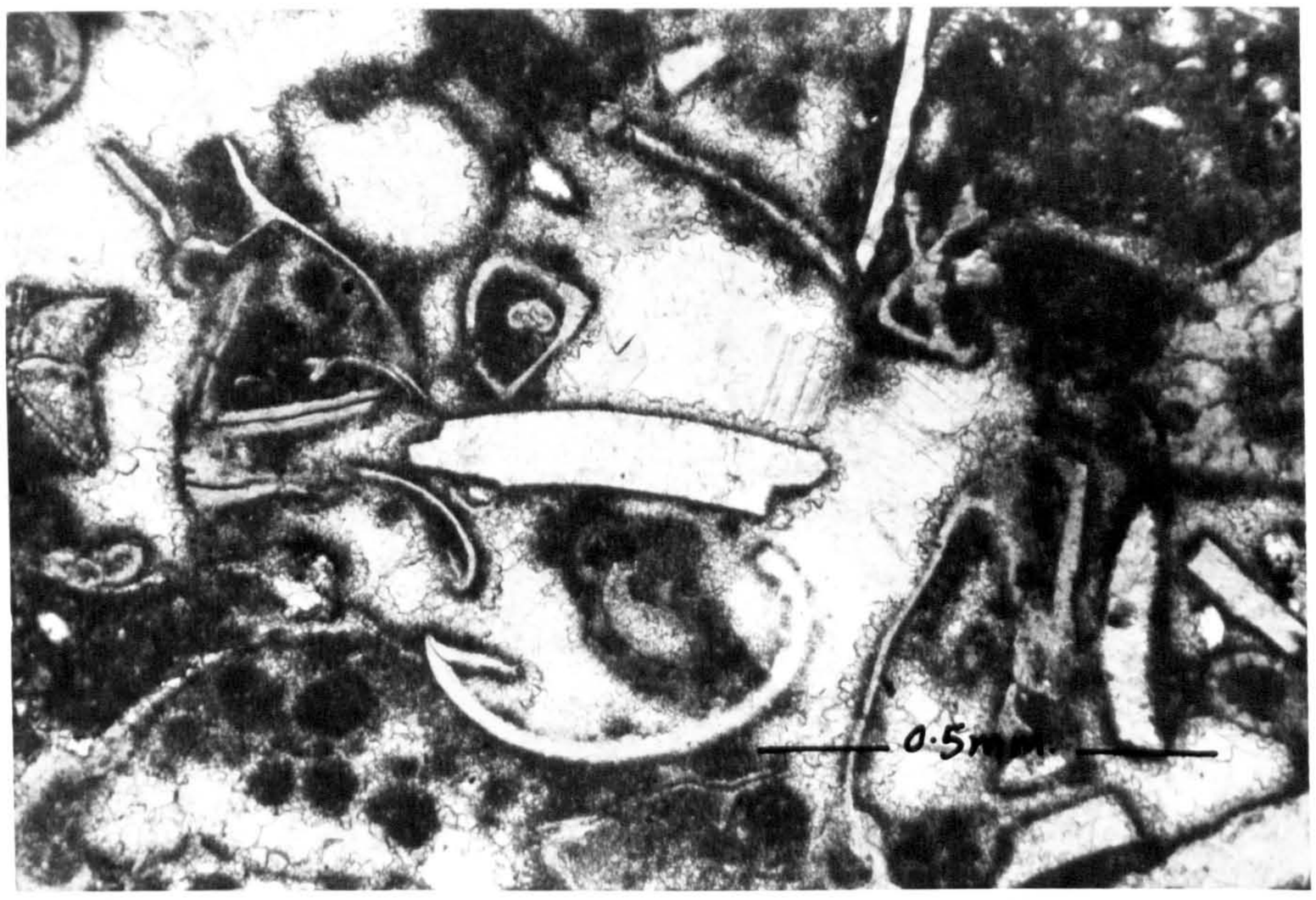

1

the first type, but differs in that the crystals have well developed terminations forming more of a zig-zag line. Under plane polarised light they appear to be joined as one crystal. A very similar calcite fabric was described by Fuchtbauer (fig.5-60, 1974) from the Rhaetian on the northern Alps and interpreted as an early cement.

3. Loosely packed fibrous crystals of non-ferroan calcite with a radiating needle-like texture (figs.6-3, 4). These needles average about 40μ in length and their width is about one tenth of their length. The crystals are not in contact with each other except at their bases, and are terminated at their ends by acutely pointed faces. This cement fringe is not of uniform thickness because of the variable lengths of the component crystals. This type of cement is the most common in the Gachsaran carbonate rocks and occurs in several different settings;

(a) It envelops allochems to form a fringe of radiating crystals (figs.6-3, 4). Where this cement has grown upon some types of Foraminifera (fig.6-5), the cement is in optical continuity with the fibrous texture of the Foraminifera (fig.6-5). The fibrous cement fringe then has a pronounced sweeping extinction as a result of the radial-fibrous arrangement of crystals. Kendall (1976) has described similar fabrics associated with Foraminifera.

(b) In some cases, this type of cement forms a centripetal lining to leached fossil cavities (fig.6-6).

(c) A replacive and displacive habit is shown by this fibrous cement, particularly in association with bivalves. The fibres extend from outside into the shell replacing the entire bivalve with a fibrous texture. The fibres, however, are large and more pronounced (figs.6-7, 8). This is thought to be mainly due to a higher stage of recrystallisation (see Section 6-4B2).

The resemblance of these fibrous calcite crystals to those forming in Recent environments (Taylor and Illing, 1969; Shinn, 1969; Pingitore, 1971;

Fig. 6-3 A biomicrite. Note the radiating needle-like texture of the calcite crystals surrounding the Foraminifera fragment. Slice p.p.l. Makhul, Iraq.

Fig. 6-4 As Fig. 6-3 but under higher power.

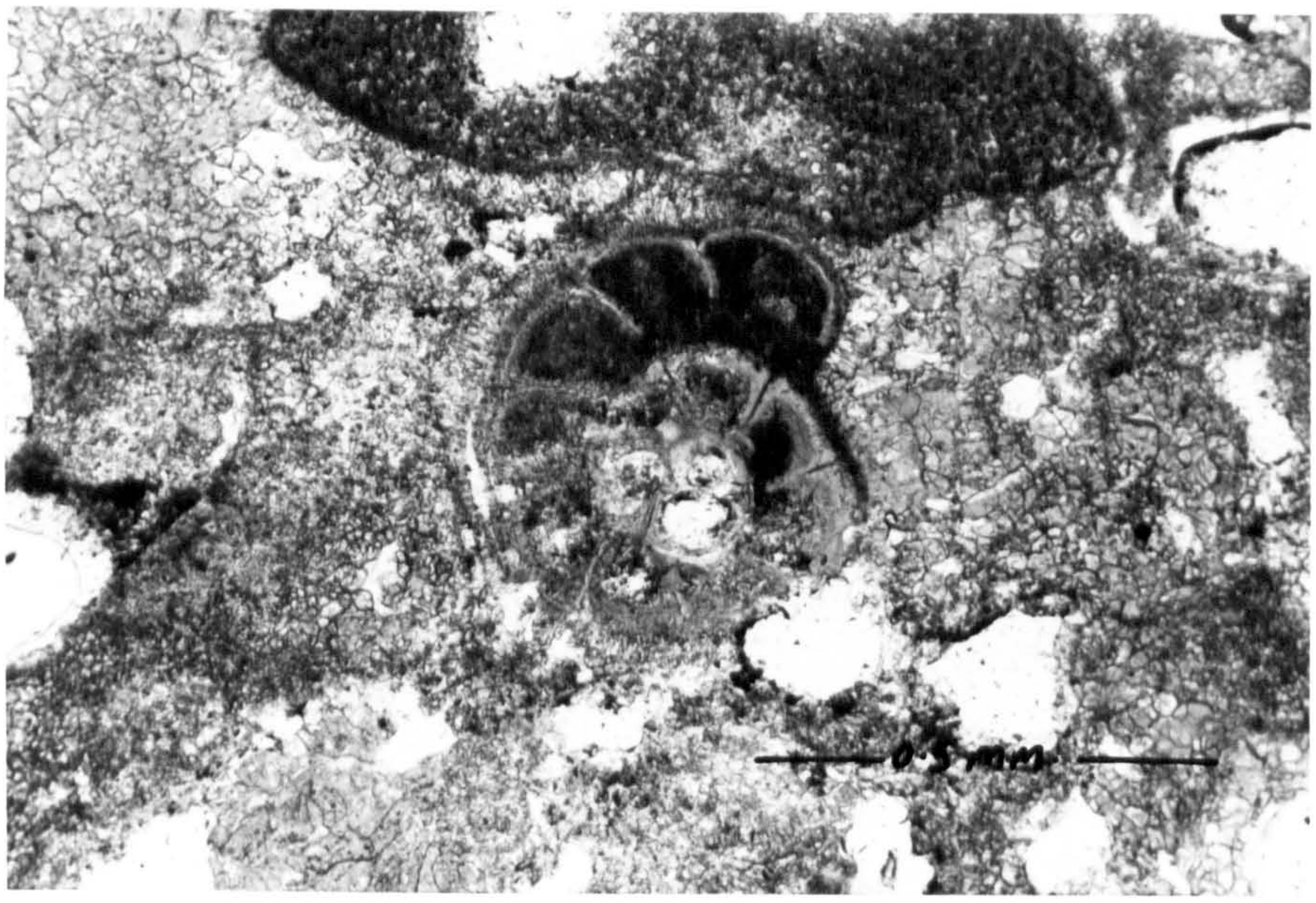

1

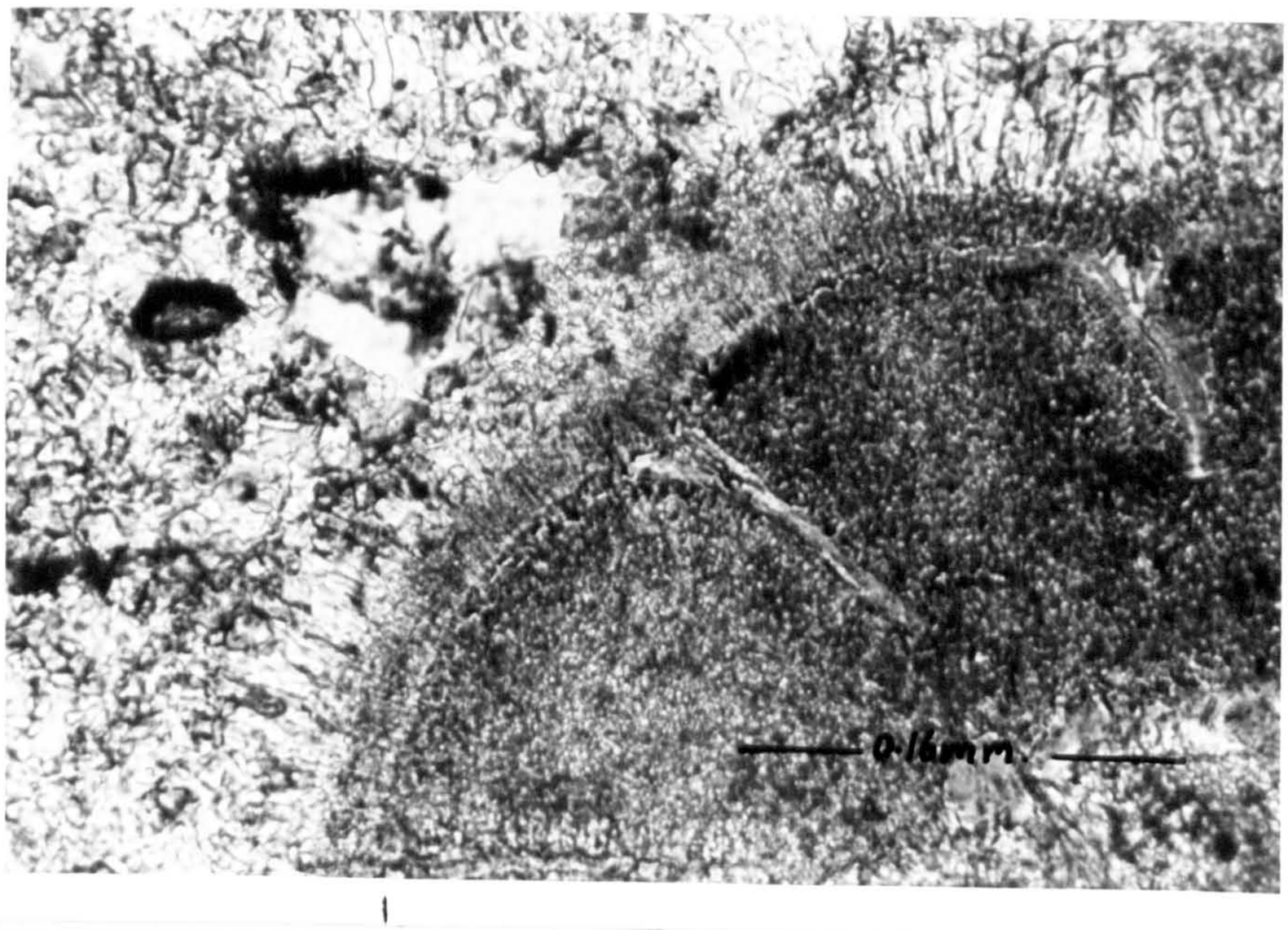

1

Fig. 6-5 A Foraminifera surrounded by an early needle-like fibrous cement. The cement crystals are in optical continuity with the fibrous crystals of the Foraminifera. The cement may well have displaced the surrounding sediment. Slice p.p.l. Hammam Al-Alil, Iraq.

Fig. 6-6 Leached chambers of a gastropod lined centripetally with radiating needle-like calcite crystals. The rest of the cavities are filled with drusy spar. Slice p.p.l. Bashiqa, Iraq.

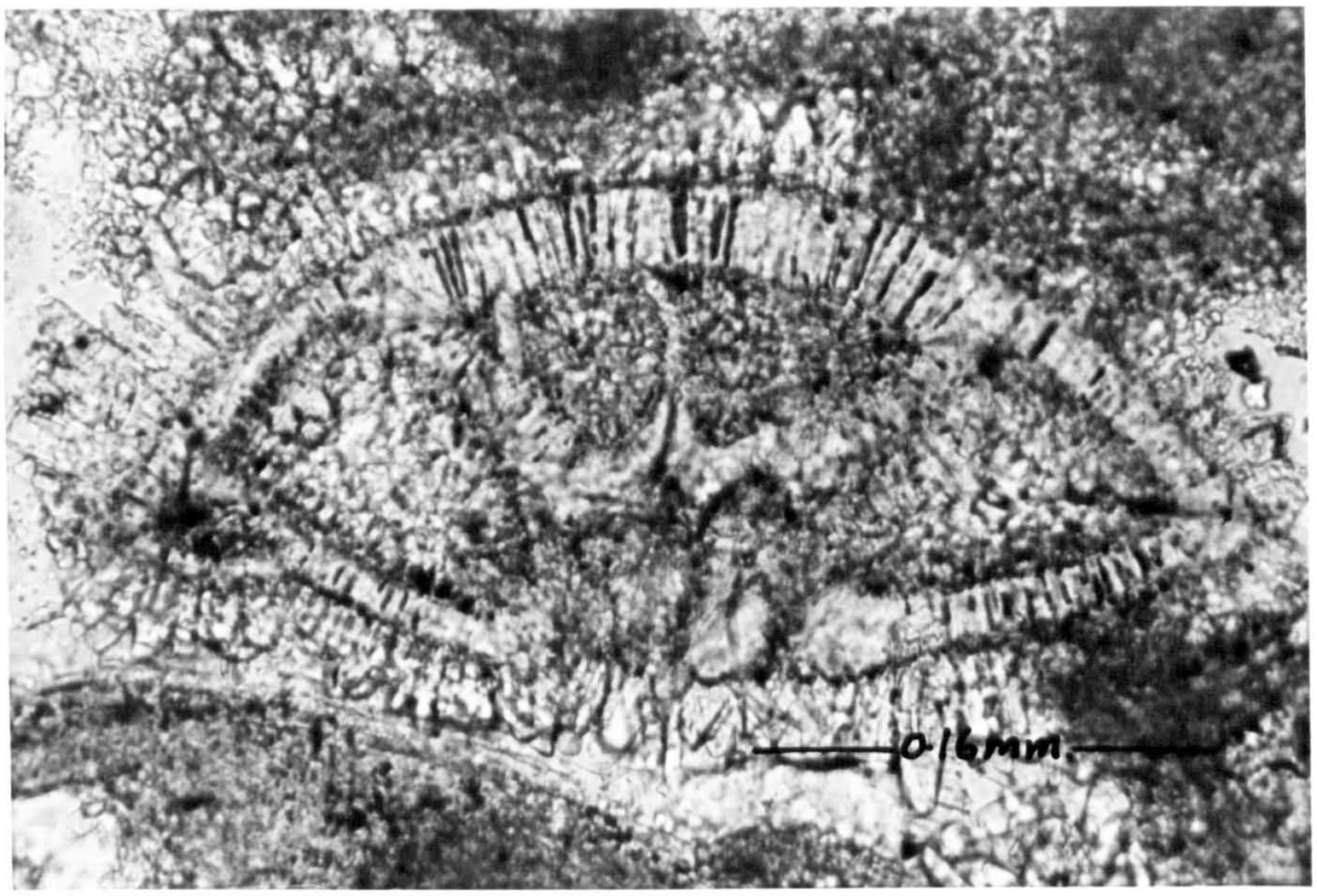

1

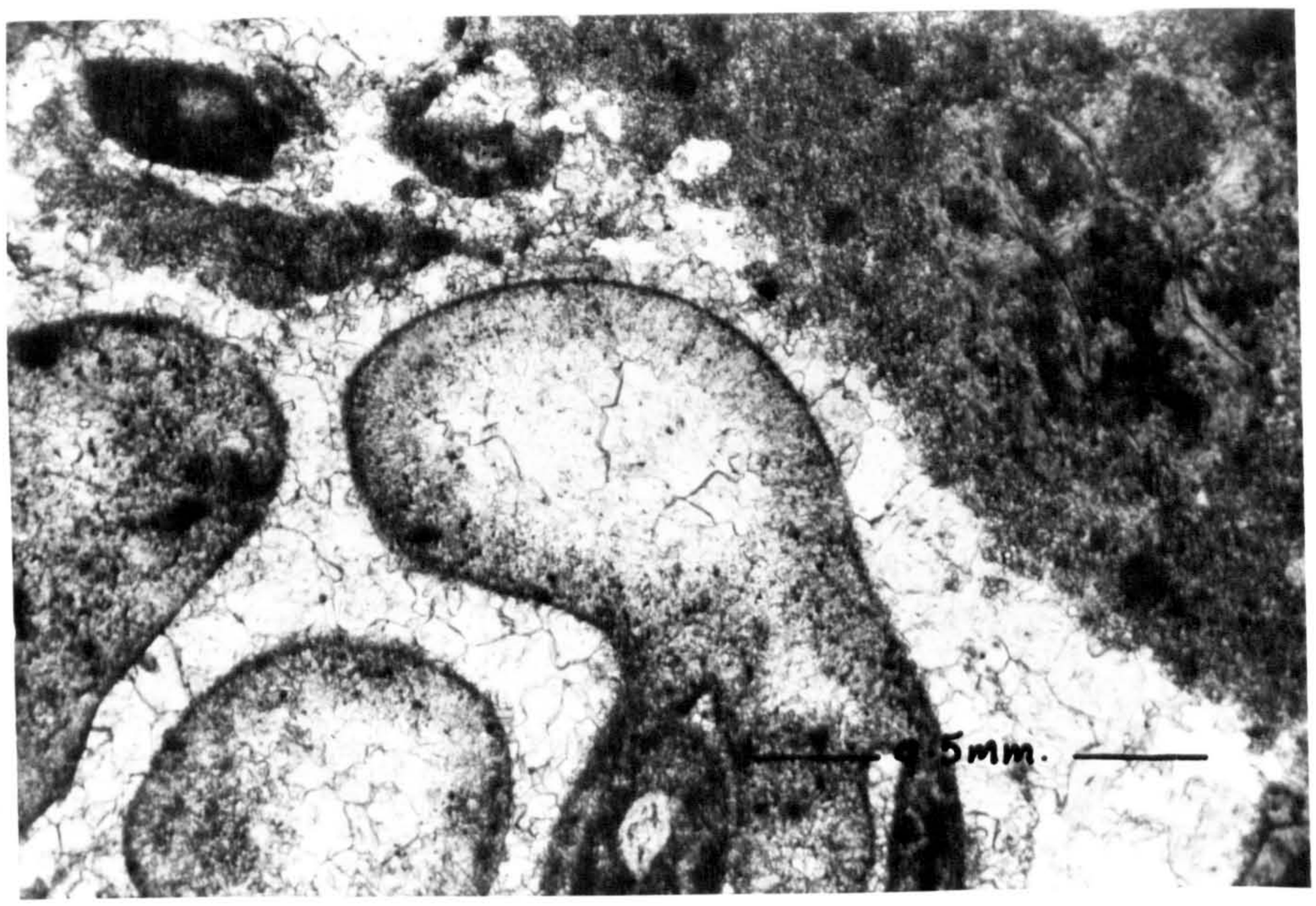

1

Fig. 6-7 A bivalve shell filled with fibrous calcite cement. The latter projects outwards replacing the wall and displacing the sediment. The cement inside the shell is in optical continuity with the cement outside, forming a sweepy extinction. Slice. crossed nicdes, Shaqlawa, Iraq.

Fig. 6-8 A bivalve shell filled with fibrous calcite cement. Note the displacing nature of these crystals. Part of the wall (micrite envelope) is broken and displaced (arrow). Slice p.p.l. Hammam Al-Alil, Iraq.

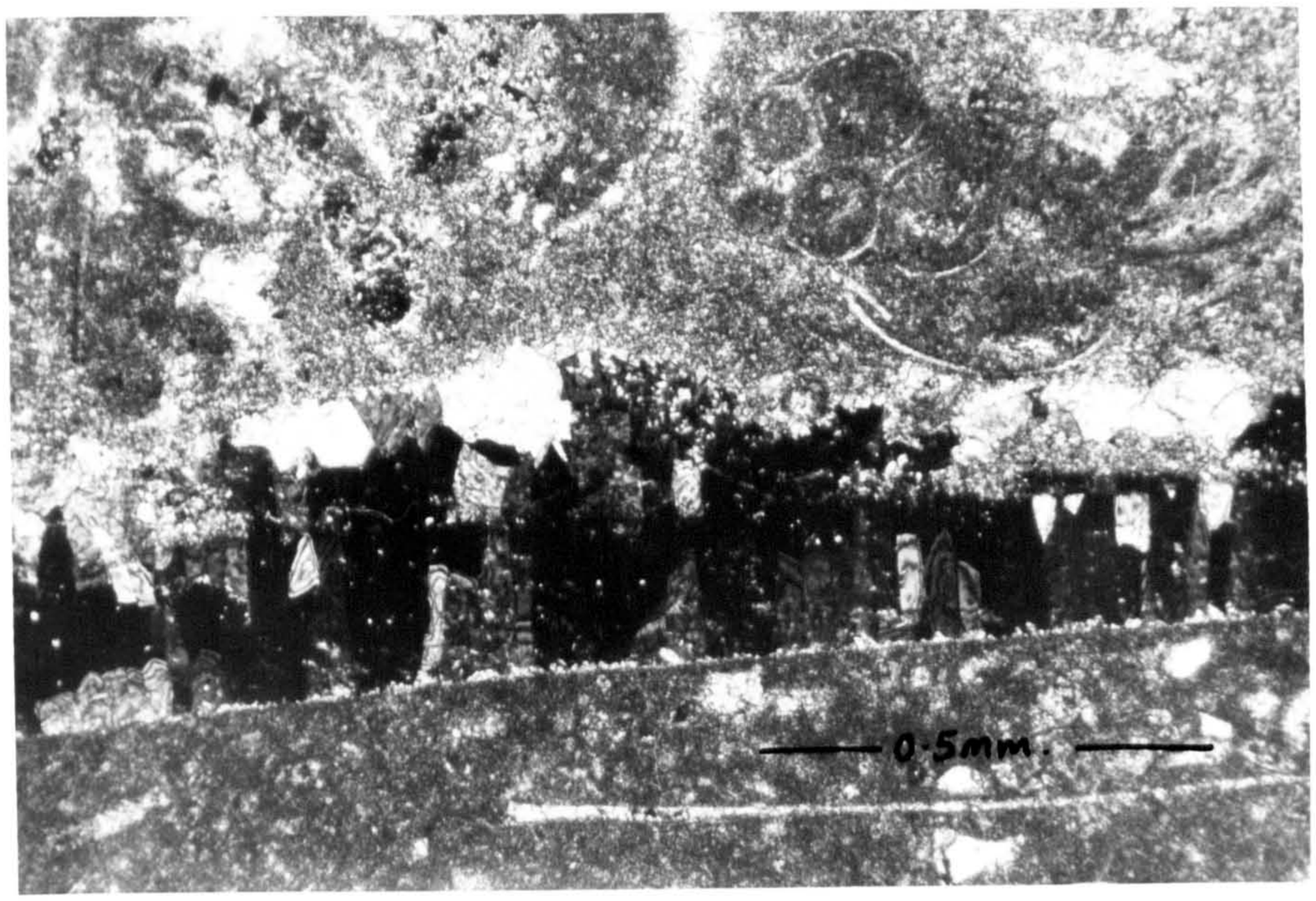
0·5mm.

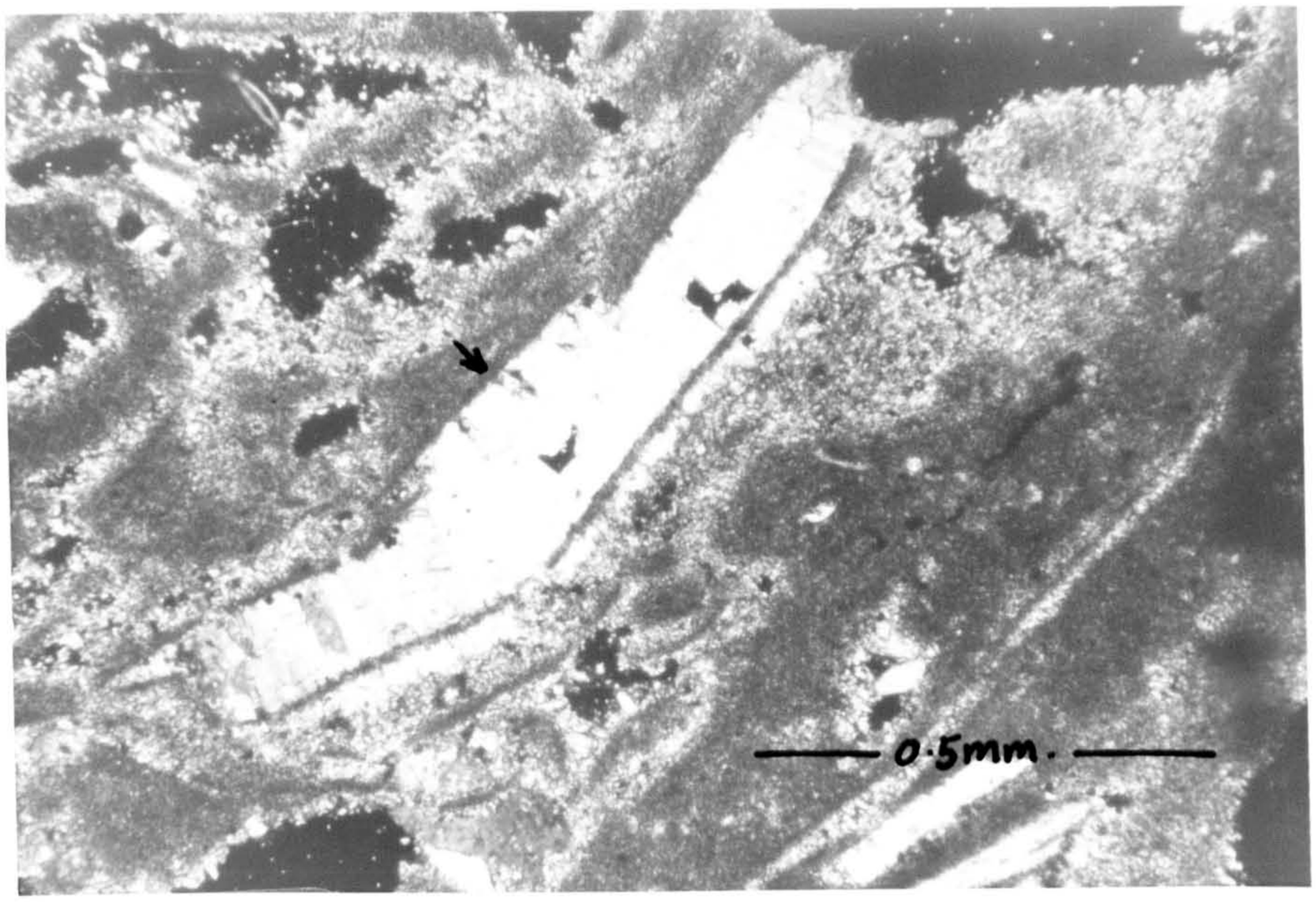
0·5mm.

Fig. 6-9 A micrite envelope in a cavity filled with drusy spar. Note the micrite attached onto the convex side of the envelope. Slice p.p.l. Makhul, Iraq.

Fig. 6-10 Micrite cement (arrows) lining the walls of a cavity filled with drusy spar. Note the dark, dull colour of the micrite cement as compared with the surrounding matrix. Slice. p.p.l. Makhul, Iraq.

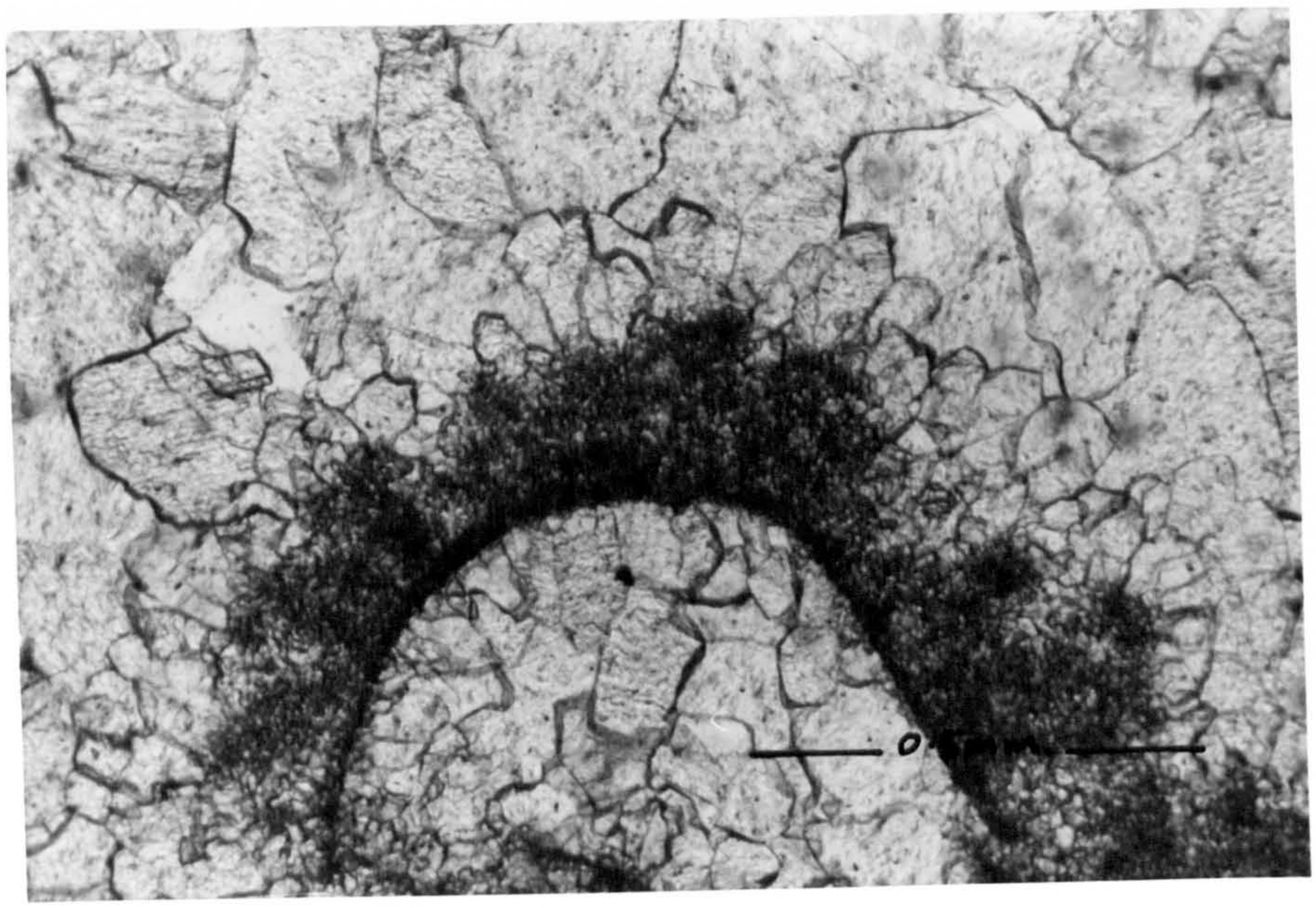
0·5mm.

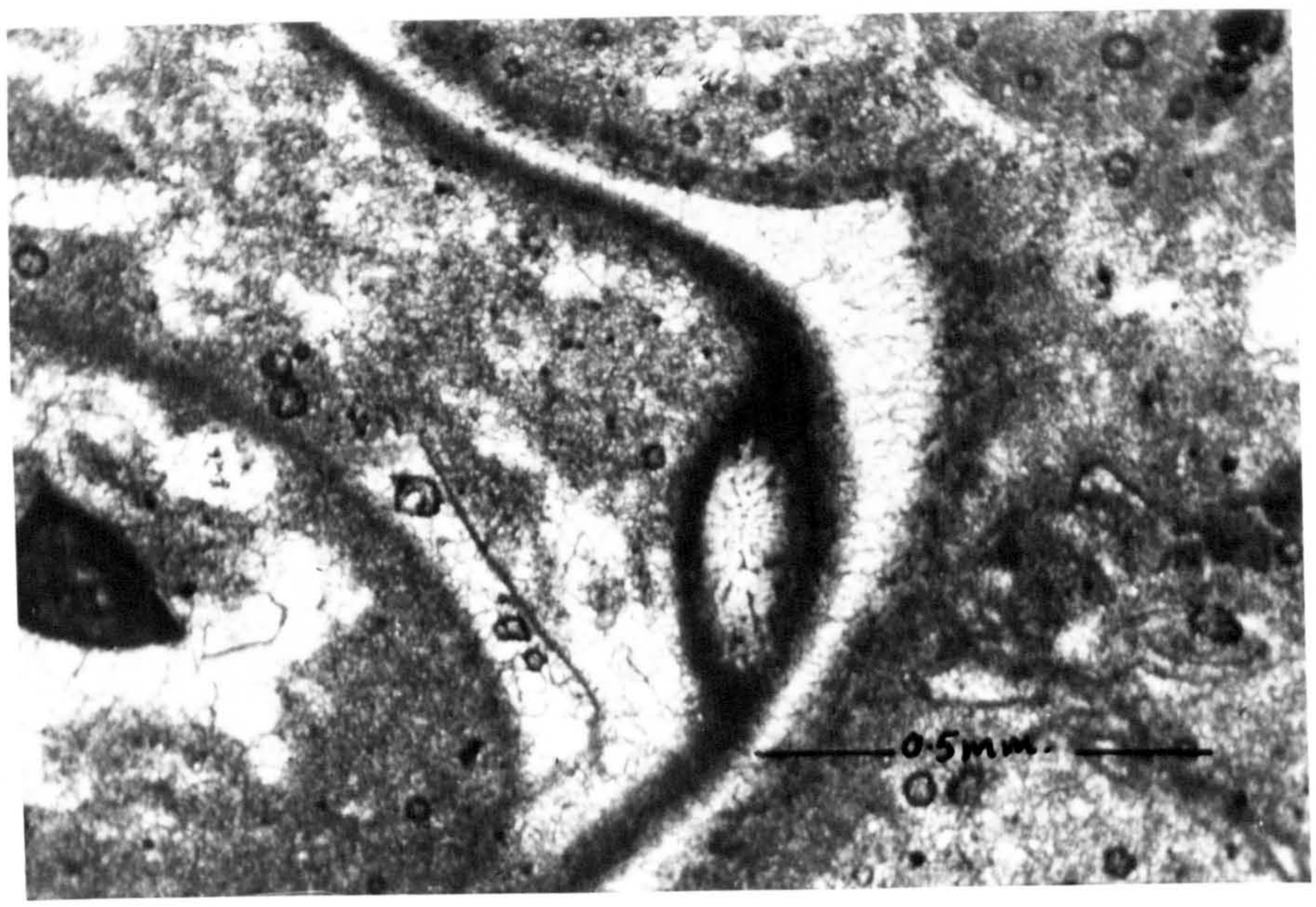
0·5mm.

and many others) suggests that they were originally of aragonite which were later replaced by low Mg-calcite.

Shinn (1969) noticed that aragonite not only fills pore spaces, but can also be a replacement, and stated (p.133) "In some cases it appears that fibrous overgrowth invades the shell and replaces the shell texture with fibrous aragonite in optical continuity with the overgrowth." Type C fibrous cement is thought to be of this type.

4. The fourth, and probably the most difficult to distinguish, is the cryptocrystalline (micritic) cement. The only criteria for distinguishing this type of cement are its geometry and relationship with allochems in the carbonate rocks. Its texture, shape and colour are generally the same, if not identical to micrite produced by algal diminution or by other means. It is therefore often very difficult to assess the importance or the occurrence of this type of cement in the Gachsaran carbonates, and in fact it has rarely been described from other limestone sequences.

In Recent carbonate sediments (e.g. Friedman, 1968b; Taylor and Illing, 1969; Shinn, 1969), a dark, dense cryptocrystalline material cements the grains and lines pores and cavities. This cement has been found to consist in most cases of high Mg-calcite, but sometimes of aragonite. Both of these would change to low Mg-calcite during the course of diagenesis. Cryptocrystalline (micritic) cements in the Gachsaran limestones occur in several forms:

(a) forming micrite envelopes; filling empty tubes in the allochems made by boring algae (see Section 6.5).

(b) cementing micrite sediments; this is shown very clearly in figure 6-9 in which a fragment of micrite envelope has been forced into a cavity now filled with drusy spar. The micrite envelope has sediment remnants attached on its convex side which, without a micrite cementing material, would have been dispersed in the cavity.

(c) in some cases, micrite cement was found to line pores and cavities in the Gachsaran carbonates (fig.6-10). Notice in the latter case the micrite cement is finer in size and more opaque in colour than the surrounding matrix.

(d) in other cases, micrite cement has been found to fill or line cavities of Foraminifera or leached shells of bivalves (figs.6-11, 12). This micrite is identified as a cement and not a mechanically deposited micrite because the latter usually occupies the lower part of the shell cavity, forming a geopetal structure (fig.6-13). Also, micrite fill, in many cases, is associated with skeletal grains and quartz grains (fig.6-14).

The micritic cement described above is thought to have developed as a cryptocrystalline high Mg-calcite similar to Recent occurrences. During subsequent diagenesis, the Mg was depleted to leave low Mg-calcite. The darker nature of some of these micritic cements is probably due to the presence of impurities.

6.3 Late Cementation

Late cementation of the Gachsaran carbonates is thought to be mainly produced through the influence of meteoric waters. Although much leaching may accompany later cementation, much of the literature suggests a reduction in porosity with time. The Gachsaran carbonate rocks were cemented by three major types of minerals; calcite, dolomite and gypsum or/anhydrite, and of these calcite is dominant.

6.3.1 Cementation by calcite

Three major fabric types can be recognised:

A. Drusy calcite mosaic. The term 'druse' was used by Bathurst (1958) to describe a type of cavity-filling mosaic which tends to increase in crystal size away from the substrate. Two types of drusy mosaic were identified in the Gachsaran carbonates.

Fig. 6-11 A gastropod chamber filled with micrite cement. Slice. p.p.l. Bashiqa, Iraq.

Fig. 6-12 A micrite cement forming a centripetal lining to a bivalve cavity. The remainder of the cavity is occupied by drusy calcite mosaic. Slice. p.p.l. Bashiqa, Iraq.

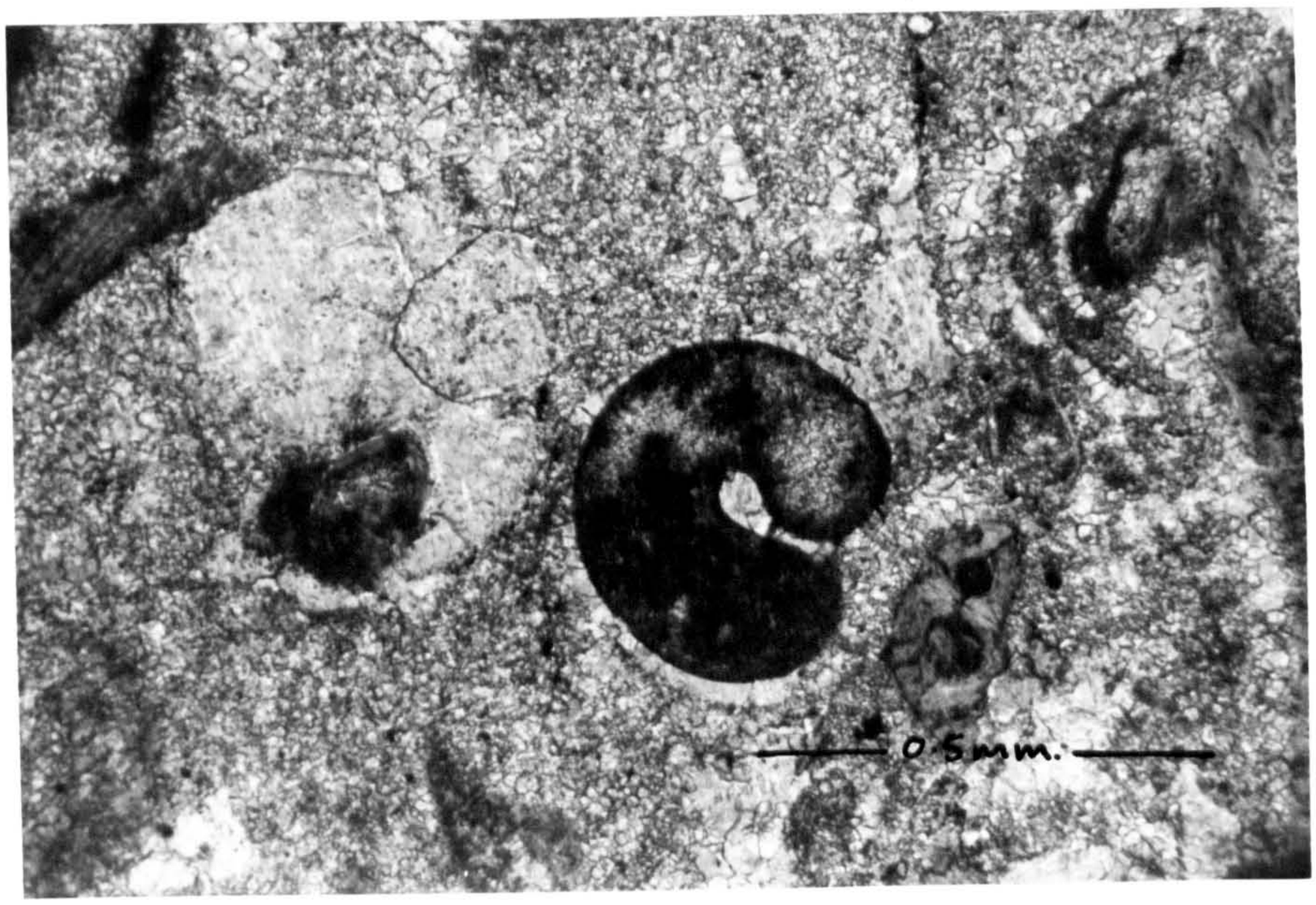
0·5mm.

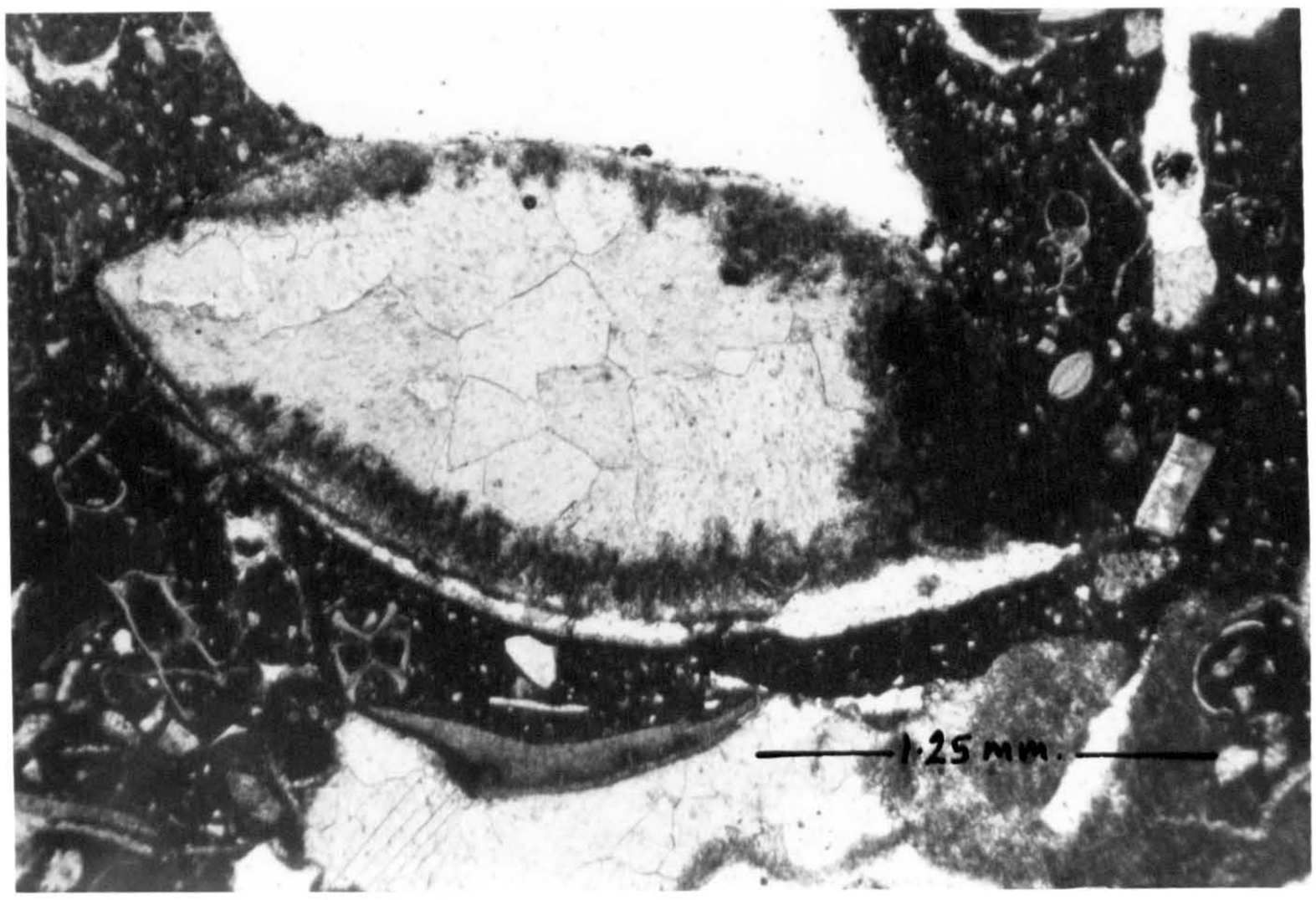
1·25 mm.

Fig. 6-13 Mechanically deposited sediment inside a skeletal test cavity forming a geopetal structure. Note that the remainder of the test is filled by sparry calcite. Slice. p.p.l. Bashiqa, Iraq.

Fig. 6-14 Mechanically deposited micrite associated with quartz grains and small skeletal fragments inside large skeletal fragment cavity. Slice. crossed nichols. Hammam Al-Alil, Iraq.

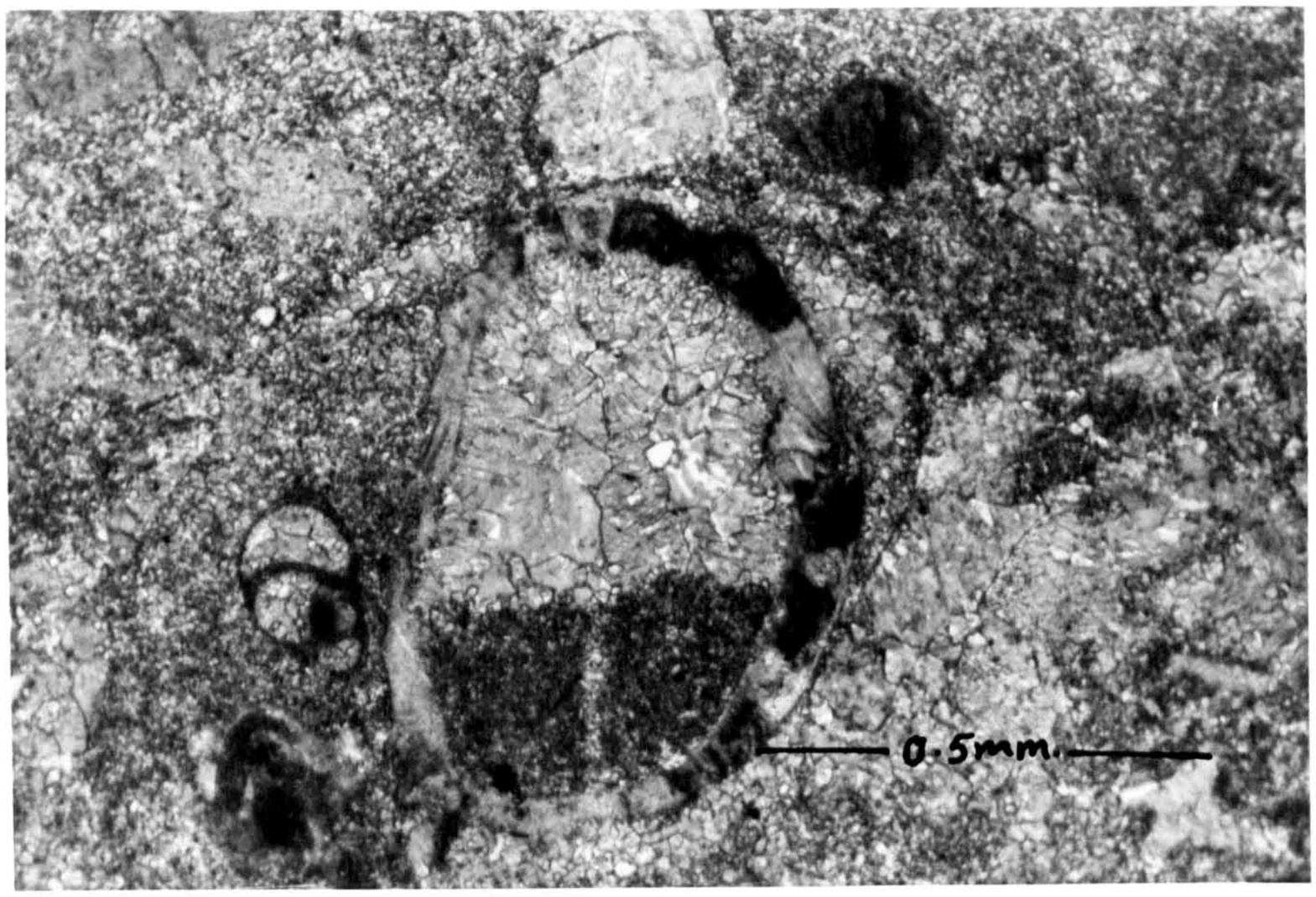
0.5mm.

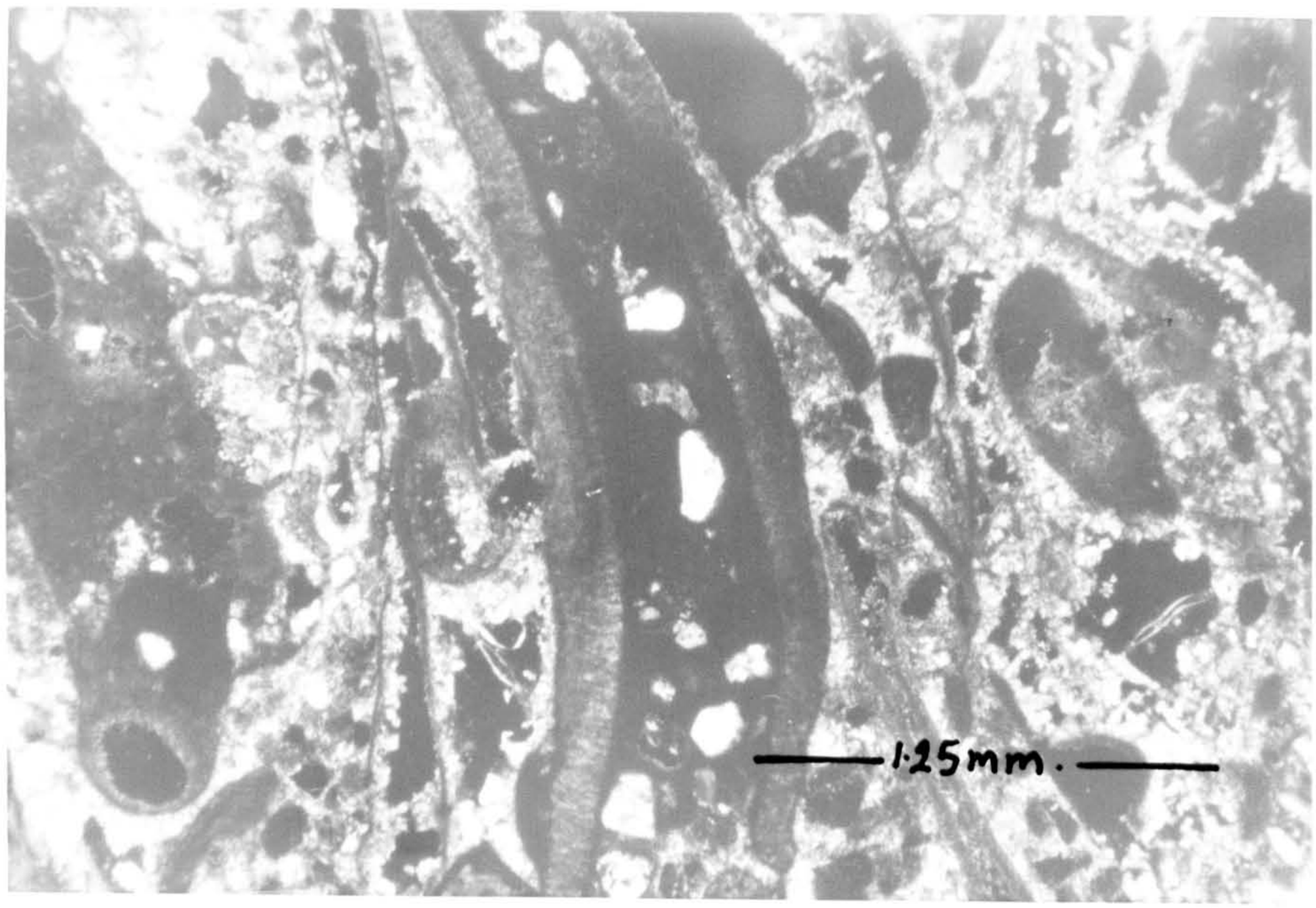
1.25mm.

In the first type the mosaic tends to increase in crystal size away from one margin of the cavity towards the other. The resultant fabric is a finer mosaic on one margin of the cavity and coarser on the other (fig. 6-15). In the second type, smaller crystals around the margins of the cavity increase in size towards the cavity centre (figs.6-16, 17). The increase in crystal size can be gradual (fig.6-17) or sharp (fig.6-16). The increase in size of the calcite crystals was interpreted by Bathurst as arising from competitive growth (Bathurst, 1975, p.422 and fig.303).

B. Granular calcite mosaic. This type of mosaic consists of more or less equidimensional crystals. Bathurst (1958) used the term 'granular' to refer to cements between allochems only. This, however, does not always seem to be the case and granular mosaic is a common cavity fill (fig.6-18), as well as a cement between the allochems.

C. Syntaxial rim mosaic. This type of calcite mosaic characterises echinoderm cementation in the Gachsaran carbonates. It usually consists of two generations of cement. The first is characterised by its numerous pyramidal faces forming a zig-zag outline, while the second envelops the first, forming one poiklotopic crystal; both generations are in optical continuity with the echinoderm fragment (fig.6-19).

Evamy and Shearman (1965, 1969) have described in detail the growing of this type of mosaic. According to them, the growth of syntaxial cement begins with the echinoderm grain filling its pores and then growing outward. As the volume of cement increases, the number of the pyramidal faces are reduced.

6.3.2 Cementation by dolomite

Dolomite rhombs (10 to 30μ) were found to line skeletal cavities and voids forming an internal rim cement (fig.6-20). This cement is either one or several crystals thick. It usually occupies the margins of voids and was not seen filling the pores completely. The centres of these voids are

Fig. 6-15 A bivalve filled with drusy spar. Note the smaller crystals of calcite on one side and the larger crystals on the other. Slice. p.p.l. Bashiqa, Iraq.

Fig. 6-16 A cavity filled with drusy spar. Note the calcite crystals increase in size towards the centre of the cavity. The increase is abrupt. Compare with Fig.6-17. Slice. p.p.l. Bashiqa, Iraq.

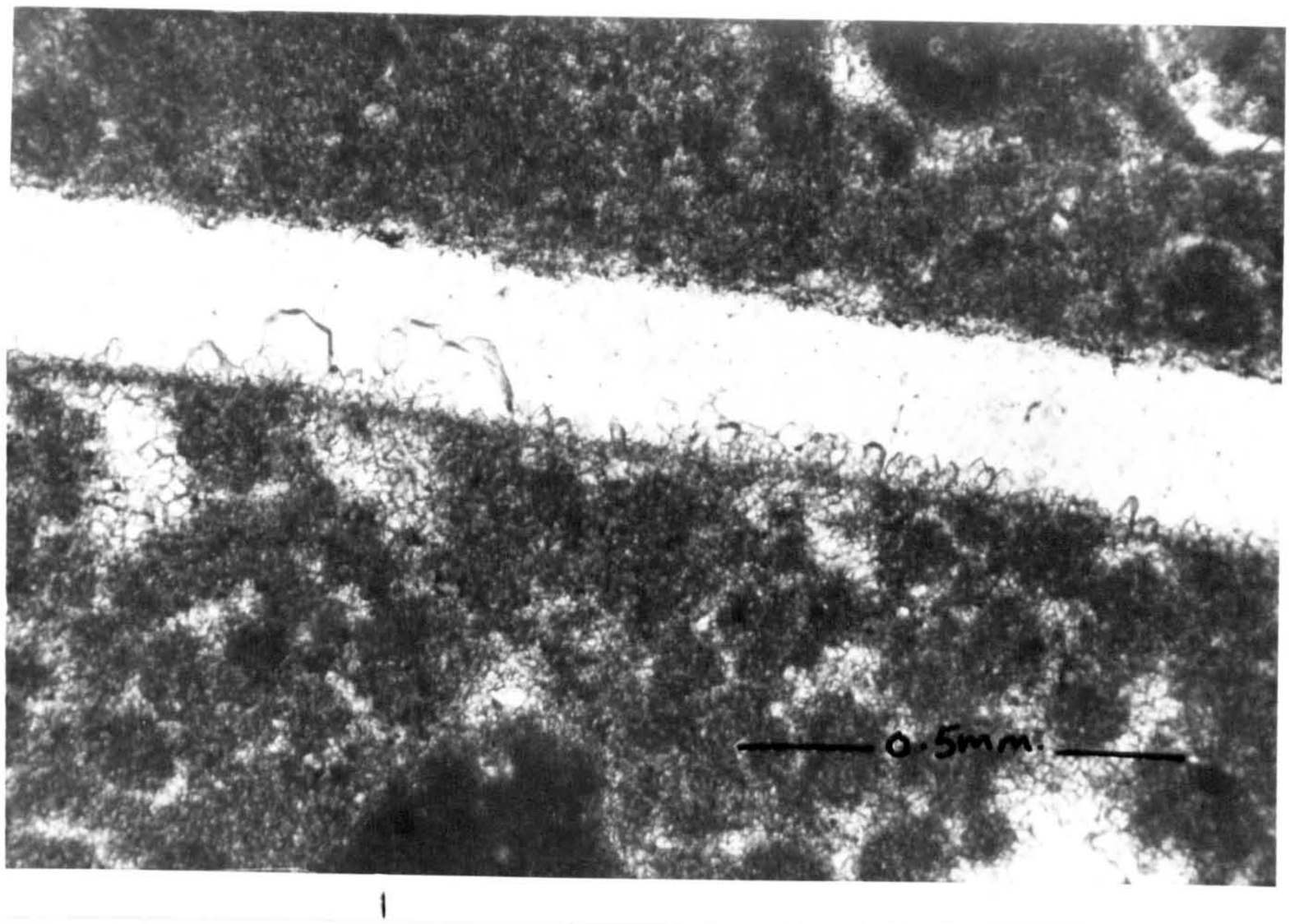
0.5mm.

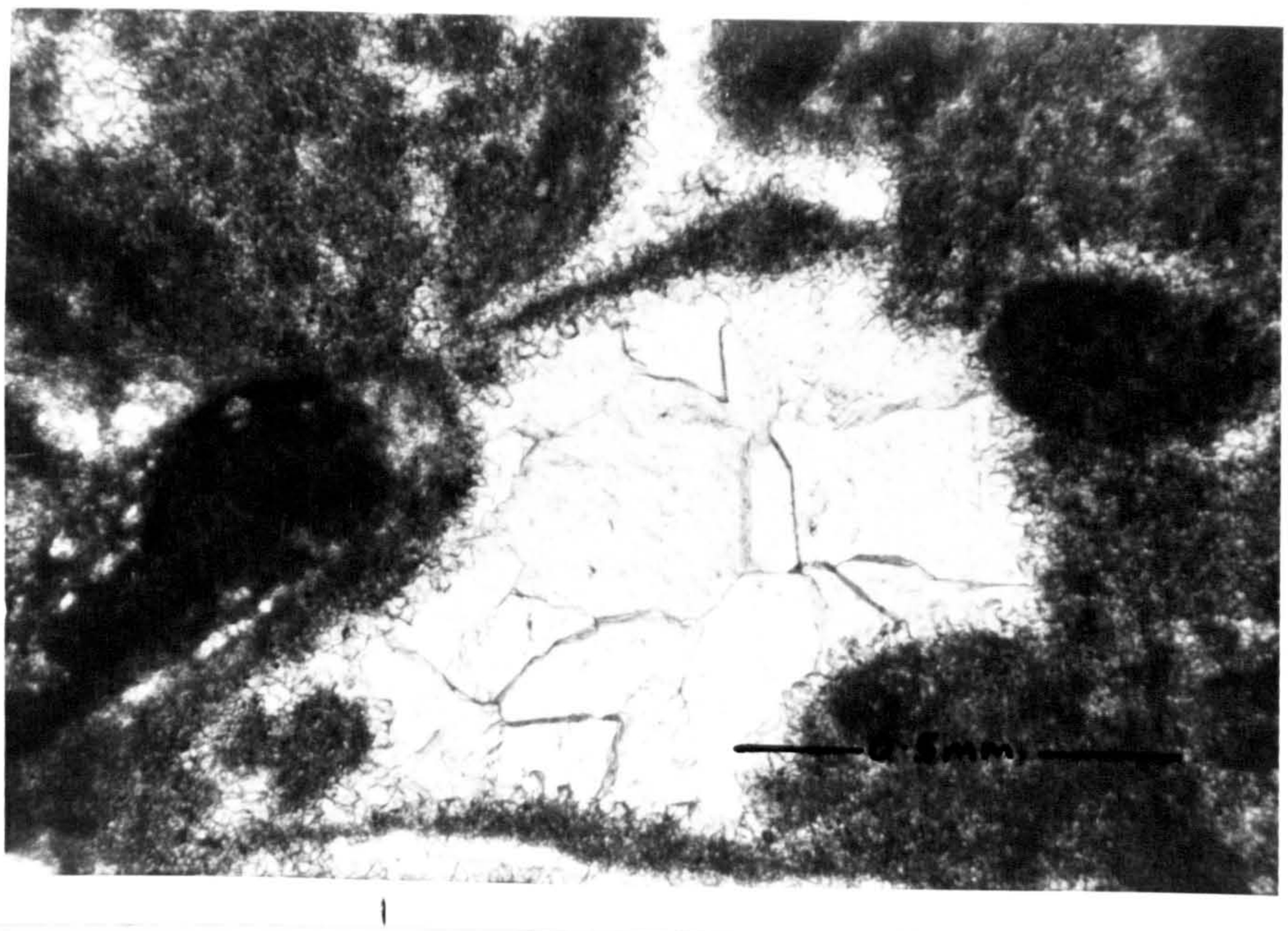
0.5mm.

Fig. 6-17 A bivalve cavity filled with drusy spar. Note the gradual increase in calcite crystal size towards the centre. Slice. p.p.l. Bashiqa, Iraq.

Fig. 6-18 A cavity filled wth granular mosaic of calcite crystals. Slice. p.p.l. Bashiqa, Iraq.

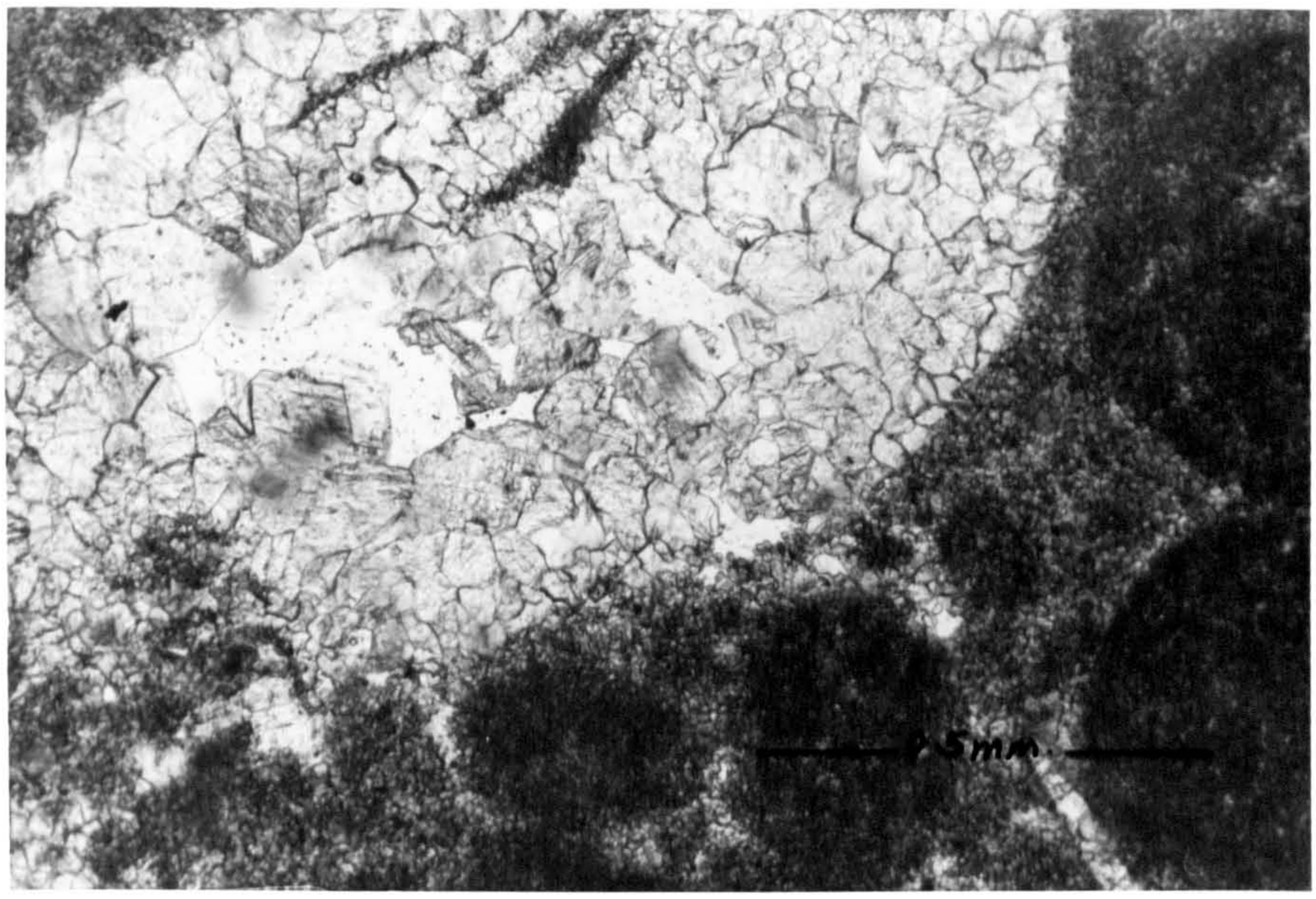

1

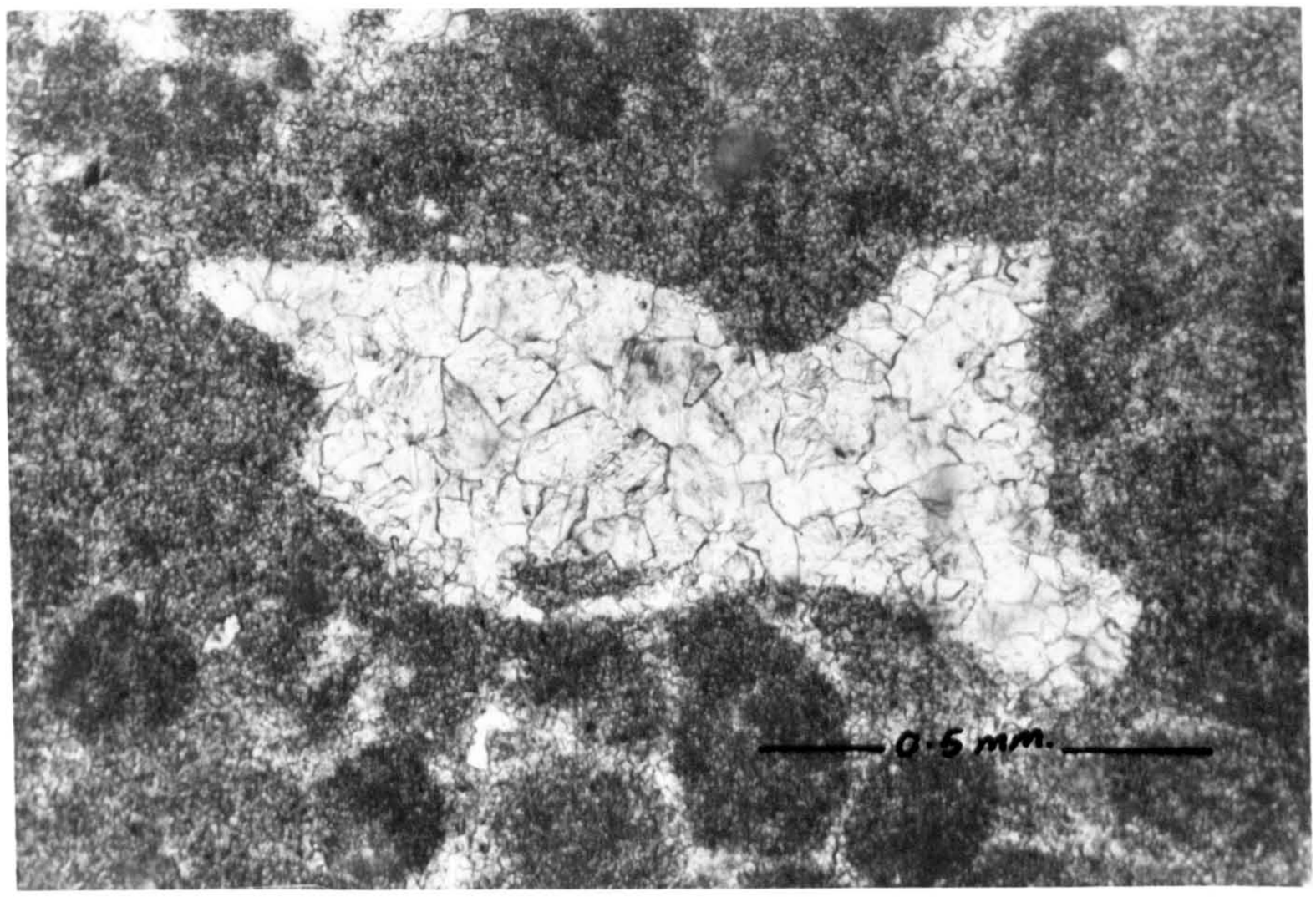

1

Fig. 6-19 An echinoderm fragment on the right cemented by syntaxial cement. Note the zig-zag pyramidal faces of the cement in the cavity as differenciated from the second generation cement filling the rest of the cavity to the left. Both generations are in optical continuity with the cement filling the echinoderm fragment. Slice. p.p.l. Hammam Al-Alil, Iraq.

Fig. 6-20 A bivalve cavity lined centripetally by dolomite rhombs. The rest of the cavity is filled with sparry calcite crystals. Slice.p.p.l. Mishraq, Iraq.

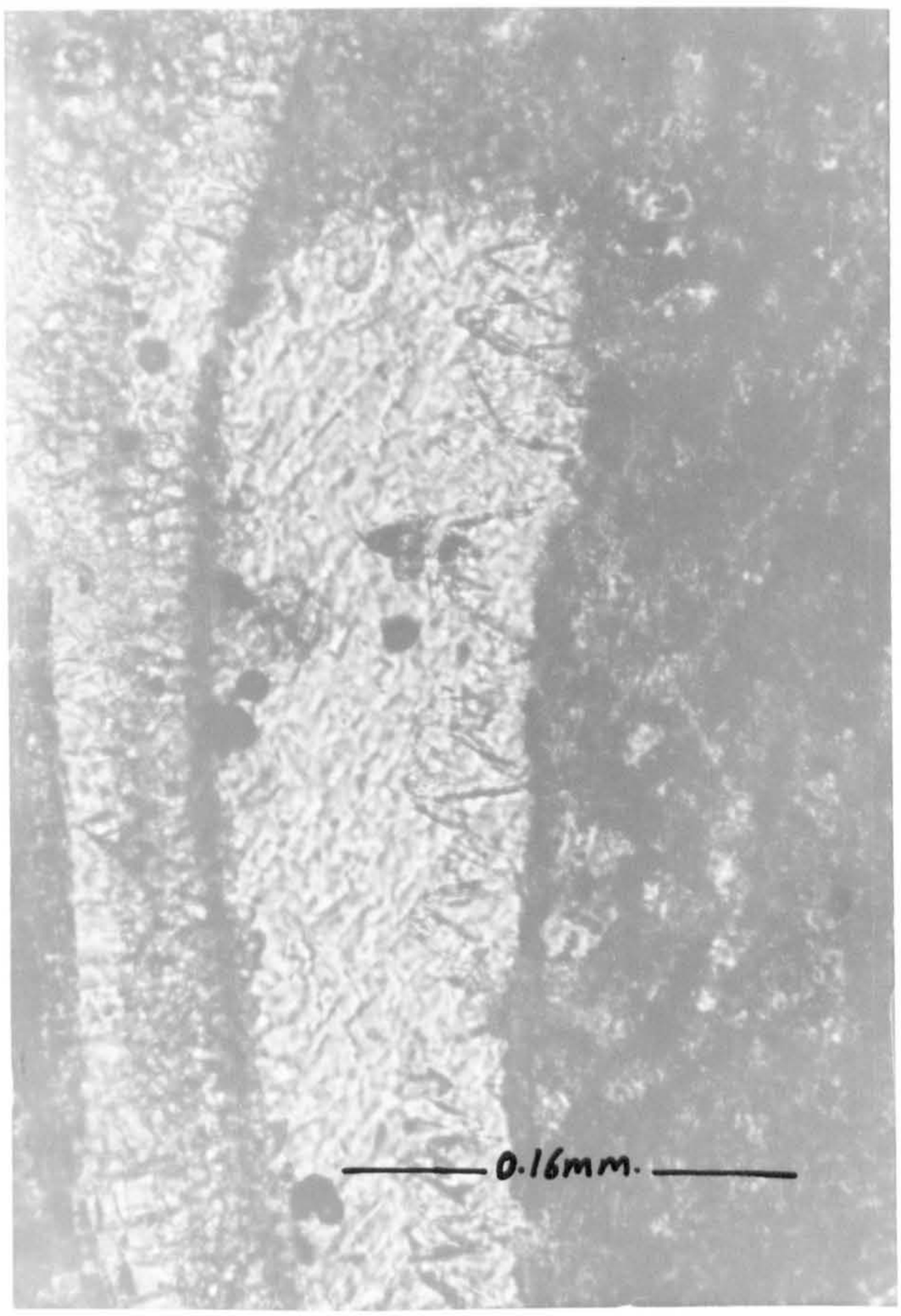
0.16mm.

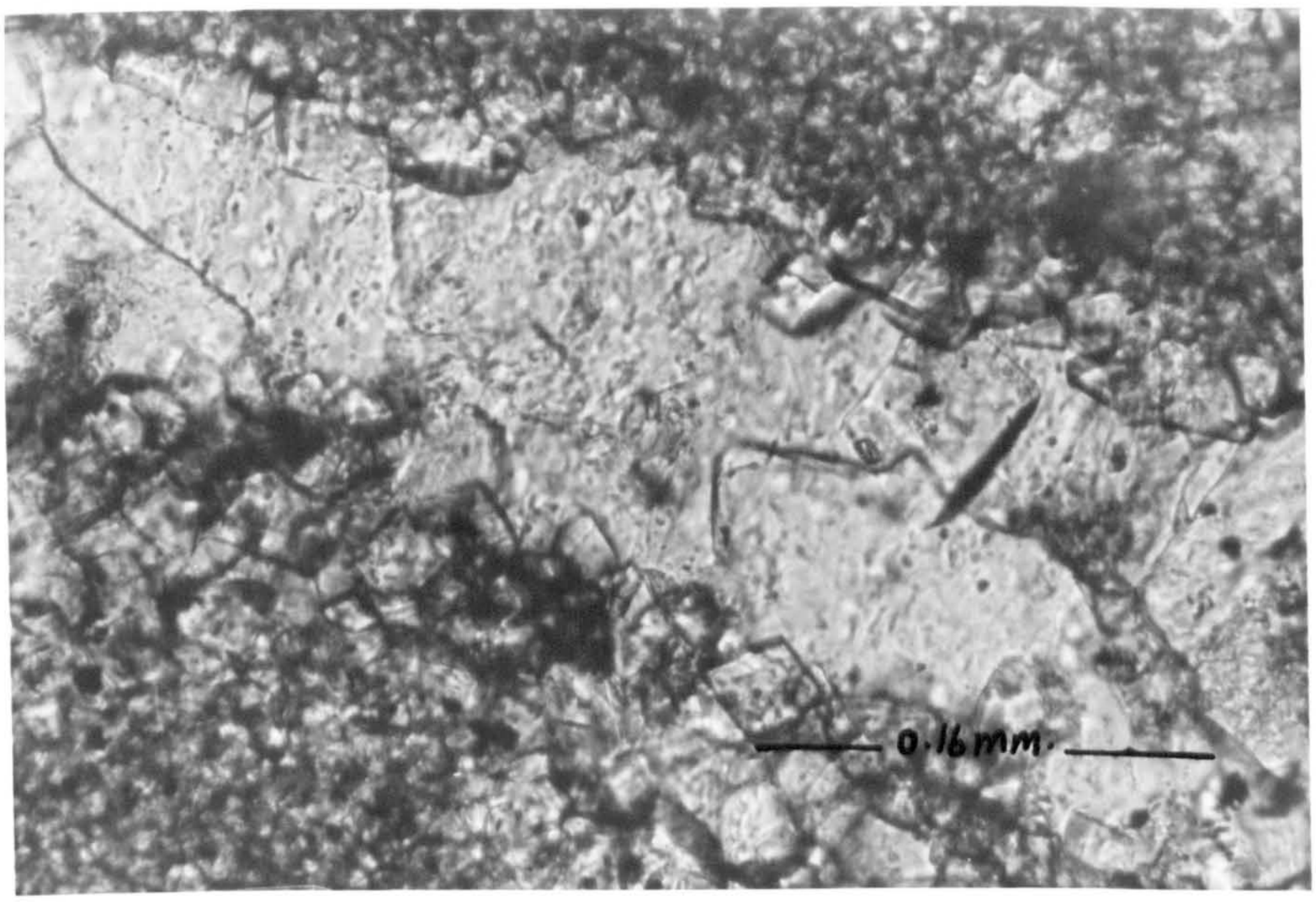
0.16mm.

occupied by sparry calcite cement. It was noticed that in such an occurrence, the matrix of the rock is also dolomitised.

From the above observations, it is suggested that cementation accompanied dolomitisation, with dissolution of the bioclasts taking place at an earlier stage.

6.3.3 Cementation by sulphates

Gypsum occurs as a cement within leached bivalve grains in some biomicritic rocks from the Gachsaran Formation. The original shapes of the bivalve grains are intact (no collapse structure)(fig.6-21). This type of cement was found to have a replacive habit as well (figs.6-21, 22). The replacive gypsum is recognised through the presence of inclusions of micrite and allochems. Lensoid crystals of gypsum were also present. In some samples the gypsum replacing the micrite rocks is of type A (fig.6-23)(see Chapter 3, Section 3.11), suggesting that this gypsum has replaced anhydrite (see Section 3.11).

The above observations indicate two stages of diagenesis. During the first stage the allochems were infilled with gypsum following the dissolution of the aragonite composed allochems. Later diagenesis included the replacement of some of the micrite matrix by gypsum. Sulphate cements were precipitated during later diagenesis, such as on uplift. The presence of lensoid gypsum crystals suggests that these sediments were deposited in an intertidal-shallow subtidal setting.

6.4 Neomorphism

The term 'neomorphism' was introduced by Folk (1965) to embrace certain diagenetic processes such as inversion, replacement and recrystallisation. Strictly, the term 'recrystallisation' is used to invoke crystal enlargement or diminution without change in mineralogy. Neomorphism thus includes recrystallisation. The term 'aggrading neomorphism' is used to describe processes that result in crystal enlargement. The term 'degrading

Fig. 6-21 A biomicrite. The bivalve cavities are filled with gypsum cement. Note that in some cases the gypsum crystals have a replacive character. Slice. crossed nichols. Hammam Al-Alil, Iraq.

Fig. 6-22 A cavity filled with gypsum crystals. Note the presence of inclusions and a Foraminifera fragment within the cemented cavity. Slice. crossed nichols. Hammam Al-Alil, Iraq.

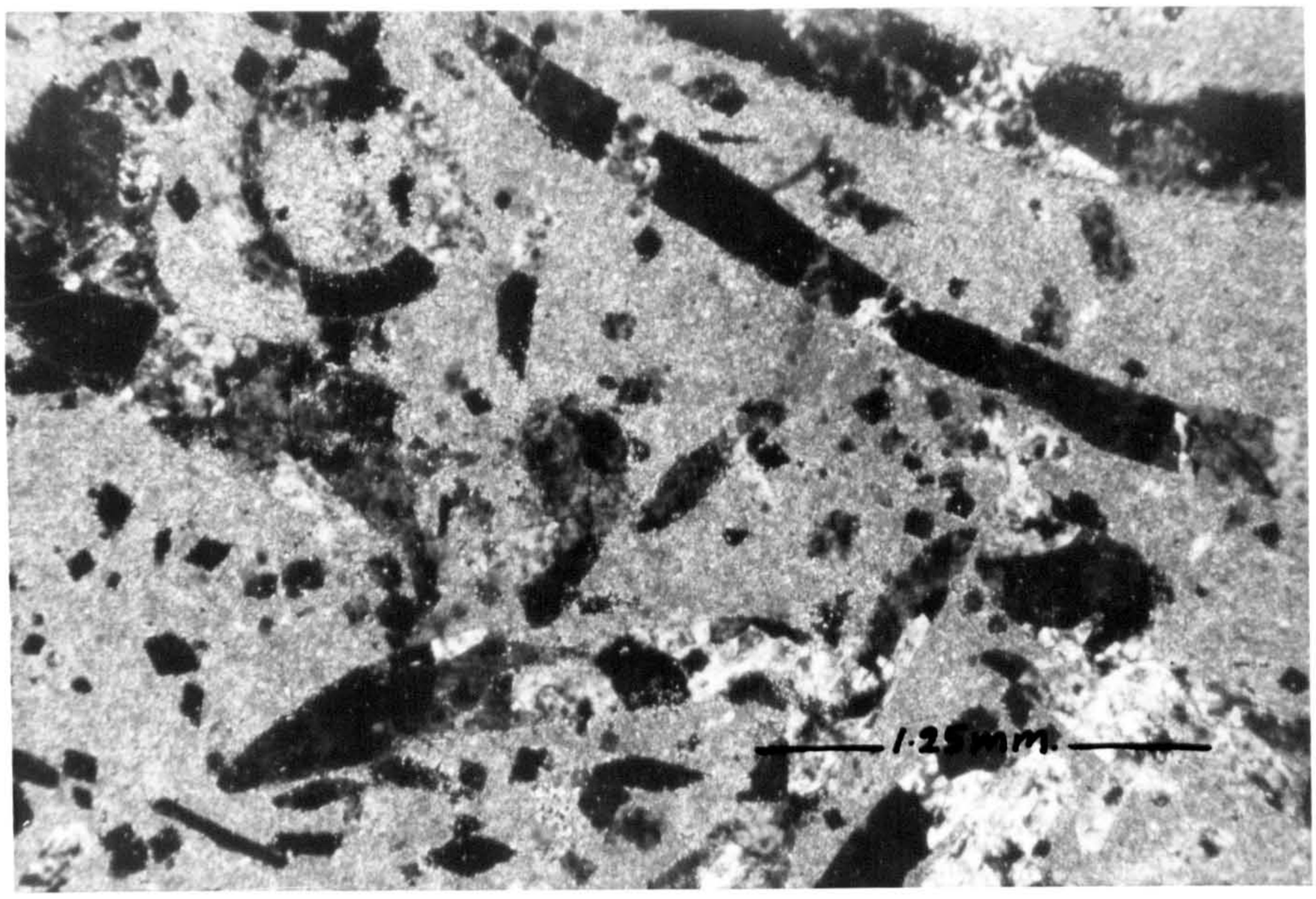
1·25mm.

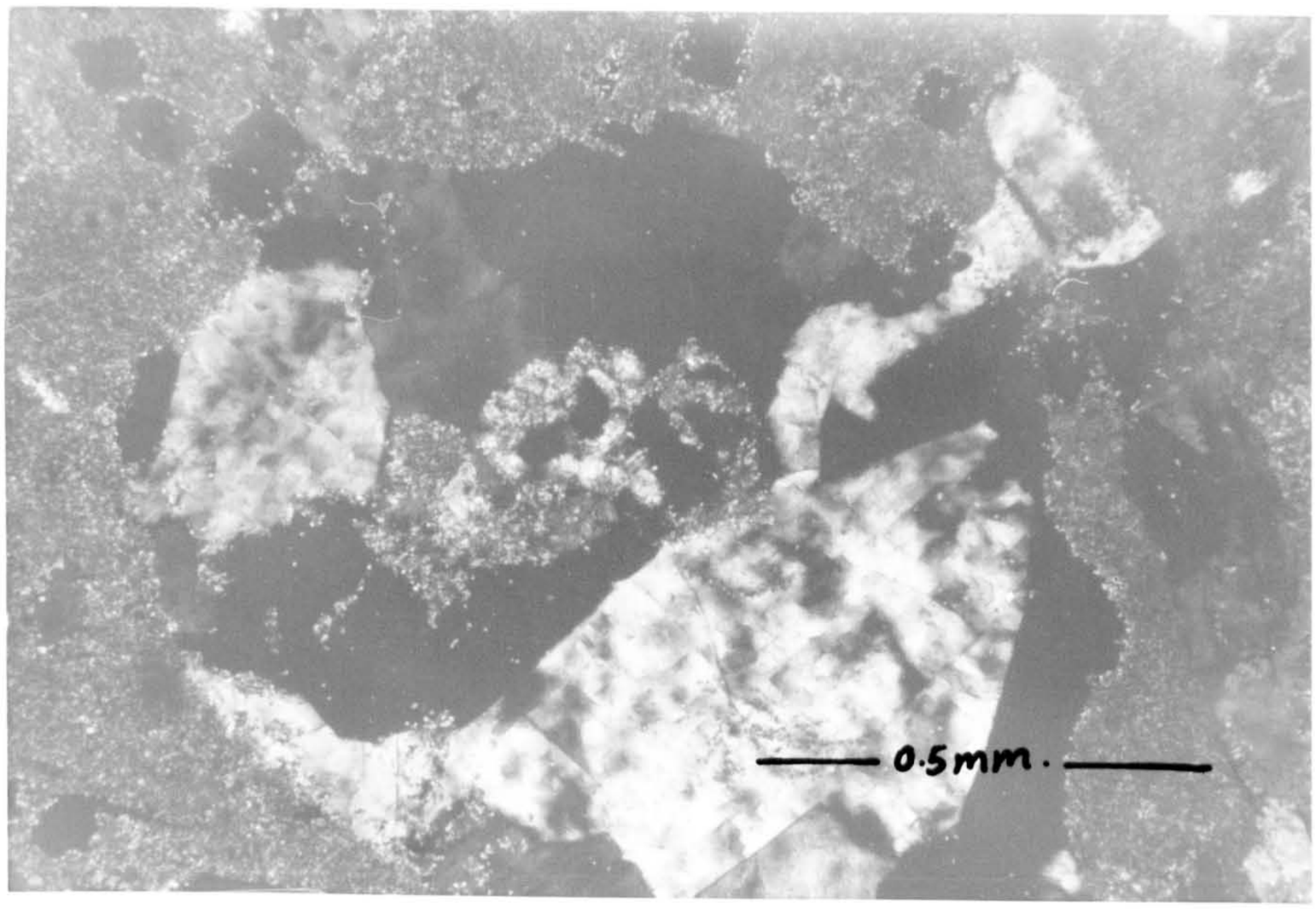
0·5mm.

Fig. 6-23 Type A gypsum filling cavities and replacing micrite matrix. Slice. crossed nicoles, Makhul, Iraq.

Fig. 6-24 Neomorphic spar. Note the relatively uniform size of the calcite crystals. Slice. crossed nicoles, Shaikh Ibrahim, Iraq.

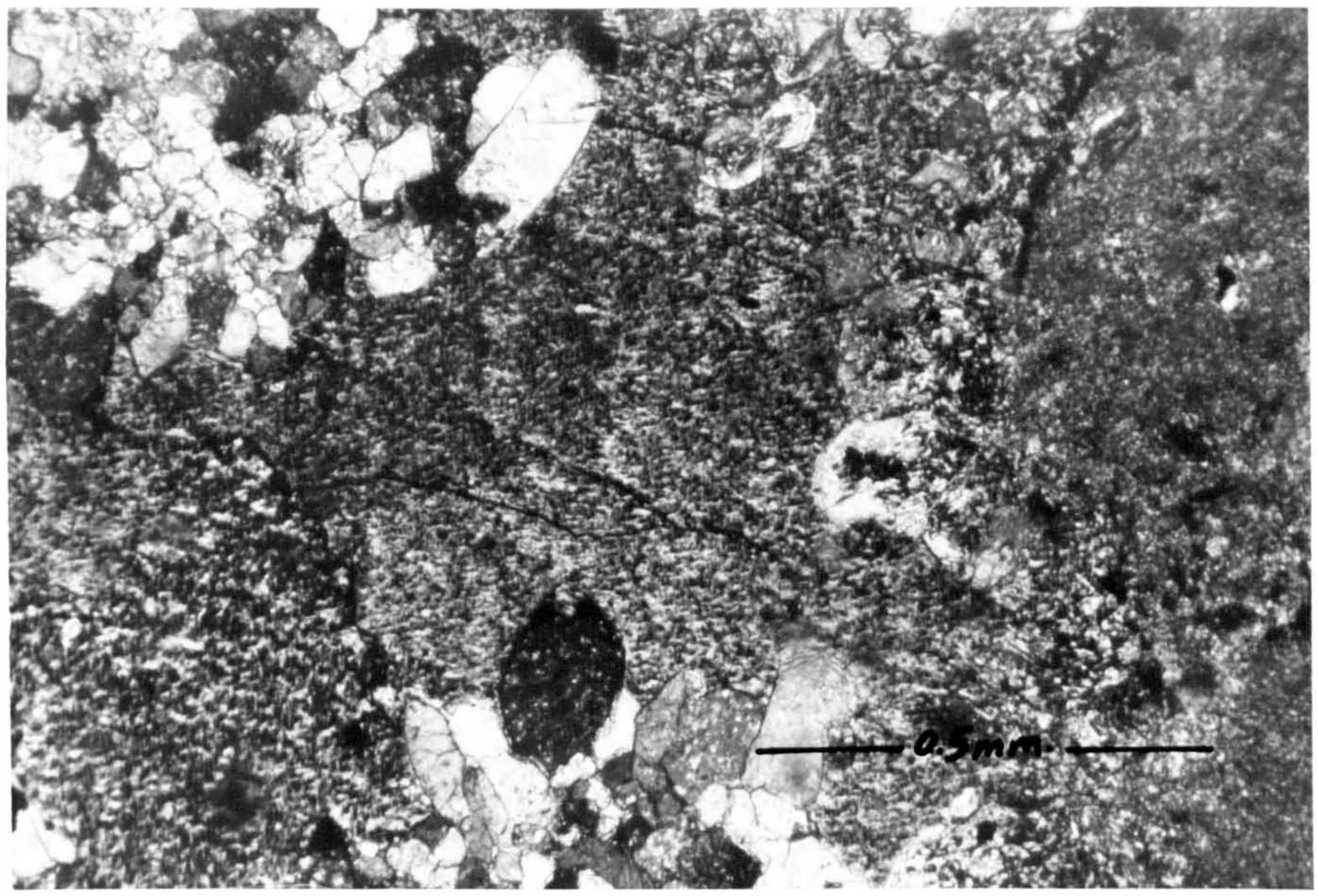

1

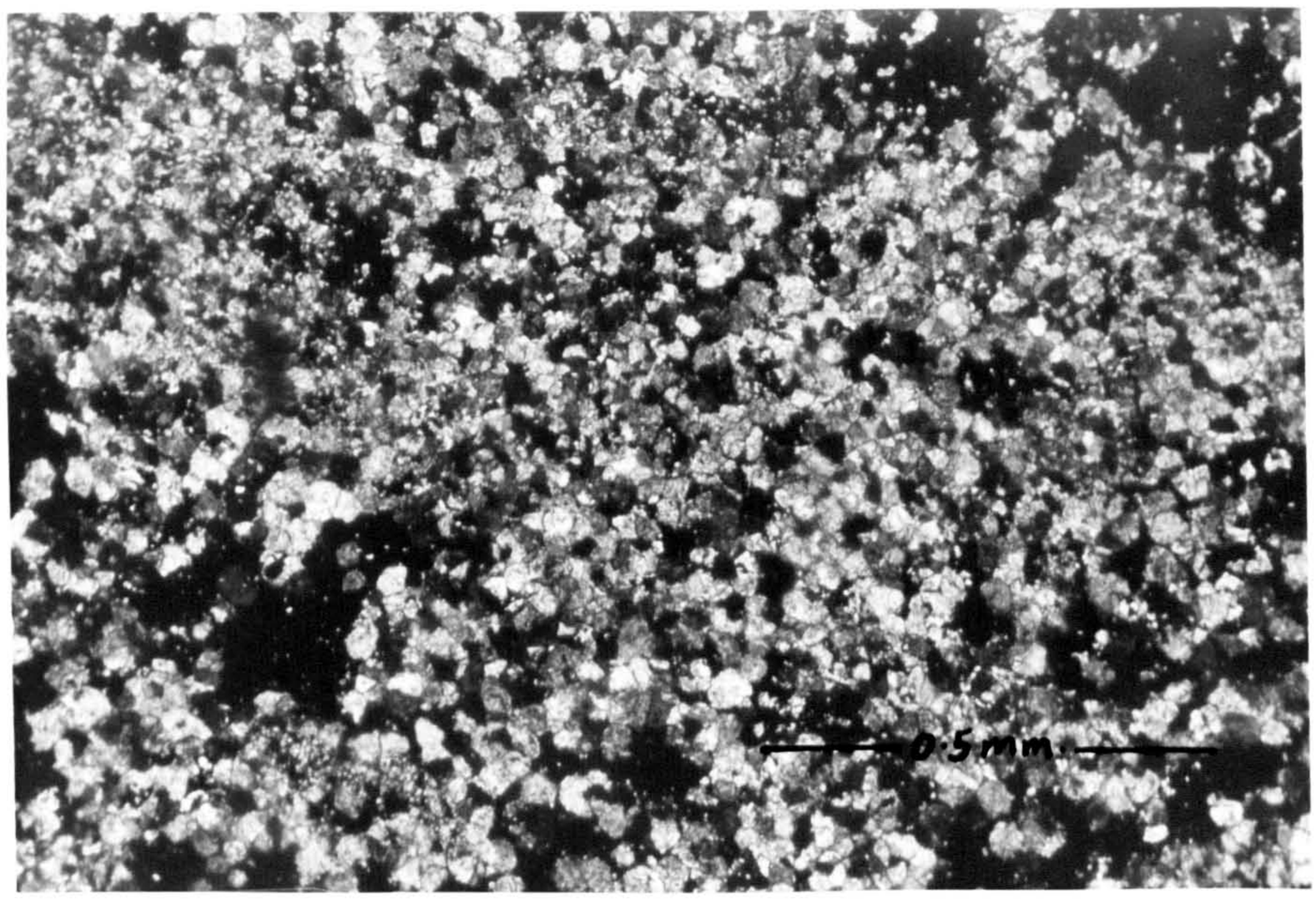

1

neomorphism' is used to describe processes that result in crystal diminution.

It is not always easy to distinguish neomorphic spar from sparry calcite cement; the criteria used here to distinguish between the two fabrics are after Bathurst (1975).

A. Matrix neomorphism. The matrix of many limestones in the Gachsaran Formation consist of micrite sized particles (1-5μ).

The term 'microspar' was used by Folk (1965) to denote 'recrystallised' micrite which has a crystal size of 5-6μ. Microspar crystals up to 10μ, however, are not uncommon.

Three types of matrix neomorphism were distinguished in the Gachsaran limestones:

1. The first type results from the gradual enlargement of all micrite crystals, maintaining a uniform crystal size through all stages of crystal enlargement (fig.6-24, see also fig.3, Folk, 1965). The term 'coalescive neomorphism' was given for this form of crystal enlargement by Folk.

2. In the second type, grain enlargement has taken place from scattered centres within the micrite matrix. These areas would increase in size to form microspar with patches of micrite, or less neomorphosed microspar retained (fig.6-25, see also fig.3, Folk, 1965). This process leads to a heterogeneous texture referred to as gramulous or clotted texture (fig. 6-26) in this work. The reasons behind the development of these two different textures were investigated by Bausch (1968) and Marschner (1968). Both have agreed that the amount of insoluble residue present within the rock is a determining factor. The more insoluble residue present, the more the neomorphism of the particles is hindered, so that the second type of texture tends to develop. This in fact is the case with most of the examples of neomorphism encountered in the Gachsaran samples.

Bathurst (1958) used the metallurgical term 'grain growth' to describe

Fig. 6-25 Neomorphic spar. Note the difference in the neomorphosed calcite crystal sizes. Slice. crossed nichols. Hammam Al-Alil, Iraq.

Fig. 6-26 A neomorphosed biomicrite showing a clotted texture. Slice. crossed nicoles, Hammam Al-Alil, Iraq.

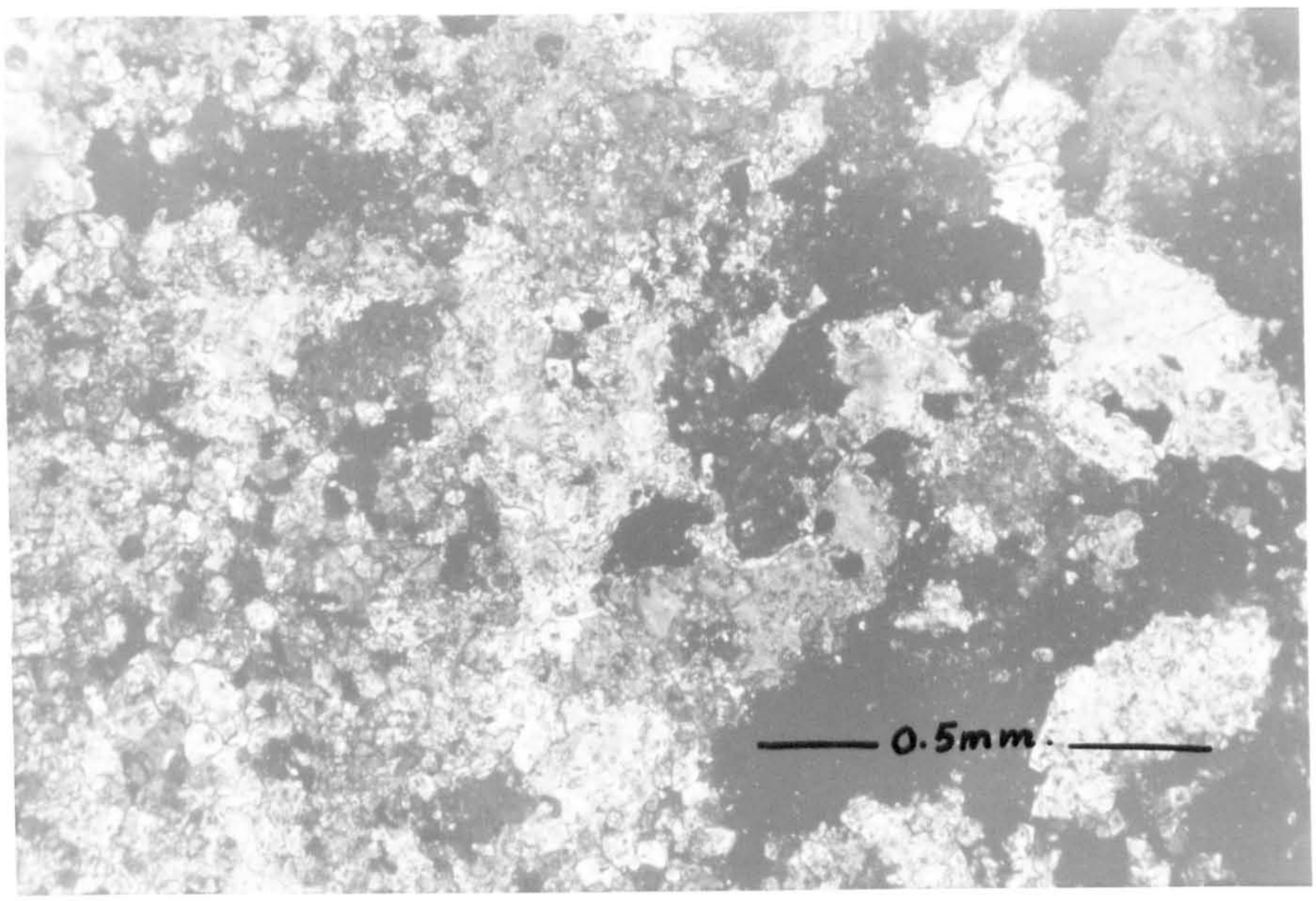

1

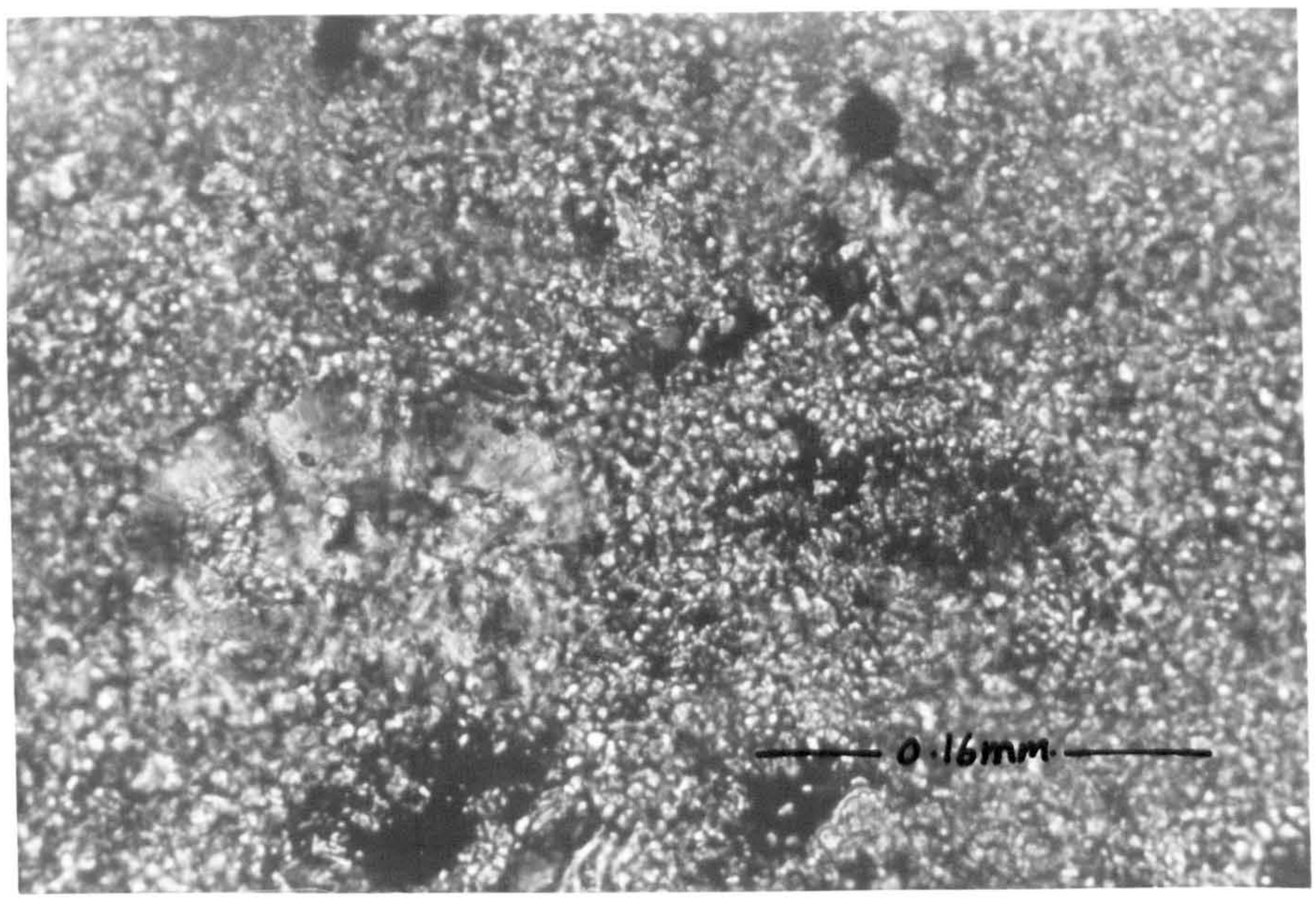

1

calcite crystal enlargement (i.e. micrite to sparite). Folk presented a convincing argument for abandoning this term which involves solid-state metamorphic-type processes and emphasised the role played by water during diagenesis. Bathurst later accepted this, and Folk's term 'aggrading neomorphism'.

Silt-sized particles - It may be important to mention, while dealing with the subject of microspar, that not all silt-sized calcite crystals are neomorphosed micrite. Indeed, silt-sized particles are not uncommon in the Gachsaran carbonates. For example, silt-sized calcite crystals frequently occupy voids within skeletal grains as part of geopetal structures (fig.6-13). The crystals have an average diameter of 10μ and their general characteristics do not show any feature which would suggest recrystallisation. Dunham (1969) and Bathurst (1975) have both confirmed that primary carbonate silt can exist. The origin of this silt was suggested by Dunham to be a combination of winnowing and solution of sediment. Bathurst expressed his doubts as to the original mineralogy of this microspar; whether it was initially aragonite or calcite.

B. Neomorphism of allochems

1. Degrading neomorphism. This type of neomorphism was first noted by Orme and Brown (1963) in crinoid ossicles. The process involves a decrease in crystal size, the opposite of aggrading neomorphism. Orme and Brown used the term 'grain diminution' to describe the replacement of a crinoid ossicle by microspar. Bathurst (1975), however, expressed his doubts about these observations and suggested that the microspar had formed by a process similar to algal micritisation. Other descriptions of degrading neomorphism have come from limestones which have been subjected to tectonic deformation or low grade metamorphism. No convincing examples of degrading neomorphism of skeletal fragments were found in the Gachsaran carbonates.

2. Aggrading neomorphism. The most easily distinguished form of aggrading neomorphism is the polymorphic replacement of fibrous aragonite by low Mg-calcite (figs.6-7, 8). The fibrous aragonite has been polymorphically replaced by low Mg-calcite. Two observations can be cited on this type of neomorphism; the first one is the displacive nature of the neomorphosed fabric (fig.6-8). The micrite envelope is broken and part of it is displaced outward by the neomorphosed calcite fibres. The second is the replacive nature of these fibres outside the bivalve shell. The fibres of calcite outside the shell are in optical continuity with those occupying its interior. Traces of original structures are still preserved, represented by impurity lines. This process and the resultant texture was also reported from the Recent sediments of the Arabian Gulf by Shinn (1969).

Blocky calcite crystals were also found to occupy bivalve shells (fig.6-27). These have the features of neomorphic spar described by Bathurst (1975). It is possible that the polymorphic type of spar recrystallised into this type. It is also possible that this type resulted from the direct neomorphism of the aragonitic shells. Also, with regard to allochems, microspar has developed within the matrix and then replaced pellets. As a result, the pellets have been rendered (fig.6-28).

C. Replacement of sulphates

This process is thought to have a wide occurrence in the Gachsaran Formation. In Fatha and Mishraq areas, it was noticed that wholesale replacement of gypsum beds by calcite has occurred, resulting in cavernous sugary limestone beds (fig.6-29). Microscopically two stages in the replacement process are observed; the first is the replacement of lath anhydrite by calcite and the second is the recrystallisation of these calcite pseudomorphs after lath anhydrite into blocky calcite spar (fig.6-30). The spars are up to .4mm. in diameter.

Fig. 6-27 A biomicrite. The bivalve cavities are occupied by blocky neomorphic calcite crystals. Traces of impurities are only faintly preserved. Slice. p.p.l. Shaqlawa, Iraq.

Fig. 6-28 A pelmicrite showing aggrading neomorphism. The micrite is replaced by neomorphic microspar. Note that the pellets are rendered as a result of neomorphism. Slice. crossed nicoles, Hammam Al-Alil, Iraq.

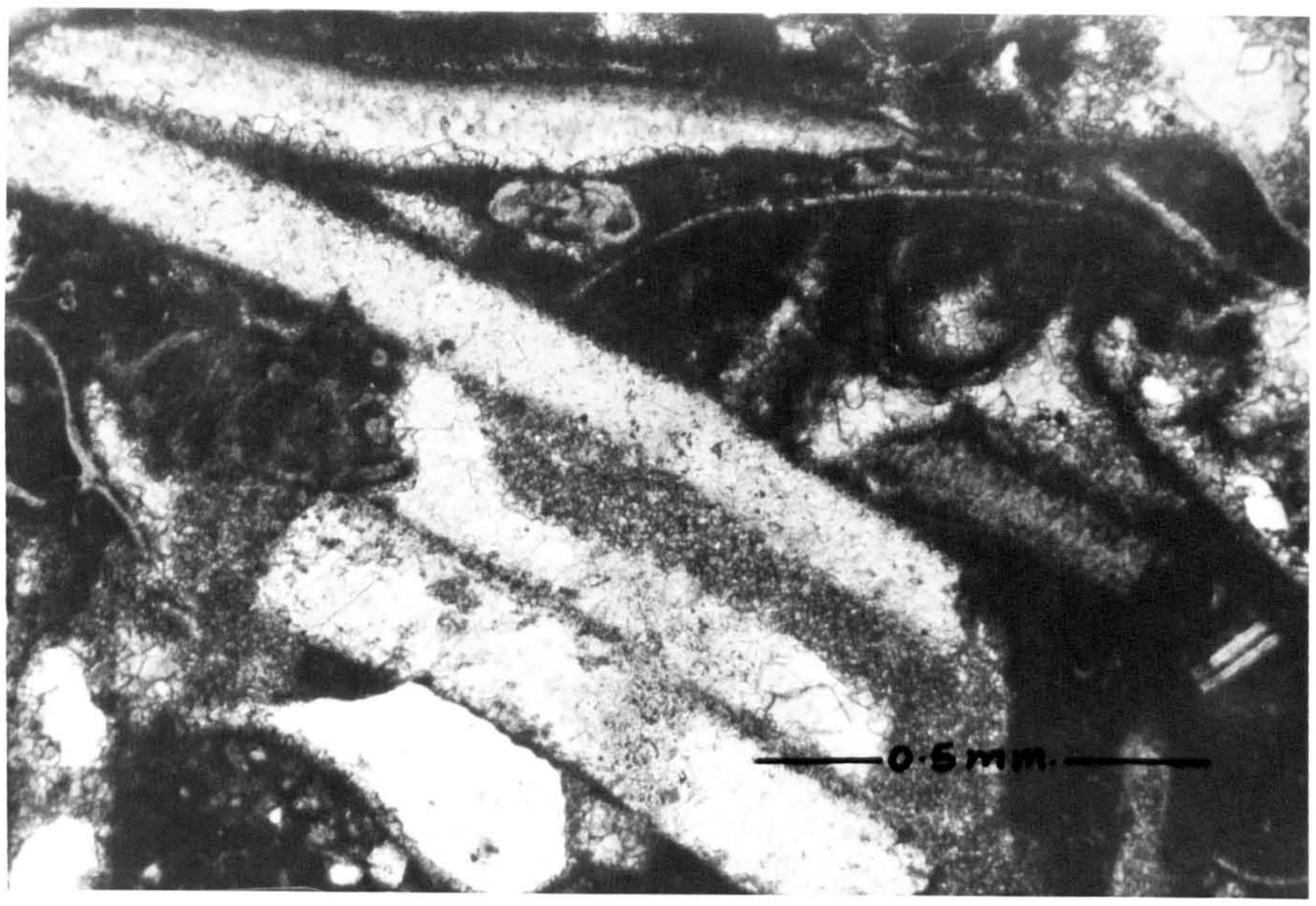

1

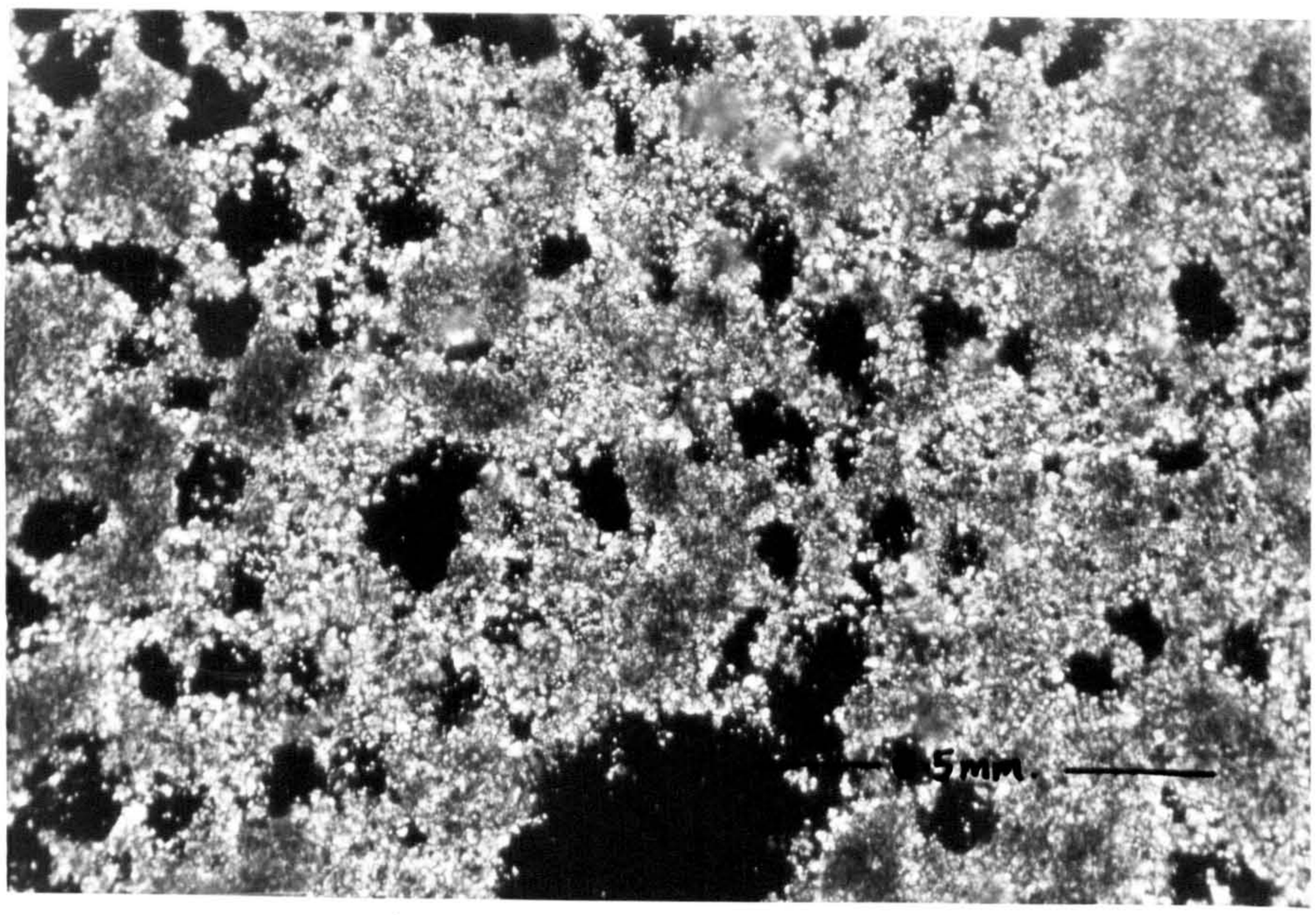

1

Fig. 6-29 Cavernous sugary limestone beds. Resulting from the wholesale replacement of gypsum beds by calcite. Hammam Al-Alil, Iraq.

Fig. 6-30 Anhydrite laths replaced partly by gypsum (g) and then by blocky calcite crystals (c). Slice. crossed nicoles, Mishraq, Iraq.

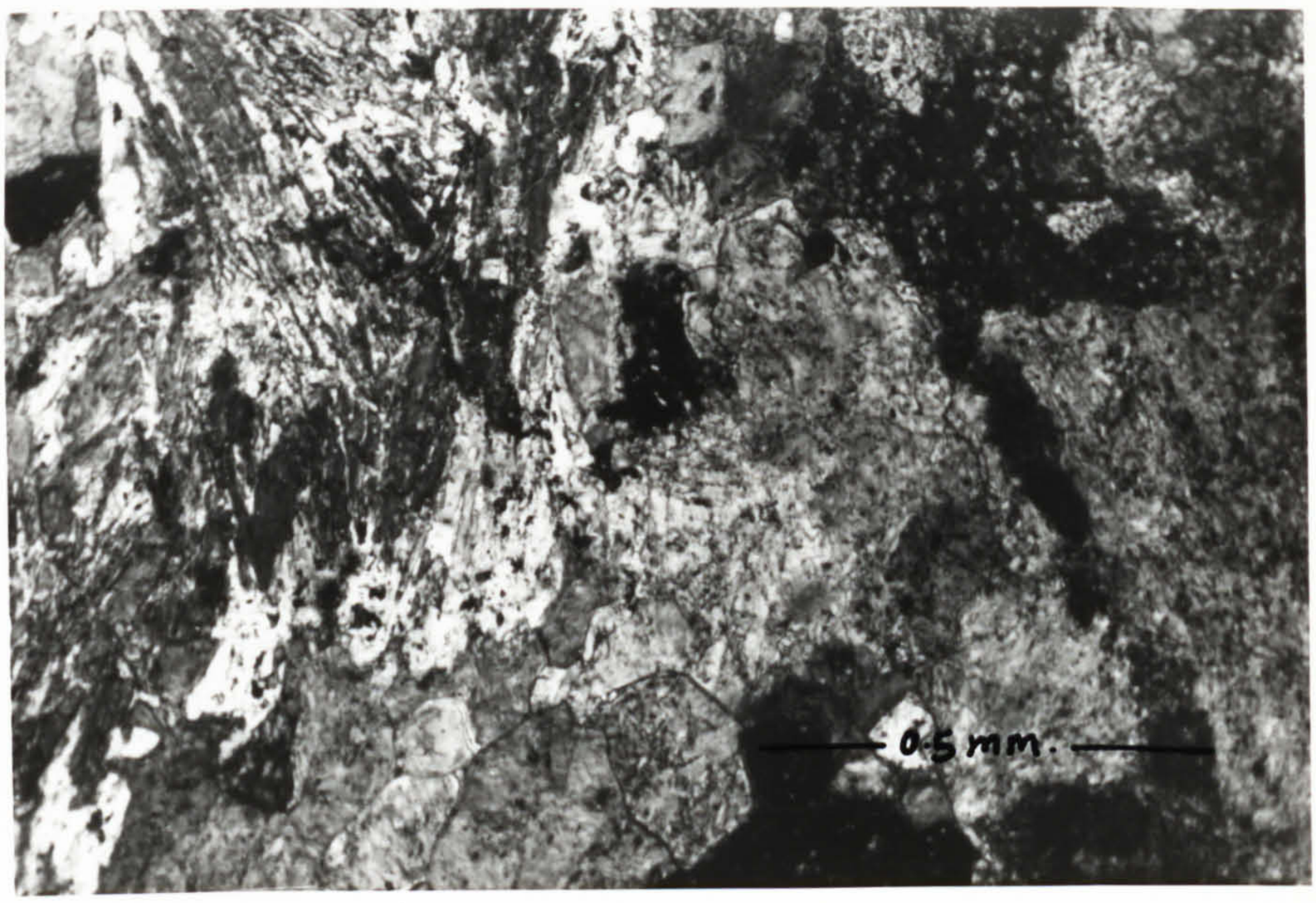
0.5 mm

6.5 Micritization

Dense micrite is often found associated with algal filaments in the Gachsaran Formation. Similar micrite has been found forming envelopes around molluscan grains and in many cases constituting the whole allochem and so obliterating its original structure to the extent of non-recognition.

The close association of micrite with algal borers has been described from many Recent environments (e.g. Wolf, 1965; Emery, et al., 1954; Ginsburg, 1957), however, no direct relationship was deduced. Bathurst (1966) pointed out that skeletal fragments and other allochems are bored by algae and that these bores are later filled by micrite. By repeated boring and infilling, the allochems can be completely micritised. Bathurst referred to this process as micritization. Such a process was found to be most common in Recent intertidal and supratidal environments (e.g. Bathurst, 1966; Taylor and Illing, 1969). Algal micritization is widespread in the Gachsaran limestones and alters the allochems producing (1) micrite envelopes, and (2) wholly micritized grains.

1. Micrite envelopes

The effects of boring, endolithic algae are first to produce a micrite envelope around allochems (figs.6-27, 31). Their formation is in the manner described by Bathurst (1966, 1975). The existence of micrite envelopes is important for the preservation of molluscan grains which were originally composed of aragonite. Aragonite, being metastable, is replaced by calcite during diagenesis. In many cases, a void stage exists between aragonite solution and calcite precipitation. The presence of a micrite envelope around an aragonite skeletal grain can preserve the grain shape if a void stage develops. Cases of broken and deformed envelopes are not uncommon (fig.6-31). The reasons for the ability of micrite envelopes to withstand considerable mechanical pressure without breaking are still remote. Kinsman (in Bathurst, 1975, pp.334) pointed out the importance of

organic matter in consolidating the micrite envelopes. The organic matter may have acted as an adhesive material giving the micrite envelopes their high elastic capability and thus, in many instances, preventing them from collapse.

Early cementation, which includes the formation of cement fringes and crusts, may also have played a role in the preservation of the moulds of aragonitic skeletal fragments. The micrite envelopes themselves can be considered as a ramification of sea-floor cementation.

2. Wholly-micritized grains

Bathurst noted that many skeletal fragments in Bimini Lagoon are completely micritised.

Micritized grains are common in the Gachsaran limestones (figs.6-32, 33) and of these, some are of skeletal origin, others are micritised ooids. There is no doubt that the non-faecal peloids have been micritized by repeated algal boring and infilling by micrite. Micritized ooids are sometimes difficult to distinguish from pellets (figs.6-32, 33). Ooids penetrated by algal mucilage have been described from the Trucial Coast by Shearman and Skipwith (1965).

6.6 Porosity

1. Interparticle porosity

This type of porosity arises from the pore space between allochems (fig.6-33). The porosity is largely dependent on the composition and texture of the sediment, which are determined by the depositional environment. The pore spaces can be partly or wholly filled by cement, thus reducing or destroying the interparticle porosity.

Interparticle porosity can be regenerated through a subsequent dissolution of cement although this may also involve solution of allochems (fig.6-34).

Fig. 6-31 Broken and deformed micrite envelopes in a biomicrite. Slice. p.p.l. Tell-Afar, Iraq.

Fig. 6-32 Micritised ooids associated with faecal pellets in an oosparite. Slice. p.p.l. Hammam Al-Alil, Iraq.

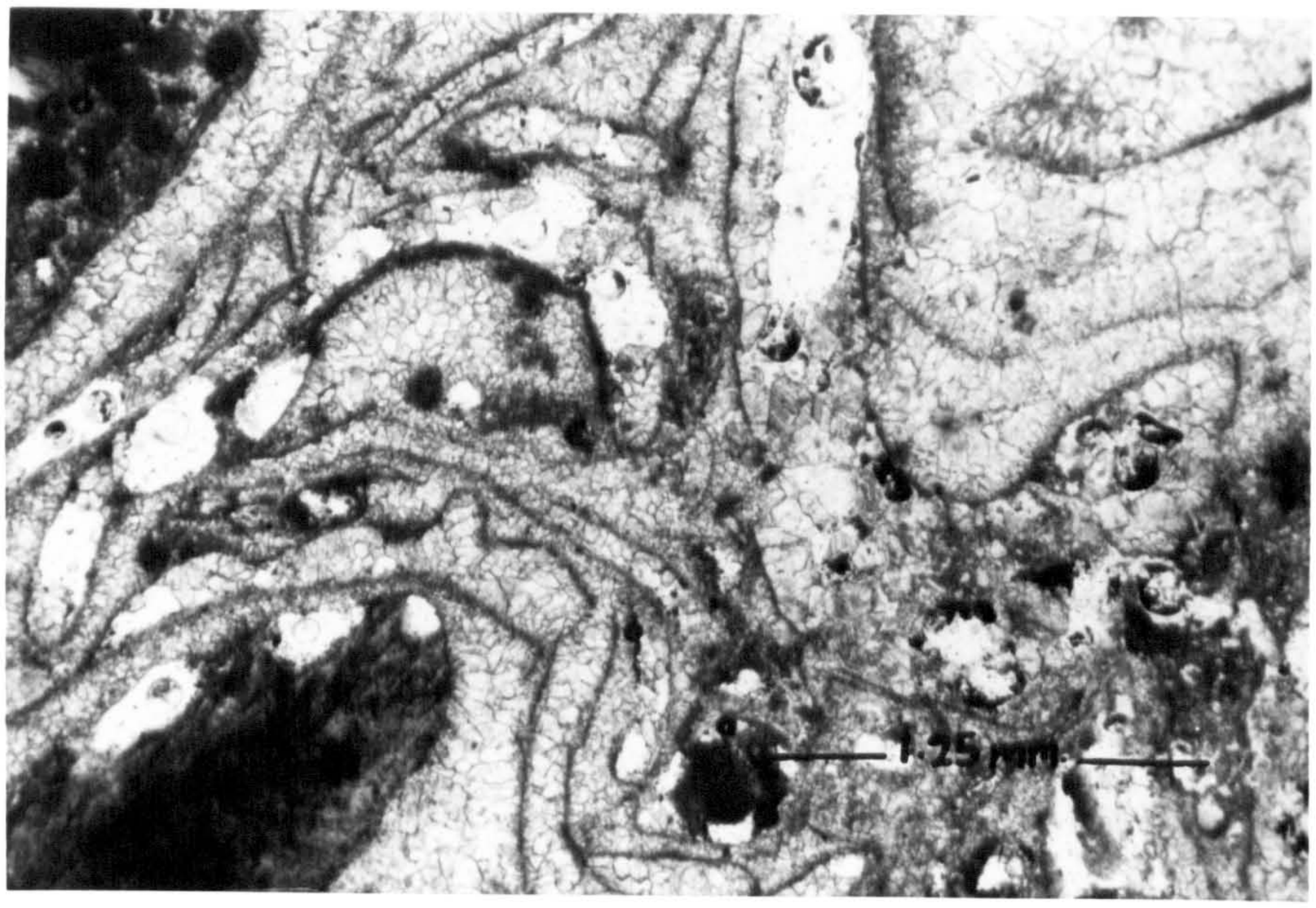

1

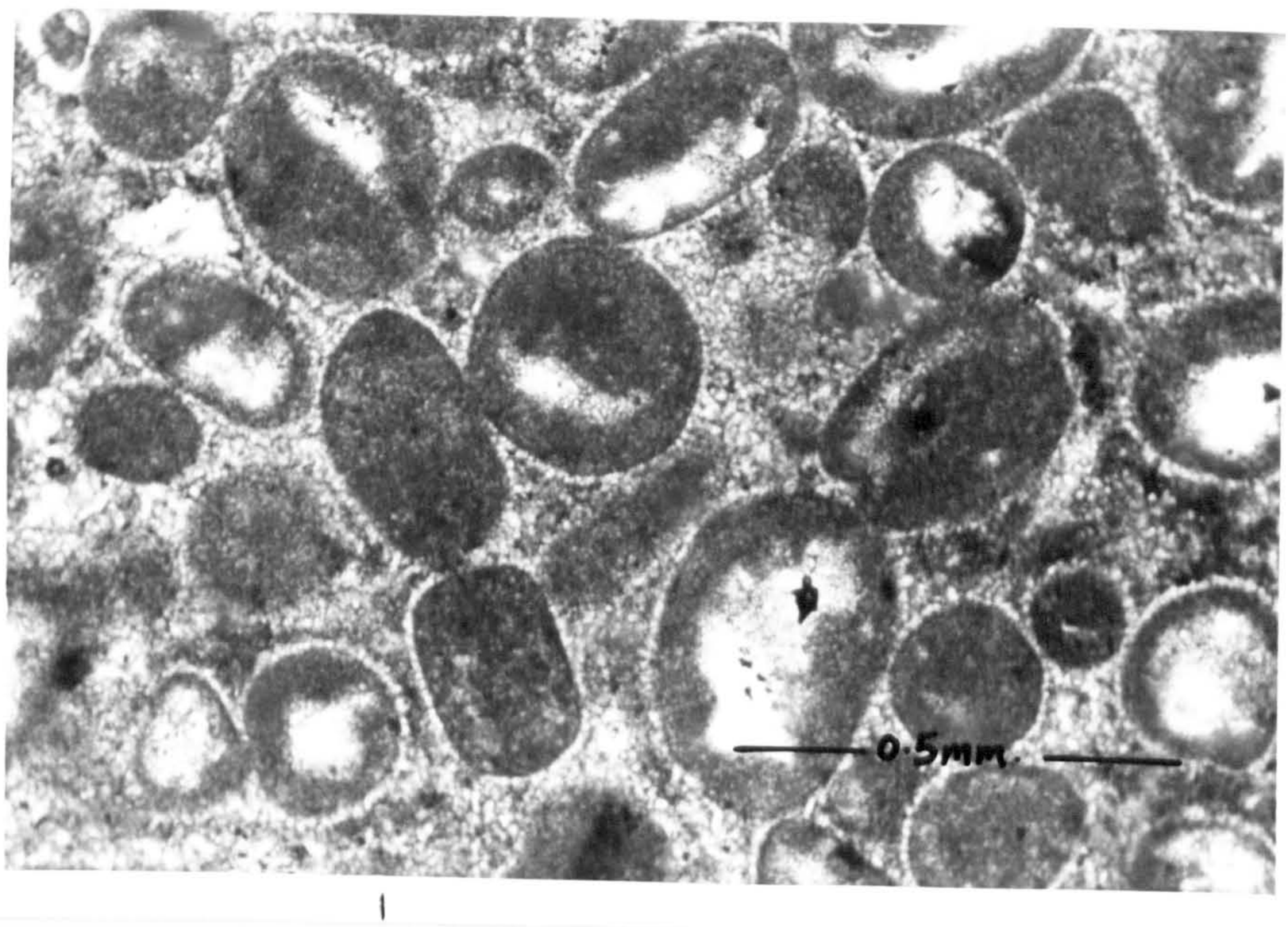

1

Fig. 6-33 Oosparite showing interparticle porosity. Note that the calcite cement is mostly present near the contact points of allochems. Slice. p.p.l. Hammam Al-Alil, Iraq.

Fig. 6-34 Interparticle porosity partly original and partly caused by dissolution of cement. Slice. p.p.l. Jabal Alan, Iraq.

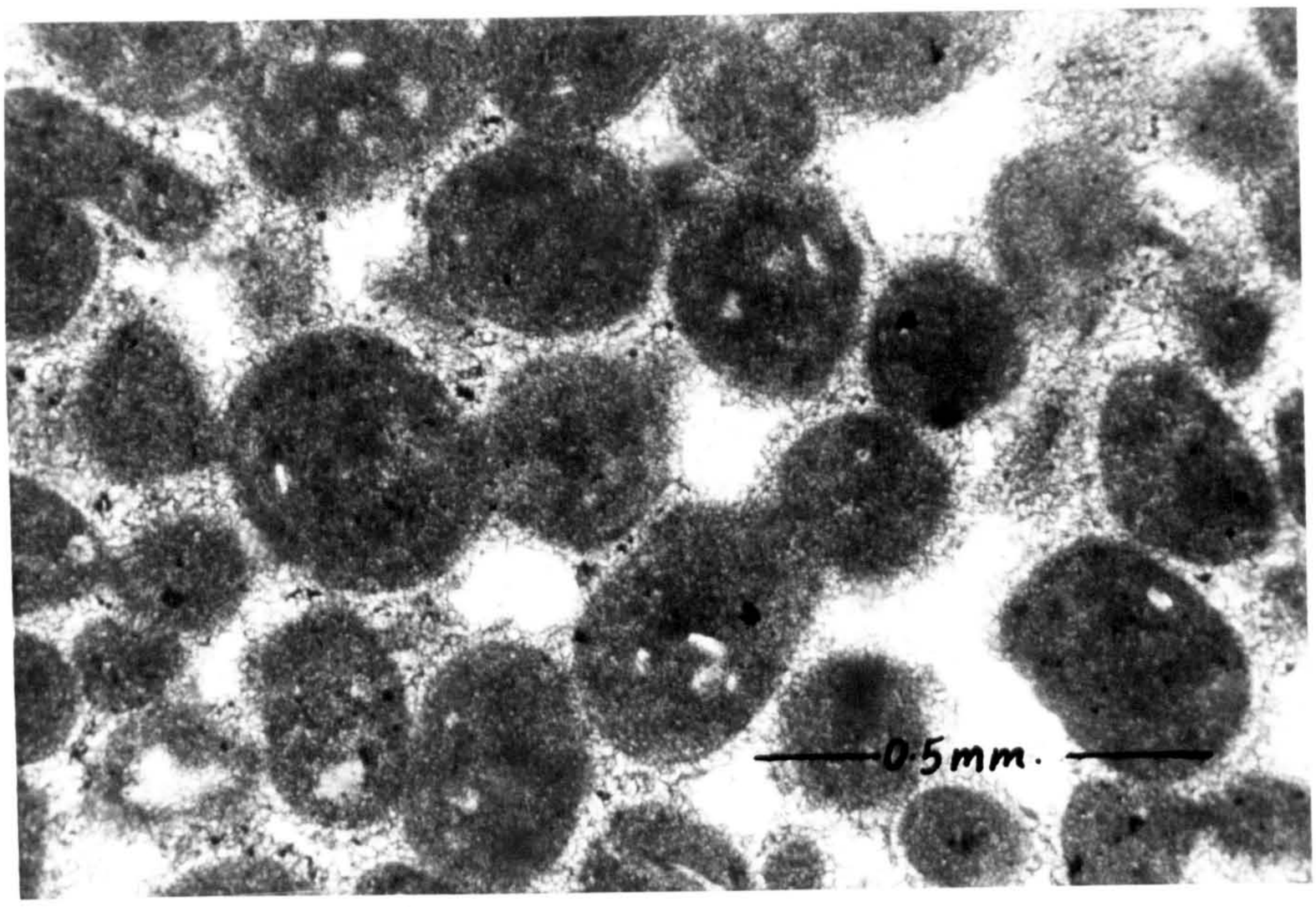
0·5mm.

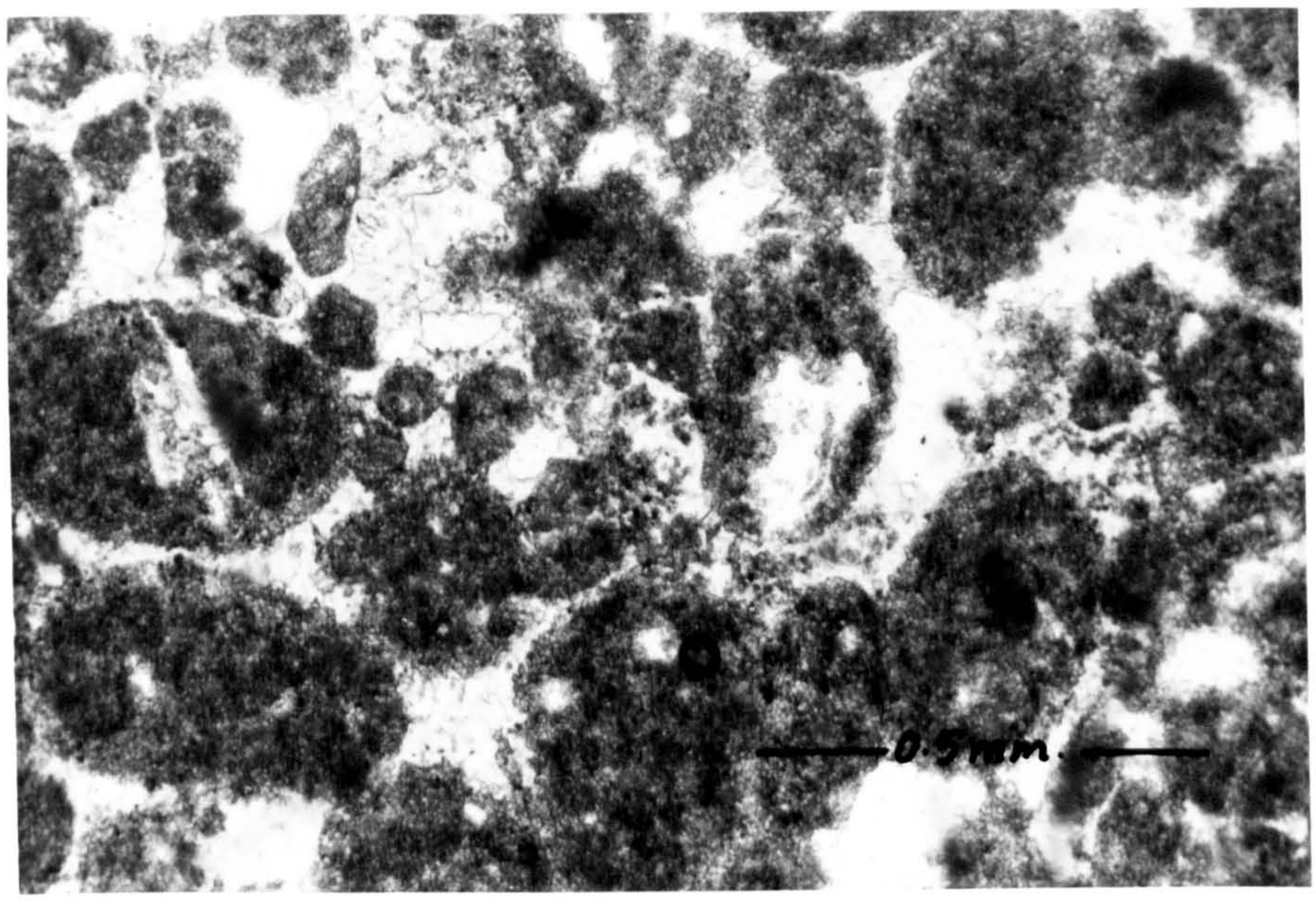
0·5mm.

Fig. 6-35 Oncolitic limestone showing mouldic porosity. Note the empty interiors of the oncolites. Slice. p.p.l. Hammam Al-Alil, Iraq.

Fig. 6-36 Bio-oosparite showing mouldic porosity. Note the leached nature of the bivalves and ooids. Slice. p.p.l. Tell-Afar, Iraq.

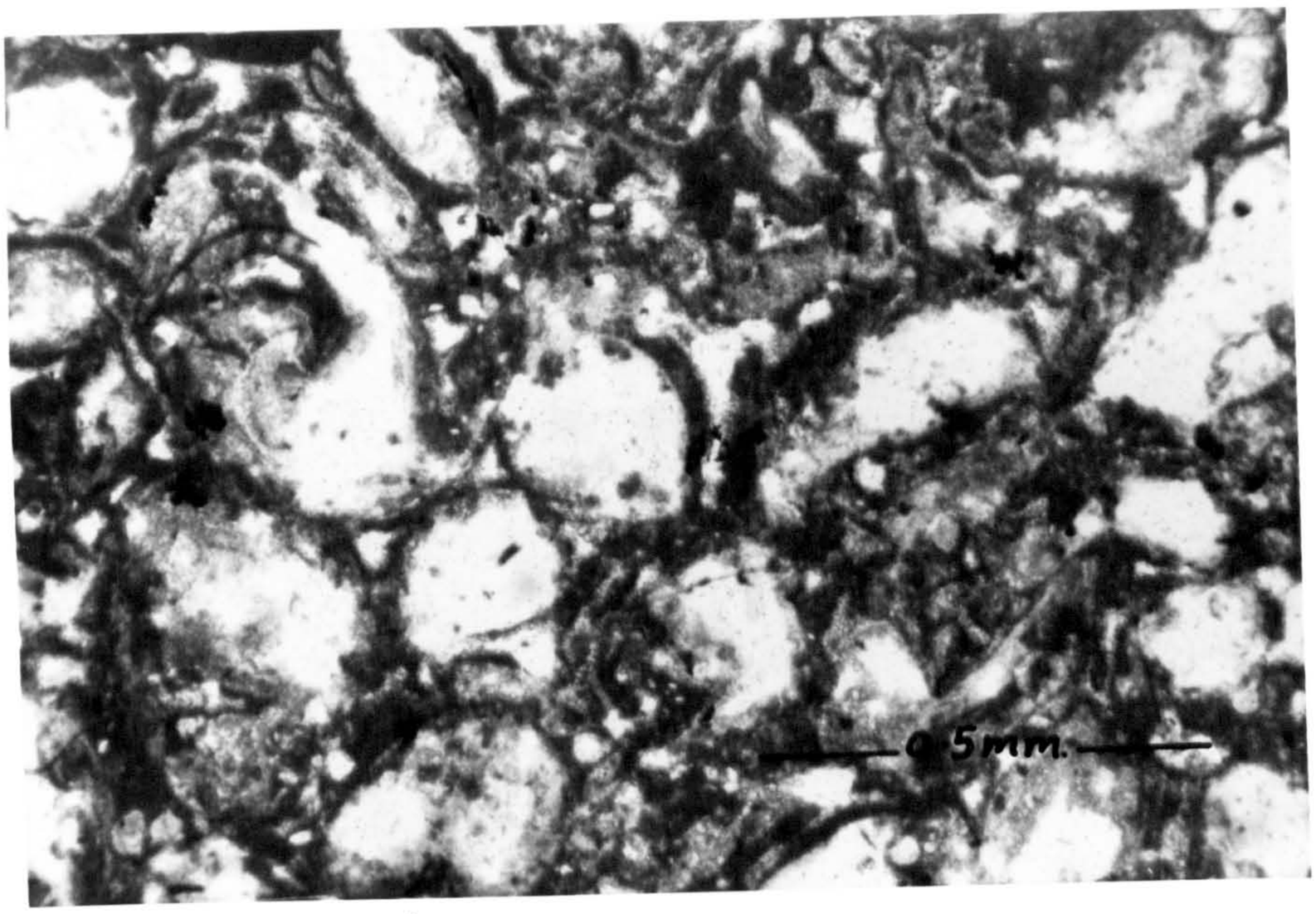
0.5mm.

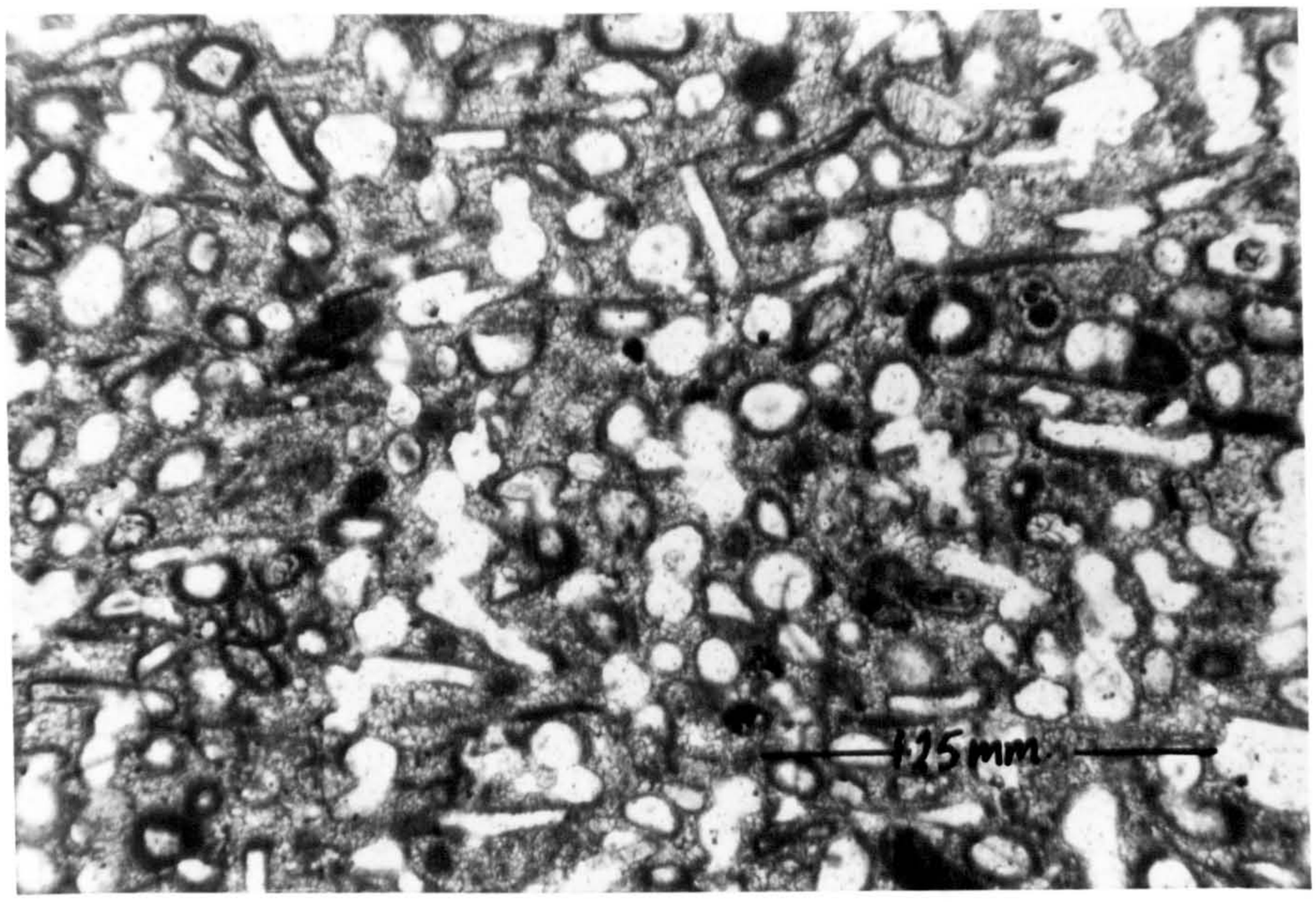
1.25mm

2. Intraparticle porosity

This is of several different types:

A. Mouldic porosity. This is caused by whole or partial solution of allochems such as oncolites (fig.6-35), ooids or skeletal fragments (fig. 6-36), or pellets (fig.6-37). In most cases the mouldic pores are connected with interparticle porosity caused largely by solution of the cement. Sediments with this type of porosity are characterised by a lack of cementing material, a fact which would indicate that leaching took place either after the sediment was cemented, or that the leached material was responsible for cementing the sediment.

B. Chambers of skeletal fragments which were later filled either by sparite (fig.6-38) or micrite (fig.6-39). This type of porosity is pre-sedimentary.

C. Sheltered porosity. This type of porosity is caused by large skeletal fragments, particularly shells, forming an umbrella structure which is not completely infilled with matrix (fig.6-40). This type is either filled with drusy cement or left open.

3. Vugs

This is the most common type of porosity found within the Gachsaran carbonates. Vugs mainly form by solution of whole areas of the rock (fig. 6-41). These pores are extremely irregular with no definite shape.

4. Fractures or veins

This type of porosity is limited in the Gachsaran carbonates, but it is very important in other limestones of the Middle East, such as the Asmari Limestone.

6.7 Compaction

Criteria used to estimate the effect of compaction in the Gachsaran carbonate rocks are: (1) the degree of orientation of the bioclasts within

a mud-supported matrix, and (2) the degree of preservation or destruction of delicate fossil fragments such as micrite envelopes, Foraminifera tests etc.

(1) A preferred orientation of skeletal fragments parallel to the bedding can be produced through compaction and through current action during deposition.

Although most of the Gachsaran carbonates have been deposited in relatively quiet water environments, examples of skeletal fragemnts showing preferred bedding-parallel alignment due to current action are not uncommon (fig.6-42).

The orientation of skeletal fragments with respect to bedding planes can be classified into random, weak, moderate and strong. Random and weak preferred orientations dominate, thus indicating that the Gachsaran carbonates have suffered no significant compaction.

(2) In most cases, delicate structures of Foraminifera and micrite envelopes are intact. However, in some cases, collapsed and broken micrite envelopes are present (fig.6-43). Based mainly on the degree of preservation of delicate fossils, limestones can be divided into those which are slightly, moderately and strongly compacted. In limestones which show moderate to strong preferred fossil orientations due to compaction, much of fossil structure shows evidence of collapse or breakage. In limestones with a random or slight preferred orientation, bioclasts and delicate structures are preserved intact.

Fig. 6-37 Pelmicrite showing mouldic porosity. Note the leached nature of the peloids. Slice. p.p.l. Shaikh Ibrahim, Iraq.

Fig. 6-38 A Miliolid showing intraparticle porosity. The pores were later filled with drusy spar. Slice. p.p.l. Makhul, Iraq.

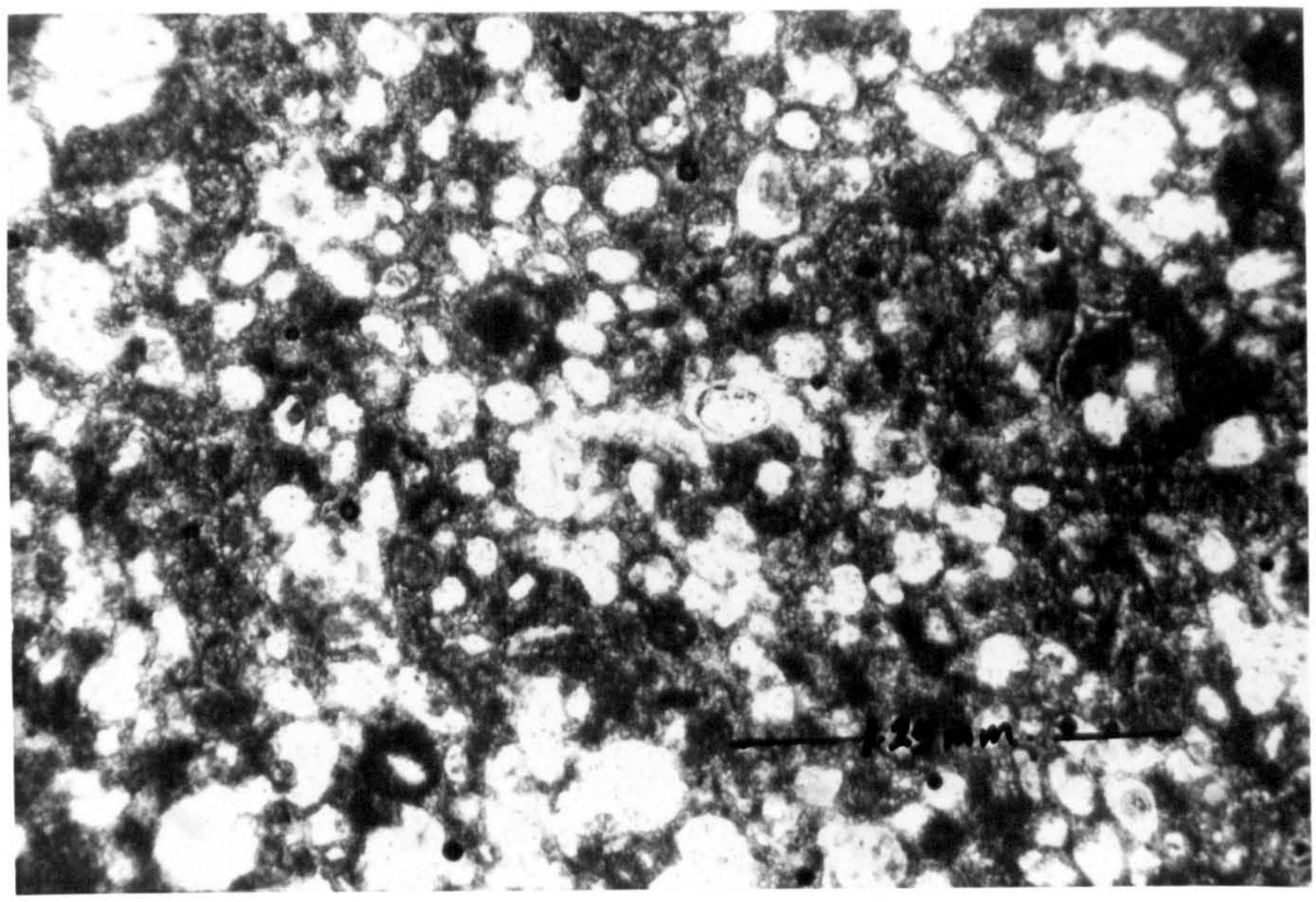

1

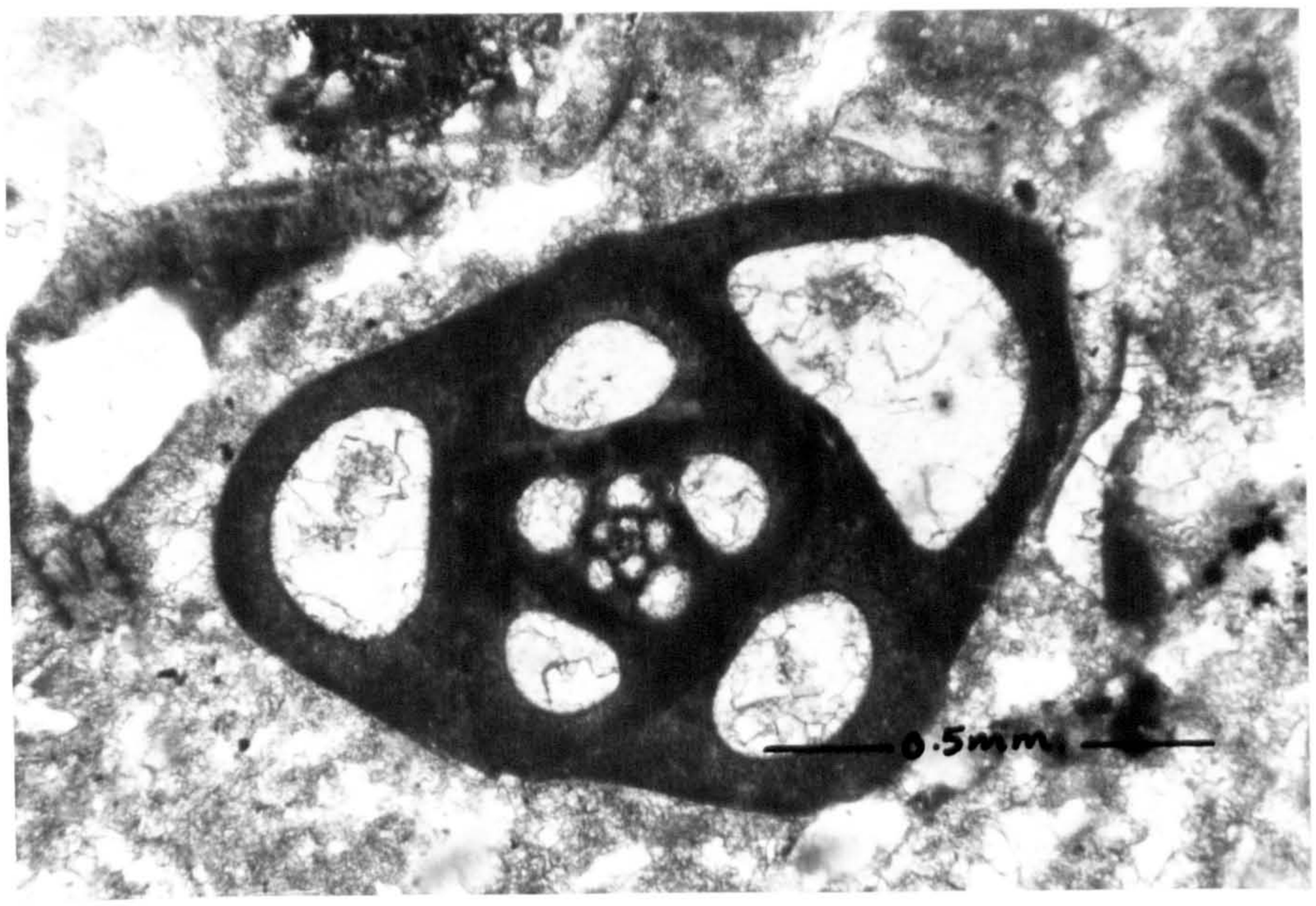

1

Fig. 6-39 Rotaliids showing intraparticle porosity. The pores are filled with micrite cement. Slice. p.p.l. Makhul, Iraq.

Fig. 6-40 Sheltered porosity. The cavity (now filled with drusy spar) is sheltered by a large skeletal Fragment. Slice.p.p.l. Tell-Afar, Iraq.

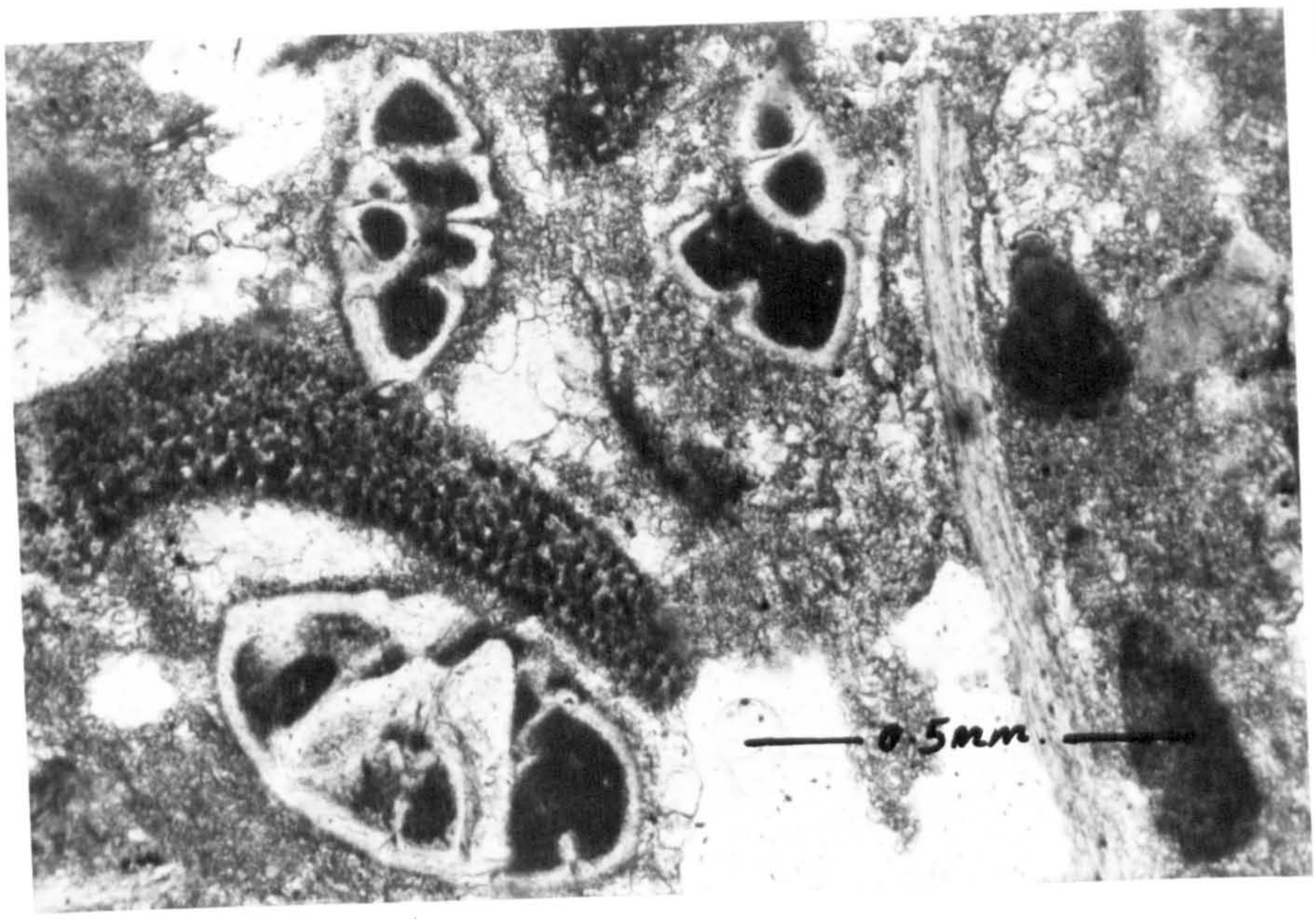

1

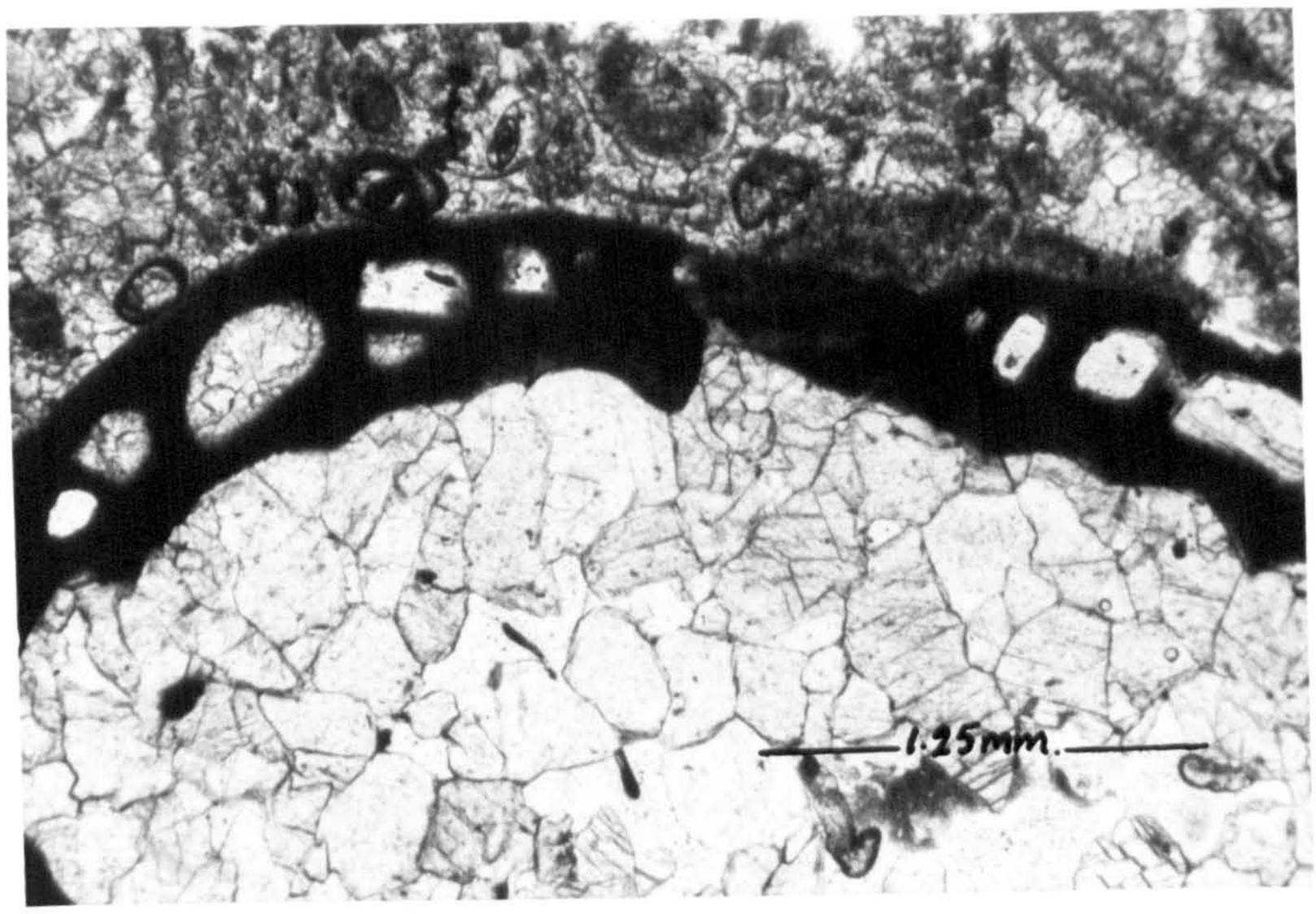

1

Fig. 6-41 Vugs. Formed by solution of whole areas of the rock. Note the irregular and non-definite shape of the pores. Slice.p.p.l. Makhul, Iraq.

Fig. 6-42 A biosparite showing preferred orientation of bivalve grains. Slice.p.p.l. Tell-Afar, Iraq.

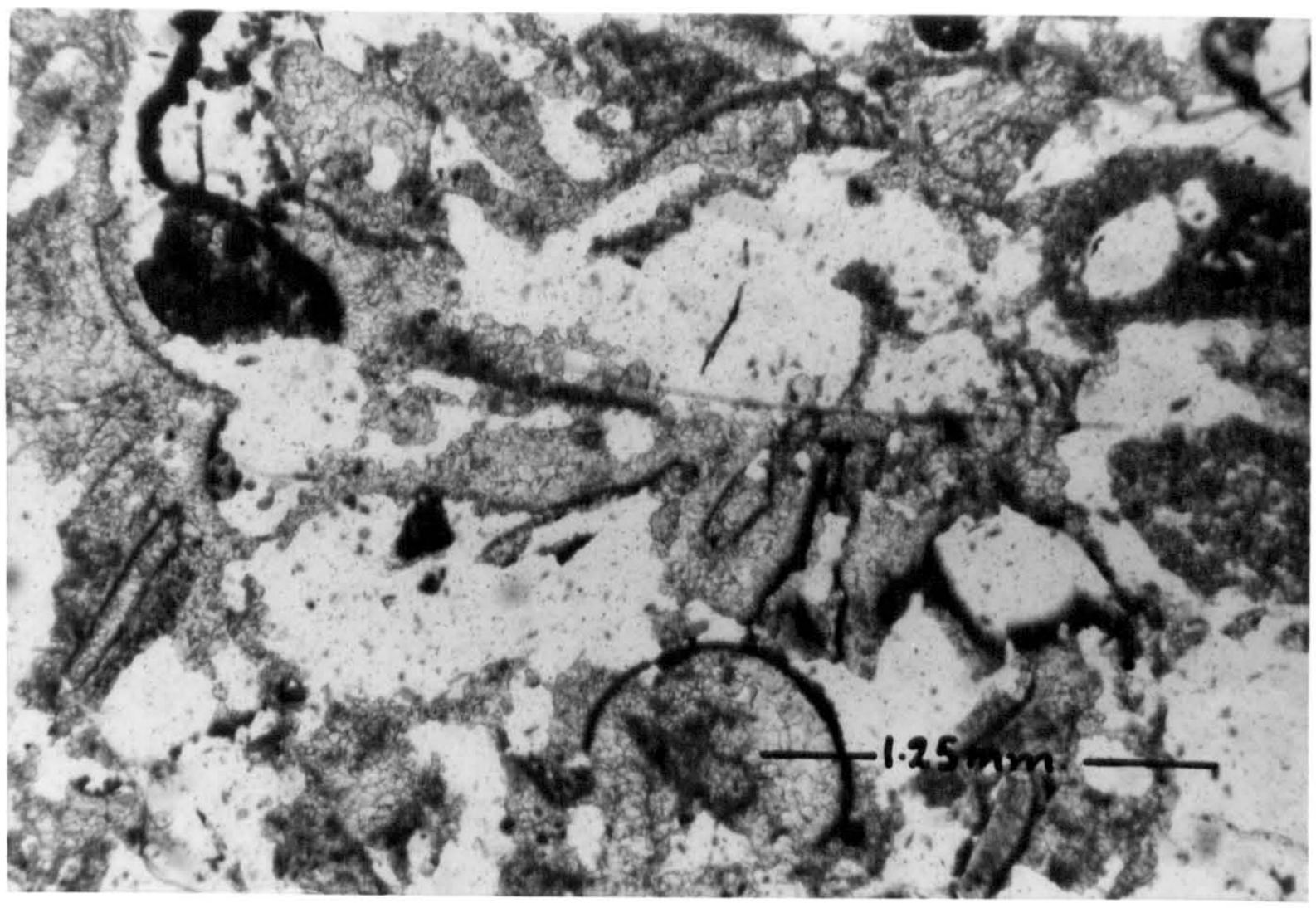

1

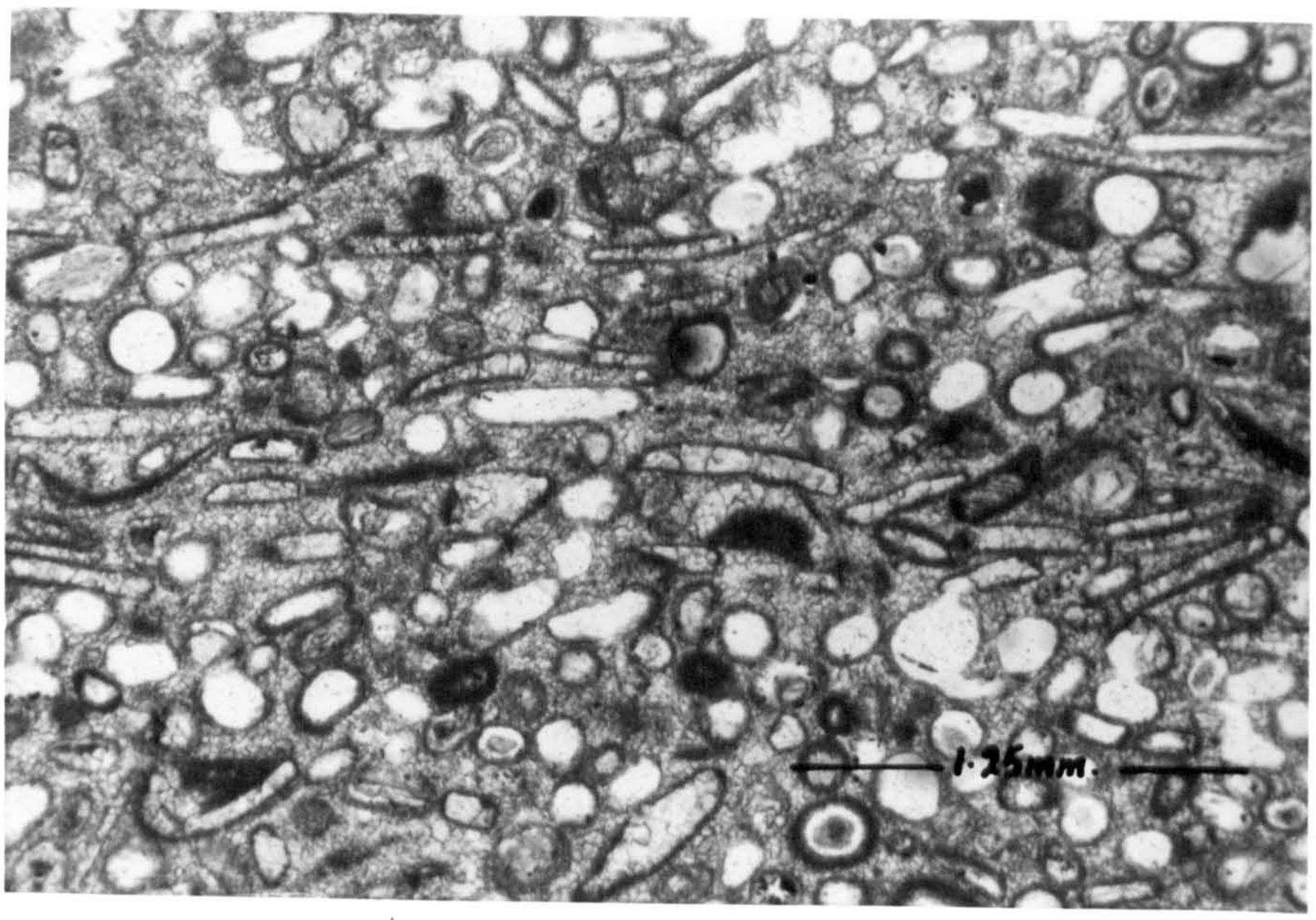

1

Fig. 6-43 A biosparite showing compaction. A skeletal grain has been forced into a bivalve fragment (arrow). Slice. p.p.l. Tell-Afar, Iraq.

Fig. 6-44 A dolostone. Note the unrhombic, very fine nature of the dolomite crystals. Slice. p.p.l. Tell-Afar, Iraq.

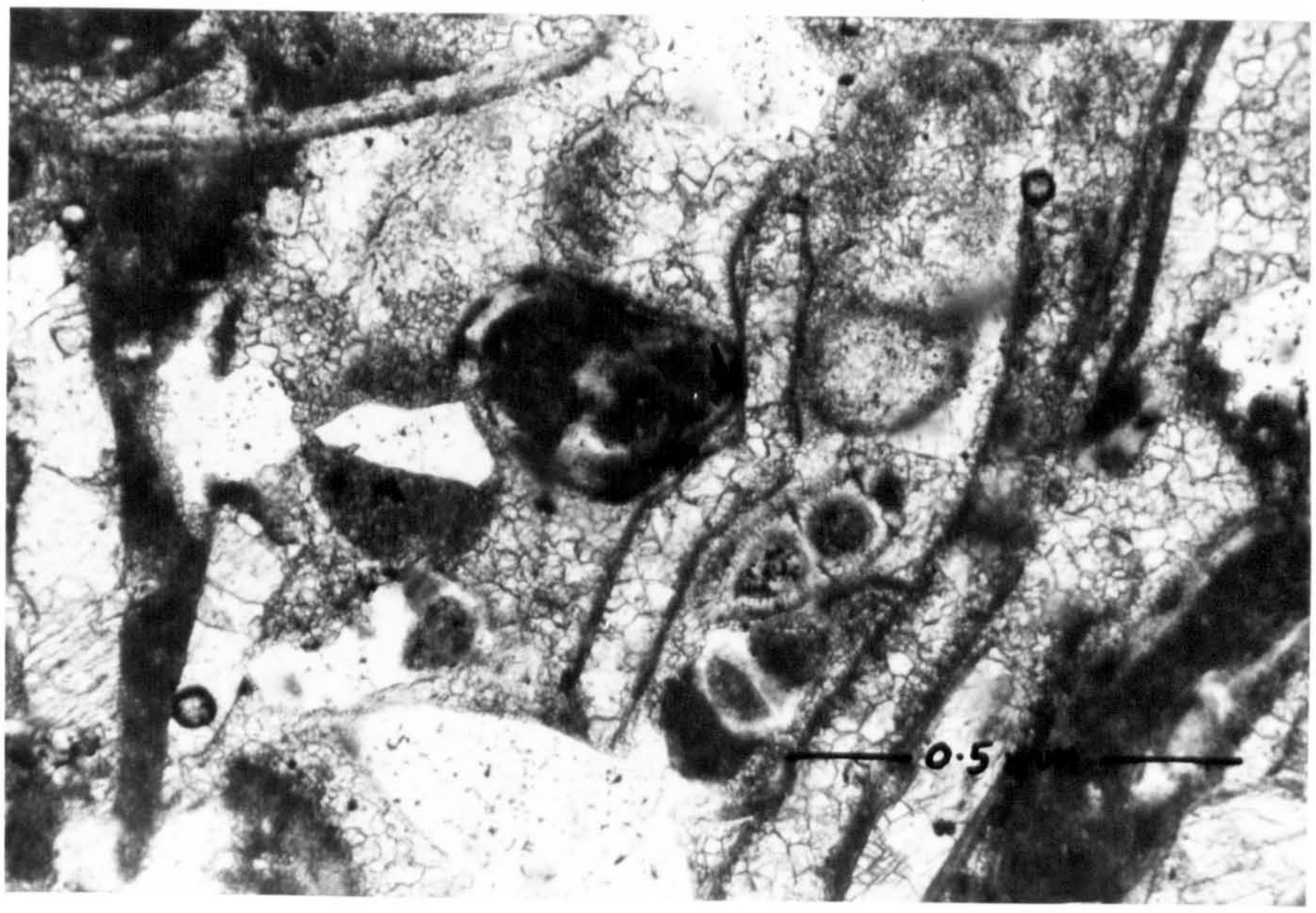
0·5

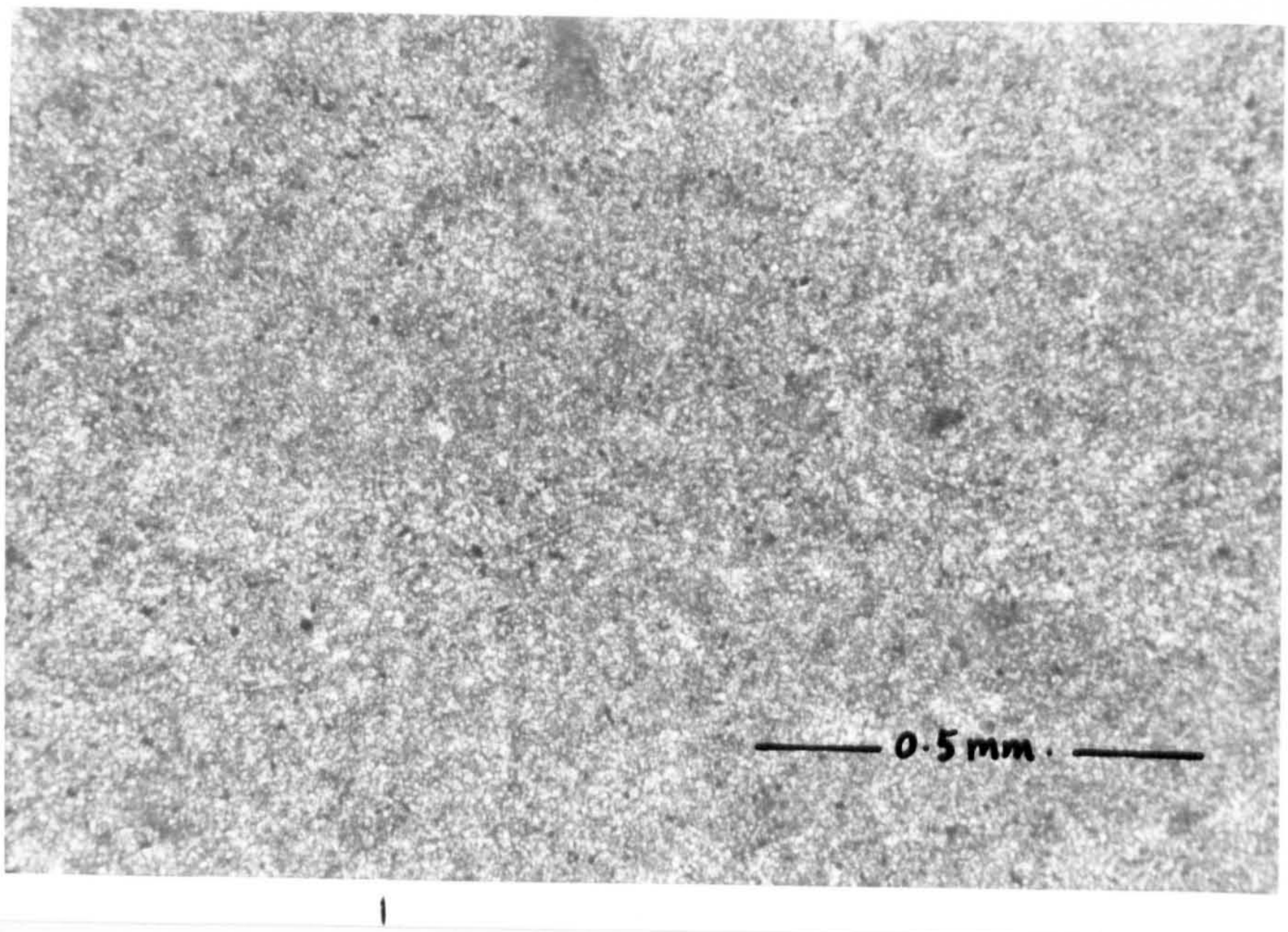
0·5 mm

6.8 Origin of Dolomites

The genesis of dolomite has attracted many workers, partly because of its still unsolved origin and partly because of its importance to oil prospectors. The literature on the mineral dolomite, the rock dolostone and the processes of dolomitisation is vast. A review of this literature is felt to be unnecessary here and the reader is referred to Friedman and Sanders (1967) and Bathurst (1975).

The detection of dolomites in Recent environments has contributed much to the understanding of its formation. The often close association of dolomite with evaporites as in Bonaire Island (Deffeyés, et al., 1965), the Arabian Gulf (Illing, et al., 1965) and Abu Dhabi (Curtis, et al., 1963) has led many to believe that most dolostones in the geological record have formed through the influence of hypersaline solutions. In such evaporating environments, it has been demonstrated that precipitation of aragonite and gypsum raises the Mg/Ca ratio of the pore waters to a value of 5:1 to 10:1, or more. This rise leads to a contemporaneous replacement of aragonite to dolomite. It has also been shown that aragonite or high Mg-calcite precipitates below such a high Mg/Ca ratio. The Mg/Ca molar ratio generally increases across a tidal flat, from the high intertidal to supratidal zones. It should be noted that consideration must be given to the nature of the saline water bordering the tidal flats. The occurrence of dolomite in the Bahamas and Florida (Shinn and Ginsburg, 1964; Shinn, et al., 1965), does not fit in completely with an evaporative model as evaporites are not present. Some might argue that the solutions reaching the supratidal flats have a high enough Mg/Ca ratio to precipitate dolomite, but not high enough to precipitate gypsum. Although this is a possibility, it should be noted that the precipitation of gypsum plays a major part in raising the Mg/Ca ratio.

Folk and Land (1975) stated that precipitation is generally rapid in

hypersaline evaporative environments which, together with the high concentration, makes it difficult for dolomite to form because of the precise Ca-Mg ordering required. Instead they postulated that aragonite or high Mg-calcite crystallises with the Mg/Ca ratio is exceptionally high, when dolomite is then forced out of solution. In order to achieve a slower rate of crystallisation, they proposed an alternative model for dolomite formation. They suggested that dolomite may form most readily by a reduction in salinity particularly in a schizohaline environment (alternating between hypersaline and near-fresh conditions, as in a floodable sabkha or a phreatic mixing zone). Diluting marine saline waters with fresh water lowers the salinity but maintains a high Mg/Ca ratio, thus crystallisation is slower and the interferring effect of foreign ions is reduced. Folk and Land noticed that dolomite crystals formed from such a model are characteristically limpid (euhedral and perfectly clear with plane mirro-like faces). The absence of evaporites from the tidal flats of the Bahamas led Folk and Land to suggest that at least some of the dolomite crusts there have formed through dilution of brines through rainfall. Applications of such a model for dolomite occurrences in the geological record may include the Middle Ordovician of Winsconsin (see Badiozamani, 1973).

Much dolomitisation is clearly a diagenetic replacement process. Such a process is usually selective as was shown by Schmidt (1965) and Lucia (1968). Schmidt established that a micritic matrix was more susceptible to dolomitisation than allochems, and of the latter, originally aragonitic bioclasts were more susceptible than calcitic ones. Lucia (1968) established that the dolomitisation sequence in Recent sediments from Bonaire was mud matrix, pellets and then shells. The susceptibility to dolomitisation deduced from the Carboniferous Limestones of Northumberland is sparry calcite infillings of veinlets, moulds and cavities, micritised bioclasts, matrix and then bioclasts (Al-Hashimi, 1972).

It is evident that a number of factors are responsible for the selective replacement of sediment by dolomite. These factors are (1) pre-dolomitisation mineralogy, (2) particle size, (3) permeability variations, and (4) organic matter (Al-Hashimi, 1972). The mineralogy of sediment or rock before dolomitisation is perhaps the most important factor in causing selective dolomitisation. For example, the unstable aragonite and high-Mg calcite could be more susceptible to dolomitisation than low-Mg calcite. Schmidt (1965) noticed that aragonitic bioclasts were selectively dolomitised, while calcitic bioclasts were less so. With regard to particle size, it has been demonstrated that, given the same conditions, lime mud would be more affected by dolomitisation than sand-sized particles because of reactivity differences. The significance and role played by organic matter in causing dolomitisation is stressed by Beales (1953), Spotts and Silverman (1966) and Al-Hashimi (1972). The permeability factor needs no comment, as more permeable sediments are more easily dolomitised than less permeable ones.

6.9 The Gachsaran Dolostones

These dolostones are classified into two main types, penecontemporaneous syngenetic and later diagenetic.

1. Penecontemporaneous dolostones

Penecontemporaneous dolomite consists of crystals less than 4 microns in size. The crystals do not acquire the usual rhombic shape of dolomite (fig.6-44). Staining techniques proved to be of little help in distinguishing this dolomite from calcitic micrite. X-ray diffraction analysis proved to be the most efficient method of determining the mineralogy of such fine grained crystals.

The dolostones are either structureless, laminated or brecciated, but always closely associated with evaporites such as gypsum or anhydrite.

They very rarely contain any skeletal fragments. The stromatolites and cryptalgal laminites within the formation were found to consist of 75% dolomite and 25% calcite. This type of very fine dolomite is considered to be primary in the sense that dolomite replaced the original carbonate sediment penecontemporaneously. This conclusion is supported by the following points;

(a) the non-rhombic shape of the dolomite crystals. This could be a result of a relatively fast rate of crystallisation,

(b) the close association of these types of rocks always with gypsum or anhydrite. Such an association indicates that these sediments have supra-tidal affinities and so are comparable with occurrences of dolomite in such Recent environments as Bonaire Island (Deffeyes, et al., 1965) and the Trucial Coast, Arabian Gulf (Curtis, et al., 1963; Kinsman, 1964, 1965; Butler, 1970). It should be noted, however, that there is no direct evidence available regarding the original composition of the carbonate mud in which the very fine dolomite developed. The relatively fast recrystallisation contemplated for these dolomites and their relatively young age (Miocene) may indicate that the original carbonate mud consisted chiefly of aragonite as in Recent marine carbonate muds.

2. Later diagenetic dolostones

The main constituents of the Gachsaran carbonate rocks are sparite, micrite and allochems consisting mainly of skeletal fragments, ooids and pellets. The three main constituents are treated separately due to their different response and susceptibility to dolomitization. It should be noted, however, that the effect of later diagenetic dolomitization on the Gachsaran limestones is very limited. This could be attributed to the presence of extensive impermeable beds of gypsum and claystone which may have acted as a seal and so inhibited the passage of ascending or descending meteoric solutions.

A. Sparry calcite

This constituent was found to be most susceptible to dolomitization. Sparry calcite (sometimes with a drusy texture) is found to fill primary cavities, leached skeletal fragments and veins. The sparry calcite most susceptible to dolomitisation is the one which fills open space voids and veins (fig.6-45). Also this type was found more readily dolomitised than the surrounding allochems and matrix. It was noticed that most of these cavities are not completely filled by sparry calcite. There is no way of telling whether this is original or the effect of later solution. If this porosity was original, then it may have played a major role in the more selective replacement of this constituent by facilitating the passage of the dolomitising fluids. Another possibility is that the sparry calcite contained ions such as Mg which would have affected the stability of calcite spar.

B. Micrite matrix

Fine dolomite rhombs (6-10μ) occur within the calcite matrix of some limestones (fig.6-46). Idiotopic texture with no visual porosity results from the complete dolomite replacement of the micrite matrix. The presence of some dolomite rhombs replacing sparry calcite infilling voids indicates that the replaced carbonate mud was lithified before dolomitization took place.

C. Allochems

Of the allochems, the bioclasts were found to be more readily dolomitised in comparison with pellets, ooids and intraclasts. Some bioclasts were found slightly altered although 'swimming' in a mass of dolomite (fig.6-45).

The features noted above suggest that the dolomite replacement is late diagenetic. The following observations support this contention.

Fig. 6-45 A cavity filled with sparry calcite. Note the replacement of calcite crystals by dolomite rhombs, also the allochems' less susceptibility to replacement. Slice. p.p.l. Mishraq, Iraq.

Fig. 6-46 A dolostone. The matrix consists of small scale dolomite rhombs, formed as a result of direct replacement of micrite by dolomite. Slice. crossed nichols. Mishraq, Iraq.

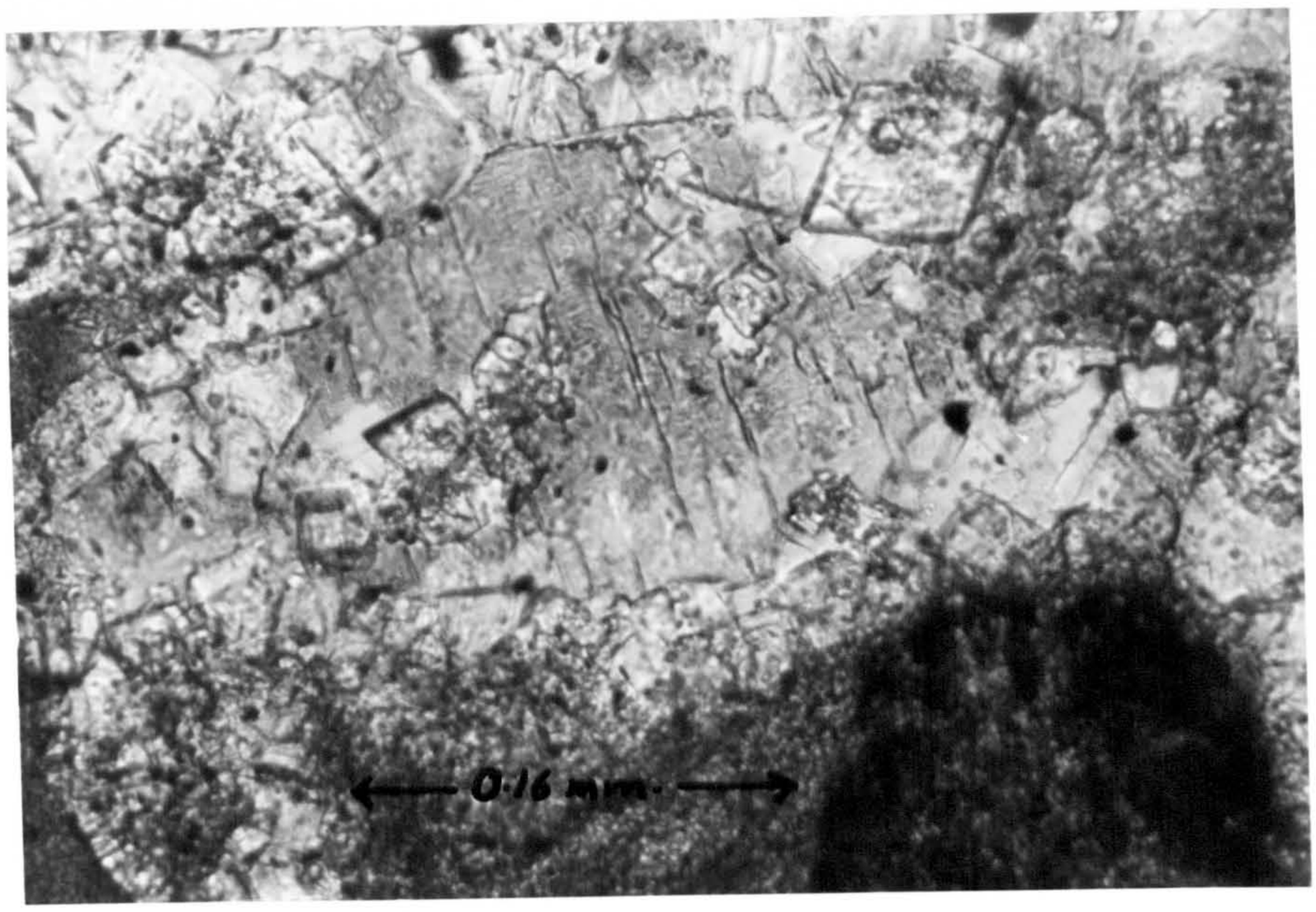

1

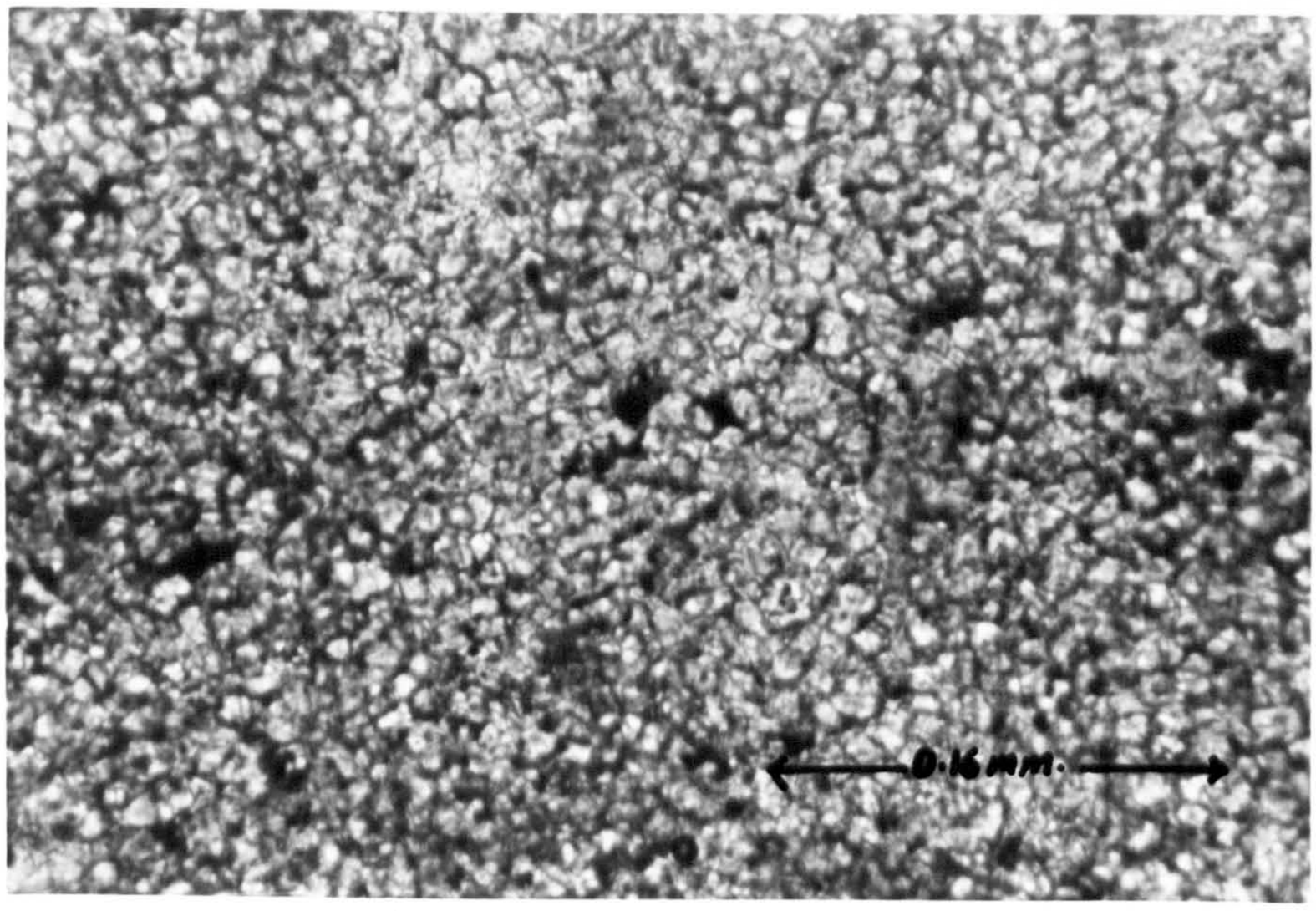

1

1. If dolomitization was early diagenetic, then one would expect that sparry calcite would not be replaced by dolomite. The fact that dolomite rhombohedra were observed replacing sparry calcite indicates that dolomitisation began after the lithification of the rock.

2. The bioclasts found within these carbonate rocks were made either of aragonite, high Mg-calcite or low Mg-calcite. If dolomitization was early, then one would expect that fossils, originally made of aragonite or high Mg-calcite, would be more susceptible to dolomitisation than the ones made of low Mg-calcite. The fact that most of these bioclasts showed relatively uniform resistance to dolomitization indicates that stabilisation of the metastable minerals of these bioclasts took place prior to dolomitization.

6.10 Dolomite Cementation

Cementation of carbonate rocks by dolomite has been dealt with in an earlier section (Section6.5).

6.11 X-Ray Analysis

X-ray diffraction techniques were used to determine the mineral content of the carbonate rocks of the Gachsaran. This technique was found to be very useful particularly for detecting the presence of dolomite in fine grained carbonates. A Philips X-ray diffractometer with Co-K_x radiation was used. Details of the method used is given in Appendix (p.).

The X-ray diffractograms for these carbonate rocks all show calcite and/or dolomite. The absence of other diffraction peaks simply indicates the lack of accessory minerals in quantities sufficient for detection at the sensitivity level employed. A calcite peak of 3.035 Å and a dolomite peak of 2.88 Å were used for determining calcite and dolomite respectively.

X-ray diffraction techniques can also be used to determine quantitatively the relative amounts of the different carbonate minerals present, and also to calculate the amount of Mg and Ca in calcites and dolomites. The simplest method for calculating the proportions of the different carbonate minerals is that of Lowenstam (1954), Turekian and Armstrong (1960). This method involves a relative measure of the maximum peaks of different minerals in the sample

$$R = \frac{hc}{hc + hd} \quad \text{or} \quad R = \frac{hd}{hd + hc}$$

hc = height of calcite peak, hd = height of dolomite peak

A more accurate method, however, involves the measure of areas occupied by the different mineral's main peaks (Pilkey, 1964). For the purpose of this work, the first method is employed to determine the percentage of dolomite to calcite in any one sample. Goldsmith and Graf (1958) distinguished between ideal and non-ideal dolomite. Ideal dolomite is that which consists of layers of carbonate sheets alternating with layers of only calcium ions

Fig. 6-47 Various curves relating the mole percent $MgCO_3$ in a calcite (or dolomite) with the position of the d(211) peak. The Goldsmith, Graf and Heard (1961) curve comes closest to the idealized curve. After Milliman (1974).

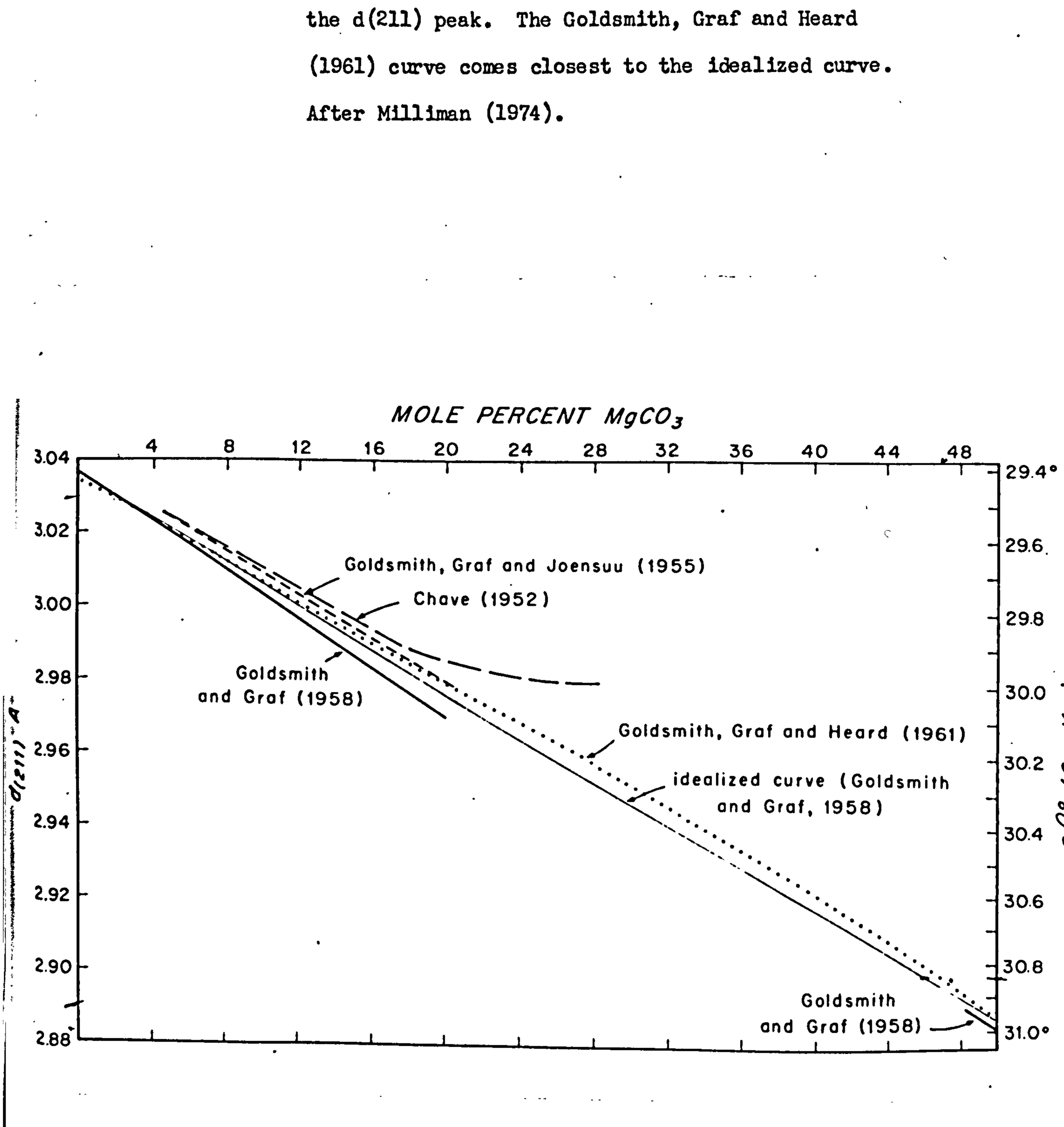

Fig. 6-48 A representative figure showing X-ray diffraction peaks of calcite and dolomite. The peaks are sharp and symmetrical.

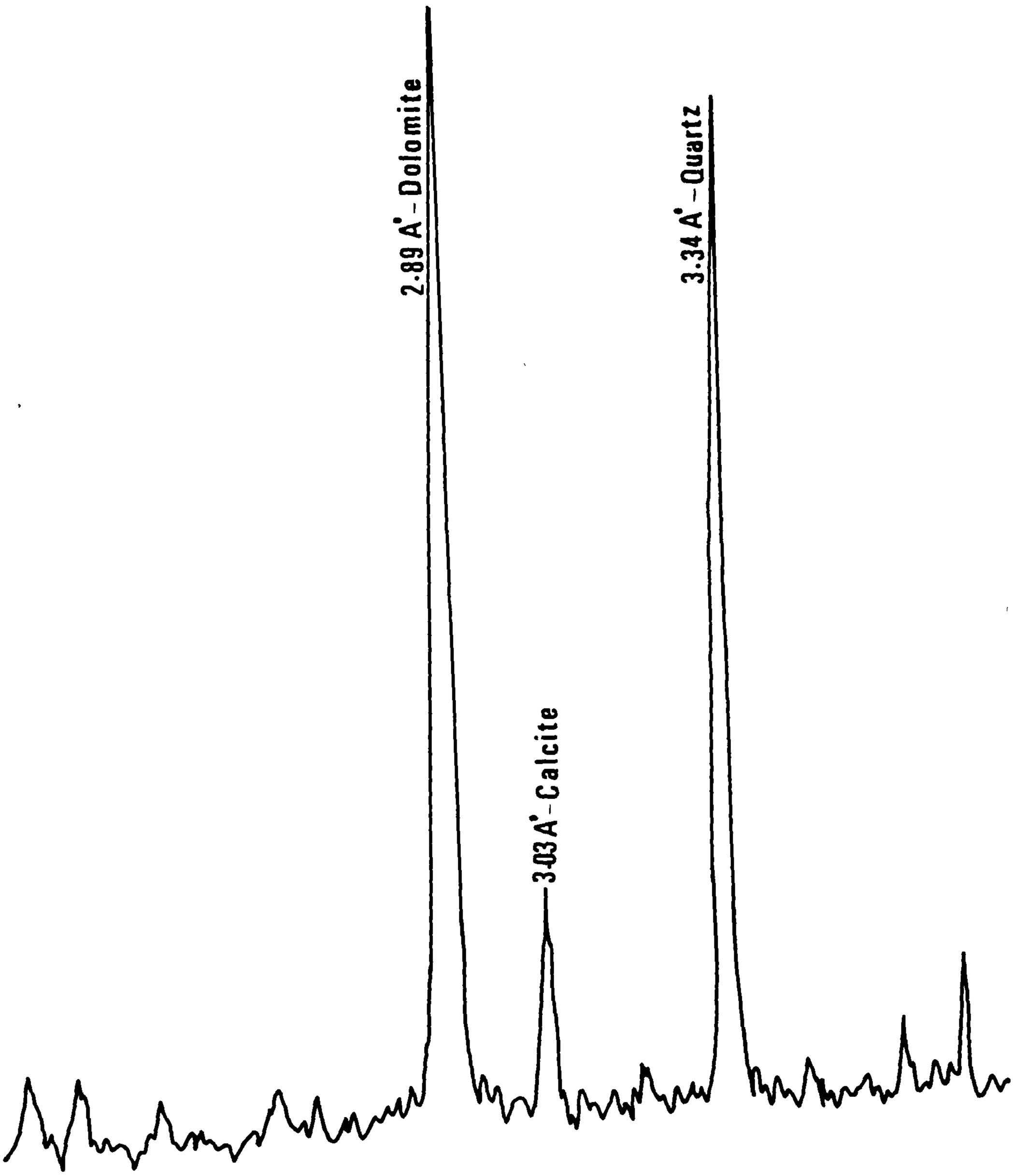

Fig 6 - 48

and only magnesium ions. It contains equal molar proportions of Mg and Ca and shows sharp ordering peak reflections in X-ray diffraction photographs. Non-ideal dolomite contains an excess of $CaCO_3$ and shows a departure from perfect ordering of calcium and magnesium atoms in the crystal structure. Such differences can be detected by X-ray analysis (for more details see Shinn, et al., 1965). Goldsmith, et al. (1958) assumed a linear relationship between the lattice constant (d211) and substitution of $MgCO_3$ in calcite (fig.6-47). Shinn, et al. (1965) have shown that dolomites with $>$ 50% $CaCO_3$ show a peak shift toward a higher d-spacing, indicating also a higher $CaCO_3$ content. Caution, however, must be applied since substitution of Fe and Mn for Mg may have the same effect (Goldsmith, et al., 1958). Milliman (1974) related the asymmetry of the X-ray pattern to the concentration of Mg in calcite.

Sharp and symmetrical X-ray patterns (fig.6-48), together with a lattice spacing of 3.035 Å, indicate the high Mg-calcite is not present in the Gachsaran samples, only low Mg-calcite. Using the curve of Goldsmith et al., all the calcites of the Gachsaran contain $<$ 2 mole% $MgCO_3$ and the dolomites $>$ 48%. The dolomites show well developed ordering peaks at 2.89 Å. It is thus concluded that the dolomites of the Gachsaran are highly ordered and are very nearly ideal.

Marschner (1969) related the vertical variation in the $CaCO_3$ excess of dolomites from a Triassic dolomitic limestone sequence to the variation in the salinity of the depositional environment. He found that dolomites with a Ca:Mg = 1:1 molar ratio formed in a depositional environment characterised by high salinity. At first sight, the results and observations on the Gachsaran carbonates support this view. One must not, however, underestimate the diagenetic processes which may transform poorly-ordered dolomites into ideal dolomites (Graf and Goldsmith, 1956; Goldsmith and

Graf, 1958). Indeed, there are many examples in the literature of ancient ideal dolomites which are not associated with evaporites (e.g. Badiozamani, 1973). It was Folk and Land (1975) who pointed out that the formation of dolomites does not necessarily require super-saline conditions and suggested that the more ordered or ideal dolomite should form in schizohaline environments. The arguments on which Folk and Land based their conclusion were that dilution of water does not reduce dolomite formation, but on the contrary, enhances its production through slow crystallisation, thus forming an ideal dolomite.

If the above arguments hold, then it is only logical to assume that the original deposited dolomite of the Gachsaran was poorly-ordered and was transformed later to the more ordered type through solution and re-crystallisation.

6.12 Summary

Micritization caused by boring algae and later infilling of bores by micrite or micrite cement was probably the first diagenetic alteration process to have affected the allochems of the Gachsaran carbonate sediments.

These limestones were cemented by at least four types of early cements. Textures of these types of cements by comparison with Recent examples suggest that they were of aragonite and high Mg-calcite. The preservation of many of the bivalve moulds by micrite envelopes probably suggests that early cementation was a factor in strengthening the envelopes.

Small non-rhombohedral dolomite crystals which are very similar to calcitic micrite constitute many of the Gachsaran dolostones. Their texture and location in the stratigraphic sequence suggest that these are very early diagenetic dolomites.

Late cementation took place during and after burial. The solutions for this cementation are considered to have been meteoric waters, with at

least some $CaCO_3$ supplied from the dissolution of aragonite bivalves and other skeletal grains. The predominant cementing material in these carbonates is calcite (drusy sparite). Examples of gypsum and dolomite cements, however, are not uncommon. Gypsum cementation is thought to have been caused mainly by sulphate-rich solutions derived from the solutions buried with the sediment and derived from the hydration of anhydrite to gypsum on uplift. Hypersaline solutions were also responsible for late dolomitization.

Neomorphism also commenced during burial caused mainly by the unstable nature of aragonite and, to a lesser extent, that of high Mg-calcite as the rocks came more in contact with connate waters. Solutions of allochems and sediment took place as well as neomorphism of micrite to coarser fabrics.

Meteoric waters percolating through the rocks along fault planes and joints may have been responsible for the replacement of some gypsum beds by cavernous, sugary limestone.

CHAPTER 7

CARBONATE'S GEOCHEMISTRY

CHAPTER 7

CARBONATE'S GEOCHEMISTRY

7.1 Introduction

The major and minor element suites of the limestones and dolostones of the Gachsaran Formation have been studied. In all, twenty-one samples were chosen, rèpresenting the major carbonate lithofacies. Thirteen of the samples are limestones, six are dolostones and two are calcareous siltstones (Table 7-1).

The major elements Ca, Mg, Fe, Na and K and the trace elements Sr, Pb, Zn, Cu and Rb were determined on the acetic-acid soluble fraction. The results are considered to represent the concentration of these elements in the carbonate phase. In addition, Na, K, Fe, Al_2O_3 and SiO_2 were determined on whole rock samples. The Hilger and Watts Atomspeck Absorption Spectrophotometer was used for these analyses. Details of the analytical methods used and preparation of samples are given in Appendix

. The results are compared with published analyses of recent and ancient carbonate sediments.

The aim of this geochemical study is to examine the relationships between major and minor elements and to assess their possible use as indicators of the original mineralogy of the sediment. The major and minor elements geochemistry could also give some information on the diagenetic changes that have taken place. Thus, it is hoped that this study may aid the interpretation of the conditions of deposition and the diagenetic history of the Gachsaran carbonate horizons.

7.2 Calcium and Magnesium

The average contents of calcium and magnesium in the Gachsaran limestones, dolostones and siltstones are given in Table 7-2.

The Ca^{+2} content of the Gachsaran limestones is somewhat variable (Table 7-1). This variability is mainly due to variations in the amounts

TABLE 7-1

	Sample No.	Location	Mineralogy & Lithology	Acetic Acid Analysis: Ca%	$CaCO_3$%	Mg%	$MgCO_3$%	Ca/Mg	Acetic acid Na_2O ppm	Whole analysis Na_2O ppm	Acetic acid K_2O ppm	Whole analysis K_2O ppm	Acetic acid Fe_2O_3 ppm	Whole analysis Fe_2O_3 ppm	Acetic acid MnO ppm	Whole analysis MnO%	Al_2O_3%	Silica%	Acetic Acid Analysis: Sr ppm	Sr/Ca(x10^3)	Zn ppm	Pb ppm	Cu ppm	Rb ppm	I.R%
1	24	Hamman Al-Alil	Limestone Pelmicrite	34.2	85.4	0.8	2.7	45.8	206	0.12	245	0.21	85	1.22	370	0.04	0.74	4.22	7361	21.55	10	-	8	5	11
2	26	Hamman Al-Alil	Limestone Cosparite	35.7	89.3	0.6	2.04	55.5	318	0.1	64	0.1	154	0.91	392	0.05	0.96	3.5	346	0.97	12	2.4	8	<4	8.5
3	66	Shaqlawa	Limestone Bromicrite	37.2	92.9	0.4	1.3	93.0	295	0.15	55	0.06	458	0.5	1528	0.15	0.52	4.3	263	0.71	30	3	9	<3	5.5
4	42	Shaikh Ibrahim	Limestone Neomorphic spar	37.8	94.6	0.35	1.2	108.0	61	0.08	46	0.05	48	0.2	76	-	0.1	2.04	312	0.82	12	2.4	13	<5	4.0
5	110	Bashiqa	Limestone Biomicrite	37.4	93.4	0.4	1.3	93.5	242	0.1	57	0.06	359	0.31	516	0.03	0.21	1.5	224	0.6	12	9.4	8.4	<3	5.2
6	108	Bakhul	Limestone Biointrasparite	38.5	95.7	0.79	2.71	48.5	264	0.38	50	0.104	43	0.75	232	0.03	0.11	2.1	388	1.01	12	-	7.1	<3	1.5
7	45	Shaikh Ibrahim	Limestone Neomorphic spar	34.6	86.6	0.3	0.95	115.3	5.0	-	128	0.31	42	0.61	186	0.03	1.15	6.0.	310	0.89	10	-	7.3	<5	12.5
8	109	Bakhul	Limestone Biosparite	37.3	93.2	0.6	1.93	62.2	115	0.1	41	0.12	371	0.46	304	0.04	0.1	2.12	386	1.04	12	8.2	9	<4	4.7
9	85	Hamman Al-Alil	Limestone Oncosparite	33.4	83.6	1.0	3.3	33.4	295	0.05	187	0.76	122	1.57	1069	0.15	1.66	7.5	308	0.92	11	29	12.2	<5	13.0
10	22-4-7	Mishraq	Limestone Oncosparite	35.1	87.86	0.6	2.04	58.5	222	0.21	118	0.23	735	0.7	140	0.02	0.92	3.52	456	1.3	12	-	6.5	<5	10.0
11	22-4-8	Mishraq	Limestone Pelmicrite	31.8	79.6	1.5	5.2	21.2	371	0.23	276	0.54	1047	1.23	183	0.04	1.95	7.35	1019	3.2	16	3	9	-	15.0
12	20-3-21	Mishraq	Limestone Biointrasparite	37.6	86.1	0.2	0.71	188.0	157	-	206	0.1	192	0.27	86	0.02	0.21	7.79	348	1.01	10	-	9	-	13.0
13	22-4-10	Mishraq	Limestone Comicrite	37.4	93.48	0.27	0.92	138.5	247	0.02	289	0.14	867	0.47	122	0.03	0.85	2.63	380	1.02	10	8.5	9	-	4.3
14	Str.	Shaikh Ibrahim	Dolostone stromatolitic	25.7	64.2	9.95	34.52	2.6	450	0.105	112	0.01	168	0.13	214	0.02	-	1.8	7003	27.3	14	9.7	6.1	<4	2.0
15	212	Hamman Al-Alil	Dolostone Pelmicrite	21.6	53.93	11.07	38.4	1.95	1631	0.204	265	0.14	502	0.45	145	0.015	0.85	3.25	480	2.23	8	14	8	<3	7.4
16	36	Tell-Afar	Dolostone Algal laminites	22.3	55.7	11.82	41.0	1.9	1122	0.204	189	0.19	103	0.4	344	0.04	0.21	2.26	127	0.57	10	14	4	<5	3.0
17	22-4-1	Mishraq	Dolostone Algal algal-bearing micrite	19.4	48.4	10.41	36.12	1.9	1689	0.223	478	0.56	2079	1.4	447	0.06	2.48	7.92	281	1.45	4	12.5	5	<5	15.0
18	20-3-18	Mishraq	Dolostone micrite	21.8	54.4	11.67	40.5	1.9	360	0.237	784	0.003	542	0.42	157	0.03	0.85	3.56	81	0.4	13	-	3	6	5.0
19	20-3-4	Mishraq	Dolostone micrite	20.5	51.12	12.63	43.8	1.6	512	0.063	318	0.1	739	0.3	143	0.03	0.42	3.43	3668	17.94	7	12.5	4	-	4.5
20	83	Hamman Al-Alil	Siltstone	4.3	10.82	4.37	15.16	1.0	380	1.63	305	1.87	123	2.6	554	0.08	8.2	42.82	97	2.24	5	7.3	7.8	<4	
21	219	Hamman Al-Alil	Siltstone	5.7	14.3	0.48	1.65	11.9	109	2.12	164	1.73	278	1.84	553	0.08	7.58	54.45	188	3.3	4	15.5	3.5	<3	

of insoluble residue present. The negative correlation between Ca^{+2} and insoluble residue (Fig.7-1) confirms this. The insoluble residue consists mainly of clay minerals and silica (quartz).

TABLE 7-2

Type of rocks	Average Ca content	Range of Ca content	Average Mg content	Range of Mg content	Average Ca/Mg
Miocene limestones	36.0	31.8-37.8	0.6	0.2 - 1.5	60.0
Miocene dolostones	21.9	19.4-25.7	11.3	9.95-12.63	2.0
Miocene siltstones	5.0	4.3- 5.7	2.4	0.48- 4.37	6.5
Upper Devonian-Lower Carboniferous lsts. (Veevers, 1969)	31.7		0.9		35.2
Mesozoic subtidal-intertidal carbonate facies (Bencini & Turi, 1974)	34.9		3.05		11.4
Dolostones from different formations (Wolf et al., 1967)	22.6		11.3		2.0
Recent Bahamian carbonates (Till, 1969)	36.6		1.13		32.4

In the limestones free of any dolomite (determined by X-ray diffraction) up to 1.5% Mg^{+2} has substituted for the Ca^{+2} in the calcite lattice.

Whereas the average Ca^{+2} content of the Gachsaran limestones is slightly higher than the average Ca^{+2} content of the Devonian/Carboniferous and Mesozoic suites (Table 7-2), the Mg content of the Gachsaran limestones is less. The Ca/Mg ratio underlines the contrast in Ca and Mg contents; the average Ca/Mg ratio is 60, while that of the Paleozoic is 35.0 and Mesozoic is 11.

Comparing the Ca and Mg contents in the Gachsaran limestones with those of the Devonian and Carboniferous carbonate rocks of the Russian

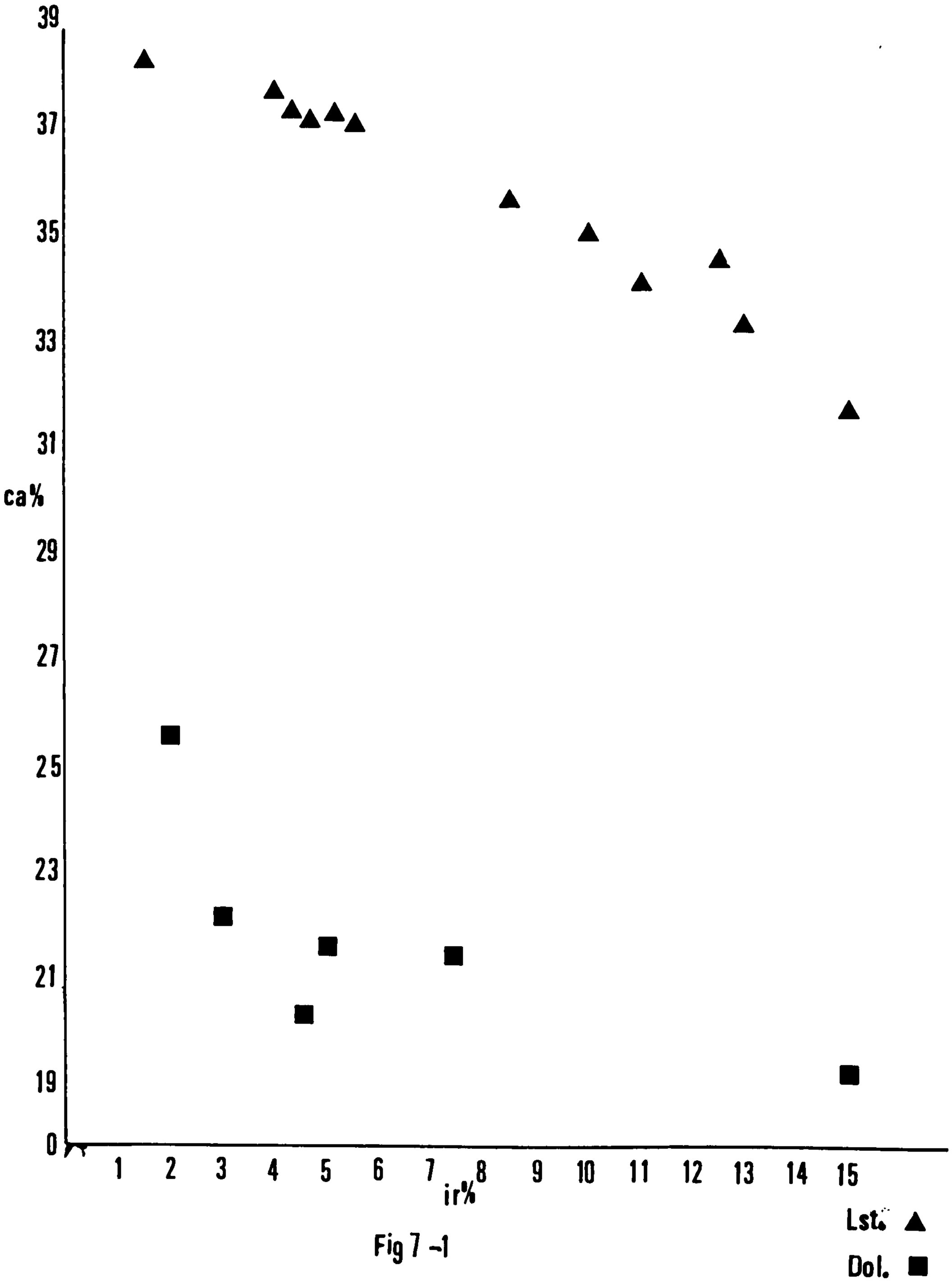
39
37
35
33
31
ca%
29
27
25
23
21
19
0
1 2 3 4 5 6 7 8 9 10 11 12 13 14 15
ir%
Lst.
Dol.

Fig 7 -1

Platform (Ca = 28%, Mg = 6%)(Vinogradov and Ronov, 1956), the Ca content of the Gachsaran limestones is higher where the Mg content of the Gachsaran limestones is much lower.

Although the Ca content in the limestones of the Gachsaran (36.0%) compares very closely to the Ca content of some recent Bahamian carbonates (Table 7.-2), there is quite a contrast in their Mg^{+2} content.

Low Mg^{+2} contents in limestones have been attributed to factors preventing hypersalinity (Veevers, 1969) or to the type of calcareous organisms perdominant in the limestones (El-wakeel and Riley, 1961; Dodd, 1967; Billings and Ragland, 1968, among others). With Recent carbonate sediments, the Mg^{+2} contents are largely dependent on the mineralogy of the sediment. Three carbonate minerals are present, aragonite, high Mg-calcite and low Mg-calcite. Aragonite generally contains less than 3000ppm Mg^{+2}, whereas high Mg-calcite contains up to 20 mole % $MgCO_3$. The mineralogy of the sediment is also determined by its skeletal and non-skeletal composition. Unless dolomitised, ancient limestones have low Mg contents since they are composed of low Mg-calcite. Gavish and Friedman (1969), for example, have noticed that Mg-calcite skeletal grains changed to low Mg-calcite without any textural changes as a result of contact with meteoric waters. Much of this Mg is thus lost during early diagenesis (Gavish and Friedman, 1969; Iand et al., 1967).

The very low Mg content of the Gachsaran limestones suggests that either the original sediment was largely composed of aragonite, or that much leaching of Mg^{+2} occurred during diagenesis, such as through contact with meteoric water. From a consideration of the petrological composition of the limestone analysed, it is likely that the original sediment was of mixed mineralogy; aragonite and high Mg-calcite. It is thus thought that the low Mg contents and the high Ca/Mg ratio represent intensive meteoric leaching.

7.3 Sodium

The average content of acid soluble and total average of Na_2O in the Miocene limestones, dolostones and siltstones of the Gachsaran Formation, together with published Na_2O values for other limestones, are listed in Table 7-3.

TABLE 7-3

	Average Na_2O content -acid soluble fraction-	Range	Total average Na_2O content
Miocene limestones	220 ppm	5-371ppm	0.12%
Miocene dolostones	961 ppm	360-1689ppm	0.17%
Miocene siltstones	245 ppm	109-380ppm	1.8%
Eocene dolostone (Land et al., 1975)	400 ppm		
Pleistocene limestones (Land and Hoops, 1973)	560 ppm		
Recent carbonates (Land and Hoops, 1973)	2485 ppm		

Land and Hoops (1973) and Veizer et al. (1977) emphasised the importance of the Na content in ancient carbonate rocks as an indicator of palaeosalinity. Veizer et al. (1977) analysed many samples from the Palaeozoic of Somerset and Prince of Wales Islands, Arctic Canada, and found that a value of 310 ppm Na_2O divided limestones deposited in hypersaline environments from those of normal marine origin. The average Na_2O content in the Gachsaran limestones is 220 ppm (Table 7-3). This figure is significantly lower than that of Pleistocene limestones (Table 7-3, Land and Hoops, 1973), and an order of magnitude lower than the Na_2O content of Recent carbonates (Table 7-3). Land and Hoops (1973), among

others, found that the sodium content decreases as re-equilibration with meteoric water takes place. The average Na_2O content in the Gachsaran dolostones is 961 ppm, which is higherthan that of Eocene dolostones (Table 7-3) and much higher than the average Na_2O content in the limestones. It is also of interest that the 961 ppm figure for the Miocene dolostones is also way above the 310 ppm value of Veizer et al. (1977). It should be noted that Veizer's figure represented an average Na_2O content of limestones and dolostones. It is suggested that for the Miocene limestones much of the sodium was lost during diagenesis. The high values for the dolostones, however, could indicate that they deposited under relatively high saline conditions, or at least very early during diagenesis before the carbonate sediments had lost their originally high Na contents.

The acid soluble Na occurs as a substitute for Ca in the calcite lattice, and may also occur in solid or liquid inclusions in the form of NaCl (Fritz and Katz, 1972; Land and Hoops, 1973). The total Na_2O, most of which is in insoluble residue (see Table 7-3), is contained in clays and silicates.

7.4 Strontium

The average content of acid soluble Sr^{+2} in the Miocene carbonates and siltstones of the Gachsaran Formation, together with published values of other carbonates are listed in Table 7-4.

TABLE 7-4

	Average Sr^{+2} content	Range	Average $\frac{Sr\%}{Ca\%} \times 10^3$
Miocene limestones	338 ppm	224-456	0.94
Miocene dolostones	342 ppm	81-480	1.1
Miocene siltstones	143 ppm	97-188	2.8
Tertiary carbonates (Kapl et al, 1952)			1.3
Mesozoic subtidal-intertidal carbonate facies (Bencini and Turi, 1974)	388 ppm		1.0
Recent carbonates, Arabian Gulf (Kinsman, 1969)	9390 ± 500 ppm		

The above values of Sr of the Gachsaran carbonates are comparable to the average Sr^{+2} content in ancient limestones (400-800 ppm)(see Table III, Wolf et al., 1967). Also the average Sr x 10^3/Ca of the Gachsaran limestones is comparable to that average of other Tertiary carbonates (Table 7-4). It should be noted, however, that the above Sr values only represent 85% of the analysed samples and more extreme values for Sr were recorded.

Two limestone samples (24, 22-4-8, see Table 7-1) yielded Sr^{+2} contents ranging from 1000-7361 ppm, both of which are pelleted micrite. Two dolostone samples (str., 20-3-4, see Table 7-1) yielded Sr^{+2} values ranging from 3000-7000 ppm, both of which are micrite rocks of algal origin. The difference between the Sr^{+2} content of Recent sediments and their Pleistocene analogues has been studied by Stehli and Hower (1961) and by Khale (1965). See also Table 7-4 for a comparison between Miocene average Sr^{+2} content and Sr^{+2} content from the Recent Arabian Gulf sediments. Gavish and Friedman (1969) compared sediments of different ages from the Mediterranean coast and noticed that a sharp decrease occurred in Sr^{+2} with time, through meteoric water diagenesis. This trend has been commented on by many authors and discussed in detail by Kinsman (1969, 1971). Kinsman attributed the rather low Sr^{+2} conent in ancient limestones to the existence of open systems during diagenesis, through which large volumes of pore fluid migrated. The strontium content of carbonate sediments is mostly attributed to the substitution of Sr for Ca in aragonite and calcite, with aragonite able to accommodate up to ten times more strontium than calcite (Holland, 1963, 1964).

In an aqueous replacement of aragonite by calcite through dissolution-reprecipitation, Kinsman showed that the initial calcite precipitated has less strontium than the original aragonite. In a closed system, further dissolution of aragonite leads to a higher Sr^{+2} concentration in the

solution so that later calcite precipitated contains more Sr^{+2}. A situation is reached in which the calcites precipitated have the same Sr^{+2} content as the original aragonite. In an open water system, the story, however, is different, and Sr^{+2} cations are lost when transformation occurs through the migrating meteoric waters. Undoubtedly, then, the amount of Sr^{+2} present within the Gachsaran carbonates represent a remnant of a much higher value.

The rather high values of Sr^{+2} of some of the samples (Table 7-1) may be significant in this respect. Sample 24 (limestone) has an Sr^{+2} content of 7361 ppm and sample str. (dolostone) has an Sr^{+2} content of 7003 ppm (Table 7-1). Although the rather exceptionally high values for Sr^{+2} in the above two samples could be explained by a more closed system of diagenesis rather than an open one (see Kinsman, 1969, 1971), it suggests that the original content of Sr^{+2} was also very high. Samples 22-4-8 and 20-3-4 (Table 7-1), however, pose a minor problem as they have intermediate values of 1000 and 3668 ppm Sr^{+2} respectively. It is possible that these samples were subjected to some leaching but not the near-complete leaching that characterises an open system. This mix of both types of diagenetic systems may have been responsible for the samples intermediate Sr^{+2} values. There are two possible reasons for the exceptionally low Sr^{+2} value of dolomite sample 20-3-18 (81 ppm, Table 7-1). The dolomite could be late diagenetic, i.e. formed after the sediment had lost its originally high Sr^{+2} and been replaced by dolomite (cf. Veizer and Demovic, 1974). Alternatively, this sample could originally have been composed of calcite.

7.5 Manganese

The average content of acid soluble MnO in the Miocene carbonates and siltstones of the Gachsaran, together with published results of other carbonates are given in Table 7-5.

TABLE 7-5

	Average MnO content - acid soluble fraction	Range ppm	Total MnO content
Miocene limestones	400 ppm	76-1528	520 ppm
Miocene dolostones	241 ppm	143-447	325 ppm
Miocene siltstones	554 ppm		800 ppm
Jurassic and Carboniferous carbonates (Barber, 1974)	1583 ppm	200-6000	
Devonian-Carboniferous limestones (Veevers, 1969)	447 ppm		
Mesozoic subtidal-intertidal carbonate facies (Becini and Turi, 1974)	76 ppm		
Recent carbonate sediments South Belize (Billings and Ragland, 1967)	160 ppm		

The MnO content of the limestones mostly cluster in the 200-500 ppm range (Table 7-1). Comparing the MnO whole sample values of the Gachsaran carbonates with those of acid-soluble values (Tables 7-1, 5), it is noted that most of the MnO is associated within the carbonate fraction rather than with the insoluble residue. The atomic radius for Mn^{+2} is 0.8 Å, and that of calcite is 0.99 Å. Mn^{+2} substitutes to 40% by weight $MnCO_3$ in the calcite lattice (Berry and Mason, 1959). Veevers (1969) related the manganese content of some Devonian and Carboniferous limestones to their insoluble residue.

Stehli and Hower (1961) noticed that a reduction occurs in the concentration of Mn along with other elements with time. It should be noted, however, that manganese is not necessarily a primary constituent but may be diagenetic. Loss of manganese from sediments may take place by ion exchange if it is associated with clay minerals.

Mn^{+2} is directly related to Fe (e.g. Gavish and Friedman, 1969), but higher values of Mn (Table 7-1) do not follow the general trend (Fig.7-2). Since Mn goes into solution more readily than Fe (Lynn and Bonatti, 1965), it is possible that higher concentration in MnO of the three samples (Table 7-1, Fig.7-2) were caused diagenetically later by travelling connate waters.

In a study of the behaviour of Mn and Zn in carbonate diagenesis, Pingitore (1978) noted four distinct situations on aragonite to calcite transformation, taking into consideration the partition coefficient of Mn: (a) autodepletion whereby the calcite is depleted in trace elements relative to the parent aragonite, through a high rate of water flow relative to the reaction rate, (b) autoenrichment, whereby calcium is preferentially removed from the diagenetic site relative to trace elements so that there is an enrichment of the calcite in trace elements, (c) alloenrichment, whereby calcite precipitated from a solution is more enriched in trace elements than the parent aragonite, and (d) allodepletion, whereby a liquid rich in Ca and poor in trace elements is flushed into the diagenetic site. In a closed system of aqueous aragonite to calcite transformation, the resulting calcite is expected to have the same amount of trace elements (Mn^{+2}) as the parent aragonite (Pingitore, 1978). In an open system, where one of the above four situations exists, depletion or enrichment of calcite in Mn^{+2} relative to the parent aragonite can occur. The MnO contents of the Gachsaran carbonates compare very closely to those of Devonian-Carboniferous limestones from the Bonaparte Gulf basin - northwest Australia (Veevers, 1969)(Table 7-5). The Gachsaran values for Mn, however, are much lower than those of Jurassic and Carboniferous carbonates (Barber, 1974)(Table 7-5), while they are a little bit higher than the MnO values of Recent carbonate sediments - south of Belize (Billings and Ragland, 1967)(Table 7-5). Also they are much higher than

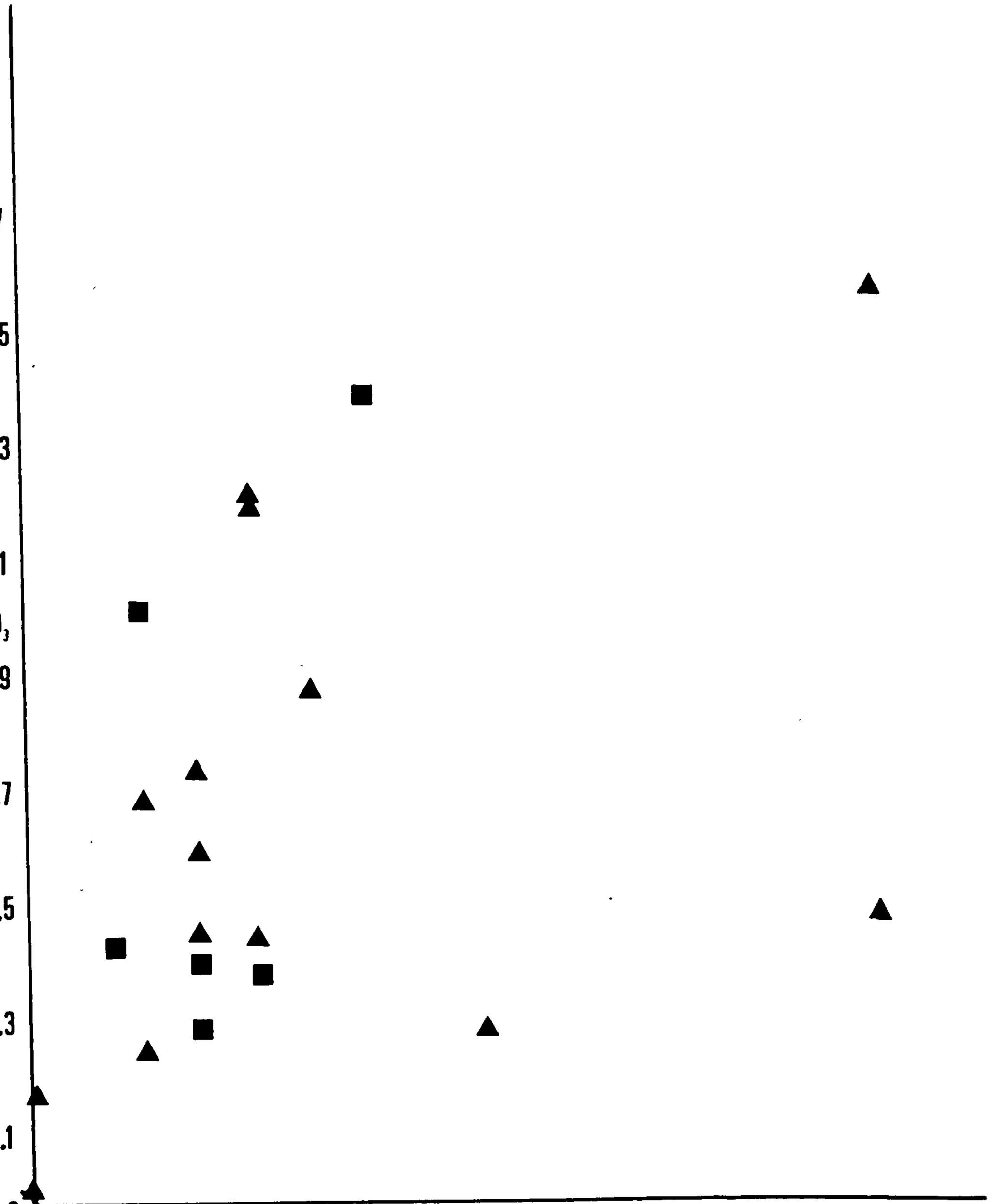

Fig.7-2

those of the Mesozoic subtidal-intertidal carbonate facies (Becini and Turi, 1974)(Table 7-5). Becini and Turi interpreted the low values of Mn as a reflection of the original carbonate mineralogy; aragonite. This conclusion emphasises the later enrichment of the Gachsaran carbonates with Mn^{+2}.

7.6 Iron

The average content of Fe_2O_3 in the Miocene limestones and siltstones of the Gachsaran Formation, together with published values of other carbonates are given in Table 7-6).

TABLE 7-6

	Average Fe_2O_3 - whole rock analysis	Average Fe_2O_3 acid soluble fraction
Miocene limestones	0.71%	348 ppm
Miocene dolostones	0.52%	696 ppm
Miocene siltstones	2.22%	200 ppm
Carboniferous-Jurassic carbonates (Barber, 1974)		
limestones	1.01%	0.63%
dolostones	4.14%	3.96%
Devonian-Carboniferous limestones (Veevers, 1969)		0.16%
Recent Bahamian carbonates (Till, 1971)		144 ppm

In limestones and dolostones, iron may be present in the lattice of the carbonate minerals (Calcite or dolomite) and/or as pyrite and ferric oxides (haematite) in the insoluble residue. The high values of Fe_2O_3 in whole rock samples compared to that of acid soluble fraction (Tables 7-1,6) shows that much the iron is present within the insoluble residue and probably in the form of ferric oxide or hydrated ferric oxide. In the

Gachsaran dolostones, the Fe_2O_3 (whole rock analysis) is less than that of limestones, the Fe_2O_3 acid soluble fraction, however, is much higher (Table 7-6). The higher concentration of acid soluble iron in dolostones may suggest that enrichment of iron took place following limestone dolomitization.

The ferroan calcite form replacing skeletal fragments has been taken as an indicator of Mg-calcite origin of the former (Richter and Fuchtbauer, 1978). Richter and Fuchtbauer suggested that the chemical instability of high-magnesium calcite is the driving force of the replacement by ferroan calcite. They also noticed that skeleton grains originally composed of low-magnesium calcite were never replaced by ferroan calcite. So, is the very low iron content in the Gachsaran carbonates compared to Carboniferous-Jurassic carbonates (Barber, 1974)(Table 7-6) and to values given for skeletal carbonates (Richter and Fuchtbauer, 1978) indicate fewer originally high Mg-calcite skeletons? Richter and Fuchtbauer gave two conditions necessary for the formation of ferroan calcite; (a) reducing environment, and (b) lack of organic matter combined with anaerobic sulphate-reducing bacteria.

7.7 Potassium

The average potassium content in the Miocene carbonates and siltstones of the Gachsaran Formation is given in Table 7-7.

TABLE 7-7

	Average K_2O content whole rock analysis	Average K_2O content acid soluble fraction
Miocene limestones	0.17%	136 ppm
Miocene dolostones	0.18%	291 ppm
Miocene siltstones	1.8%	235 ppm

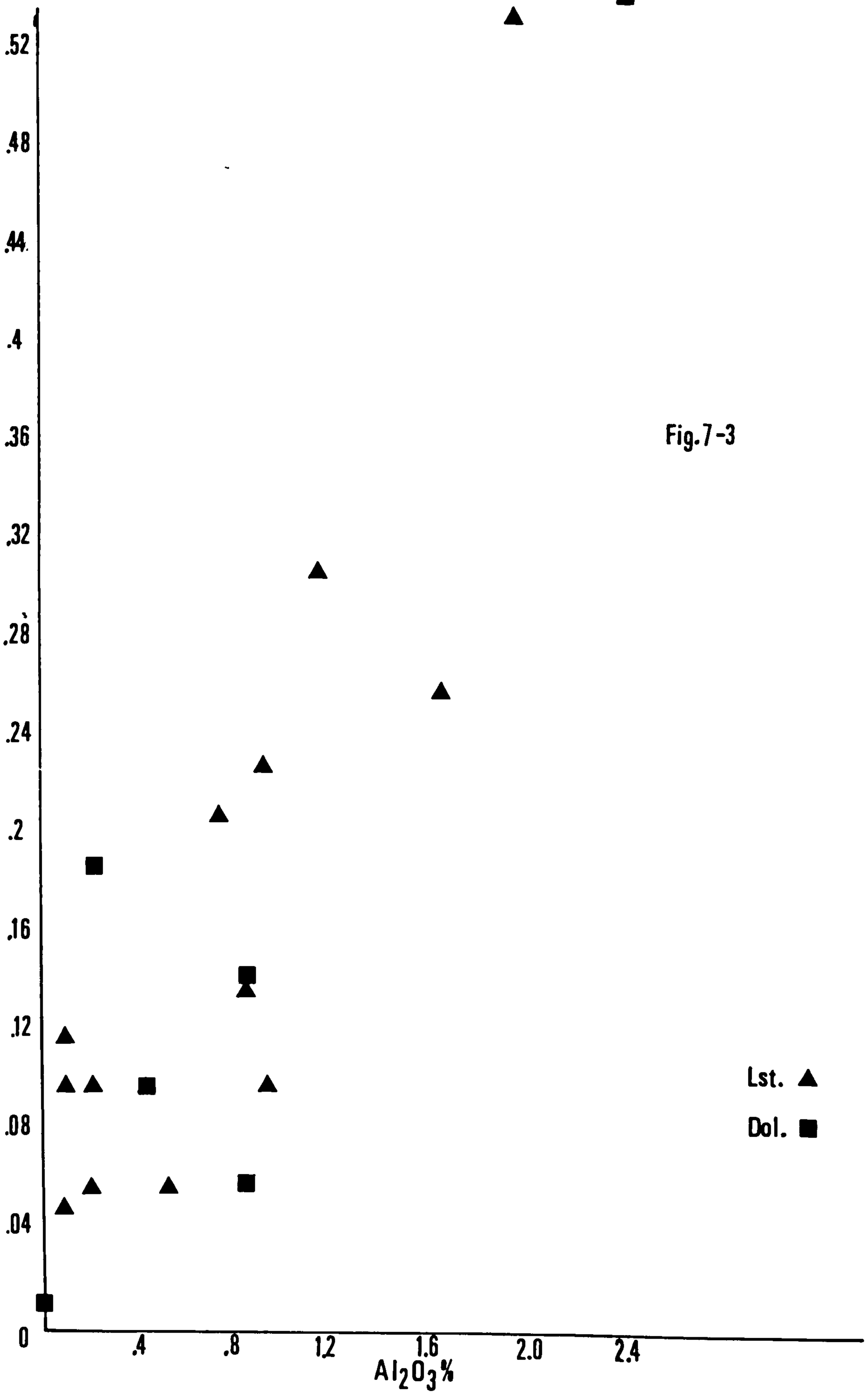

Fig. 7-3

Potassium in both limestones and dolostones is believed to be mainly present in the clay mineral fraction of the insoluble residue (Table 7-7). Thus its content is expected to rise with the rise of the amount of argillaceous material. A plot of K_2O against Al_2O_3 (Fig.7-3) shows a positive correlation and confirms the clay mineral association of K_2O. Variations in K_2O content (Table 7-1) are probably reflections of the different argillaceous contents.

7.8 Aluminium

The average aluminium content in the Miocene carbonates and siltstones of the Gachsaran Formation is listed in Table 4-8.

TABLE 7-8

	Average Al_2O_3 content	Range
Miocene limestones	7300 ppm	1000-19500 ppm
Miocene dolostones	8016 ppm	0-24800 ppm
Miocene siltstones	7.89%	7.58-8.2%

The aluminium contents of the Gachsaran carbonates show considerable variability (Tables 7-1,8). The aluminium is present mainly within clay minerals like K, and a positive correlation exists between the two elements (Fig.7-3). Aluminium in both limestones and dolostones appears to be totally confined to the insoluble residue (Fig.7-4).

7.9 Silica

The average silica content in the Miocene limestones, dolostones and siltstones of the Gachsaran Formation is given in Table 7-9. The limestones and dolostones show relatively equal amounts of silica (Table 7-1). The relatively high amount of silica in siltstones is understandable. The silica is positively correlated with the insoluble residue as it

Fig. 7-4

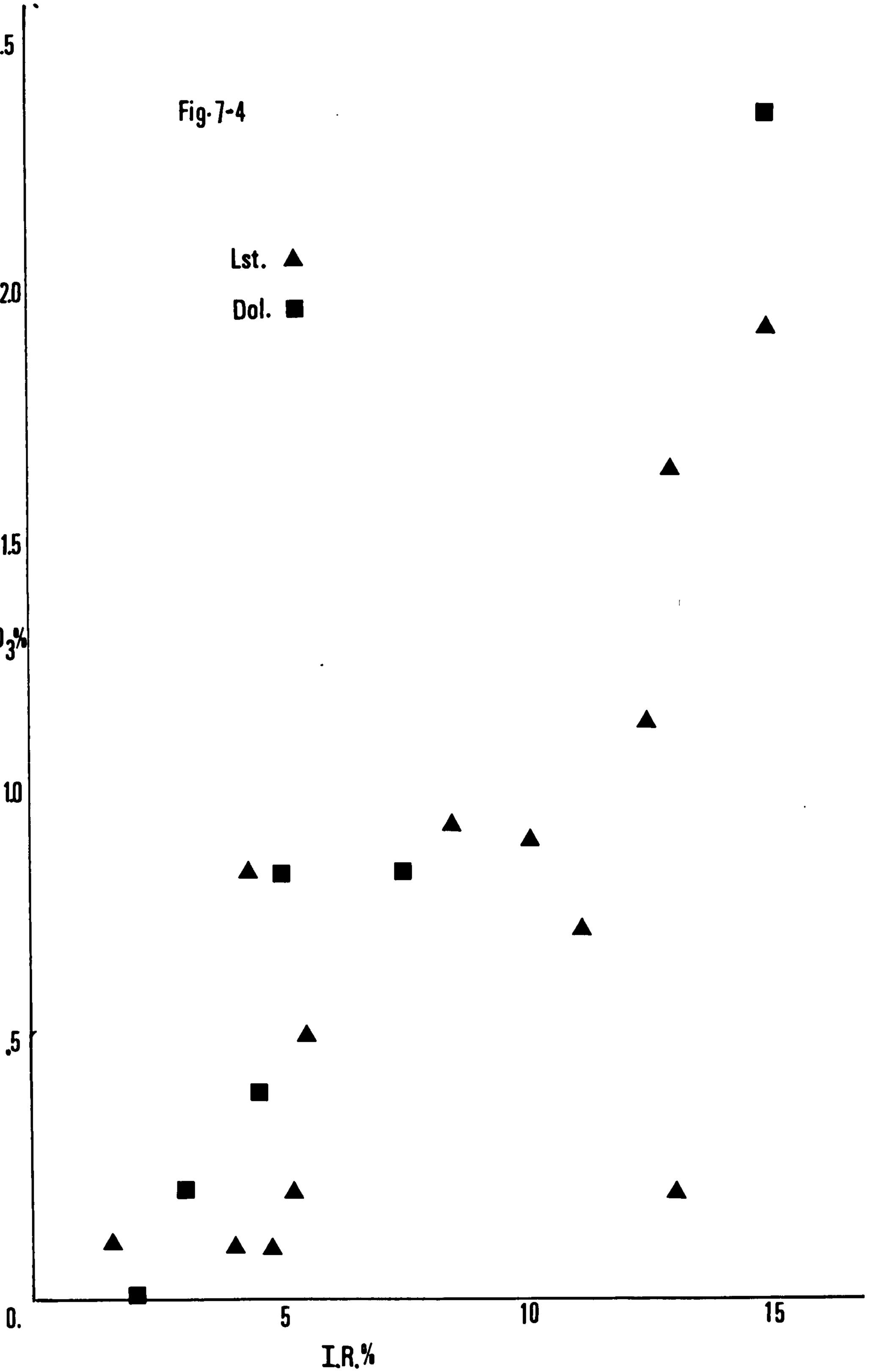

TABLE 7-9

	Average SiO_2 content	Range
Miocene limestones	4.2%	1.5-7.79%
Miocene dolostones	3.7%	1.8-7.92%
Miocene siltstones	48.64%	

constitutes a large part of it. Silica in both limestones and dolostones may be present as detrital quartz, authigenic quartz or chalcedony, as opaline or microcrystalline silica, and a smaller proportion is present within clay minerals.

7.10 Zinc, Copper, Lead and Rubidium

The average acid-soluble contents of the trace elements Zn, Cu, Pb and Rb of the Gachsaran carbonates and siltstones are given in Table 7-10.

TABLE 7-10

	Average Zn	Average Cu	Average Pb	Average Rb
Miocene limestones	13 ppm	9 ppm	5 ppm	$<$ 3 ppm
Miocene dolostones	10 ppm	5 ppm	11 ppm	$<$ 3 ppm
Miocene siltstones	5 ppm	6 ppm	11 ppm	$<$ 4 ppm
Devonian-Carboniferous carbonates (Veevers, 1969)	2.5 ppm		9.6 ppm	
Lower Carboniferous carbonates (Dickson and Barber, 1976)	5 ppm	1.4 ppm	0.9 ppm	

In limestones and dolostones, the behaviour of the major elements such as Ca, Mg and Fe are well known; their mineral associations are easy

to determine by chemical analysis, X-ray diffraction and by staining techniques. This is not so with trace elements. Their distributions may be a function of their concentrations in polygenetic carbonate minerals, non-carbonate detrital minerals and their authigenic products, organic matter and amounts adsorbed on all these minerals.

Zn, Cu, Pb and Rb show distinctly different behaviour from that of the other elements described here. They rarely exceed 10 ppm in the acid soluble fraction (Tables 7-1,10) and thus, only small amounts of these elements are adsorbed on mineral grains or are substituting in carbonates. It is expected that higher concentrations of these elements are associated with the insoluble residue.

Organic matter contents controls to a marked degree the trace elements in the bulk composition of carbonate skeletons and rocks (Wolf, et al., 1967). Krauskopf (1955), among others, stated that carbonates rich in organic matter may be enriched in Mo, Vi, Ni, Pb, Cu, Ag, As, Ge, I and Br. He further suggested that Pb, Zn, Ni and Cu may react with H_2S liberated from decaying organic matter and precipitate as sulphides. The contents of the trace elements Zn, Pb and Cu in the Gachsaran carbonates are higher than other carbonate rocks (Table 7-10). However, the Gachsaran carbonates are rich in organic matter, and this may have played an important role in terms of concentrating the trace elements Zn, Cu and Pb.

Zn^{+2} follows the same behaviour as Mn^{+2} in carbonates (see section on manganese) as opposed to Sr and Mg (Pingitore, 1978). Zn^{+2} also substitutes in the calcite lattice, but not to such an extent as Mn^{+2} (Berry and Mason, 1959).

7.11 Summary

The high values of Ca^{+2} suggest that the Gachsaran limestones are fairly pure. Like most other limestones, they have low values of Mg, Sr and Na, compared with Recent carbonate sediments. There are, however,

some interesting differences; the very low Mg in the limestones, exceptionally high Sr values in some of the samples and higher content of Na in dolostones. The low Mg^{+2} contents of the Gachsaran limestones suggests that either the parent sediments were dominantly of aragonite, with little Mg-calcite, or that much leaching of Mg^{+2} occurred during early diagenesis such as through contact with meteoric waters. It has also been suggested that other trace elements (Na and Sr) have been affected by this same process.

The Na content has been taken as a salinity indicator. Higher values of Na in dolostones suggests that they were precipitated in a more saline environment than the limestones.

The controversy of Sr^{+2} content in the Gachsaran carbonates suggests two possible forms of diagenesis; a closed system or an open system. A mixture of both processes may have affected any one sample. Sr^{+2} values up to 7000 ppm in the carbonates suggest that the parent sediment was more likely composed of aragonite.

Higher values of Mn suggest that at least these samples were enriched in Mn later on in an open system of diagenesis. Higher concentrations of iron in dolostones suggest that enrichment of iron took place following limestone dolomitization. The question is asked whether the relatively low iron content of the Gachsaran carbonates suggest low content of high Mg-calcite skeletons, or that the high organic content which characterises the Gachsaran carbonates have hindered ferroan calcite formation.

Potassium and Aluminium are directly correlated with each other and with the insoluble residue, their contents depending mostly on the amount of argillaceous material present.

The higher values of trace elements Zn, Cu and Pb compared to other ancient limestones have been effected by higher concentrations of organic matter in the Gachsaran carbonates.

CHAPTER 8

SYNTHESIS OF GACHSARAN SEDIMENTATION AND TECTONIC CONTEXT

CHAPTER 8

SYNTHESIS OF GACHSARAN SEDIMENTATION AND TECTONIC CONTEXT

8.1 Resumé of stratigraphy

The Gachsaran Formation (formerly the Lower Fars Formation) consists of gypsum-anhydrite, halite, limestone and mudrock. The formation was deposited in a NW-SE oriented basin extending from north-eastern Syria, through northern and north-eastern Iraq into south-western Iran. This Mesopotamian Basin was situated on the north and north-eastern leading edge of the Arabian plate. In Iraq, the Gachsaran Formation rests on the Jeribe Limestone Formation (Lower Miocene) in the central part of the Mesopotamian Basin. Towards the margins of the basin, it rests disconformably on older strata, in particular, the Eocene Pila Spi Formation on the north-eastern side of the basin, in northeast Iraq. The four units into which the Gachsaran Formation has been divided in the Kirkuk area (Transition, Saliferous, Seepage and Upper Red Beds) by Bellen et al. (1959) on the basis of borehole cores, cannot be recognised in surface exposures. A distinction can be made, however, between a lower group with sulphates, many limestones and fewer mudrocks, and an upper group of sulphates, mudrocks, but few limestones.

Although there is much scope for detailed micropalaeontological work on the Gachsaran, it appears that the base is diachronous, being of Lower Miocene age (Burdigalian) in southwest Iran, Middle Miocene (Langhian to Serravallian) in Iraq, and possibly Middle to Upper Miocene (Serravallian to Tortanian) in Syria (see Chapter 2). In terms of sediment thickness, the Gachsaran is quite variable. Apart from the formation thinning towards the basin margins, there are variations in thickness within the basin itself. The maximum thickness in Iraq is around 600m., but in northern Iraq, where the author has carried out fieldwork, thicknesses are generally less than

300m. Thickness variation within the basin reflect a more positive or more negative behaviour of the basin floor, producing areas with a lower or higher rate of subsidence. The underlying control could be fault movements in the basement. Thickness variations could also be complicated by salt tectonics.

8.2 Resumé of facies of the Gachsaran Formation

Four principal lithofacies are present within the Gachsaran Formation: gypsum-anhydrite, halite, limestone and mudrock.

Gypsum-anhydrite: These constitute about 70% of the formation near the central part of the basin in Iraq. Horizons of gypsum-anhydrite typically range in thickness from 1.5 to 15 metres; exceptionally, some may be thicker. At surface outcrops, the sulphate is present as gypsum, typically of alabastrine type, whereas in the subsurface, the sulphate is anhydrite. The anhydrite preserved at depth is present as subfelted and felted lath, blocky and fibroradiate types. There is evidence for a gypsum precursor to subfelted anhydrite. Four types of secondary gypsum were recognised, with three varieties forming by direct hydration of anhydrite. The sulphate beds are characterised by a nodular appearance, nodules being generally in the range of 1 to 15cm. In some cases, nodular gypsum is overlain by a bedded or layered variety, with individual beds ranging from 2 to 5cm. in thickness, and consisting of planar, undulating and somewhat contorted layers, but continuous laterally for many metres.

Although gypsum -anhydrite can form in both subaqueous and subaerial environments (eg. Dean et al., 1975), the nodular sulphate of the Gachsaran shows many similarities to anhydrite being precipitated at the present time within supratidal sediments of sabkhas along the Trucial Coast of the Arabian Gulf (see Chapter 3). The bedded sulphate occurring above the nodular variety could represent an enterolithic anhydrite which also forms in supratidal areas, but the continuity of bedding argues against this. Two

alternatives were given: that it formsthrough sulphate precipitation with algal layers (cf. algal mat-gypsum mush alterations of the Abu Dhabi Sabkha), or that it accumulated subaqueously in shallow lagoonal situations. Whatever the origin, its occurrence above nodular sulphate suggests a depositional site landwards of a sabkha, possibly within or around back-sabkha lagoons (cf. Leeder and Zeidan, 1972).

Halite: Halite does not crop out but it is reported from boreholes from the centre of the basin (see Chapter 3). Halite can be precipitated subaerially in sabkha situations (eg. Shearman, 1970) and subaqueously in shallow or deep water environments (eg. King, 1947). Stocklin noted the presence of polyhalite in association with the halite in south-western Iran. The halite is interpreted to have precipitated at times when the basin was partially or completely cut off from the world's ocean. The presence of polyhalite may suggest that the basin was desiccated, at least in some places.

Limestone: The limestone horizons constitute 10-15% of the Gachsaran Formation in northern Iraq. These horizons range from several centimetres to several metres in thickness. Microfacies exhibited by these limestones include pelsparites, pelmicrites, biosparites, biomicrites, intrasparites, intramicrites, oosparites and oncolitic limestones. The most common biota are Foraminifera and bivalves, also gastropods, ostracods, bryozoa, echinoids and crustacean fragments. Some limestones contain stromatolites and cryptalgal laminites. Non-algal laminites also occur, associated with calcite pseudomorphs after nodular anhydrite and locally with bioturbation structures. Sedimentary structures also include symmetrical ripples formed by wave oscillation and herringbone cross-bedding. Some limestones are either partly or completely dolomitized. The dolomite is very fine-grained and usually occurs within micrites and cryptalgal limestones. The latter may also contain lozenge-shped calcite pseudomorphs after gypsum. The

depositional environment of these limestones is interpreted as shallow subtidal to intertidal. Biosparites, oosparites and oncolitic limestones are interpreted as forming under agitated shallow subtidal conditions. The laminated limestones, very similar to examples described from lake situations (Picard, 1972; Tucker, 1978) are interpreted as forming in high intertidal ponds, lagoons or lakes. Their association with replaced nodules of anhydrite is taken to indicate subaerial conditions and desiccation of the lagoon or pond. Pelleted micrites, cryptalgal laminites and stromatolitic limestones were deposited on intertidal flats. Limestones with pseudomorphs after gypsum formed in high intertidal situations.

Mudrock: The mudrock horizons constitute 15-50% of the Gachsaran Formation in northern Iraq. Most of these horizons are massive and structureless. Occasional thin beds of limestones several centimetres in thickness occur within these horizons. The mudrock horizons generally attain several metres in thickness but may be as thick as 30m.

Two types of mudrock were distinguished. The distinction was based on colour, Foraminifera and clay mineral content. The green mudrocks are dominated by benthic Foraminifera, but other fossils including bivalves, ostracods, echinoids, gastropods are also common. Clay minerals are dominated by illite, but montmorillonite, mixed layers and kaolinite are also present. These mudrocks are interpreted as deposited in hypersaline lagoons. The red mudrocks are dominated by planktonic Foraminifera. Clay minerals are dominated by nearly equal proportions of montmorillonite and illite. Kaolinite is also present but in lower concentrations than the green mudrocks. These mudrocks are interpreted as having been deposited in relatively deeper water restricted marine situations. The possibility of some mudrocks being of Aeolian origin is not excluded.

8.3 Facies and cycle interpretations

When a number of lithological units are repeated through a succession,

the succession is referred to as cyclic. Basically, there exist two types of cycle: asymmetrical cycles (ABC ABC) and symmetrical cycles (ABCBA)(Duff et al., 1967). In this sense, much of the Gachsaran is cyclic (asymmetrical), the common rhythm being mudrock, limestone and gypsum (Figs.2-7,8-1). As noted above, the mudrocks can be interpreted as relatively deeper water, subtidal; the limestones are largely shallow subtidal to intertidal, and the gypsum-anhydrite beds are interpreted as of sabkha (i.e. supratidal) origin. The typical cycle then can be interpreted in terms of sabkha progradation, whereby supratidal sediments (the sulphates) built out laterally, seawards, over intertidal and shallow subtidal carbonate sediments, which in turn prograded over deeper water muds. Such sabkha cycles have been described from many other sequences in the geological record (eg. Wood and Wolfe, 1969; Bosellini and Hardie, 1973). Variations from the mudrock-limestone-gypsum rhythm are not uncommon. In the lower part of the formation, sequences may consist of limestone-gypsum cycles with little or no mudrock. These cycles represent sedimentation in an area distant from any continental influence so that only carbonate sediments accumulated in subtidal and intertidal environments. Towards the margins of the basin and in the upper part of the succession, sequences show a paucity of limestone and the succession consists largely of mudrock and gypsum horizons (see Fig.2-7). In these cases, the cycle mudrock-gypsum is simply a reflection of an increased fine-grained clastic input to the basin. The predominance of mudrock and paucity of limestones in the higher part of the Gachsaran is a consequence of the greater influx of terrigenous material during later Gachsaran time. The upward change in character of the mudrock thus suggests a change in the pattern of deposition. The number of sabkha cycles developed is variable, depending on location within the basin. Generally, there are between 20 and 30 cycles present, each with a thickness of around 20 metres. Sabkha progradation, a depositional mechanism, gives rise

Generalized Section

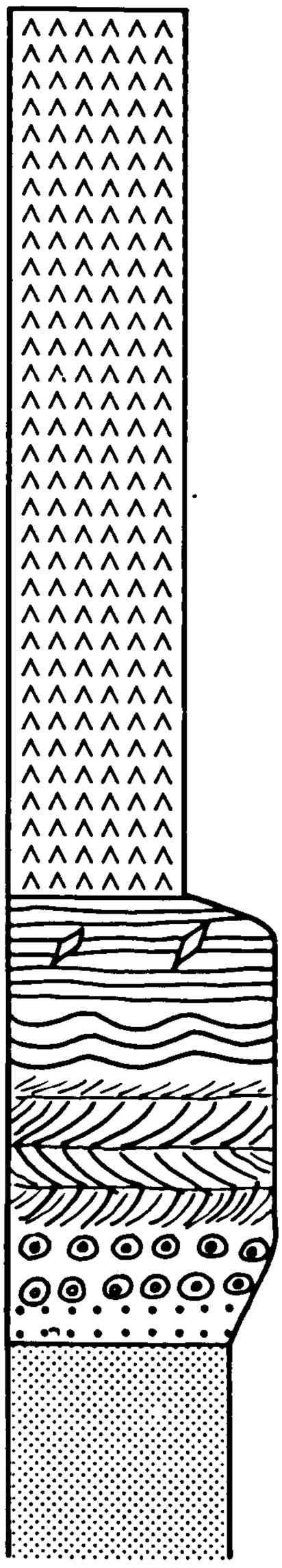

Gypsum

mainly alabastine
nodular in lower part, bedded in upper
locally contorted, probably after anhydrite

Limestone

pelleted, oolitic or bioclastic,
locally cross-stratified, wave rippled,
laminated, stromatolitic or bioturbated,
pseudomorphs after gypsum common.
Fossils: bivalves, gastropods, bryozoa,
foram inifera and ostracods

Clay

green or red in colour,
structureless or laminated,
locally calcareous,
Fossils: occasionally bivalves, also forams.

Fig. 8-1

to a sabkha cycle (eg. Shearman, 1966), and this could well be the main mechanism producing each Gachsaran cycle. An alternative, however, is a fall in sea-level (regression) which would lead to widespread sabkha development over intertidal-supratidal deposits. A rise in sea-level (transgression) is required to repeat the cycle of deposition.

Factors controlling sea-level changes and thus producing the repetition of cycles include changes in climate and the effect of large scale tectonic movements (Blatt et al., 1972). Attention is thus focussed on the tectonic context of the Mesopotamian Basin, and on the climatic events of the earth at that time, both of which could have affected the relative position of sea-level and giving rise to transgressions or regressions to initiate new cycles.

8.3 Tectonic context of the Mesopotamian Basin

The Mesopotamian Basin is a zone of thick sediment accumulation located on the north-eastern edge of the Arabian plate. The suture zone between the Arabian plate and the Iranian and Turkish plates to the northeast and north is situated along the line of the Zagros-Taurus mountain belt. It is now accepted by many people that an ocean, Tethys, was located between the Arabian plate and Iranian-Turkish plates from the early Mesozoic, and that this ocean closed at the end of the Cretaceous, in Middle Maestrichtian time. This closure is marked by the emplacement of ophiolites in the Zagros-Taurus mountain belt (Takin, 1972; Haynes and MacQuillan, 1974; Stoneley, 1974).

The collision of the Iranian and Arabian plates brought about folding and thrusting of the sedimentary cover on the leading edges of the two plates and the formation of a mountain range, the forerunner of the Zagros-Taurus range. In such a continent collision as this, sedimentary basins can form adjacent to the suture zone (Dickinson, 1974; Mitchell and Reading, 1978). These basins may develop (a) towards the leading edge of the plate being subducted, before or after collision; the peripheral basin of Dickinson

(1974), (b) upon fragments of un-subducted ocean floor (remnant-ocean basins), or (c) through strike-slip fault movements within the collision belt.

There were no significant compressional movements along the margin of the Arabian plate during the interval Late Cretaceous to late Miocene, only vertical, epeirogenic movements and local block faulting. Evidence for this is provided by the absence of angular unconformities in the Tertiary of Iraq (only disconformities and non-sequences are present) and the many rapid vertical and lateral facies changes in the Lower Tertiary. It is envisaged that from the late Cretaceous the Arabian plate was moving northwards, attached to the Iranian-Turkish plates, which were also moving in a similar direction, at a comparable rate. The reason for this subsidence and the persistence of the Mesopotamian Basin is thought to be the cooling of the crust in this area following the closure of the Tethyan ocean in the late Cretaceous. The Taurus-Zagros orogeny at the end of the Miocene and into the Pliocene resulted from regional changes in the rates of plate motion which produced a preferential northward movement of the Arabian plate relative to the Iranian-Turkish plates, and thus the crumpling and folding of the Tertiary and older sediments deposited between and on the margins of these plates. The uncoupling of the Arabian-Turkish/Iranian plates and the compression in the Zagros-Taurus area was due to collision of the Turkish/Iranian plates with the Eurasian plate to the north.

With regard to the tectonic movements during the Miocene and their influence on Gachsaran deposition and cyclicity, Table 8-1 documents the tectonic events around the Arabian plate. Of note are (i) the absence of seafloor spreading in the Red Sea area during the Middle Miocene; spreading here took place before and after Gachsaran deposition (Girdler and Styles, 1978), (ii) the stratigraphic evidence for extensive vertical movements

Table 8-1

	SOUTH & WEST NORTH & EAST	MAJOR EVENTS
PLIOCENE 5 MIOCENE 24 OLIGOCENE 37 EOCENE 55 PALAEOCENE 65 Maestr. CRETACEOUS 137 JURASSIC	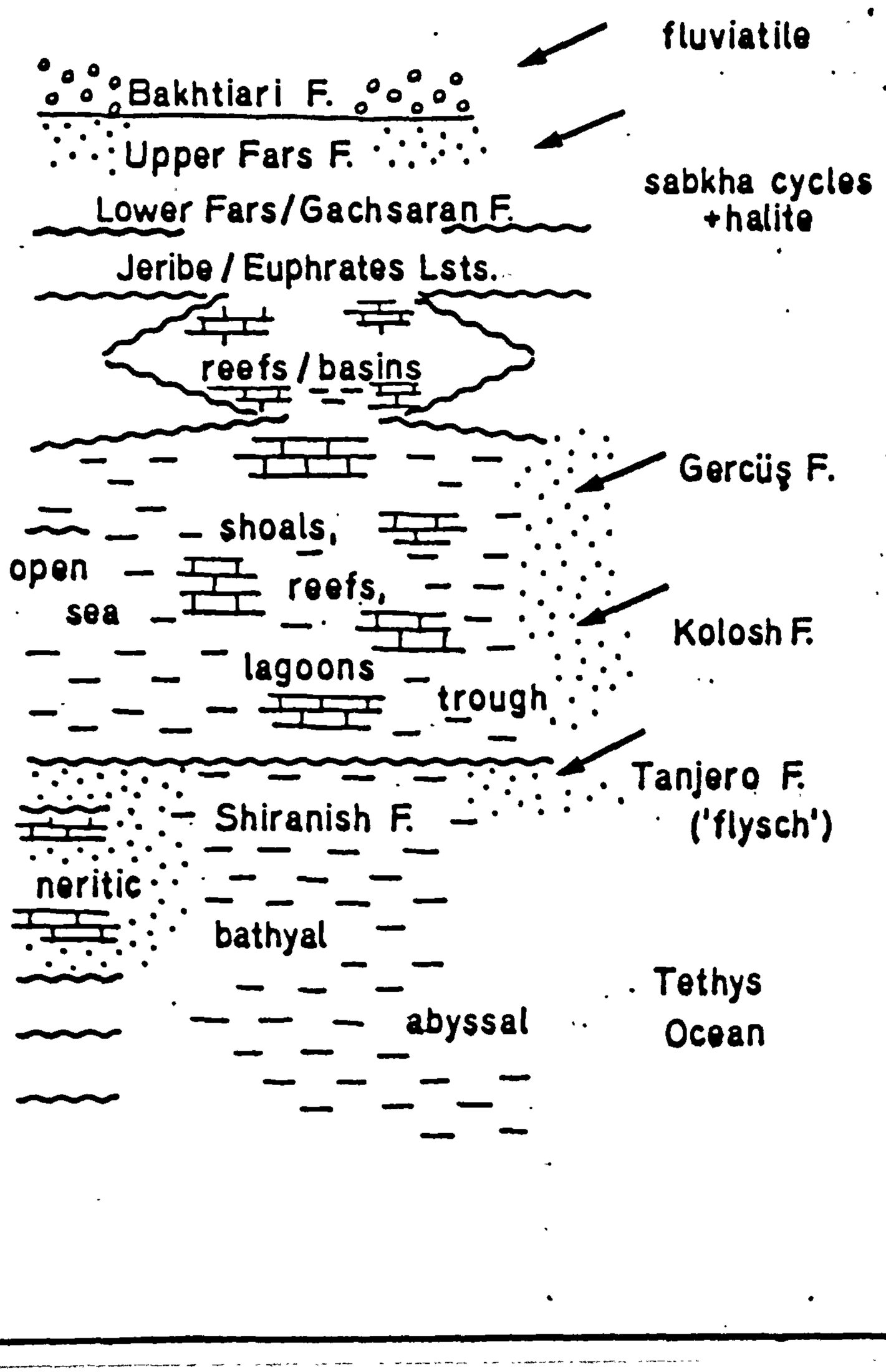	Zagros - Taurus orogeny through Afro - Arabia / Eurasia collision event. Sedimentation in Mesopotamian Basin, with detritus from N.E. and N. Rapid lateral and vertical facies changes, and non-sequences, reflecting dominantly vertical tectonic movements. Arabia - Iran - Turkey moving north as one plate. CLOSURE OF OCEAN, Zagros - Taurus ophiolite emplacement. OCEAN (TETHYS) separating Arabian plate from Iranian - Turkish plates. In Iraq sedimentation on N. and N.E. leading edge of Arabian plate in continental margin setting.

along the western side of the Arabian plate in the Levant area during the Middle Miocene (Gvirtzman and Buchbinder, 1978), and (iii) the uplift of the Oman Peninsula from the late Oligocene - early Miocene. These points, together with the clear high subsidence rates of the Mesopotamian Basin, show that vertical crustal movements were important during the Miocene and só may have been a factor in the repetition of Gachsaran cycles. The uplift of the Oman Peninsula is considered most significant since this could have produced an isolation of the Mesopotamian Basin from the Indian Ocean and permitted the precipitation of halite. Partial isolation of the basin at other times may have led to the development of restricted faunas within some limestones or claystones. On a more regional scale, the Miocene in the Alpine-Mediterranean area was a period of strong plate movements (Dewey et al., 1973; Bernoulli, 1978) which could well have affected sea-level in the Mesopotamian Basin, and thus contributed towards the cyclicity.

8.4 Climatic considerations

An arid climate clearly existed during the Miocene in the Middle East and permitted the precipitation of the gypsum-anhydrite, halite and polyhalite of the Gachsaran Formation. Climate, however, may have been instrumental in the development of the sabkha cycles by causing changes in the extent of the polar ice caps and thus causing eustatic changes of sea-level. The 'Great Ice Age' of the Pleistocene is a well-documented major glaciation, but it is now clear that the glaciation of the Antarctic began during the Miocene, and possibly in the Oligocene. There is much evidence from the Indian, Pacific and Southern Oceans for changes in the pattern of sedimentation during the Miocene, which can be related directly to the development of an ice cap on Antarctica (eg. Bandy, 1968; Jacobs, 1974). It is difficult to assess the importance of eustatic sea-level changes in the Gachsaran Formation. Detailed mapping is required to

identify limestones or mudrocks persistent over the whole basin which could thus have been formed through a eustatic sea-level rise.

8.5 Summary

A consideration of the lithofacies and sequences of the Gachsaran Formation shows that the cycles of mudrock-limestone-gypsum or mudrock-gypsum or limestone-gypsum, can be interpreted in terms of sabkha progradation. The type of cycle is controlled by the terrigenous clastic input into the basin; mudrock-gypsum cycles being more common toward basin margins and in the upper part of the formation. Several factors are likely to have been involved in the repetition of the cycles, but as yet it is difficult to assess the importance of each. Vertical tectonic movements were common during the Middle Miocene on and around the Arabian plate and active subsidence was taking place in the Mesopotamian Basin. Uplift of the Oman Peninsula may have led to a partial or complete isolation of the basin from the Indian Ocean. The Miocene was also a period of active plate movements in the Alpine-Mediterranean area. All these tectonic movements could have affected relative sea-level. Eustatic sea-level changes as a result of fluctuations in the ice cover of the Antarctic may also have been important.

APPENDIX I

PEEL TAKING AND STAINING OF CARBONATE ROCKS

Peel Taking

The procedure used is as follows:

1. The rock sample is first ground or cut to make an even surface. The surface of the sample is then polished with 400, 800 and finally 1000 fine grade carborundum powder.
2. The rock surface is then etched with 1.5% HCl for about 60 seconds, then washed with distilled water and left to dry.
3. The rock sample is then placed horizontally. A piece of plasticine or a tray of sand might help in this matter.
4. The sample surface is flooded with a minimum of ethyl acetate from a teat pipette. Before the ethyl acetate is allowed to dry, the peel sheet is placed on one edge of the sample and lowered gently so that the meniscus of fluid precedes the sheet, thus excluding bubbles that may form.
5. The peel is left to dry for 5 or 10 minutes and then removed in one smooth continuous motion.
6. The peel is then placed between two slides and the slides are firmly plastered to prevent crinkling.

The peel is now ready for study.

Staining

The staining technique described here is after Dickson (1965). This technique is used for both slides and peels. The solutions used for staining are Alizarin red S and Potassium ferricyanide mixed in the ratio of 3:2. After etching, the slides or rock samples are immersed in the solution for about one minute and then immersed in Alizarin red S to intensify the colour, washed and left to dry.

This staining procedure imparts the following colours:

Calcite - pink to red, depending on the orientation of the crystals

Ferroan calcite - mauve to royal blue depending on the percentage of iron present

Dolomite - remains colourless

Ferroan dolomite - pale to deep turquoise.

APPENDIX II

METHODS USED FOR BREAKING DOWN AND WASHING FORAMINIFERA SAMPLES

Each sample is put in a beaker with the number of the sample recorded on the beaker. Beakers are then filled with water and heated on a hot-plate. The softer samples need only 5 to 10 minutes of gentle heating. Only enough water should be added to prevent caking around the walls of the beaker. Harder samples (limestones) are very difficult to process. A simple mortar crusher is used first to crush the limestones into small fragments. These fragments are then boiled for several hours. They are then washed through filter paper and the residue is placed in an oven for several hours. The samples are then cooled quickly, sometimes using a refrigerator, then placed in the oven again. This process is repeated several times, and if still needed, boiled again.

The samples are then sieved through different sized meshes and stored in a number of jars, each of which bears the number of the sample and the size of the mesh it has been passed through. The samples are then ready for the picking process.

A more precise method for breaking down Foraminifera which requires special equipment and apparatus is given by Hulme (1961).

APPENDIX III

X-ray diffraction techniques

These techniques are used for:

1. The identification of clay minerals in mudstones and the determination of their relative percentages,
2. The identification of calcium and dolomite in carbonate rocks and the determination of their relative percentages. Also for measuring up the $MgCO_3$ content of calcite by measuring the shift in the position of the $d_{(104)}$ reflection.
3. The identification of gypsum and anhydrite in sulphate rocks and to check up their crystal ordering.

Techniques used for Qualitative Analysis

Techniques used here for the separation and mounting of the 2 μ fraction of clay minerals are after Gibbs (1965) and Zaim (1977). The preparation and mounting of the carbonate and sulphate samples are techniques used by the Department of Geology in the University of Newcastle upon Tyne.

Mudrock

1. About 50 - 100gm of the mudstone samples are crushed in an agate mortar into a fine powder.
2. The powdered samples are then placed in 1000m.l. beakers and filled with .3M acetic acid to dissolve any associated calcium carbonate.
3. The mixture is stirred periodically until reaction ceases; reaction may last for more than one day.
4. The impotent liquid is decanted and additional acid is added. The process is repeated until reaction ceases.

5. The acid is then decanted and distilled water is used to wash up the sample.
6. The samples are then treated with H_2O_2 in the manner described by Zaim (1977) to remove the associated organic matter.
7. The samples are then washed again and stirred in the same beaker. Settling is allowed to continue for two hours. After this period, only the fine fraction below 2 μ clay material remains in suspension.
8. Ten m.l. of the 2 μ clay saturated solution is then drained by means of an eye dropper and centrifuged onto a glass slide. The centrifuging is done by means of a super centrifuge at 18000 rpm.
9. The glass slide is then picked up and allowed to dry at room temperature ready for X-ray running. Glossy transparent smears give the best results.
10. The samples are then kept in a desiccator till they are run by Philips X-Ray Diffractometer using CuK_x radiation. The clay smears are run between 2 - $27^{o}2\emptyset$ at a speed of 1^{o}/minute.
11. The samples are checked after the first running and then glycolated. Heating in a muffle furnace at $550^{o}C$ for one hour follows glycolation. These different procedures were found necessary to detect different clay minerals present (see text).

<u>Carbonates and Sulphates</u>

1. The samples are crushed with a tungsten steel pestle and then ground in a creston ball mill.
2. A small part of the powder is is placed in an agate mortar with a small amount of powdered quartz as a standard, and hand-ground for a couple of minutes. A few drops of acetone are added and hand-grinding continued for a further few minutes.
3. Using an eye dropper, a few drops of the mixture are put on a

glass slide. The slide is then gently shaken to allow the material to spread evenly to obtain a smear with a uniform thickness.

4. The samples are then run using a Philips X-Ray Diffractometer with a CuK_x radiation. The strongest peak intensities for calcite, dolomite, gypsum and anhydrite are used after correcting with the standard.

Quantitative Analysis of Clay Minerals

Ratio of the (001) peak areas is used to estimate the amount of each clay mineral present within the Gachsaran mudrock. The most serious problem with this method, however, is the multi-component assemblages present within their basal reflections overlapping, and where to place the background base line. The placing of the base line was treated by Gjems (1967) "...this curve is approximately horizontal at the higher angles in the diagrams, but rises sharply at lower angles towards $0^{\circ}2\emptyset$". The simpler method used is that to measure (001) peak intensities. The results obtained from the two procedures were divided by two to minimise the percentage of error. Many factors affect the peak intensities of clay minerals and results obtained may at best be regarded as semi-quantitative (Mackenzie and Mitchell, 1966; Thorez, 1976).

The most important clay minerals found were illite, followed by montmorillonite, mixed layers and kaolinite (see Table 7-1 in text).

APPENDIX IV

METHODS OF CHEMICAL ANALYSIS

The selected samples were crushed and then chemically analysed by means of two methods:

1. Bernas (1968) Bomb technique.
2. Extraction with dilute acetic acid (or dilute hydrochloric acid).

Both methods are based on atomic absorption spectrophotometry and are the standard techniques followed in the chemical analysis laboratory at the Department of Geology in the University of Newcastle upon Tyne.

The elements determined were Ca, Mg, Na, K, Fe, Mn, Al, Si, Sr, Zn, pb, Cu and Rb.

1. Bernas Bomb Technique

Weigh 100mg of selected samples and transfer them to teflon bombs. Moisten them with 0.5ml. of aqua regia and add 5ml. hydrofluoric acid (AR, 40%). Swirl to break up sample aggregates, replace the lid and insert bombs into steel cases and screw on caps. Heat in oven at 110°C for about 2 hours. Remove and allow to cool, keeping the bombs upright throughout.

Leave to cool, remove the vessels from their cases and tranfer the contents to polystyrene vials containing 2g. boric acid. Wash the lids and the vessels with hot water, thoroughly scrub the interior of the vessels with a polystyrene rod. Do not exceed 70ml. total volume of solution and washings for each vial. Place the covers on the vials and (if necessary) warm gently until all the boric acid and the precipitated fluorites have dissolved. (Several hours may be needed for rocks containing much Mg.)

Cool the solutions, dilute to 200ml. in volumetric flasks and transfer immediately to plastic bottles. Insoluble carbonaceous matter should be filtered off during the transfer.

The appropriate dilutions are then prepared for each element.

A blank solution and a matching blank dilution are also made for the blank determination. One blank solution per batch is thought to be sufficient. One or two standard rocks should also be taken throughout the whole procedure.

2. Analysis of carbonate minerals in rocks by extraction with dilute acetic acid (or dilute hydrochloric acid).

Weigh .5g of selected samples and transfer to 250ml. or 125ml. conical beakers. Add to each 40ml. 3.0% (V/V) acetic acid (AR). For dolomites 20ml. 10% (V/V) hydrochloric acid was used as solvent.

Stand overnight and then dilute to 50ml. in volumetric flasks after addition of .5ml. perchloric acid (60% Aristar). Any significant residue may be separated by decantation or by using a dropper, washed, dried and weighed, to obtain a wt % insoluble residue.

The solutions may be used directly for determination of K, Na, Pb, Ni, Cr, Cu, Co, Ag, Li, Rb and Zn, using the normal composite standard solutions for all. For Fe, Mn, Mg at the 1% level, a x 25 dilution is required. For Sr at 200-2000ppm level, prepare x 2.5 dilution with La added (3000 ug/ml La), i.e. transfer 10ml. of main solutions to 25ml. volumetric flasks, add .75ml. La base solution (100mg/ml La) and dilute to the mark. Use Sr std. with 3000 ug/ml La added and determine Sr.

For CaO at a 50% level use a x 500 dilution prepared by pipetting 10ml. of the 25 dilution into 200ml. flasks, adding 6ml. La base solution and diluting to the mark. Use CaO standards prepared with added La (3ml. La base solution per 100ml. CaOstd.), a 10 ug/ml CaO standard is appropriate.

The batches of standards and of rock solutions are then passed through a Higler and Watts Atomspek Atomic Absorption Spectrophotometer. The absorbance is recorded on a chart and the peak heights read and

compared with an average of the two nearer standard peaks.

$$\text{Conc. of sample solution (mg/ml)} = \text{peak height (sample)} \times \frac{\text{standard value}}{\text{peak height of standard sol.}}$$

REFERENCES

AITKEN, J.D., 1967. Classification and environmental significance of cryptalgal limestones and dolomites, with illustrations from the Cambrian and Ordovician of south-western Alberta. J. Sediment. Petrol., 37, 1163-1178.

AL-ANSARI, N.A., 1973. Geology of the southern part of Jabal Makhul. M.Sc. Thesis, University of Baghdad (unpublished).

ALEXANDERSON, T., 1969. Recent littoral and sublittoral high-Mg calcite lithification in the Mediterranean. Sedimentology, 12, 47-61.

ALEXANDERSON, T., 1972. Micritization of carbonate particles: processes of precipitation and dissolution in shallow marine sediments. Geol. Inst. Univ. Uppsala, Bull. (N.S.3), 7, 201-236.

AL-HASHIMI, W.S., 1972. Sedimentological studies of the limestone members of the Middle Limestone Group in Northumberland. Ph.D. Thesis, University of Newcastle upon Tyne (unpublished), p.386.

AL-KHERSAN, H., and AL-SADDIKI, A., 1970. The Jeribe Limestone Formation. Iraq National Oil Co. (unpublished report), p.52.

AL-KHERSAN, H., and AL-SADDIKI, A., 1972. Microfacies of the Jeribe Limestone. Eighth Arab. Petrol. Cong. (Algiers), 97, p.22.

ALLEN, D.G., 1971. The origin of sheet fractures in the Galole Creek copper deposits, British Columbia. Can. J. Earth Sci., 8, 704-711.

AL-MUBARAK, M., 1973. The Geology of Fatha-Mosul area. National Iraqi Mineral Co. (unpublished report).

AL-NAQIB, K.M., 1967. Geology of the Arabian Peninsula, south-western Iraq. Geol. Survey Prof. Paper, 560-G. United States Dept. of the Interior.

AL-OMARI, F., and SADIK, A., 1973. Geological studies on Gebel Maqlub area, northern Iraq. Journ. Geol. Soc. Iraq., VI, 66-82.

AMERICAN COMMISSION ON STRATIGRAPHIC NOMENCLATURE, 1961. Code of stratigraphic nomenclature. Am. Assoc. Petroleum Geologists Bull., 45, 645-655.

AL-SAADONI, G., 1978. The sedimentology of the Lower Fars Formation. M.Sc. Thesis, University of Bristol (unpublished).

ARTHURTON, R.S., and HEMINGWAY, J.E., 1972. The St. Bees Evaporites: a carbonate evaporite formation of Upper Permian age in West Cumberland, England. Proc. of the Yorkshire Geol. Soc., 38, 565-592.

AWRAMIK, S.M., 1971. Precambrian columnar stromatolite diversity: reflection of Metazoan appearance. Science, 174, 825-827.

BADIOZAMANI, K., 1973. Dorag dolomitization model, Ordovician, Wisconsin. J. Sediment. Petrol., 43, 965-984.

BAKER, N.E., and HENSON, F.R.S., 1952. Geological conditions of oil occurrence in Middle East Fields. Am. Assoc. Petroleum Geologists Bull., 36, 1885-1901.

BAKER, E.T., 1973. Distribution and composition of suspended sediment in the bottom waters of the Washington continental shelf and slope. J. Sediment. Petrol., 43, 812-821.

BANDY, O.L., 1956. Ecology of Foraminifera in north-eastern Gulf of Mexico. (ibid.) Prof. Paper, 274-G.

BANDY, O.L., and ARNAL, R.E., 1957. Distribution of Recent Foraminifera off West Coast of Central America. Am. Assoc. Petroleum Geologists Bull., 41, 2037-2053.

BANDY, O.L., and ARNAL, R.E., 1960. Concepts of Foraminiferal palaeoecology. Am. Assoc. Petroleum Geologists Bull., 44, 1921-1932.

BANDY, O.L., 1968. Cycles in Neogene palaeoceanography and eustatic changes. Palaeogeography, Palaeoclimatol., Palaeoecol., 5, 63-75.

BARBER, C., 1974. Major and trace element association in limestones and dolomites. Chem. Geol., 14, 273-280.

BATHURST, R.G.C., 1958. Diagenetic fabrics in some British Dinantian limestones. Liverpool-Manchester J. Geol., 2, 11-36.

BATHURST, R.G.C., 1966. Boring algae, micrite envelopes and lithification of molluscan biosparites. J. Geol., 5, 15-32.

BATHURST, R.G.C., 1969. Bimini Lagoon. In: H.G.Multer (ed.), Field Guide to some Carbonate Rock Environments: Florida Keys and Western Bahamas. Fairleigh Dickson University, Madison, N.J., 62-66.

BATHURST, R.G.C., 1975. Carbonate sediments and their diagenesis. Developments in Sedimentology 12, Amsterdam, Elsevier, p.658.

BAUSCH, W.M., 1968. Clay content and calcite crystal size of limestones. Sedimentology, 10, 71-75.

BEALES, F.W., 1953. Dolomitic mottling in Pallisser (Devonian) limestone, Banff and Jaspar National Parks, Alberta. Am. Assoc. Petroleum Geologists Bull., 37, 2281-2293.

BEALES, F.W., 1965. Diagenesis in pelleted limestones. In: L.C. Pray and R.C. Murray (eds.), Dolomitization and Limestone Diagenesis: a Symposium. Soc. Econ. Palaeontologists Mineralogists Spec. Publ., 13, 49-70.

BEAVER, P., 1966. Clay minerals and geomorphology in four Carribbean Islands. Clay Miner. Bull., 6, 371.

BELLEN, R.G. Van, DUNNINGTON, H.V., WETZEL, R., and MORTON, D.M., 1959. Lexique stratigraphique Internationale; Dubertret, L., ed., Asie, Fasc., 10a, Iraq. p.333.

BENCINI, A., and TURI, A., 1974. Mn distribution in the Mesozoic carbonate rocks from Lima Valley, Northern Apennines. J. Sediment. Petrol., 44, 774-782.

BERRY, L.G., and MASON, B., 1959. Mineralogy. W.H. Freeman and Company, San Francisco, p.612.

BERNAS, B., 1968. A new method for decomposition and comprehensive analysis of silicates by atomic absorption spectrometry. Anal. Chem., 40, 16-82.

BILLINGS, G.K., and RAGLAND, P.C., 1968. Geochemistry and mineralogy of the Recent reef and lagoonal sediments south of Belize (British Honduras). Chem. Geol., 3, 135-153.

BISCAYE, P.E., 1965. Mineralogy and sedimentation of Recent deep sea clay in the Atlantic Ocean and adjacent seas and oceans. Geol. Soc. Am. Bull., 76, 803-831.

BLACK, M., 1933. The algal sediments of Andros Island, Bahamas. Royal Soc. London Philos. Trans. Ser. B., 222, 165-192.

BOSELLINI, A., and HARDIE, L.A., 1973. Depositional theme of a marginal marine evaporite. Sedimentology, 20, 5-27.

BRAUNAGEL, L.H., and STANLEY, K.O., 1977. Origin of variegated red beds in the Cathedral Bluss Tongue of the Wasatch Formation (Eocene), Wyoming. J. Sediment. Petrol., 47, 1201-1219.

BROMELY, R.G., 1970a. Borings as trace fossils and Entobia Outacea Portlock, as an example. In: Crimes, T.P. and Harper, J.C. (eds.), Trace fossils. Geol. Spec. Issue, 3, 49-90.

BROWN, L.S., 1931. Cap-rock petrography. J. Sediment. Petrol., 15, 509-529.

BROWN, P.R., 1964. Petrography and origin of some Upper Jurassic beds from Dorset, England. J. Sediment. Petrol., 34, 254-269.

BUCHER, W.H., 1918. On oolites and spherulites. J. Geol., 26, 593-609.

BUNDY, W.M., 1956. Petrology of gypsum-anhydrite deposits in south-western Indiana. J. Sediment. Petrol., 26, 240-252.

BURGESS, I.C., and HOLLIDAY, M.A., 1974. The Permo-Triassic rocks of the Hilton Borehole, Westmorland. Bull. Geol. Survey of Great Britain, 46, 11-34.

BUSK, H.G., and MAYO, H.T., 1918. Some notes on the Geology of the Persian Oil Fields. Jour. Inst. Petr. Techn., 5, 3-26.

BUTLER, G.P., 1965. Early diagenesis in the Recent sediments of the Trucial Coast of the Persian Gulf. M.Sc. Thesis, University of London (unpublished), p.251.

BUTLER, G.P., 1970. Holocene gypsum and anhydrite of the Abu Dhabi Sabkha, Trucial Coast: an alternative explanation of origin. In: Rau, J.L. and Dellwig, L.F. (eds.), Third Symposium on Salt, Northern Ohio Geol. Soc., 120-152.

CARROLL, D., and STARKEY, H.C., 1959. Leaching of clay minerals in limestone environments. Geochim. Cosmochim. Acta., 16, 83-87.

CAYEUX, L., 1935. Les Roches Sedimentaires de France. Roches Carbonatees. Masson, Paris, 463.

CLOUD, Jr., P.E., and BARNES, V.E., 1948. The Ellenburger group of central Texas. Texas Univ. Bur. Econ. geol., Pub.4621, p.437.

CLOUD, Jr., P.E., 1962. Environment of calcium carbonate deposition west of Andros Island, Bahamas. U.S. geol. Profess. Papers, 350, 1-138.

CONYBEARE, C.E.B., and CROOK, K.A.W., 1968. Manual of sedimentary structures, Dept of National environment, Bureau of mineral resources, Geology and Geophysics Bull., 12.

CTYROKY, P.A., KARIM, S., and VESSEM, E.J. Van., 1975. Miogypsina and Borelis in the Euphrates Limestone Formation in the Western Desert of Iraq. In: N. Jb. Geol. Palaont. Abh., 148, i, 33-49.

CUFF, 1969. Lattice disorder in anhydrite. Proc. Geol. Soc. Lond.

CURTIS, R., EVANS, G., KINSMAN, D.J.J., and SHEARMAN, D.J., 1963. Association of dolomite and anhydrite in the Recent sediments of the Persian Gulf. Nature, 197, 679-680.

DAVIES, G.R., 1970. Algal-laminated sediments, Gladstone Embayment, Shark Bay, Western Australia. Am. Assoc. Petroleum Geologists, Mem., 13, 169-205.

DAVIES, P.J., BUBELA, B., and FERGUSON, J., 1978. The formation of ooids. Sedimentology, 25, 703-730.

DEAN, W.E., DAVIES, G.R., and ANDERSON, R.Y., 1975. Sedimentological significance of nodular and laminated anhydrite. Geology, 3/7, 367-372.

DEER, W.A., HOWIE, R.A., and ZUSSMAN, J., 1962. Gypsum. In rock forming minerals, 5, 202-218.

DEFFEYES, K.S., LUCIA, F.J., and WEYL, P.K., 1965. Dolomitization of Recent and Plio-Pleistocene sediments by marine evaporite waters on Bonaire, Netherlands Antilles. In: L.C. Pray and R.C. Murray (eds.), Dolomitization and limestone diagenesis: a Symposium. Soc. Econ. Palaeontologists, Mineralogists, Spec. Pub., 13, 71-88.

DE GROOT, K., 1969. The chemistry of submarine cement formation at Dohat Hussain in the Persian Gulf. Sedimentology, 12, 63-68.

DEWEY, J.F., PITMAN, W.C.III, RYAN, W.B.F., and BONNIN, J., 1973. Plate tectonics and the evolution of the Alpine system. Geol. Soc. Am. Bull., 84, 3137-3180.

DICKINSON, W.R., 1974. Plate tectonics and sedimentation. In: Dickinson, W.R. (ed.), Tectonics and Sedimentation, Spec. Publ., Soc. econ. Paleont. Miner., Tulsa, 22, 1-27.

DICKSON, J.A.D., and BARBER, C., 1976. Petrography, chemistry and origin of early diagenetic concretions in the Lower Carboniferous of the Isle of Man. Sedimentology, 23, 189-211.

DODD, J.R., 1967. Magnesium and strontium in calcareous skeletons: A review. J. Palaeontology, 41, 1313-1329.

DONAHUE, J.D., 1965. Laboratory growth of pisolite grains. J. Sediment. Petrol., 35, 251-256.

DUFF, P.M.D., HALLAM, A., and WALTON, E.K., 1967. Cyclic Sedimentation. Developments in Sedimentology, Amsterdam (Elsevier), p.280.

DUNHAM, R.J., 1962. Classification of carbonate rocks according to depositional texture. In: W.E. Ham (ed.), Classification of Carbonate Rocks. Am. Assoc. Petroleum Geologists Bull., Tulsa, Okla., 108-121.

DUNHAM, R.J., 1969. Early Vadose silt in Townsend Mound (reef), New Mexico. In: G.M. Friedman (ed.), Depositional Environments in Carbonate Rocks: a symposium. Soc. Econ. Palaeontologists, Mineralogists, Spec. Pub., 14, 139-181.

DUNNINGTON, H.V., 1958. Generation migration, accumulation, and dissipation of oil in Northern Iraq. In: Weeks, L.G. (ed.), Habitat of Oil. Am. Assoc. Petroleum Geologists, 1194-1251.

DUNNINGTON, H.V., 1968. Salt-tectonic features of Northern Iraq. Geol. Soc. Am. Spec. Paper, 88, 184-227.

EARDLEY, A.J., 1938. Sediments of Great Salt Lake, Utah. Am. Assoc. Petroleum Geologists Bull., 22, 1305-1411.

EL WAKEEL, S.K., and RILEY, J., 1961. Chemical and mineralogical studies of deep sea sediments. Geochim. Cosmochim. Acta, 25, 110-146.

EMERY, K.O., TRACEY, J.I., and LADD, H.S., 1954. Geology of Bikini and nearby atolls. U.S. Geol. Surv., Profess. Papers, 260 A, 1-265.

EVAMY, B.D., and SHEARMAN, D.J., 1965. The development of overgrowths from echinoderm fragments. Sedimentology, 5, 211-233.

EVAMY, B.D., and SHEARMAN, D.J., 1969. Early stages in development of overgrowths on echinoderm fragments in limestones. Sedimentology, 12, 317-322.

EVANS, G., MURRAY, J.W., BIGGS, H.E.J., BATE, R., and BUSH, P.R., 1973. The oceanography, ecology, sedimentology and geomorphology of parts of the Trucial Coast Barrier Island complex, Persian Gulf. In: B.H. Purser (ed.), The Persian Gulf, Springer-Verlag, Berlin. Heidelberg. New York.

FARROW, G.E., 1971. Back-reef and lagoonal environments of Aldabra Atoll, distinguished by their crustacean burrows. In: Stoddart, D.R. and Yonge, C.M. (eds.), Regional variations in Indian Ocean coral reefs. Zool. Soc. London, Symp., 28, 455-500.

FOLK, R.L., 1959. Practical petrographic classification of limestones. Am. Assoc. Petroleum Geologists Bull., 43, 1-38.

FOLK, R.L., 1962. Spectral subdivision of limestone types. In: W.E. Ham (ed.), Classification of carbonate Rocks. Am. Assoc. Petroleum Geologists Bull., Tulsa, Okla., 62-84.

FOLK, R.L., 1965. Some aspects of recrystallization in ancient limestones. In: L.C. Pray and R.C. Murray (eds.), Dolomitization and Limestone Diagenesis: a Symposium. Soc. Econ. Palaeontologists, Mineralogists, Spec. Publ., 13, 14-48.

FOLK, R.L., and LAND, L.S., 1975. Mg/Ca ratio and salinity: two controls over crystallization of dolomite. Am. Assoc. Petroleum Geologists Bull., 59, 60-68.

FORBES, B.G., 1958. Folded Permian gypsum of Ripon Parks, Yorkshire. Geol. Soc. Yorkshire Proc., 31, 351-358.

FOSTER, R.J., 1972. The solid geology of northeast Caithness. Ph.D. Thesis, University of Newcastle upon Tyne, p.334.

FREEMAN, T., 1962. Quiet water oolites from Laguna Madre, Texas. J. Sediment. Petrol., 32, 475-483.

FRIEDMAN, G.M., and SANDERS, J.E., 1967. Origin and occurrence of dolostones. In: G.V. Chilingar, H.J. Bissell and R.W. Fairbridge (eds.), Carbonate Rocks: origin, occurrence and classification. Elsevier, Amsterdam, 267-348.

FRIEDMAN, G.M., 1968b. The fabric of carbonate cement and matrix and its dependence on the salinity of water. In: G. Muller and G.M. Friedman (eds.), Recent Developments in carbonate Sedimentology in Central Europe. Springer, Berlin, 11-20.

FRIEDMAN, G.M., and KOLESAR, P.T., 1971. Fresh water carbonate cements. In: O.P. Bricker (ed.), Carbonate Cements, 122-123.

FRITZ, P., and KATZ, A., 1972. The sodium distribution of dolomite crystals. Chem. Geology, 72, 170-194.

FREY, R.W., 1970. Trace fossils of Fort Hays Limestone Member of Niobrara Chalk (Upper Cretaceous), west-central Kansas. Univ. Kansas Paleont. Contr., Art.53, p.41

FREY, R.W., 1975. The realm of ichnology, its strengths and limitations. In: Frey, R.W. (ed.), The Study of Trace Fossils, 13-38, Berlin. Heidelberg. New York (Springer).

FUCHTBAUER, H., 1974. Sediments and sedimentary rocks. Sedimentary Petrology, part 2. E. Schweizerbart'she Verlagsbuchhandlung (Nagele u. Ober-miller) Stuttgart, H64p.

GARRET, P., 1970. Phanerozoic stromatolites: non-competitive ecologic restriction by grazing and burrowing animals. Science, 169, 171-173.

GAURTNER, H.R.Von., 1932. Petrographie und Palaogeographische stellung der Gipse vom Sudrande des Harzes. Preuss. Geol. Landesanst. Jahrb., 53, 655-694.

GAVISH, E., and FRIEDMAN, G.M., 1969. Progressive diagenesis in Quarternary to late Tertiary carbonate sediments: sequence and time scale. J. Sediment. Petrol., 39, 980-1006.

GEBELEIN, C.D., 1974. Biologic control of stromatolite microstructure: implications for Precambrian time stratigraphy. Am. J. Sci., 274, 575-598.

GIBBS, R.J., 1965. Error due to segregation in quantitative clay mineral X-ray diffraction mounting technique. Am. Min., 50, 741-751.

GILL, W.D., and ALA, M.A., 1972. Sedimentology of Gachsaran Formation (Lower Fars Series), southwest Iran. Am. Assoc. Petroleum Geologists Bull., 1965-1974.

GINSBURG, R.N., 1957. Early diagenesis and lithification of shallow water carbonate sediments in south Florida. In: R.J. Leblanc and J.G. Breeding (eds.), Regional Aspects of Carbonate Deposition. Soc. Econ. Palaeontologists, Mineralogists, Spec. Publ., 5, 80-99.

GINSBURG, R.N., 1960. Ancient analogues of recent stromatolites: Internat. Geol. Cong., 21st. Repts. Pt.22, 26-35.

GINSBURG, R.N., SHINN, A.E., and SCHROEDER, J.H., 1967. Submarine cementation and internal sedimentation within Bermuda reefs (abs.). Geol. Soc. Am., Progr. Ann. Meeting, 78-79.

GIRDLER, R.W., and STYLES, P., 1978. Seafloor spreading in the western Gulf of Aden. Nature, 271, 615-617.

GJEMS, O., 1967. Studies on clay minerals and clay mineral formation in sail profiles in Scandinavia. Medd. Norske Skogf., 81, 302-415.

GOLDMAN, M.I., 1952. Deformation, metamorphism, and mineralization in gypsum-anhydrite cap-rock, Sulphur Salt Dome, Louisiana. Geol. Soc. America Mem., 50, p.169.

GOLDRING, R., 1964. Trace fossils and the sedimentary surface in shallow water marine sediments. In: Van Straaten, L.M.G.U. (ed.), Deltaic and shallow marine deposits. Developments in Sedimentology, 1, 136-143.

GOLDSMITH, J.R., and GRAF, D.L., 1958. Structural and compositional variations in some natural dolomites. J. Geol., 66, 678-693.

GRABAU, A.W., 1904. On the classification of sedimentary rocks. Am. Geologist., 33, 228-247.

GRAF, D.L., and GOLDSMITH, J.R., 1956. Some hydrothermal synthesis of dolomite and protodolomite. J. Geol., 64, 173-186.

GVIRTZMAN, G., and BUCHBINDER, B., 1978. The Late Tertiary of the Coastal Plain and Continental Shelf of the Levant region and its bearing on the history of the Eastern Mediterranean. In: Initial Reports, Deep Sea Drilling Project, 42, 1195-1222.

HADDING, A., 1958. Origin of the lithographic limestones: Publications from Institutes of Mineralogy, Palaeontology and Quarternary Geology, University of Lund, Sweden. No.41 (Kungl. Fysiografiska Sallskapets & Lund Forhaudlingar Bd.28,Nr.4).

HAM., W.E., 1962. Economic geology and petrology of gypsum and anhydrite in Blaine County. Oklahoma Survey Bull., 89, 100-151.

HARDIE, L.A., 1967. The gypsum-anhydrite equilibrium at one atmosphere pressure. Am. Mineralogist, 52, 171-200.

HASSAN, F., and EL-DASHLOUTY, S., 1970. Miocene Evaporites of the Gulf of Suez region and their significance. Am. Assoc. Petroleum Geologists, 54, 1686-1695.

HAYNES, S.J., and MACQUILLAN, H., 1974. Evolution of the Zagros Suture Zone, Southern Iran. Geol. Soc. Am. Bull., 85, 739-744.

HEDBERG, H.D., (ed.), 1976. International Stratigraphic Guide. pp.xvii + 1-200. Wiley.

HENSON, F.R.S., 1951. Observations on the geology and petroleum occurrences of the Middle East. 3rd World Petroleum Cong. (The Hague). Proc. Sec.1, 118-140.

HEYBROEK, F., 1965. The Red Sea Miocene Evaporite Basin. In: Salt basins around Africa, London Inst. Petroleum, 17-40.

HOLLAND, C.H., et al., 1978. A guide to stratigraphical procedure. Geol. Soc. Lond. Spec. Rep., 10, 1-18.

HOLLIDAY, D.W., 1966. Nodular gypsum and anhydrite rocks in the Billefjorden region, Spitsbergen. Arbok norsk. Polarinst., 65-73.

HOLLIDAY, D.W., 1967. Secondary gypsum in Middle Carboniferous rocks of Spitsbergen. Geol. Mag., 104, 171-177.

HOLLIDAY, D.W., 1968. Early diagenesis in Middle Carboniferous nodular anhydrite of Spitsbergen. Geol. Soc. Yorkshire Proc., 36, 277-292.

HOLLIDAY, D.W., 1970. The petrology of secondary gypsum rocks: a review. J. Sediment. Petrol., 40, 2, 734-744.

HOLLIDAY, D.W., 1971. Origin of Lower Eocene gypsum-anhydrite rocks, southeast St. Andrew, Jamaica. Trans. Inst. Min. Metall. (Sect.B: Appl. Earth Sci.), 80, B305-315.

HOLLIDAY, D.W., 1973. Early diagenesis in nodular anhydrite rocks. Trans. Inst. Min. Metall., B82; B81-84.

HOLLIDAY, D.W., 1970. The petrology of secondary gypsum rocks: a review. J. Sediment. Petrol., 40, 734-744.

HOFFMAN, P., 1976. Stromatolite morphogenesis in Shark Bay, Western Australia. In: Walter, M.R. (ed.), Stromatolites, 261-272, Amsterdam (Elsevier).

HOFMANN, H.J., 1969. Attributed of stromatolites. Geol Surv. Canada, 39, 1-45.

HSU, K.J., MOTADERT, L., BERNOULLI, D., CITA, M.B., ERIKSON, A., GARRISON, R.E., KIDD, R.B., MELIERES, F., MULLER, C., and WRIGHT, R., 1978. History of the Mediterranean salinity crisis. In: Initial Reports of the Deep Sea Drilling Project, National Science Foundation, V.XLII, p.1.

HUBERT, J.F., and REED, A.A., 1978. Red Bed diagenesis in the East Berlin Formation, Newark Group, Connecticut Valley. J. Sediment. Petrol., 48, 175-184.

HUDSON, J.D., 1970. Algal limestones with pseudomorphs after gypsum from the Middle Jurassic of Scotland. Iethaia, 3, 11-40.

HULME, S.G., 1961. A mechanized method of breaking down and washing Foraminiferal rock samples. Micropaleontology, 7, 107-113.

ILHAN, E., 1967. Toros-Zagros folding and its relation to Middle East Oil fields. Am. Assoc. Petroleum Geologists Bul.., 51, 5, 651-667.

ILLING, L.V., 1954. Bahaman calcareous sands. Am. Assoc. Petroleum Geologists Bull., 38, 1-95.

ILLING, L.V., WELLS, A.J., and TAYLOR, J.C.M., 1965. Penecontemporary dolomite in the Persian Gulf. In: L.C. Pray and R.C. Murray (eds.), Dolomitization and limestone diagenesis: a symposium. Soc. Econ. Palaeontologists Mineralogists, Spec. Publ., 13, 89-111.

INTERNATIONAL SUBCOMMISSION ON STRATIGRAPHIC CLASSIFICATION, Report No.76: Terminology and Usage, 297-323. (1972).

JACOBS, M.B., 1974. Clay mineral changes in Antarctic deep-sea sediments and Cenozoic climatic events. J. Sediment. Petrol., 44, 1079-1086.

JAMES, G.A., and WYND, J.D., 1965. Stratigraphic nomenclature of Iranian oil consortium agreement area. Am. Assoc. Petroleum Geologists Bull., 49, 2182-2245.

JOHNSON, J.H., 1951. An introduction to the study of rock building algae and algal limestones. Colo. School Mines. Quart., 46,

JONES, D.J., and HUDSON, J.M., 1949. Notes on field work on the Lower Fars stratigraphy. Unpublished report G.R. 87, National Iraqi Oil Company.

KAHLE, C.F., 1965b. Strontium in oolitic limestones. J. Sediment. Petrol., 35, 846-856.

KENDALL, G.G.St.C., and SKIPWITH, Sir P.A. d'E Bt., 1968. Recent algal mats of a Persian Gulf lagoon. J. Sediment. Petrol., 38, 1040-1058.

KERR, S.D., and THOMSON, A., 1963. Origin of nodular and bedded anhydrite in Permian shelf sediments, Texas and New Mexico. Am. Assoc. Petroleum Geologists Bull., 47, 1726-1732.

KING, R.H., 1947. Sedimentation in Permian Castile sea, Am. Ass. Petroleum Geologists Bull., 31, 470-477.

KINSMAN, D.J.J., 1964. The Recent carbonate sediments near Halat el Bahrani, Trucial Coast, Persian Gulf. In: L.M.J.U. Van Straaten (ed.), Deltaic and Shallow Marine Deposits. Elesevier, Amsterdam, 185-192.

KINSMAN, D.J.J., 1964b. Recent carbonate sedimentation near Abu Dhabi, Trucial Coast, Persian Gulf. Thesis, Imp. Coll. Sci. Technol.,

KINSMAN, D.J.J., 1965. Dolomitization and evaporite development, including anhydrite, in lagoonal sediments, Persian Gulf. Geol. Soc. Am., Spec. Papers, 82, 108-109. (Abstract).

KINSMAN, D.J.J., 1966. Gypsum and anhydrite of Recent age, Trucial Coast, Persian Gulf. In: Second Symposium on Salt, Northern Ohio Geol. Soc., 1, 302-306.

KINSMAN, D.J.J., 1969. Modes of formation, sedimentary association and diagnostic features of shallow water and supratidal evaporites. Am. Assoc. Petroleum Geologists Bull., 53, 830-840.

KINSMAN, D.J.J., 1971. Diagenetic history of limestone determined from Sr^{+2} distribution. In: Carbonate cements, ed. Bricker, O.P. Johns Hopkins Press, p.376.

KINSMAN, D.J.J., 1969. Interpretation of Sr^{+2} concentrations in carbonate minerals and rocks. J. Sediment. Petrol., 39, 486-508.

KINSMAN, D.J.J., and PARK, R.K., 1976. Algal belt and coastal sabkha evolution, Trucial Coast, Persian Gulf. In: Walter M.R. (ed.), Stromatolites. Amsterdam (Elsevier), 421-434.

KODAMAH, H., SHIMODA, S., and SUDO, T., 1969. Hydrous mica complexes: their structure and chemical composition. Proc. Intern. Clay Conf., Tokyo, V.1, 185-196.

KRAUSKOPF, K.B., 1955. Sedimentary deposits of rare metals. Econ. Geol., 50th Anniv. 1905-1955, 411-463.

KRAUSKOPF, K.B., 1967. Introduction to geochemistry. New York, McGraw-Hill Book Co., p.721.

KRUMBEIN, W.C., and SLOSS, L.L., 1951. Stratigraphy and sedimentation, San Francisco, W.H. Freeman and Co., p.497.

KULP, J.L., TUREKIAN, K.K., and BOYD, D.W., 1952. Sr contents of limestones and fossils. Geol. Soc. Am. Bull., 63, 701-716.

LAND, L.S., 1967. Diagenesis of skeletal carbonates. J. Sediment. Petrol., V.37, 914-930.

LAND, L.S., 1971. Phreatic versus meteoric diagenesis of limestones: evidence from a fossil water table in Bermuda. In: O.P. Bricker (ed.), Carbonate Cements. 133-136.

LAND, L.S., and HOOPS, G.K., 1973. Sodium in carbonate sediments and rocks: a possible index to the salinity of diagenetic solutions. J. Sediment. Petrol., 43, 614-617.

LAND, L.S., SALEM, M.R.I., and MORROW, D.W., 1975. Paleohydrology of ancient dolomites: geochemical evidence. Am. Assoc. Petroleum Geologists Bull., 59, 1602-1625.

LEEDER, M.R., and ZEIDAN, R., 1977. Giant Late Jurassic sabkhas of Arabian Tethys. Nature, 268, 42-44.

LEES, G.M., 1938. Geology of the oil field belt of Iran and Iraq. Science of Petrol., 1, 140-148.

LŒBLICH, A.R., Jr., and TAPPAN, H., 1964. Sarcodina, chiefly 'the carnoebians' and Foraminiferida. In: Moore, R.C. (ed.), Treatise on invertebrate paleontology. Geol. Soc. Am. New York, pt.C, vols.1-2, p.900.

LOGAN, B.W., 1961. Cryptozoon and associated stromatolites of Shark Bay, Western Australia. J. Geol., 69, 517-533.

LOGAN, B.W., REZAK, R., and GINSBURG, R.N., 1964. Classification and environmental significance of algal stromatolites. J. Geol., 72, 68-83.

LOGAN, B.W., HOFFMAN, P., and GEBELEIN, C.D., 1974. Algal mats, cryptalgalfabrics and structures, Hamelin Pool, Western Australia. Am. Assoc. Petroleum Geologists Mem., 22, 140-194.

LOREAU, J.P., and PURSER, B.H., 1973. Distribution and ultrastructure of Holoune ooids in the Persian Gulf. In: B.H. Purser (ed.) The Persian Gulf, Springer-Verlag, Berlin, Heidelberg, New York, 279-328.

LOWENSTAM, H.A., and EPSTEIN, S., 1957. On the origin of sedimentary aragonite needles of the Great Bahama Banks. J. Geol., 65, 364-375.

LOWENSTAM, H.A., 1954. Factors affecting the aragonite: calcite ratios in carbonate-secreting marine organisms. J. Geol., 62, 284-321.

LUCIA, F.J., 1968. Recent sediments and diagenesis of south Bonaire, Netherlands, Antilles. J. Sediment. Petrol., 38, 845-858.

MACDONALD, G.J.F., 1953. Anhydrite-gypsum equilibrium relations. Am. Jour. Science, 251, 884-898.

MACKENZIE, R.C., and MITCHELL, B.D., 1966. Clay mineralogy. Earth Science Rev., 2, 47-91.

MAIKIEM, W.R., and BEBOUT, D.G., and GLAISTER, R.P., 1969. Classification of anhydrite: a practical approach. Bulletin of Canadian Petroleum Geology, 17, 2, 194-233.

MARSHALL, J.F., and DAVIES, P.J., 1975. High magnesium calcite ooids from the Great Barrier Reef. J. Sediment. Petrol., 45, 285-291.

MARSCHNER, H., 1968. Relationship between carbonate grain size and non-carbonate content in carbonate sedimentary rocks. In: G. Muller and G.M. Friedman (eds.), Carbonate Sedimentology in Central Europe. Springer-Verlag, Berlin.

MARSCHNER, H., 1969. Hydrocalcite ($CaCO_3.H_2O$) and nesquehonite ($MgCO_3.3H_2O$) in carbonate scales. Science, 165, 1119-1121.

MASSON, P.H., 1955. An occurrence of gypsum in southwest Texas. J. Sediment. Petrol., 25, 172-177.

MATTER, A., 1967. Tidal flat deposits in the Ordovician of Western Maryland. J. Sediment. Petrol., 37.

MATTHEWS, R.K., 1966. Genesis of Recent lime mud in southern British Honduras. J. Sediment. Petrol., 36, 428-454.

McWHAE, J.R.H., 1953. The Carboniferous Breccias of Billefjirden, Vest-Pitsbergen. Geol. Mag., 95, 287-298.

METWALLI, M.H., PHILIP, G., and MOUSSLY, M.M., 1974. Petroleum-bearing formations in north-eastern Syria and northern Iraq. Am. Assoc. Petroleum Geologists Bull., 58, 1781-1796.

MILLIMAN, J.D., 1966. Submarine lithification of carbonate sediments. Science, 153, 994-997.

MILLIMAN, J.D., 1974. Marine Carbonates. Recent sedimentary carbonates (part 1). Springer, Berlin, p.375.

MILLIMAN, J.B., and BARRETTO, H.T., 1975. Relict magnesian calcite oolite and subsidence of the Amazon Shelf. Sedimentology, 22, 137-145.

MILLOT, G., 1970. Geology of clays. Springer-Verlag, N.Y., p.429.

MITCHELL, A.H.G., and READING, H.G., 1978. Sedimentation and Tectonics. In: Reading, H.G. (ed.), Sedimentary Environments and Facies, 439-476.

MONTY, C.L.V., 1967. Distribution and structure of recent stromatolitic algal mats, Eastern Andros Island, Bahamas. Ann. Soc. Geol. Belg., 90, 55-99.

MONTY, C.L.V., 1972. Recent algal stromatolitic deposits, Andros Island, Bahamas. Preliminary Report. Geol. Rundschau, 61, 742-783.

MONTY, C.L.V., 1976. The origin and development of cryptalgal fabrics. In: Walter, M.R. (ed.), Stromatolites, Amsterdam (Elsevier), 193-250.

MONTY, C.L.V., 1965. Recent algal stromatolites in the Windward Lagoon, Andros Island, Bahamas. Ann. Soc. Geol. Belg., 88, 269-276.

MOSSOP, G.D., and SHEARMAN, D.J., 1973. Origins of secondary gypsum rocks. Inst. Mining, Metal., 1-8.

MURRAY, R.C., 1964. Origin and diagenesis of gypsum and anhydrite. J. Sediment. Petrol., 34, 512-523.

MURRAY, J.W., 1973. Distribution and ecology of living Benthic Foraminiferids.

McBRIDE, E.F., 1974. Significance of colour in red, green purple, olive brown, and grey beds of Difunta Group, north-eastern Mexico. J. Sediment. Petrol., 44, 760-773.

McKEE, E.D., and GUSTSCHICK, R.C., 1969. History of Redwall limestone of northern Arizona. Geol. Soc. Am., Mem., 114, 1-726.

NEUMAN, A.C. and LAND, L.S., 1975. Lime-mud deposition and calcareous algae in the Bight of Abaco, Bahamas: a budget. J. Sediment. Petrol., 45, 763-786.

NEWELL, N.D., PURDY, E.G., and IMBRIE, J., 1960. Bahamian oolitic sand. J. Geol., 68, 481-497.

O'BRIEN, C.A.E., 1950. Tectonic problems of the oil field belt of south-west Iran. Report 18th Int. Geol. Cong., 1948. Proceedings Section E, 45-58.

O'BRIEN, C.A.E., 1957. Salt diapirism in south Persia. Geol. Mijnbouw, 19, 357-376.

OGNIBEN, L., 1957. Secondary gypsum of the Sulphur Series, Sicily, and the so-called integration. J. Sediment. Petrol., 27, 64-79.

OLDERSHAW, A.E., and SCOFFIN, T.P., 1967. The source of ferroan and non-ferroan calcite cements in the Halkin and Wenlock limestones. J. Geol., 5, 309-320.

ORME, G.R., and BROWN, W.W.M., 1963. Diagenetic fabrics in the Avonian limestones of Derbyshire and North Wales. Proc. Yorkshire Geol. Soc., 34, 51-66.

OWEN, R.M.S. and NASR, S.N., 1958. Stratigraphy of Kuwait - Basra area. In: Weeks, L.G. (ed.), Habitat of Oil. Am. Assoc. Petroleum Geologists Bull., 1252-1278.

PAMIC, J., SESTINI, G., and ADIB, D., 1979. Alpine magnetic and metamorphic processes and plate tectonics in the Zagros Range, Iran. Geol. Soc. Amer. Bull., 90, 569-576.

PARK, R., 1976. A note on the significance of lamination in stromatolites. Sedimentology, 23, 379-393.

PARKER, F.L., 1954. Distribution of the Foraminifera in the north-eastern Gulf of Mexico. (ibid.), 111, 453-588.

PETIJOHN, F.P., 1957. Sedimentary rocks, 2nd Ed., New York, Harper & Bros.

PHLEGER, F.B., 1951, Ecology of Foraminifera of northwest Gulf of Mexico. Geol. Soc. Am., Mem., 46.

PICARD, M.D., and HIGH, L.R., 1972b. Criteria for recognising lacustriner rocks. In: Recognition of Ancient Sedimentary Environments, Rigby, J.K. and Hamblin, W.K. (eds.), Spec. Publ. Soc. Econ. Paleont. Miner., Tulsa, 16, 108-145.

PILGRIM, G.E., 1908. The Geology of the Persian Gulf and the adjoining portions of Persia and Arabia. Mem. Geol. Survey India, 34, 1-177.

PILKEY, O.H., 1964. Mineralogy of the fine fraction of certain carbonate cores. Bull. Marine Sci. Gulf and Caribbean, 14, 126-139.

PINGITORE, N.E., 1971. Submarine precipitation of void-filling needles in Pleistocene coral. In: O.P. Bricker (ed.), Carbonate Cements, 68-71.

PINGITORE, Jr. N.E., 1978. The behaviour of Zn^{2+} and Mn^{2+} during carbonate diagenesis: theory and applications. J. Sediment. Petrol., 48, 799-814.

PLAYFORD, P.E., and COCKBAIN, A.E., 1976. Modern algal stromatolites at Hamelein Pool, a hypersaline barred basin in Shark Bay, Western Australia. In: Walter M.R. (ed.), Stromatolites, Amsterdam (Elsevier), 389-412.

PORRENGA, D.H., 1967. Clay mineralogy and geochemistry of Recent sediments in tropical areas. Stolk-Dort, Dordrecht, Netherlands, p.145.

POSNJAK, E., 1938. The system $CaSO_4$-H_2O. Am. J. Science, 35A, 247-272.

PURDY, E.G., 1963a. Recent calcium carbonate facies of the Great Bahama Bank. 1. Petrography and reaction groups. J. Geol., 71, 334-355.

PURDY, E.G., 1963b. Recent calcium carbonate facies of the Great Bahama Bank. 2. Sedimentary facies. J. Geol., 71, 472-497.

RATEEV, M.A., GORBUNOVA, Z.H., LISITZYA, A.P., and NOSOV, G.L., 1969. The distribution of clay minerals in the oceans. Sedimentology, 13, 592-596.

REINECH, H.E., and SINGH, I.B., 1973. Depositional sedimentary environments, with reference to Terrigenous clastics. Springer-Verlag, Berlin, p.439.

REYNOLDS, R.C. and HOWER, J., 1970. The nature of interlayering in mixed-layer illite-montmorillonite. Clays Clay Min., 18, 23-36.

RICHTER, D.K., and FUCHTBAUER, H., 1978. Ferroan calcite replacement indicates former magnesian calcite skeletons. Sedimentology, 25, 843-860.

RICKE, H.H., and CHILINGARIAN, G.V., 1974. Compaction of argillaceous sediments. Amsterdam (Elsevier), p.424.

RILEY, C.M., and BYRNE, J.V., 1961. Genesis of primary structures in anhydrite. J. Sediment. Petrol., 31, 553-559.

ROONEY, L.F., and FRENCH, R.R., 1968. Allogenic quartz and the origin of penemosaic texture in evaporites of the Detroit River Formation (Middle Devonian) in Northern Indiana. J. Sediment. Petrol., 38, 755-765.

ROSS, C.S., 1945. Minerals and mineral relationships of the clay minerals. J. Am. Ceram. Soc., 28, 173-183.

RUSNAK, G.A., 1960. Some observations of Recent oolites. J. Sediment. Petrol., 30, 471-480.

SANDBERG, P.A., 1975. New interpretations of Great Salt Lake ooids of ancient non-skeletal carbonate mineralogy. Sedimentology, 22, 497-537.

SAYYAB, A., and KURESHY, A.A., 1967. The benthonic Foraminifera of the Lower Fars Formation (Lower Miocene) from Shathatha, Karbala, Iraq. Bull. College of Science, Baghdad, 10, 139-149.

SCHALLER, W.T., and HENDERSON, E.P., 1932. Mineralogy of drill cores from the potash field of New Mexico and Texas. Bull. U.S. Geol. Survey, 833, 124p.

SCHMIDT, V., 1965. Facies, diagenesis, and related reservoir properties in the Gigas Beds (Upper Jurassic), north-western Germany. In: L.C. Pray and R.C. Murray (eds.), Dolomitization and limestone diagenesis. Soc. Econ. Paleontologists Mineralogists, Spec. Publ., 13, 124-168.

SCHREIBER, B.C. and FRIEDMAN, G.M., 1976. Depositional environments of Upper Miocene (Messinian) evaporites of Sicily as determined from analysis of intercalated carbonates. Sedimentology, 23, 255-270.

SHAWKAT, M.G., and TUCKER, M.E., 1978. Stromatolites and sabkha cycles from the Lower Fars Formation (Miocene) of Iraq. Geol. Rdsch., 67, 1-14.

SHEARMAN, D.J., and SKIPWITH, P.A.d'E, 1965. Organic matter in Recent and ancient limestones and its role in their diagenesis. Nature, 208, 1310-1311.

SHEARMAN, D.J., 1966. Origin of marine evaporites by diagenesis. Trans. Inst. Min. Metall., B,75, B,208-215.

SHEARMAN, D.J., and FULLER, J.G., 1969. Anhydrite diagenesis, calcitization and organic laminites, Winnepegosis Formation (Middle Devonian), Saskatchewan. Bull. Canad. Petrol. Geol., 17, 496-525.

SHEARMAN, D.J., TWYMAN, J., and KARIMI, M.Z., 1970. The genesis and diagenesis of oolites. Proc. Geologists Assoc. (Engl.), 81, 561-575.

SHEARMAN, D.J., 1970. Recent halite rock (Baja California), Mexico. Inst. Mining Metal., Trans., 79, 155-162.

SHEARMAN, D.J., MOSSOP, G., DUNSMORE, H., and MARTIN, M., 1972. Origin of gypsum veins by hydraulic fracture. Trans. Inst. Min. Metall. (Sect.B: App. Earth Sci.), 81, B149-155.

SHINN, E.A., and GINSBURG, R.N., 1964. Formation of Recent dolomite in Florida and the Bahamas. Am. Assoc. Petrol. Geologists Bull., 48, p.547 (abstract).

SHINN, E.A., GINSBURG, R.N., and LLOYD, R.M., 1965b. Recent supratidal dolomite from Andros Island, Bahamas. In: L.C. Pray and R.C. Murray (eds.), Dolomitization and limestone diagenesis: a symposium. Soc. Econ. Paleontologists Mineralogists, Spec. Publ., 15, 112-123.

SHINN, E.A., 1969. Submarine lithification of Holocene carbonate sediments in the Persian Gulf. Sedimentology, 12, 109-144.

SHINN, E.A., 1973. Carbonate coastal accretion in an area of longshore transport, NE Qatar. In: Purser, B.H. (ed.), The Persian Gulf, Springer-Verlag, Berlin, 179-192.

SHINN, E.A., 1973. Sedimentary accretion along the leeward, SE coast of Qatar Peninsula, Persian Gulf. In: B.H. Purser (ed.) The Persian Gulf, Springer-Verlag, Berlin, 199-210.

SORBY, H.C., 1979. The structure and origin of limestones. Proc. Geol. Soc. London, 35, 56-95.

SPOTTS, J.H., and SILVERMAN, S.R., 1966. Organic dolomite from point Fermin, California. Am. Mineralogist, 51, 1144-1155.

STEHLI, F.G., and HOWER, J., 1961. Mineralogy and early diagenesis of carbonate sediments. J. Sediment. Petrol., 31, 358-371.

STEWART, F.H., 1953. Early gypsum in the Permian evaporites of north-eastern England. Proc. Geol. Assoc., 64, 33-39.

STEWART, F.H., 1949. The petrology of the evaporites of the Eskdale No.2 boring, East Yorkshire. Part I. The Lower Evaporite Bed. Mineralog. Mag., 28, 621-675.

STÖCKLIN, J., 1968. Salt deposits of the Middle East. Geol. Soc. Amer. Spec. Pap., 88, 157-181.

STOCKMAN, K.W., GINSBURG, R.N., and SHINN, E.A., 1967. The production of lime mud by algae in South Florida. J. Sediment. Petrol., 37, 633-648.

STONELEY, R., 1974. Evolution of the continental margins bounding a former southern Tethys. In: Burk, C.A., and Drake, C.L. (eds.), Geology of Continental Margins, Springer, New York, 889-903.

SUGDEN, W., 1951. Report on the stratigraphy and structure of the Lower Fars of the Kirkuk field. Iraq Petrol. Co. Ltd., (unpublished report), p.64.

TAKIN, M., 1972. Iranian Geology and Continental Drift in the Middle East. Nature, 235, 147-150.

TAYLOR, J.M.C., and ILLING, L.V., 1969. Holocene intertidal calcium carbonate cementation, Qatar, Persian Gulf. Sedimentology, 12, 69-107.

THOREZ, J., 1976. Practical identification of clay minerals: a handbook for teachers and students in clay mineralogy. Editions G. Lelotte, Belgique, p.90.

THOMPSON, A.M., 1970. Geochemistry of color genesis in Red Bed sequence, Juniata and Bald Eagle Formations, Pennsylvania. J. Sediment. Petrol., 40, 599-615.

TUTZ, G., and MULLER, G., 1971. High-magnesium calcite and aragonite cementation in Recent Beachrocks, Fuerteventura, Canary Islands, Spain. In: O.P. Bricker (ed.), Carbonate Cements, 4-5.

TILL, R., 1971. Are there geochemical criteria for differentiating reef and non-reef carbonates? Am. Assoc. Petroleum Geologists Bull., 55, 523-528.

TUCKER, M.E., 1976. Replaced evaporites from the late Precambrian of Finnmark, Artic Norway. Sed. Geol., 16, 193-204.

TUCKER, M.E., 1977. Stromatolite biostromes and associated facies in the late Precambrian Porsanger Dolomite Formation of Finnmark, Arctic Norway. Palaeogeography, Palaeoclimatol., Palaeoecol., 21, 55-83.

TUCKER, M.E., 1978. Triassic lacustrine sediments from South Wales: shore-zone clastics, evaporites and carbonates. In: Matter, A. and Tucker, M.E. (eds.), Modern and Ancient Lake Sediments, 205-224.

TURCKIAN, K.K., and ARMSTRONG, R.L., 1960. Magnesium, strontium and barium concentrations and calcite/aragonite ratios of some Recent molluscan shells. J. Marine Res., 18, 133-151.

TWENHOFEL, W.H., 1950. Coral and other organic reefs in geologic column. Bull.Am. Assoc. Petroleum Geologists. 34, 182-202.

USDOWSKI, H.E., 1963. Der Rogenstein des norddeutschen Unteren Buntsandsteins, ein Kalkoolith des marinen Faziesbereichs. Fortschr. Geol. Rheinland Westfalen, 10, 337-342.

VAN DER MAREL, H.W., 1966. Quantitative analysis of clay minerals and their admixtures. Cont. Mineral. and Petrol., 12, 96-138.

VEEVERS, J.J., 1969. Associations of fossils, grain-types and chemical constituents in the Upper Devonian and Lower Carboniferous limestones of the Bonaparte Gulf Basin, Northwest Australia. J. Sediment. Petrol., 39, 1118-1131.

VEIZER, J., and DEMOVIC, R., 1974. Strontium as a tool in facies analysis. J. Sediment. Petrol., 44, 93-115.

VEIZER, J., LEMIEUX, J., JONES, B., GIBLING, M.R., and SAVELLE, J., 1977. Sodium: Paleosalinity indicator in ancient carbonate rocks. Geology, 5, 177-179.

VER PLANK, W.E., 1952. Gypsum in California. California division of Mines Bull., 163, 151.

VINOGRADOV, A.P., AND RONOV, A.B., 1956. Composition of the sedimentary rocks of the Russian Platform in relation to the history of its tectonic movements. Geochemistry (USSR)(Eng. trans.), 533-559.

WAGNER, C.W., and TOGT, C. Van Der, 1973. Holocene sediment types and their distribution in the southern Persian Gulf. In: Purser, B.H. (ed.), The Persian Gulf, Springer, Berlin, 123-156.

WALKER, T.R., 1967. Formation of Red Beds in Ancient and Modern Deserts. Geol. Soc. Am. Bull., 78, 353-368.

WALTON, W.R., 1955. Ecology of living Benthonic Foraminifera, Todos Santos Bay, Baja California. J. Palaeontology, 29, 952-1018.

WEAVER, C.E., 1959. The clay petrology of sediments. Clays Clay Min., Proc. 6th Natl. Conf. N.A.S.N.R.C., Pergamon Press, 154-187.

WEST, I.M., 1964. Evaporite diagenesis in the Lower Purbeck Beds of Dorset. Proc. Yorkshire Geol. Soc., 34, 315-330.

WEST, I.M., 1965. Macrocell structure and enterolithic veins in British Purbeck gypsum and anhydrite. Proc. Yorkshire Geol. Soc., 35, 47-58.

WILLIAMS, H., TURNER, F.J., and GILBERT, C.M., 1954. Petrography. W.H. Freeman and Co., San Francisco, p.406.

WOLF, K.H., 1965. "Gain-diminution" of algal colonies to micrite. J. Sediment. Petrol., 35, 420-427.

WOLF, K.H., CHILINGAR, G.V., and BEALES, F.W., 1967. Elemental composition of sedimentary carbonates, 23-149 in Chilingar, G.V., Bissell, H.J., and Fairbridge, R.W. (eds.), Developments in Sedimentology, 9B, Carbonate rocks: physical and chemical aspects. Elsevier Publ. Co., p.413.

WOOD, G.V., and WOLFE, M.J., 1969. Sabkha cycles in the Arab/Darb Formation off the Trucial Coast of Arabia. Sedimentology, 12.

ZAIM, M., 1977. Clays in the River Yare. Ph.D. Thesis , School of Environmental Sciences, University of East Anglia (unpublished), p.278.

ZEN, E-An., 1965. Solubility measurements in the system $CaSO_4$-NaCl-H_2O at 35°, 50° and 70° and one atmospheric pressure. J. Petrology, 6, 124-164.